

**PALEOENVIRONMENTAL RECONSTRUCTION
OF JAMES AND GRANITE LAKES IN THE TEMAGAMI REGION
OF NORTHEASTERN ONTARIO: FROM THE RETREAT OF THE
LAURENTIDE ICE SHEET TO THE PRESENT**

Robert E. A. Boudreau, M.Sc., C.D.

A thesis submitted to the Faculty of Graduate Studies and Research
in partial fulfilment of
the requirements for the degree of

Doctor of Philosophy

in

The Faculty of Graduate Studies and Research

Ottawa-Carleton Geoscience Centre and Department of Earth Sciences
Carleton University
Ottawa, Ontario
May 2004

©2004 Robert E. A. Boudreau



Library and
Archives Canada

Bibliothèque et
Archives Canada

Published Heritage
Branch

Direction du
Patrimoine de l'édition

395 Wellington Street
Ottawa ON K1A 0N4
Canada

395, rue Wellington
Ottawa ON K1A 0N4
Canada

Your file *Votre référence*
ISBN: 0-612-97813-3
Our file *Notre référence*
ISBN: 0-612-97813-3

NOTICE:

The author has granted a non-exclusive license allowing Library and Archives Canada to reproduce, publish, archive, preserve, conserve, communicate to the public by telecommunication or on the Internet, loan, distribute and sell theses worldwide, for commercial or non-commercial purposes, in microform, paper, electronic and/or any other formats.

The author retains copyright ownership and moral rights in this thesis. Neither the thesis nor substantial extracts from it may be printed or otherwise reproduced without the author's permission.

AVIS:

L'auteur a accordé une licence non exclusive permettant à la Bibliothèque et Archives Canada de reproduire, publier, archiver, sauvegarder, conserver, transmettre au public par télécommunication ou par l'Internet, prêter, distribuer et vendre des thèses partout dans le monde, à des fins commerciales ou autres, sur support microforme, papier, électronique et/ou autres formats.

L'auteur conserve la propriété du droit d'auteur et des droits moraux qui protègent cette thèse. Ni la thèse ni des extraits substantiels de celle-ci ne doivent être imprimés ou autrement reproduits sans son autorisation.

In compliance with the Canadian Privacy Act some supporting forms may have been removed from this thesis.

Conformément à la loi canadienne sur la protection de la vie privée, quelques formulaires secondaires ont été enlevés de cette thèse.

While these forms may be included in the document page count, their removal does not represent any loss of content from the thesis.

Bien que ces formulaires aient inclus dans la pagination, il n'y aura aucun contenu manquant.


Canada

ABSTRACT

This dissertation, divided into three separate sections, investigates the paleoenvironmental history of James and Granite lakes, by examining the sedimentary, hydrogeochemical and micropaleontological history found in the lake sediments.

Chapter One introduces this dissertation and leads to the field methods outlined in Chapter Two. Chapter Three investigates the Holocene sedimentary history of the area, outlining changes in climate that occurred after the retreat of the Laurentide Ice Sheet more than $10,800 \pm 220$ yr. BP. As indicated by the sediment types found, three paleoclimatic regimes existed during the Holocene. A glacial fluvial (sand) regime existed until $10,800 \pm 220$ yr. BP as the Laurentide Ice Sheet retreated from the area. This was followed by an ice-marginal glacial lake regime, which deposited silts and clays from 10,800 to 10,700 yr BP. Finally, from 10,700 yr. BP to the present a mesotrophic lacustrine environment prevailed and has deposited 3.5 m of gyttja, the mass accumulation of which mirrors the relative water level of the system.

The geochemistry of the bottom sediment, and lake waters indicate that two chemically separate water types, carbonate poor, Na-K waters enter James Lake from the north and mix with anthropogenic influenced waters in the south. These anthropogenically influenced waters are Mg-SO₄ rich and found adjacent to the abandoned Northland Pyrite Mine waste rock pile on the southwestern shore of James Lake. Although an inlet stream to Granite Lake is adjacent to the waste rock pile, metals dissolving from the waste rock generally precipitate before the waters reach Granite Lake

to the south. Indications are that the James and Granite Lake system, as a whole, has been exposed to these metals since 8400 yr. BP.

Palynology indicates that the forest in the area since the Holocene warm period has been a mixed Great-Lakes St. Lawrence type. The James and Granite lakes system has cycles of high and low water, as shown by cyclic high and low diversity populations of arcellaceans. Within these cycles, the high nutrient indicator *Cucurbitella tricuspis*, found in conjunction with the algae *Pediastrum* indicates generally eutrophic conditions in the lakes.

DEDICATION

To my parents Val and Bernice, whom I am sure thought I would never finish this undertaking; to my daughter Lindsay, who once wanted to be a scientist, may she find it again; to my brothers Tom, Gary and Shawn; and to Alice who encouraged me.

ORIGINAL RESEARCH CONTRIBUTIONS

The extent of the contributions to this doctoral dissertation from other researchers is listed as follows: F. A. Michel, G. Mason and A. Kumar collected sediment core in James Lake from 1995 to 1996. R. E. A. Boudreau, R. T. Patterson and F. A. Michel collected core in James and Granite lakes from 1997 to 2002. Sediment-water interface sediment samples were collected in James Lake by A. Kumar from 1996 to 1997, and by R. E. A. Boudreau in James and Granite lakes from 1998 to 2002. Pore water samples were obtained by F. A. Michel and R. E. A. Boudreau from piezometers in James Lake during 1999, and water chemistry data were collected by F. A. Michel and R. E. A. Boudreau from 1997 to 2003, and helped by J. Galloway during 2002, in James and Granite lakes. Sub-bottom profiles were obtained by R. E. A. Boudreau in James and Granite lakes from 2001 to 2003.

^{14}C dates were analyzed by the University of Waterloo Isotope Laboratory using liquid scintillation, while small samples were sent to New Zealand for analysis by AMS. ICP-AES and GFAAS analyses were done by Seprotech Laboratories, ARECO Canada Inc., and Caduceon Environmental Laboratories in Ottawa, while sample preparation for these analyses was performed by F. A. Michel and R. E. A. Boudreau. Pollen samples were chemically macerated and slides prepared by A. Kumar, and the pollen counts were performed by J. Galloway. With the exception of assistance with field work, and as listed above, all sample preparation, SEM work, analysis, etc., was completed by R. E. A.

Boudreau in consultation with F. A. Michel and R. T. Patterson.

This doctoral dissertation was written by R. E. A. Boudreau and submitted for comments to F. A. Michel and R. T. Patterson, and the final draft presented here represents the style and content edits suggested by my supervisors.

ACKNOWLEDGEMENTS

I would like to acknowledge and thank the many people who helped, supported and guided me through this research. My supervisors Dr. Tim Patterson and Dr. Fred Michel who introduced me to my field site at James and Granite lakes in northeastern Ontario, and taught me patience through long days at the field camp.

I would like to acknowledge also the many students who participated in the Environmental Science Field camp from 1999 to 2004 who, through their enthusiasm to learn, helped collect data which were used to decipher the Holocene environmental puzzle at this research site. I thank Lewis Ling, who aided me with the Scanning Electron Microscope at the Carleton University Research Facility for Electron Microscopy, Sheila Thayer for helping me with administration and answering my many questions over the years, and Ildi Munro for being a friend and encouraging me to continue.

I would like to thank Tim, Fred and Alice Chang for their time proof reading and helping me edit the manuscript of this dissertation; and I thank my committee, especially Dr. Jim Cheetham and Dr. Danielle Fortin, and my external examiner, Dr. Barry Warner.

This research was partially funded by the Natural Sciences and Engineering Research Council of Canada (NSERC) Discovery Grant to R. Timothy Patterson, funding provided by Frederick A. Michel and a Student Research Award from the Cushman Foundation for Foraminiferal Research.

TABLE OF CONTENTS

Abstract	ii
Dedication	iv
Original Research Contributions	v
Acknowledgements	vii
Table of Contents	viii
List of Tables	xiv
List of Figures	xvi
List of Plates	xx

CHAPTER ONE

INTRODUCTION	1
Background	1
Objectives	4
Format	5
REFERENCES	5
FIGURES	9

CHAPTER TWO

METHODS	11
----------------	-----------

Introduction	11
Field Methods	11
Sediment Samples	11
Sediment Cores	11
Sediment/Water Interface Samples	12
Water Samples	13
Water Chemistry	13
pH	13
Water Temperature	14
Electrical Conductivity	15
Oxygen	15
Sub-bottom Profiles	15
Laboratory Methods	16
Radiocarbon (¹⁴ C) Dating	16
Stratigraphy	17
Palynology	17
Chemistry	18
Micropaleontology	18
REFERENCES	19
TABLES	21
FIGURES	26

CHAPTER THREE

PALEOSEDIMENTARY MODEL OF THE JAMES AND GRANITE LAKES SYSTEM, USING PALEOLIMNOLOGICAL PROCESSES AS QUATERNARY PALEOINDICATORS	41
ABSTRACT	41
INTRODUCTION	42
Background	41
ANALYSIS AND RESULTS	45
Sedimentary profiles	45
Core compaction and compression	46
Sub-bottom profiles	52
Radiocarbon dating	53
Mass Accumulation Rate	56
Mass Compression Rate	56
Paleoindicators	57
DISCUSSION	59
CONCLUSIONS	63
REFERENCES	64
TABLES	70
FIGURES	76
PLATE	92
APPENDIX A	93

CHAPTER FOUR

AQUATIC CHEMISTRY	98
ABSTRACT	98
INTRODUCTION	99
ANALYSIS and RESULTS	101
Anions and Cations	101
Water Properties	102
Trace Metals	105
Bulk Sediment Chemistry	107
DISCUSSION	110
Water Stratification	110
Major Ion Chemistry	110
Dissolution/Precipitation Chemistry	112
Bulk Sediment Chemistry	114
CONCLUSION	115
REFERENCES	115
TABLES	118
FIGURES	132

CHAPTER FIVE

APPLICATION OF MICROPALAEONTOLOGICAL PROXIES TO ASSESS HOLOCENE PALEOENVIRONMENTAL AND PALEOCLIMATIC CHANGES IN JAMES AND GRANITE LAKES	148
ABSTRACT	148
INTRODUCTION	149
ANALYSIS and RESULTS	152
Shannon – Weaver Diversity Index	154
Cluster Analysis	155
Pollen Cluster Analysis	157
DISCUSSION	159
The end of the Pleistocene	159
Post Younger Dryas warming period	159
Post Younger Dryas cool period	160
Early Holocene warming	160
Holocene Hypsithermal	160
Medieval Warm Period and Little Ice Age	161
Present Conditions	162
Possible impact of beavers on lake ecology	163
CONCLUSIONS	164
SYNONYMY	165
REFERENCES	179

TABLES	190
FIGURES	206
PLATES	220
CONCLUSIONS	222

LIST OF TABLES

Table 2.1	Prefixes used in maps for sampling of different materials	21
Table 2.2	Data for James Lake piston core JL 95-5	22
Table 2.3	Data for James Lake push core JL 97-1	22
Table 2.4	Data for James Lake push core JL 97-2	22
Table 2.5	Data for James Lake push core JL 97-3	23
Table 2.6	Data for James Lake push core JL 97-4	23
Table 2.7	Data for James Lake Livingstone core JL 98-3	23
Table 2.8	Data for James Lake Livingstone core JL 99-1	24
Table 2.9	Data for James Lake Livingstone core JL 99-7	25
Table 2.10	Data for James Lake Livingstone core JL 01-2	26
Table 2.11	Data for James Lake Livingstone core JL 01-8	26
Table 2.12	Data for Granite Lake Livingstone core GL 99-2	27
Table 2.13	Data for Granite Lake Livingstone core GL 98-3	27
Table 2.14	Data for Granite Lake Livingstone core GL 99-4	28
Table 3.1	Zone Key for sediment layers in Stratigraphic columns	70
Table 3.2	Porosity and density data for Granite lakes	71
Table 3.3	Sediment compression data for the James and Granite lakes system	72
Table 3.4	^{14}C data from James and Granite lakes	73
Table 3.5	Bulk sedimentation rates for James and Granite lakes	74

Table 3.6	Mass accumulation rates, compaction rates and mass compression rates for James and Granite lakes	75
Table 4.1	Trace metal pore-water chemistry from the sediment-water interface in James Lake	118
Table 4.2	Trace metal pore-water chemistry from piezometers in James Lake	119
Table 4.3	Cation and anion data from James and Granite lakes	120
Table 4.4	Bulk sediment chemistry from sediment-water interface sediment samples	122
Table 4.5	Electrical conductivity and pH data from piezometers in James Lake	123
Table 4.6	Water depth, pH, electrical conductivity and water temperatures from James and Granite lakes	124
Table 4.7	pH, electrical conductivity, oxygen concentration and water temperatures from James and Granite lakes	125
Table 4.8	Bathymetric temperature profile data for James and Granite lakes	126
Table 4.9	Water hardness compared with total dissolved solids and pH in James and Granite lakes	127
Table 4.10	Bulk sediment chemistry data from sediment-water interface sediment samples from James Lake	130
Table 5.1	Taxonomic unit counts, Shannon diversity, fractional abundances and standard error for sediment-water interface samples and core sediment samples from James and Granite lakes.	190
Table 5.2	Taxonomic unit counts, Shannon diversity, fractional abundances and standard error for core pollen sediment samples from James and Granite lakes.	204

LIST OF FIGURES

Figure 1.1	Map showing location of James and Granite lakes	9
Figure 1.2	Map showing Hudson Bay, Great Lakes and St. Lawrence drainage divides in relation to the James and Granite lakes site.	10
Figure 2.1	Map showing coring sites in James and Granite lakes.	29
Figure 2.2	Using the Livingstone coring device from a raft in James Lake.	30
Figure 2.3	Map showing locations of sediment-water interface samples in James and Granite lakes.	31
Figure 2.4	Map showing positions where water samples, pH, temperature, specific conductivity and oxygen measurements were collected in James and Granite lakes.	32
Figure 2.5	Map showing locations of sub-bottom profile runs in James Lake.	33
Figure 2.6	Map showing locations of sub-bottom profile runs in Granite Lake.	34
Figure 2.7	Legend Key for Figures 2.7a – e	35
Figure 2.7a	Stratigraphic column for James Lake core JL 99-1	36
Figure 2.7b	Stratigraphic column for James Lake core JL 99-7	37
Figure 2.7c	Stratigraphic column for James Lake core JL 01-2	38
Figure 2.7d	Stratigraphic column for Granite Lake core GL 98-3	39
Figure 2.7e	Stratigraphic column for Granite Lake core GL 99-4	40
Figure 3.1	Stratigraphic columns for James and Granite lake cores JL 99-7, JL 01-2, JL 99-1, GL 99-4 and GL 98-3	76
Figure 3.2	Void ratio plotted against depth	77

Figure 3.3	Density, porosity and compaction curves for Granite Lake core GL 99-4	78
Figure 3.4	Sub-bottom sonar profile for run #9 in James Lake	79
Figure 3.4A	Close-up of sub-bottom sonar profile for run #9 showing Basin A and the position of core JL 99-1	80
Figure 3.4B	Close-up of sub-bottom sonar profile for run #9 showing Basin B and the position of core JL 01-8	81
Figure 3.5	Sub-bottom sonar profile for run #23 in James Lake	82
Figure 3.6	Sub-bottom sonar profile for run #1 in James Lake	83
Figure 3.7	Graph of uncalibrated ^{14}C dates against depth for James and Granite lakes	84
Figure 3.8	Calibration dates for James Lake core JL 99-1	85
Figure 3.9	Calibration dates for James Lake core JL 99-7	86
Figure 3.10	Calibration dates for Granite Lake core GL 99-4	87
Figure 3.11	Graph of mass accumulation rates against ^{14}C ages	88
Figure 3.12	Graph of mass compression rates against depth	89
Figure 3.13	Relative water depths, phases and climate for the James and Granite lakes system	90
Figure 4.1	Map showing locations of sediment-water interface pore-water and sediment-water interface sediment samples from James and Granite lakes	132
Figure 4.2	Trilinear plot of sediment-water interface pore waters for James and Granite lakes	133
Figure 4.3	Map showing water types as indicated in the Trilinear plots for James and Granite lakes	134
Figure 4.4	Map showing pH for surface and bottom waters for James and Granite lakes	135

Figure 4.5	Map showing electrical conductivity in James and Granite lakes	136
Figure 4.6	Graph showing bathymetric temperature profile for Granite Lake	137
Figure 4.7	Semi-log graph showing bathymetric temperature, oxygen and total dissolved solid profiles for the Northland Pyrite Mine trench	138
Figure 4.8	Semi-log graph showing bathymetric temperature, oxygen and total dissolved solid profiles for James Lake	139
Figure 4.9	Bathymetric map of James and Granite lakes indicating the hypolimnion, metalimnion and epilimnion zones based on temperature profiles	140
Figure 4.10	Graph showing logarithms of molar concentrations of metals plotted against pH for sediment-water interface pore-water sites in James and Granite lakes	141
Figure 4.11	Graph showing logarithms of molar concentrations of metals plotted against pH for piezometer pore-water sites in James Lake	142
Figure 4.12a	R-mode vs Q-mode cluster diagram for sediment-water interface bulk sediment chemical analysis for James Lake	143
Figure 4.12b	R-mode vs Q-mode cluster diagram for sediment-water interface bulk sediment chemical analysis for James lake without phosphorus	144
Figure 4.13	Map showing lake bottom sediment zones, indicating iron and phosphorus concentrations from sediment-water interface bulk sediment chemistry from James Lake	145
Figure 4.14	R-mode vs Q-mode cluster diagram for sediment-water interface bulk sediment chemical samples combined with bulk sediment core chemical samples from James Lake	146
Figure 4.15	Stratigraphic columns for cores from James Lake indicating core sediment zones	147

Figure 5.1	Graph of Shannon diversity against taxonomic counts for sediment-water interface stations in the James and Granite lakes system	206
Figure 5.2	R-mode vs Q-mode cluster diagram for sediment-water interface samples and core sediment samples in the James and Granite lakes system.	207
Figure 5.2a	R-mode vs Q-mode cluster relationships for assemblages I, II and III in the James and Granite lakes system	208
Figure 5.2b	R-mode vs Q-mode cluster relationships for assemblages IV and V in the James and Granite lakes system	209
Figure 5.3	Map showing sediment-water interface assemblages in the James and Granite lakes system	210
Figure 5.4	Sawtooth diagram for taxa in James Lake core JL 99-1	211
Figure 5.5	Sawtooth diagram for taxa in James Lake core JL 99-7	212
Figure 5.6	Sawtooth diagram for taxa in James Lake core JL 01-2	213
Figure 5.7	Sawtooth diagram for taxa in Granite Lake core GL 98-3	214
Figure 5.8	Sawtooth diagram for taxa in Granite Lake core GL 99-4	215
Figure 5.9	Stratigraphic relationships between assemblages	216
Figure 5.10	R-mode vs Q-mode cluster diagram for pollen assemblages in the James and Granite lakes system	217
Figure 5.11	Sawtooth diagram for pollen in James and Granite lakes	218

LIST OF PLATES

Plate 3.1	Gastropods, pelecypods and charophytes from James and Granite lakes	90
Plate 5.1	Centropyxid arcellaceans from James and Granite lakes	220
Plate 5.2	More arcellaceans from James and Granite lakes	221

APPENDICES

Appendix A to Chapter 3	93
Original volume	93
Initial and final void ratio	94
Change in height of a layer	94
Time Model	96

CHAPTER ONE

INTRODUCTION

This dissertation was undertaken to describe the paleoenvironmental and Holocene history of James and Granite lakes, and to increase our understanding of the post-glacial history in the Temagami region of northeastern Ontario.

Background

James and Granite lakes are two small lunate, mesotrophic lakes, located west of highway 11, approximately 10 km north of Temagami in northeastern Ontario (Figure 1.1). These lakes lie within hilly terrain (315 to 410 masl), in the Southern Structural sub-province near a local surface water divide. Granite Lake is underlain by a quartz monzonite batholith of Algomian age (2700 to 2650 Ma; Stockwell et al., 1970), that intrudes metamorphosed Keewatin volcanics (2710 to 2700 Ma; Goodwin and Ridler, 1970); the contact strikes N 15° E just west of southern James Lake. Pyrite, pyrrhotite and minor chalcopyrite (Hewitt, 1967) are found in parallel felsic tuff zones near the contact with the quartz monzonite, outcropping on the southwestern shore of James Lake, at the Northland Pyrite Mine site (Savage, 1953). To the east of the felsic tuff zone are deformed intermediate to mafic pillow lavas and gabbros. Within the broader geological framework these rocks are overlain by undeformed conglomerates, sandstones and mudstones of the Cobalt Group (> 2160 Ma; Collins, 1925; Young, 1971; Young and

Church, 1966; and Frarey and Roscoe, 1970), which in turn are subsequently intruded by the Nipissing diabase. Neither of these last two rock types are found in the immediate study area. The research site is situated on the western edge of a north-west trending graben of Precambrian age that was reactivated during the Cretaceous-Tertiary period (Kumapareli and Saull, 1966). Lake Timiskaming sits in the centre of this structure.

The Wisconsinan maximum occurred 22,000 yr. BP, when the Laurentide Ice Sheet extended from the Tazwell Moraine (State of Illinois) to the NE coast of Labrador and Baffin Island (Lliboutry, 1999; Marshall et al., 2000). The ice covered most of Hudson Bay, as well as the Great Lakes and St. Lawrence drainage basins (Figure 1.2). The northward retreat of the Laurentide Ice Sheet led to a massive ponding of meltwaters between the ice front and the Laurentian – Mississippi watershed, which lasted until 12,500 yr. BP (Coakley et al., 1998).

As the ice retreated northward pro-glacial lakes flooded the Great Lakes basins. A series of lakes occupying the Lake Huron basin were dominated by the high level stand of the main Lake Algonquin. With the retreating ice sheet forming the northern edge of the lake, it covered the isostatically depressed area north of the current Lake Huron and extended eastward to North Bay. Re-entrants in the ice caused temporary flooding of ice free areas into the Temagami area. As new outlets opened, lake levels declined (Veillette, 1994; Vincent and Hardy, 1994).

As the ice cleared the Lake Timiskaming Valley and areas north of the study area, Lake Ojibway-Barlow formed and eventually covered much of northern Ontario and the Hudson Bay drainage basin. Varve chronology (Hughes, 1965) and an absolute shell

date within the Tyrell Sea (Boissonneau, 1968) indicate that Lake Ojibway-Barlow began to form around 10,800 yr. BP.

By 10,000 yr. BP, the ice sheet had retreated from the Ottawa River Valley to the south, and to the northeast of Lake Timiskaming, creating the “Ayley” Phase of glacial Lake Barlow between the retreating glacier and the McConell Moraine to the south (Vincent and Hardy, 1994).

Lake sediment cores from North America and Europe indicate that an increase in cold climate pollen species, and a decrease in warm climate species occurred beginning 12,000 yr. BP (the Younger Dryas cool event), and lasted up to 1500 yrs (Björck et al., 1996; Gorham et al., 2001). Following the Younger Dryas, a boreal forest dominated the Canadian Shield, consisting of white and black spruce, balsam fir, and jack pine associated with birch and aspen in the uplands, and tamarack in the lowlands, until the climate began to warm after 9000 yr. BP (Liu, 1990). The Holocene Hypsithermal, from approximately 7000 to 3000 yr. BP, produced a more arid and warmer climate in northeastern Ontario (Dean et al., 1996; Liu, 1990; Vance et al., 1995) replacing the boreal forest with a mixed boreal – Great Lakes – St. Lawrence Forest, which is the mature forest type found at this site today. The above trees are found today in association with white, red and jack pine, hemlock and maple.

Pro-glacial lake sediments (varved clays) were investigated in the vicinity of Lake Timiskaming (glacial Lake Barlow) by Antevs (1925), and the sediment water interfaces of various lakes, including James Lake, were recently investigated using arcellaceans (thecamoebians) as proxies for modern environmental change (Kumar and Patterson, 1999; Patterson and Kumar, 2000) and as paleoenvironmental indicators (Medioli and

Scott, 1988; Patterson et al., 1996; Patterson and Kumar, 2000; Reinhardt et al., 1998). The sediment chemistry of James Lake was investigated in the immediate vicinity of the Northland Pyrite Mine waste rock pile (Mason, 1998); and the vegetation history of the northern Great Lakes region was investigated using pollen (Liu, 1990; Ritchie, 1987; Terasmae, 1980), and northeastern Ontario was identified as a region where more pollen research was required (Liu, 1990).

Objectives

The main objective for this research was to reconstruct the post glacial and Holocene paleoenvironmental history in the Temagami area of northeastern Ontario, from the retreat of the Laurentide Ice Sheet to the present. The effect of acid mine drainage from an abandoned pyrite mine, at the former Northland Pyrite Property, located on the southwestern shore of James lake (Savage, 1953), was investigated. To construct the paleoenvironmental history of the site, sediment water interface sediment chemical and physical analyses was compared to sedimentary analysis of cores under James and Granite (control) lakes.

The Northland Pyrite Company mine, which went into operation in 1906, caused environmental stress that continued to influence the lake environment since the mine was abandoned in 1911. This study utilizes hydrogeochemistry, sediment chemistry, sedimentology, the geology of the site and changes in flora and fauna as they are related to changes caused by fluctuating lake levels; and the effect of introduced pollution effects or anthropogenic influences.

Format

This dissertation is divided into three main sections. The first section investigates the Holocene sedimentary record as determined using various field and laboratory methods (Chapter Two), then builds a stratigraphic time model using ^{14}C dating techniques. This sedimentary model, which includes mass accumulation through the Holocene, is described in Chapter Three.

The second section investigates the chemistry of the sediment and waters of the two lakes, the marsh between the lakes and the abandoned Northland Pyrite Property. This investigation considered the effect of waters influenced by acid mine drainage, beaver, and runoff from the nearby highway 11, with the natural waters entering James Lake from the north. This information is used to formulate a chemical model as described in Chapter Four.

The last section, investigated in Chapter Five, examines the microfauna (arcellacean populations) within the system, both present and past, to investigate short-term environmental changes in the system. Microflora (pollen) were examined to investigate long term changes in the vegetation.

Finally, general overall conclusions are presented in Chapter Six.

REFERENCES

Antevs, E., 1925, Retreat of the Last Ice-sheet in Eastern Canada: Geological Survey
Memoir 146, v. 2061: Ottawa, Printer to the King's most Excellent Majesty, 1 -
142 p.

- Boissonneau, A. N., 1967, Glacial history of Northeastern Ontario II. The Timiskaming-Algoma area, *Canadian Journal of Earth Sciences*, v. 5 (97), p. 97-109.
- Collins, W. H., 1925, North shore of Lake Huron: Geological Survey of Canada, Memoir 143, 160 p.
- Frarey, M. J. and Roscoe, S. M., 1970, The Huronian Supergroup north of Lake Huron, in *Symposium on basins and geosynclines of the Canadian Shield: Geological Survey of Canada, Paper 70-40*, p. 143-157.
- Goodwin, A. M., and Ridler, R. H., 1970, The Abitibi orogenic belt, in A. J. Baer, ed., *Symposium on Basins and Geosynclines of the Canadian Shield: Geological Survey of Canada, Paper 70-40*, p. 1-30.
- Hewitt, D. F., 1967, Pyrite Deposits of Ontario, *Mineral Resources Circular No. 5*, Ontario Department of Mines, p. 40 - 70.
- Hughes, O. L., 1965, Surficial geology of part of the Cochrane district, Ontario, Canada. *In International studies on the Quaternary*, Wright, H. E., Jr., and Frey, D. G., ed., Geological Society of America, Special Paper 84, p. 535 - 565.
- Kumar, A., and Patterson, R. T., 1999, Arcellaceans (thecamoebians): new tools for monitoring long and short term changes in lake bottom acidity: *Environmental Geology*, v. 39, p. 689 - 697.
- Liu, K.-B., 1990, Holocene Paleoecology of the Boreal Forest and Great Lakes-St. Lawrence Forest in Northern Ontario: *Ecological Monographs*, v. 60, p. 179-212.
- Marshall, S. J., Tarasov, L., Clarke, G. K. C., and Peltier, W. R., 2000, Glaciological reconstruction of the Laurentide Ice Sheet: physical processes and modelling challenges: *Canadian Journal of Earth Sciences*, v. 37, p. 769 - 793.

- Mason, G., 1998, A study of the effects of past mining activities on James Lake sediment chemistry, BSc. Thesis (unpublished), Carleton University, pp. 52.
- Medioli, F. S., and Scott, D. B., 1988, Lacustrine thecamoebians (mainly arcellaceans) as potential tools for palaeolimnological interpretations: *Palaeogeography, Palaeoclimatology, Palaeoecology*, v. 62, p. 361 - 386.
- Patterson, R. T., Barker, T., and Burbidge, S. M., 1996, Arcellaceans (Thecamoebians) as proxies of Arsenic and Mercury contamination in Northeastern Ontario lakes: *Journal of Foraminiferal Research*, v. 26, p. 172 - 183.
- Patterson, R. T., and Kumar, A., 2000, Assessment of Arcellacean (Thecamoebian) Assemblages, Species, and Strains as Contaminant Indicators in James Lake, Northeastern Ontario, Canada: *Journal of Foraminiferal Research*, v. 30, p. 310 - 320.
- Reinhardt, E. G., Dalby, A. P., Kumar, A., and Patterson, R. T., 1998, Arcellaceans as Pollution Indicators in Mine Tailing Contaminated Lakes Near Cobalt, Ontario, Canada: *Micropaleontology*, v. 44, p. 131 - 148.
- Ritchie, J. C., 1987, *Postglacial vegetation of Canada*: Melbourne, Australia, Cambridge University Press, 178 p.
- Savage, W. S., 1953, Report on Northland Pyrite Property, Candela Option. Best Township.
- Stockwell, C. H., McGlynn, J. C., Emslie, R. F., Sanford, B. V., Norris, A. W., Donaldson, J. A., Fahrig, W. F. and Currie, K. L., 1970, Geology of the Canadian Shield, in Douglas, R. J. W., ed., *Geology and economic minerals of Canada*: Canadian Geological Survey, Economic Geology Report No. 1, p. 43-150.

- Terasmae, J., 1980, Some problems of late Wisconsin history and geochronology in northeastern Ontario: *Canadian Journal of Earth Sciences*, v. 17, p. 361 - 381.
- Veillette, J. J., 1994, Evolution and Paleohydrology of Glacial Lakes Barlow and Ojibway: *Quaternary Science Reviews*, v. 13, p. 945 - 971.
- Vincent, J.-S., and Hardy, L., 1994, The evolution of Glacial Lakes Barlow and Ojibway, Quebec and Ontario: *Geological Survey Bulletin 316*, p. 18 p.
- Young, G. M., 1971, Stratigraphic and sedimentological framework of the Huronian rocks of the Southern Province of the Canadian Shield (abstract): *Geological Association of Canada, Mineralogical Association of Canada, Annual Meeting, Sudbury, Ontario, Abstracts of Papers, 1971*, p. 75-76.
- Young, G. M. and Church, W. R., 1966, The Huronian System in the Sudbury District and adjoining areas of Ontario; A review: *Geological Association of Canada, Proceedings v. 17*, p. 65-82.

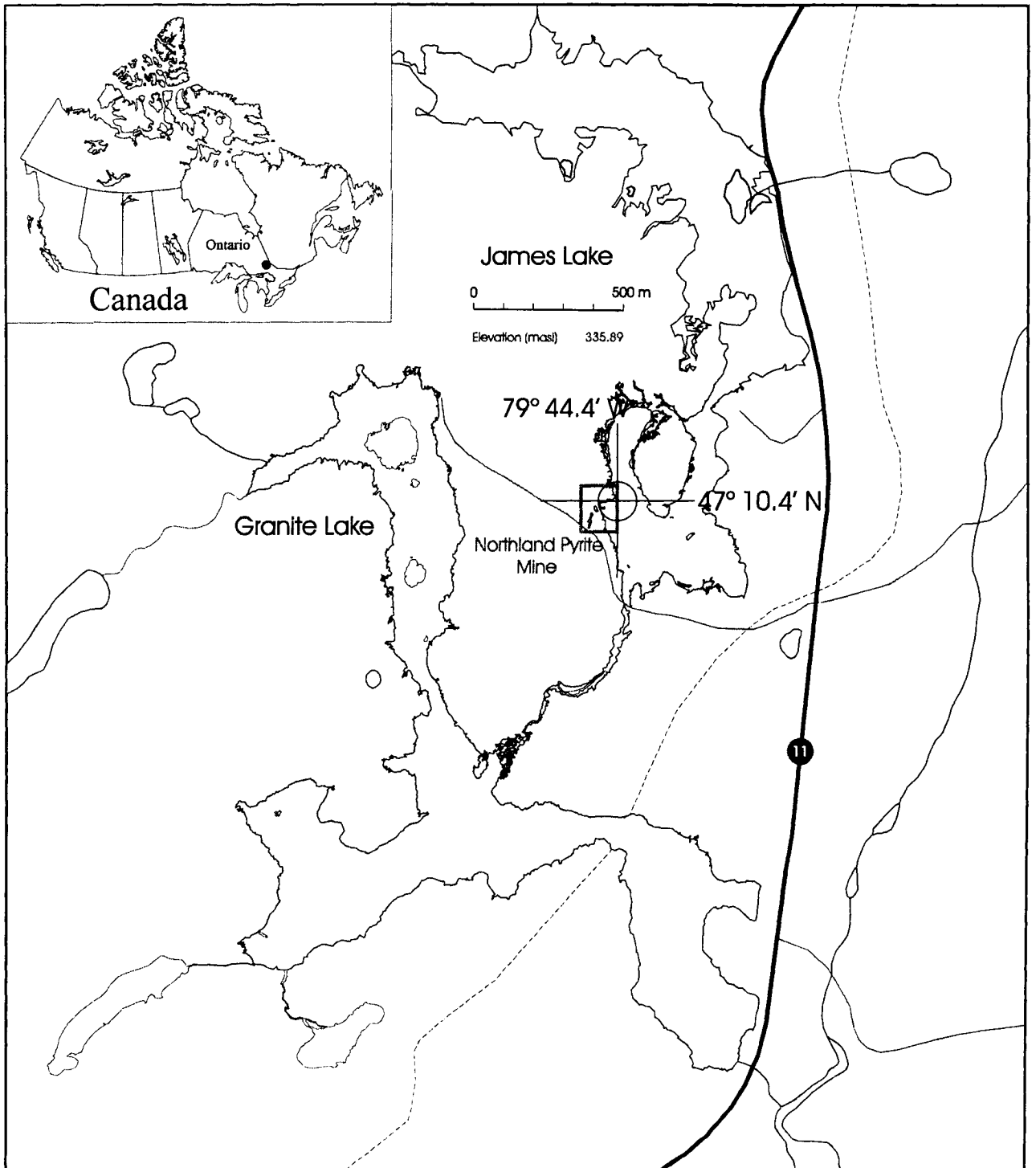


Figure 1.1 - James and Granite lakes, located near highway 11, 10 km north of Temagami in northeastern Ontario. The Northland Pyrite Mine site is located on the southwestern shore of James Lake (see box). Dashed lines denotes the route of a natural gas pipeline.

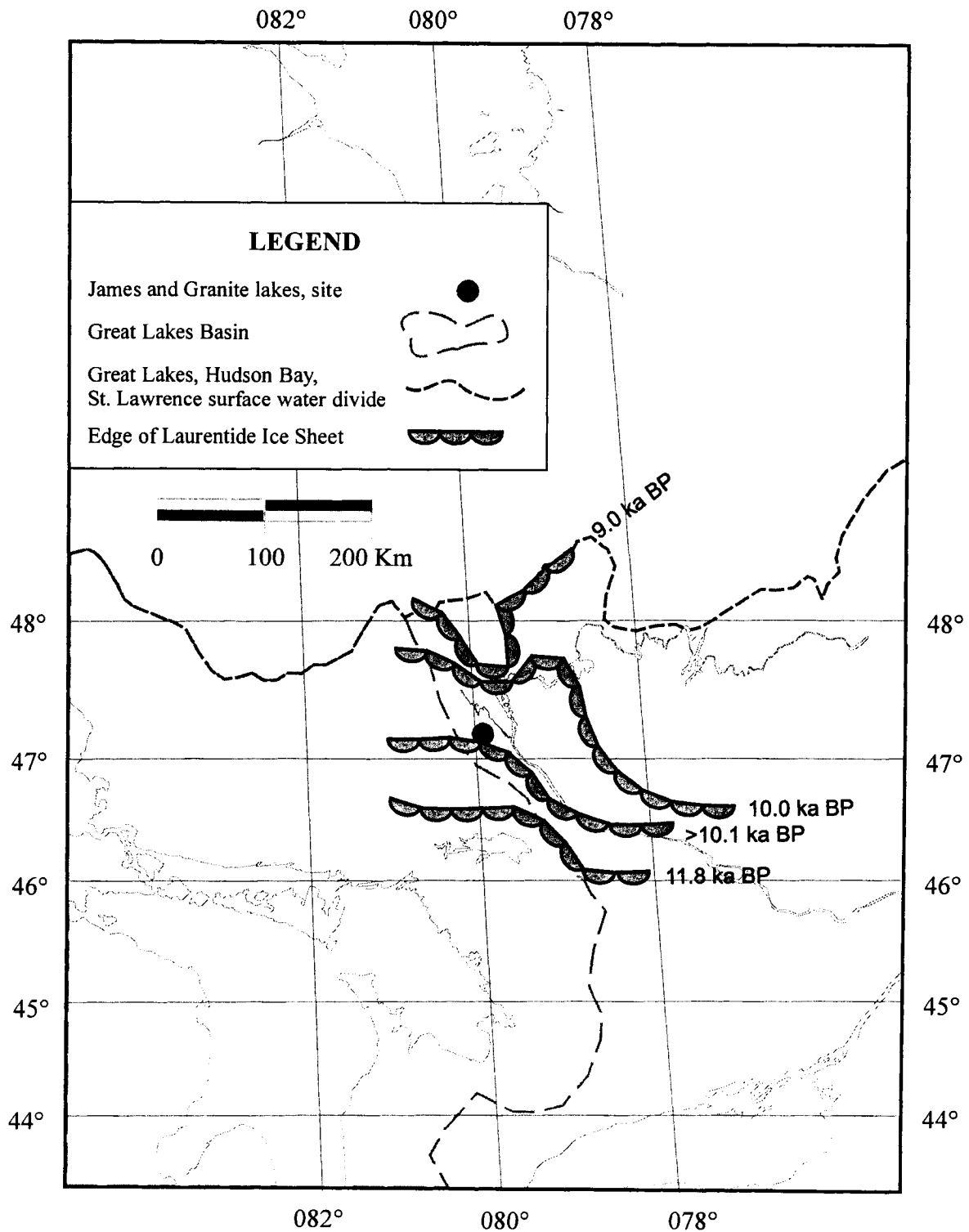


Figure 1.2 - Map indicating Hudson Bay, Great Lakes, St. Lawrence drainage divide in relation to the site under investigation, and the Laurentide Ice Sheet at various times during the Late Wisconsin Glaciation (after Veillette, 1994; and, after Vincent and Hardy, 1994).

CHAPTER TWO

METHODS

Introduction

Field data were collected from 1995 to 2002, during the last two weeks of August, and concurrent with Carleton University's second-year Environmental Science field course. Field work included the collection of sediment cores and sediment-water interface sediment samples, water property data (pH, surface and bottom water temperatures, temperature profiles, and electrical conductivity readings), sub-bottom profiles and bathymetric transects. The locations of these sample sites were determined using a hand held Trimble Scout Global Positioning unit and corroborated using triangulation.

Field Methods

Sediment Samples

Sediment Cores: James and Granite lakes were sampled from 1995 to 2002 using various coring techniques. During August 1995 a piston corer (Wright et al., 1964), deployed from a five meter boat, was used to obtain 17 cm-long (JL 95-5; prefixes Table 2.1) cores from the bottom of the pond adjacent to the mine trench at the Northland Pyrite Mine Co. site on the southwest shore of James Lake (Fig. 2.1). During the winter of 1997, four additional cores were obtained by augering through the ice, and pushing a 3.81

cm diameter PVC pipe into the sediment to obtain 104 cm (JL 97-1; Mason, 1998; Kumar, 1999; and Patterson and Kumar, 2000a), 159 cm (JL 97-2; (Mason, 1998), 102 cm (JL 97-3; (Mason, 1998)) and 98 cm (JL 97-4; (Mason, 1998) sediment cores. In August 1998, a 278 cm long core (JL 98-3) was obtained from James Lake, and a 248 cm long core was obtained from Granite Lake using a Livingstone corer (Deevey, 1964) from a raft (Fig. 2.2) anchored over the coring site. Additionally, in August 1999, again using a Livingstone corer, 363 cm (JL 99-1) and 456 cm (JL 99-7) cores were obtained from James Lake, and 60 cm (GL 99-2) and 428 cm (GL 99-4) cores were obtained from Granite Lake. Finally, during August 2001, the Livingstone coring method was again used to obtain 409 cm (JL 01-2) and 388 cm (JL 01-8) cores from James Lake.

Sediment core (1998 to 2000) was extruded from the aluminum core barrels, using a wooden dowel, while holding the core barrel steady. Stratigraphy and other details of interest are recorded in Tables 2.2 to 2.14. The sediments were packaged using plastic food wrap and aluminum foil, then stored horizontally in a cold room until transport. In the laboratory these archived cores were stored in a cold room at 4°C until sampled for further study.

Sediment-Water Interface Samples: Seventy-six sediment-water interface sediment samples were acquired from 1996 to 2002 in James and Granite Lakes at the locations indicated in Figure 2.3 (see Chapter Five). Thirty-five of these samples were obtained from James Lake in 1996 and 1997, and reported in a previous study (Kumar, 1999; Patterson and Kumar, 2000a, b). These samples were obtained using an Eckman Type Box corer with an opening of 15 cm by 15 cm, and unless objects of interest such as

gastropods or pelecypods were found, only the top two or three cm of slimy sediment was collected. This material was stored in 100 ml jars, spiked with 70% isopropyl alcohol to prevent decay, archived and stored in a cold room until transport back to the laboratory. Finally, fourteen sediment samples were sent to Areco Canada of Nepean, Ontario, for bulk sediment analysis.

Water Samples

Water chemistry: Nine water samples were obtained from James Lake in the vicinity of the waste rock pile, one water sample from the creek between James and Granite lakes, and one water sample from Granite Lake. Of the nine water samples from James Lake, seven were from pore waters obtained using a Nalgene 'Mityvac' handpump through piezometers placed into the lake bottom sediment near the Northland Pyrite Mine waste rock pile (Figure 2.4). The other two samples were taken from surface waters near JLP 99-3, and between JLP 99-6 and JLP 99-7. In addition, 24 water samples from 12 sediment-water interface stations were obtained in 1997 from James Lake. One of the 1997 water samples from each station, and all of the 1999 water samples were filtered to remove sediment using 1.2 μm filters, acidified to 1% nitric acid and refrigerated.

Chemistry is reported in Chapter Four.

pH: Fifty-two surface and bottom water pH readings were obtained using a Horiba Compact Twin pH meter (B-213) at locations in James and Granite lakes indicated in Figure 2.4. Fifteen pH measurements were taken over two days from seven piezometer sites near the Northland Pyrite Mine waste rock pile during the August 2001 Field Camp.

Twelve pH measurements were also obtained from James Lake and three from James Lake Creek during the August 2001 Field Camp. Eleven pH measurements were obtained from Granite Lake and eleven from the vicinity of the Northland Pyrite Mine during the August 2002 Field Camp. Fifteen additional pH measurements were taken in James Lake, Granite Lake and the James Lake Creek during the 2003 Field Camp.

Water temperature: Fifty-three surface and bottom water temperature measurements, and three temperature profiles were obtained between 1999 and 2003. Thirty-one temperature measurements were obtained from 1999 to 2002 using a Fish Hawk temperature probe with a digital depth counter, and twenty-two temperature measurements were taken in 2003 using a YSI (Yellow Springs Industries) Model 85 Handheld Oxygen, Conductivity, Salinity and Temperature System. Twelve temperatures were recorded in James Lake during the August 2001 Field Camp; and, eleven temperatures were recorded in Granite Lake and eight recorded in the vicinity of the Northland Pyrite Mine during the August 2002 Field Camp. Twenty-one temperatures were recorded in James Lake, seven in the James Lake Creek and three in Granite Lake during the August 2003 Field Camp. A twenty-six reading, bathymetric profile was recorded from Granite Lake at GLTPr 99 (Fig. 2.4) during the August 1999 Field Camp. A sixteen reading temperature profile was taken in the Northland Pyrite Mine trench at NPMTPr 03, and a fifteen reading temperature profile was obtained in northern James Lake at JLTPr 03.

Electrical conductivity: Twenty-four electrical conductivity measurements ($\mu\text{S}/\text{cm}$) were taken, using a Lisle-Metrix Ltd, Canlab C51D Conductivity Meter, on the waters from the vicinity of the Northland Pyrite Mine in southwest James Lake. Fourteen measurements were taken over two days from pore waters at each of the piezometers in James Lake, and ten readings from the surface waters in the vicinity of the Northland Pyrite Mine during the August 2002 Field Camp. Twenty-two electrical conductivity measurements ($\mu\text{S}/\text{cm}$) were taken using the YSI Model 85 metering system during the August 2003 Field Camp. Eleven were in James Lake, seven in the James Lake Creek and three in Granite Lake.

Oxygen: The oxygen content (mg/L) of the lake water was measured using the YSI Model 85 metering system at the twenty-two locations indicated during the August 2003 Field Camp where electrical conductivity measurements were taken (above).

Sub-bottom Profiles

Thirty-five sub-bottom profiles were compiled from James Lake during the August 2001 Field Camp (Fig. 2.5), and forty sub-bottom profiles were compiled from Granite Lake during the August 2002 Field Camp (Fig. 2.6). These profiles were obtained using a Knudsen 320 B/P Echosounder with a dual frequency transponder transmitting at 50 kHz (high frequency) and at 28 kHz (low frequency), and digitally recorded using a SCSI interface. The interface provided a full-function user interface with Microsoft Windows[®] 98 using a Panasonic Toughcoat laptop computer. The system and equipment, developed by Knudsen Engineering Ltd. of Perth, Ontario, was operated from a five meter

aluminum boat with an outboard engine. The system used an extremely precise quartz crystal timebase control, which gives a scale parameter for sound speed that is effectively zero (in theory; Knudsen Manual, 2000). However, to confirm a time-distance ratio, the runs were conducted at low speed with 15 second time checks. The echograms which intersected coring locations JL 99-1, JL 99-7, JL 01-2, GL 98-3 and GL 99-4 were enhanced with Adobe® Photoshop 6.0 and reported in Chapter Three.

Laboratory Methods

Radiocarbon (^{14}C) Dating

To determine sedimentation rates in James and Granite lakes, eight samples containing visible plant fibres or wood fragments were extracted from three of these cores, at or close to sediment horizons as indicated in Figure 2.7, and sent to the University of Waterloo Isotope Laboratory for ^{14}C analysis using liquid scintillation, while small samples were sent to New Zealand for analysis by Accelerator Mass Spectroscopy (AMS). Three ^{14}C samples from JL 99-1, two ^{14}C samples from JL 99-7, and three C^{14} samples from GL 99-4 were dated. In addition, to determine the effect of compaction on the lake bottom sediments, 10 samples from core GL 99-4 were analyzed for porosity and density. These 20 compaction samples were measured for volume, using a measuring tape (five cm long samples with a diameter of five cm, total core split in half), and weighed using an OHAUS 800 Series Triple Beam Balance scale. The samples were then dried over several days using a Corning PC100 hotplate stove on low heat,

until desiccated, then reweighed. The results of this process are discussed in Chapter Three.

Stratigraphy

Five additional cores from James and Granite lakes (JL 99-7, JL 01-2, JL 99-1, GL 99-4 and GL 98-3) were extruded by hand, measured for depth using a measuring tape, and the stratigraphy recorded (Tables 2.8, 2.9, 2.10, 2.13 & 2.14). Pelecypods, gastropods and charophytes were recovered from cores JL 99-1, JL 01-2 and GL 98-3, and their stratigraphic positions recorded in Figure 2.7.

Palynology

To define the Holocene forest and plant associations from the retreat of the Laurentide Ice Sheet to the present, thirty-one sediment sub-samples were selected for palynological analysis (Fig. 2.7). Twenty samples from core JL 99-1, and 11 samples from core GL 99-4 were sieved using a 230-mesh Tyler (63 μm) screen in order to remove coarse material. The remaining finer sediment was then weighed and processed by Dr. Arun Kumar (Carleton University), who chemically macerated the sediment and prepared slides for palynological analysis using the methods of de Vernal et al. (1999). These slides were quantitatively analyzed for pollen using a Leitz Wetzlar Stereo biological research microscope, and the information recorded in tables in Chapter Five.

Chemistry

Twelve sediment-water interface pore-water samples, and nine piezometer pore-water samples were analyzed for twenty-five metals by Seprotech Laboratories of Ottawa, Canada, using Inductively Coupled Plasma Atomic Emission Spectroscopy (ICP-AES), except that arsenic and lead were analyzed using Graphite Furnace Atomic Absorption (GFAAS). Twelve pore-water samples from James Lake were analyzed by Areco Canada Inc. of Ottawa, Canada, and one pore-water sample from Granite Lake was analyzed by Caduceon Environmental Laboratories of Ottawa, Canada, using the method outlined above for cations and Ion Chromatography for anions.

Micropaleontology

Two-hundred and thirty-five sediment samples were cut from five of the above cores at regular intervals, and at horizons of interest (Fig. 2.7). These samples, approximately 20 cc in volume, were stored in 100 cc specimen jars and spiked with 70% isopropyl alcohol to prevent bacterial decomposition. Sixty-one sediment samples from JL 99-1, 45 sediment samples from JL 99-7, 51 sediment samples from JL 01-2, 24 sediment samples from GL 98-3, 54 sediment samples from GL 99-4 and 76 sediment-water interface sediment samples were prepared for micropaleontological analysis of arcellaceans by sieving using a 35-mesh Tyler (500 μm) screen to retain coarse organic material and a 325-mesh Tyler (44 μm) screen to retain finer material. The coarse organic material, such as seeds, charophytes, aphids, gastropods and pelecypods were removed, and placed into 16 dram vials for analysis and identification. One cc of the finer material was then subdivided into aliquots for quantitative analysis using a wet

splitter (Scott and Hermelin, 1993). The 1866 wet aliquots were then analyzed for arcellaceans and charophytes using an Olympus SZH10 Zoom Stereo Research microscope, and the data recorded in tables in Chapter Five. Scanning electron micrographs of arcellaceans were obtained using a JEOL 6400 Scanning Electron Microscope at the Carleton University Research Facility for Electron Microscopy (CURFEM). These digital images were then compiled into plates using Adobe® Photoshop 6.0. Digital images of larger specimens were obtained using a Nikon Coolpix 995 camera with a resolution of 3.34 megapixels and compiled into plates using Adobe® Photoshop 6.0, and recorded in Chapters Three and Five.

REFERENCES

- Deevey, E.S.J., 1964, Sampling Lake Sediments by Use of the Livingstone Sampler, *in* Kummel, B., and Raup, D., eds., Handbook of Paleontological Techniques: San Francisco and London, W. H. Freeman and Company, 852 p.
- de Vernal, A., Henry, M., and Bilodeau, G., 1999, Techniques de préparation et d'analyse en micropaléontologie: Les Cahiers du GEOTOP, Université du Québec à Montréal, v. 3.
- Kumar, A., 1999, Micropaleontological Applications in Environmental Studies: Arcellaceans as Proxies of Chemical Pollution in Lakes, and Foraminifera as Proxies for Holocene Paleoseismic and Paleoclimatic Record in Oceans [Ph.D. thesis]: Ottawa, Ontario, Carleton University 239 p.

- Mason, G., 1998, A study of the effects of past mining activities on James Lake sediment chemistry [B.Sc. Honours thesis]: Ottawa, Carleton University 28p.
- Patterson, R.T., and Kumar, A., 2000a, Assessment of Arcellacean (Thecamoebian) Assemblages, Species, and Strains as Contaminant Indicators in James Lake, Northeastern Ontario, Canada: *Journal of Foraminiferal Research*, v. 30, p. 310 - 320.
- , 2000b, Use of Arcellacea (Thecamoebians) to Gauge Levels of Contamination and Remediation in Industrially Polluted Lakes, *in* Martin, R.E., ed., *Environmental Micropaleontology, Volume 15: Topics in Geobiology*: New York, Kluwer Academic/Plenum Publishers, p. 257 - 278.
- Scott, D.B., and Hermelin, J.O.R., 1993, A device for precision splitting of micropaleontological samples in liquid suspension: *Journal of Paleontology*, v. 67, p. 151 - 154.
- Wright, H.E., Livingstone, D.A., and Cushing, E.J., 1964, Coring Devices for Lake Sediments, *in* Kummel, B., and Raup, D., eds., *Handbook of Paleontological Techniques*: San Francisco and London, W. H. Freeman and Company, 852 p.

Table 2.1 – Prefixes used in maps and text for sampling of different materials

Sampling Prefixes	
<i>Prefix</i>	<i>Sample Type</i>
JL/GL	James/Granite Lake core site
JL/GLB	James/Granite Lake Box core
JLP	James Lake Piezometer
JL/GLW	James/Granite Lake Water sample
JL/GLpH	James/Granite Lake pH & Temperature measurement
JL/GL/NPMTPr	James/Granite Lake/Northland Pyrite Mine Temperature Profile
JLM	James Lake Marsh core site

Table 2.2 - Piston core collected by the students of the Environmental Field Camp during late August 1995 in the pool adjacent to the Northland Pyrite Mine Co. Site on the southwest shore of James Lake at position indicated in Fig. 2.1.

JL 95-5	<i>Compaction</i>	<i>Depth (cm)</i>	<i>Sediment</i>	<i>Color</i>	<i>Munsell Code</i>
<i>H₂O</i>		~100	→ S/W interface		
<i>1</i>		0 - 15	Fe Silt	moderate reddish brown	10 R 4/6
<i>2</i>		15 - 16	Stoney-Sandy silt	dark yellowish brown	10 YR 4/2
<i>3</i>		16 - 17	Gyttja	olive black	5 Y 2/1

Table 2.3 - Push core collected by Dr. Michel and Greg Mason through the ice in south west James Lake during the winter of 1997 at position indicated in Fig. 2.1.

JL 97-1	<i>Compaction</i>	<i>Depth [ice] (cm)</i>	<i>Sediment</i>	<i>Color</i>	<i>Munsell Code</i>
<i>H₂O</i>		60 [55]	→ S/W interface		
<i>1</i>	87.39%	0 - 20	Fe Silt	moderate reddish brown	10 R 4/6
<i>2</i>		20 - 48	Gyttja	olive black	5 Y 2/1
<i>3</i>		48 - 80	Gyttja	light brown	5 YR 5/6
<i>4</i>		80 - 96	Gyttja	dark yellowish brown	10 YR 4/2
<i>5</i>		96 - 103	Fe Gyttja	brownish black	5 YR 2/1
<i>6</i>		103 - 104	Sandy-silt	olive gray	5 Y 4/1

Table 2.4 - Push core collected by Dr. Michel and Greg Mason through the ice in south west James Lake during the winter of 1997 at position indicated in Fig. 2.1.

JL 97-2	<i>Compaction</i>	<i>Depth [ice] (cm)</i>	<i>Sediment</i>	<i>Color</i>	<i>Munsell Code</i>
<i>H₂O</i>		192 [60]			
<i>1</i>	30.32%	0 - 16	Gyttja	olive black	5 Y 2/1
<i>2</i>		16 - 29	Gyttja	olive black to dark yellowish brown	5 Y 2/1 to 10 YR 4/2
<i>3</i>		29 - 159	Gyttja	dark yellowish brown	10 YR 4/2

Table 2.5 - Push core collected by Dr. Michel and Greg Mason through the ice in south west James Lake during the winter of 1997 at position indicated in Fig. 2.1.

JL 97-3	Compaction	Depth [ice] (cm)	Sediment	Color	Munsell Code
<i>H₂O</i>		140 [70]	→ S/W interface		
<i>1</i>	40.80%	0 - 25	Gyttja	olive black	5 Y 2/1
<i>2</i>		25 - 66	Gyttja	moderate brown	5 YR 4/4
<i>3</i>		66 - 85	Gyttja	dark yellowish brown	10 YR 4/2
<i>4</i>		85 - 102	Silt (shell bits)	grayish brown	5 YR 3/2

Table 2.6 - Push core collected by Dr. Michel and Greg Mason through the ice in south west James Lake during the winter of 1997 at position indicated in Fig. 2.1.

JL 97-4	Compaction	Depth [ice] (cm)	Sediment	Color	Munsell Code
<i>H₂O</i>		155 [70]	→ S/W interface		
<i>1</i>	32.13%	0 - 48	Gyttja	olive black	5 Y 2/1
<i>2</i>		48 - 92	Gyttja	dark yellowish brown	10 YR 4/2
<i>3</i>		92 - 98	Silt	grayish brown	5 YR 3/2

Table 2.7 - Livingston Core taken from southeast James Lake during August 1998 at position indicated in Fig. 2.1.

JL 98-3	Compaction	Depth (cm)	Sediment	Color	Munsell Code
<i>H₂O</i>		150	→ S/W interface		
<i>1</i>	63.11%	0 - 25	Gyttja (watery)	dark yellowish brown	10 YR 4/2
<i>2</i>		25 - 71	Gyttja	dark yellowish brown	10 YR 4/2
<i>3</i>	77.19%	71 - 121	Gyttja	dark yellowish brown to moderate brown	10 YR 4/2 to 5 YR 4/2
<i>4</i>		121 - 159	Gyttja	moderate brown to dark yellowish brown to olive black	5 YR 4/2 to 10 YR 4/2 to 5 YR 2/1
<i>5</i>	79.68%	159 - 214	Gyttja	brownish gray	5 YR 4/1
<i>6</i>		214 - 234	Silty-clay	medium light gray	N 6
<i>7</i>		234 - 250	Fat Silty-clay	medium light gray	N 6
<i>8</i>	100%	250 - 268	Silty-clay	medium light gray	N 6

Table 2.8- Livingston Core taken from southwest James Lake during August 1999 at position indicated in Fig. 2.1.

JL 99-1	Compaction	Depth (cm)	Sediment	Color	Munsell Code
<i>H₂O</i>		100			
<i>1</i>		0 - 15	Fe Silt	moderate reddish brown	10 R 4/6
<i>2</i>		15 - 43	Fibrous Gytija	olive black	5 Y 2/1
<i>3</i>		43 - 117	Gytija	dusky yellow-brown to dark yellowish-brown	10 YR 2/2 to 10 YR 4/2
<i>4</i>		117 - 177	Gytija	dusky yellowish-brown	10 YR 2/2
<i>5</i>		177 - 216	Rhythmic Layered Gytija	1) blackish red 2) grayish brown 3) dusky yellow brown	1) 5 R 2/2 2) 5 YR 3/2 3) 10 YR 2/2
<i>6</i>		216 - 217	Peat?	dusky yellow-brown	10 YR 2/2
<i>7</i>		217 - 316	Rhythmic Layered Gytija	1) blackish red 2) grayish brown 3) dusky yellow brown	1) 5 R 2/2 2) 5 YR 3/2 3) 10 YR 2/2
<i>8</i>		316 - 363	Mottled Silty-clay	medium dark gray to dark greenish-gray	N 4 to 5 GY 4/1

Table 2.9 - Livingston Core taken from northern James Lake during August 1999 at position indicated in Fig. 2.1.

JL 99-7	Compaction	Depth (cm)	Sediment	Color	Munsell Code
<i>H₂O</i>		130			
<i>1</i>	87.57%	0 - 25	Gyttja	mixed black and dark yellowish-brown	5 YR 2/1 and 10 YR 4/2
<i>2</i>		3 - 25	Gyttja	dark yellowish-brown (0.5 cm organics)	10 YR 4/2
<i>3</i>		25 - 118	Watery Gyttja	dark yellowish-brown	10 YR 4/2
<i>4</i>		118 - 247	Rhythmic layered Gyttja	1) blackish red 2) grayish brown 3) dusky yellowish-brown	1) 5 R 2/2 2) 5 YR 3/2 3) 10 YR 2/2
<i>5</i>		247 - 247.5	Peat	dusky yellowish-brown	10 YR 2/2
<i>6</i>		247.5 - 249	Rhythmic layered Gyttja	1) blackish red 2) grayish brown 3) dusky yellowish-brown	1) 5 R 2/2 2) 5 YR 3/2 3) 10 YR 2/2
<i>7</i>		249 - 250.5	Peat	dusky yellowish-brown	10 YR 2/2
<i>8</i>		250.5 - 344	Rhythmic layered Gyttja	1) blackish red 2) grayish brown 3) dusky yellowish-brown	1) 5 R 2/2 2) 5 YR 3/2 3) 10 YR 2/2
<i>9</i>		344 - 346	Gyttja	olive black	5 Y 2/1
<i>10</i>		346 - 376	silty fine-sand	light olive gray	5 Y 6/1
<i>11</i>		376 - 385	Rhythmic layered silt and fine-sand	olive gray	5 Y 4/1
<i>12</i>		385 - 387	medium-grained sand	light olive gray	5 Y 6/1
<i>13</i>		387 - 407	Rhythmic layered silt and fine-sand	olive gray	5 Y 4/1
<i>14</i>		407 - 408	medium-grained sand	light olive gray	5 Y 6/1
<i>15</i>		408 - 433	Rhythmic layered silt and fine-sand	olive gray	5 Y 4/1
<i>16</i>		433 - 437	medium- coarse-grained sand (dewatering features)	light olive gray	5 Y 6/1
<i>17</i>		437 - 452	Rhythmic layered silt and fine-sand	olive gray	5 Y 4/1
<i>18</i>		452 - 456	medium-grained glaciofluvial sand	greenish gray	5 GY 6/1

Table 2.10 - Livingston Core taken from southern James Lake during August 2001 at position indicated in Fig. 2.1.

JL 01-2	Compaction	Depth (cm)	Sediment	Color	Munsell Code
<i>H₂O</i>		150			
1	95.19%	1 - 84	Gyttja	dusky brown to grayish brown	5 YR 2/2 to 5 YR 3/2
2		84 - 124	Gyttja	grayish brown	5 YR 3/2
3	99.03%	124 - 237	Rhythmic Layered Gyttja	1)(0.5 - 2.0 cm) dusky yellow brown 2)(0.5 - 1.5 cm) very dusky red	1) 10 YR 2/2 2) 10 R 2/2
4	101.96%	237 - 252	Peat (cattail rootlets)	dusky yellowish brown	10 YR 2/2
5		252 - 260	Rhythmic Layered Gyttja	1)(0.5 - 2.0 cm) dusky yellow brown 2)(0.5 - 1.5 cm) very dusky red	1) 10 YR 2/2 2) 10 R 2/2
6		260 - 276	Peat (cattail rootlets)	dusky yellowish brown	10 YR 2/2
7		276 - 323	Rhythmic Layered Gyttja	1)(0.5 - 2.0 cm) dusky yellow brown 2)(0.5 - 1.5 cm) very dusky red	1) 10 YR 2/2 2) 10 R 2/2
8	95.29%	323 - 349	Rhythmic Layered Gyttja	1) very dusky red 2)dark yellowish brown	1) 10 R 2/2 2) 10 YR 4/2
9		349 - 371	Silt	dark yellowish brown to medium gray	10 YR 4/2 to N 6
10		371 - 382	Silty-clay	gray	N 6
11	103.85%	382 - 396	Silt and Clay Varves	1) silt: (~0.5 cm) gray-blue	1) 5 PB 5/2 2) 5 G 6/1
12		396 - 409	Massive Clay	2) clay: (0.5 - 0.75 cm) greenish-gray	5 G 6/1

Table 2.11 - Livingston Core taken from southeast James Lake during August 2001 at position indicated in Fig. 2.1.

JL 01-8	Compaction	Depth (cm)	Sediment	Color	Munsell Code
<i>H₂O</i>		300			
1		0 - 45	Rhythmic layers of Silt and Gyttja	1) Silt: moderate red 2) Gyttja: olive black	1) 5 R 4/6 2) 5 Y 2/1
2		45 - 57	Gyttja	olive black	5 Y 2/1
3		57 - 98	Gyttja to fine Gyttja	olive black to moderate brown	5 Y 2/1 to 5 YR 4/4
4	101.90%	98 - 118	Gyttja	olive black	5 Y 2/1
5		118 - 128	Silt	moderate yellowish-brown	10 YR 5/4
6		128 - 130	Gyttja	olive black	5 Y 2/1
7	100.94%	130 - 388	Gyttja	dark yellowish brown	10 YR 4/2

Table 2.12 - Livingston Core taken from southwest Granite Lake during August 1999 at position indicated in Fig. 2.1.

GL 99-2	Compaction	Depth (cm)	Sediment	Color	Munsell Code
<i>H₂O</i>		500			
1		0 - 5	Sand (fine, coarsening with depth)	dark yellowish-brown (top 2 cm Fe stained)	10 YR 4/2 (Fe stain: 5 R 4/6)
2		5 - 10	medium-grain sand	dark yellowish-brown	10 YR 4/2
3		10 - 25	coarse-grain sand	dark yellowish-brown	10 YR 4/2
4		25 - 60	medium-grain sand	dark yellowish-brown	10 YR 4/2
all sand grains angular; qtz, feld and lithic frags. (Till)					

Table 2.13 - Livingston Core taken from southeast Granite Lake during August 1999 at position indicated in Fig. 2.1.

GL 98-3	Compaction	Depth (cm)	Sediment	Color	Munsell Code
<i>H₂O</i>		150			
1	90.22%	0 - 28	Gyttja	dusky yellow-brown	10 YR 4/2
2		28 - 37	Peat	olive gray	5 Y 3/2
3		37 - 68	Silty-clay	pale olive	10 Y 6/2
4		68 - 75	Fine sand (pelecypods, pine needles)	pale olive	10 Y 6/2
5		75 - 93	Silty-clay	light olive gray	5 Y 5/2
6		93 - 115	Clay	light olive gray	5 Y 5/2
7		115 - 152	Silty-clayey-sand	grayish olive	10 Y 4/2
8		152 - 159	Silty-clay	light olive gray	5 Y 5/2
9		159 - 238	Fat clay	grayish olive	10 Y 4/2
10		238 - 248		grayish-blue	5 PB 5/2

Table 2.14 - Livingston Core taken from northwest Granite Lake during August 1999 at position indicated in Fig. 2.1.

GL 99-4	Compaction	Depth (cm)	Sediment	Color	Munsell Code
<i>H₂O</i>		200			
<i>1</i>	101.08%	1 - 68	Gyttja (grass and worms)	dark yellowish-brown	10 YR 4/2
<i>2</i>		68 - 72	Gyttja	dark reddish-brown	10 R 3/4
<i>3</i>		72 - 76	Gyttja	dark yellowish-brown	10 YR 4/2
<i>4</i>		76 - 79	Gyttja	dark reddish-brown	10 R 3/4
<i>5</i>		79 - 81	Gyttja	dark yellowish-brown	10 YR 4/2
<i>6</i>		81 - 86	Gyttja	dark reddish-brown	10 R 3/4
<i>7</i>		86 - 94	Gyttja	dark yellowish-brown	10 YR 4/2
<i>8</i>	102.08%	94 - 123	Gyttja (grass)	dusky-blue	5 PB 3/2
<i>9</i>		123 - 189	Rhythmic layered Gyttja	1) dark reddish-brown 2) dusky-blue	1) 10 R 3/4 2) 5 PB 3/2
<i>10</i>		189 - 189.5	Peat and bark	dark yellowish-brown	10 YR 4/2
<i>11</i>	103.125%	189.5 - 224	Rhythmic layered Gyttja (4 - 5 cm layers)	1) dark reddish-brown 2) dusky-blue	1) 10 R 3/4 2) 5 PB 3/2
<i>12</i>		224 - 225	Peat (rootlets)	dark yellowish-brown	10 YR 4/2
<i>13</i>		225 - 285	Rhythmic layered Gyttja (4 - 5 cm layers)	1) dark reddish-brown 2) dusky-blue	1) 10 R 3/4 2) 5 PB 3/2
<i>14</i>		285 - 292	Firm Silt (gastropods)	light brown	5 YR 5/6
<i>15</i>		292 - 311	uneven Gyttja layers (gastropods and pelecypods)	1) pale yellowish-brown 2) dark yellowish-brown	1) 10 YR 6/2 2) 10 YR 4/2
<i>16</i>		311 - 313	Fine Gyttja	pale yellowish-brown	10 YR 6/2
<i>17</i>		313 - 353	Gyttja	dark yellowish-brown	10 YR 4/2
<i>18</i>		353 - 357	Gyttja	dark reddish-brown	10 R 3/4
<i>19</i>		357 - 388	Clay	light olive gray	5 Y 6/1
<i>20</i>		388 - 428	Rhythmic layered Varves (52 varves)	1) grayish-blue 2) greenish-gray	1) 5 PB 5/2 2) 5 GY 6/1
<i>21</i>		428 -	Sand	moderate brown	5 YR 3/4

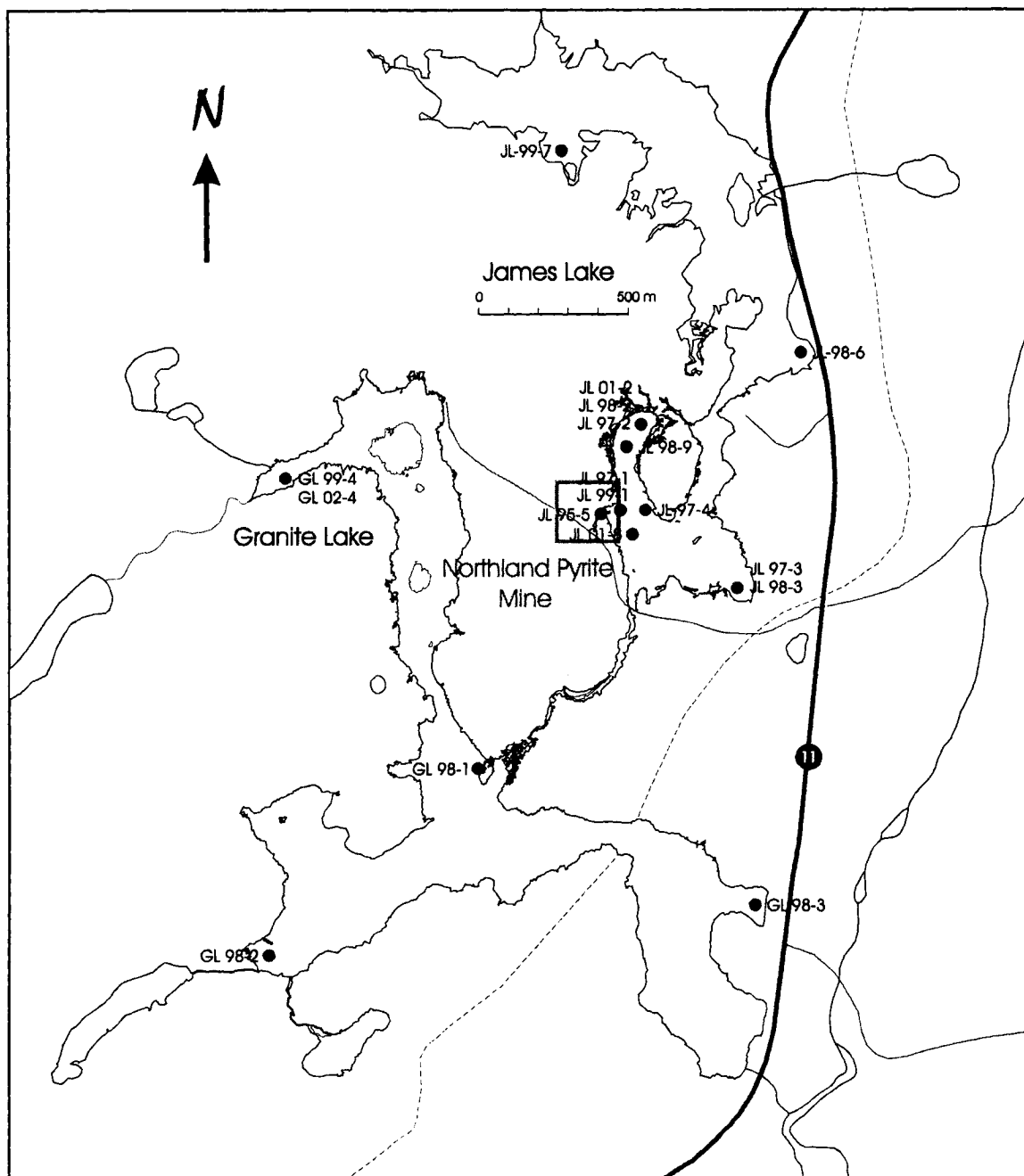


Figure 2.1 - Coring sites in James and Granite lakes from 1995 to 2002. The Northland Pyrite Mine site is outlined by a box on the southwestern shore of James Lake.



Figure 2.2 - Using the Livingstone Coring device from a raft in James Lake, adjacent to the waste rock pile left at the Northland Pyrite Mine site.

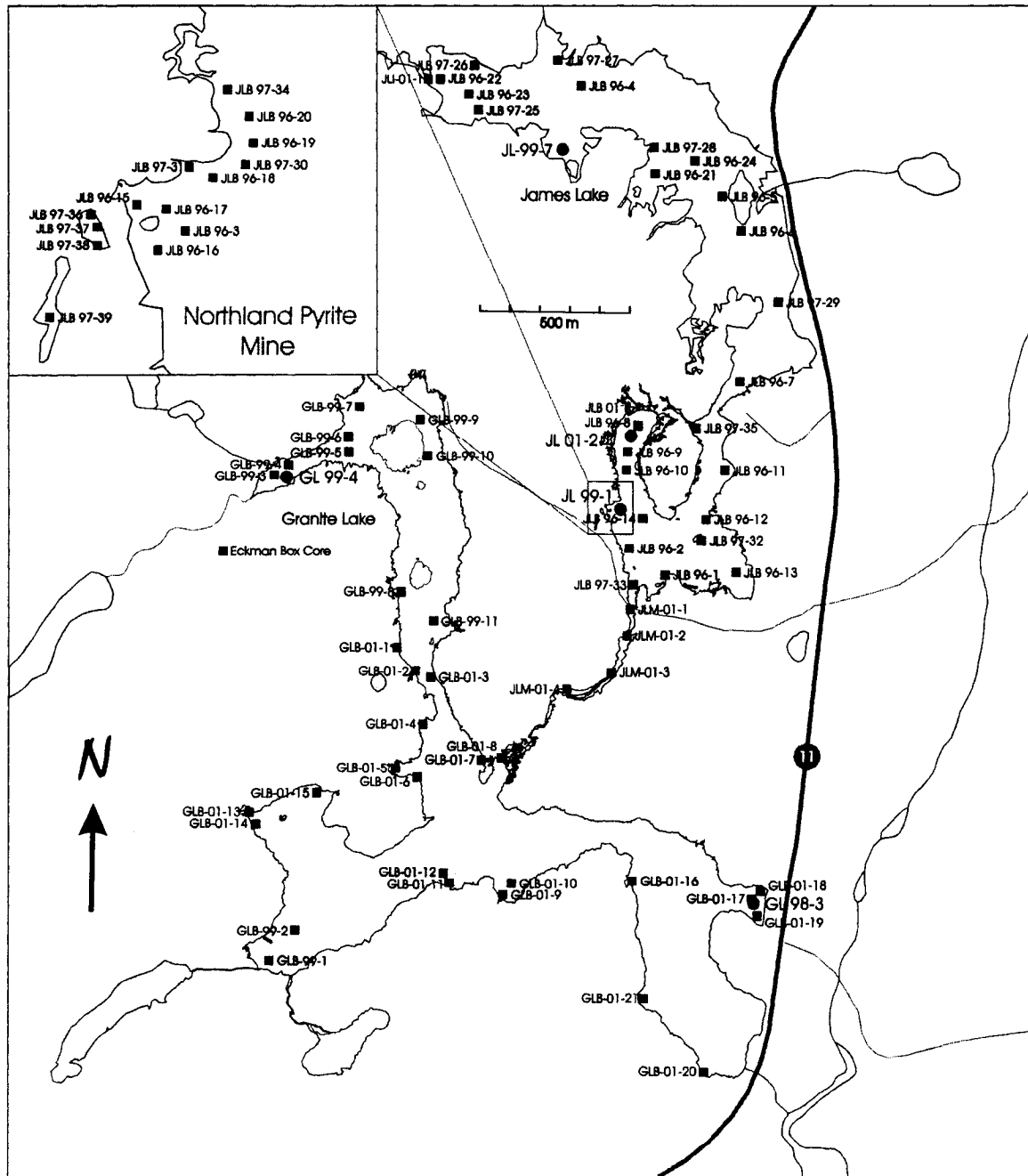


Figure 2.3 - Locations of sediment-water interface samples taken between 1996 and 2002 in the area of James and Granite lakes. The 35 samples from James Lake taken from 1996 to 1997 were previously reported (Kumar, 1999; Patterson and Kumar, 2000a, b). The inset locates samples collected near the waste rock pile in southwestern James Lake.

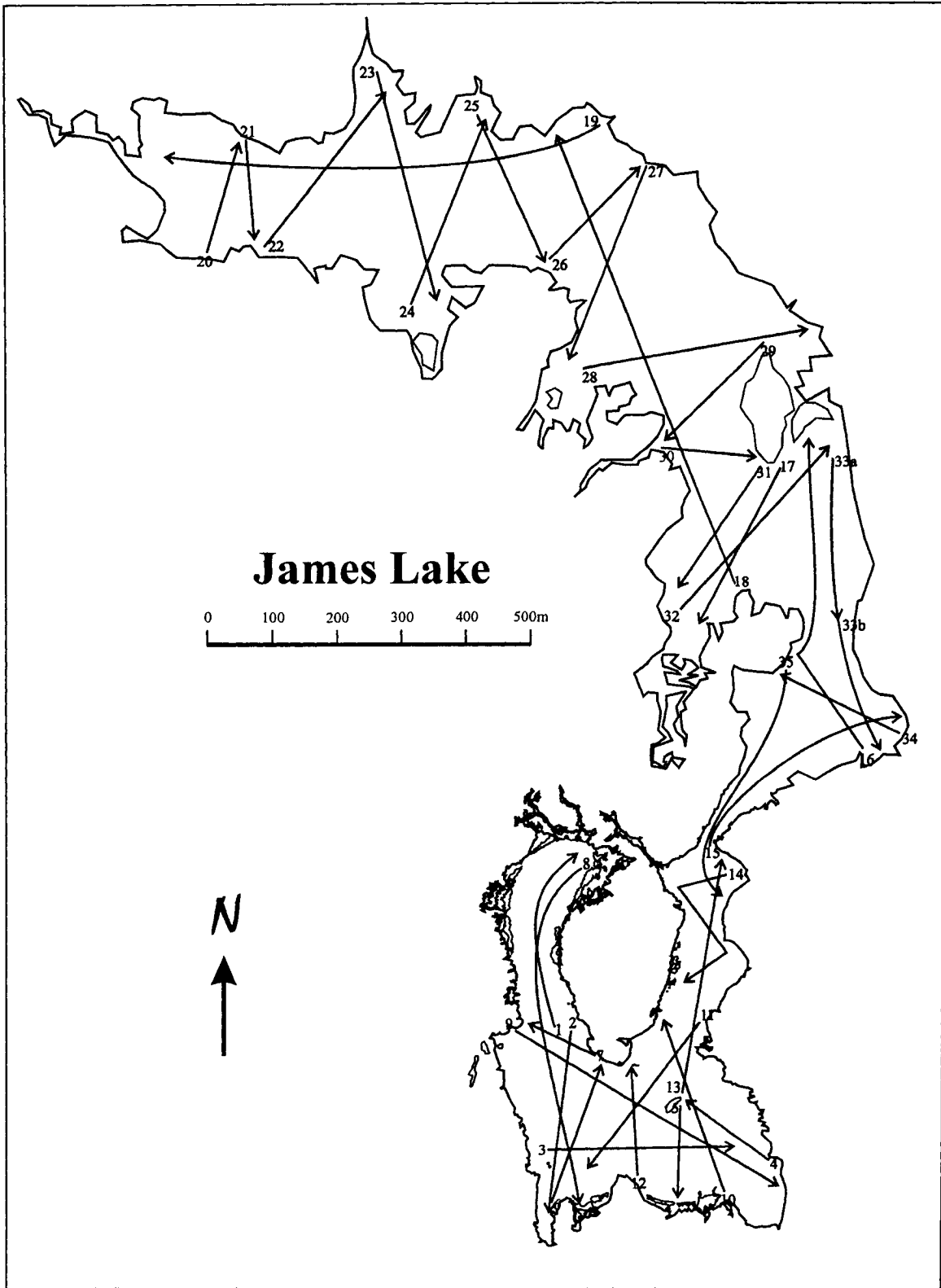


Figure 2.5 - August, 2001 sub-bottom profile runs for James Lake.

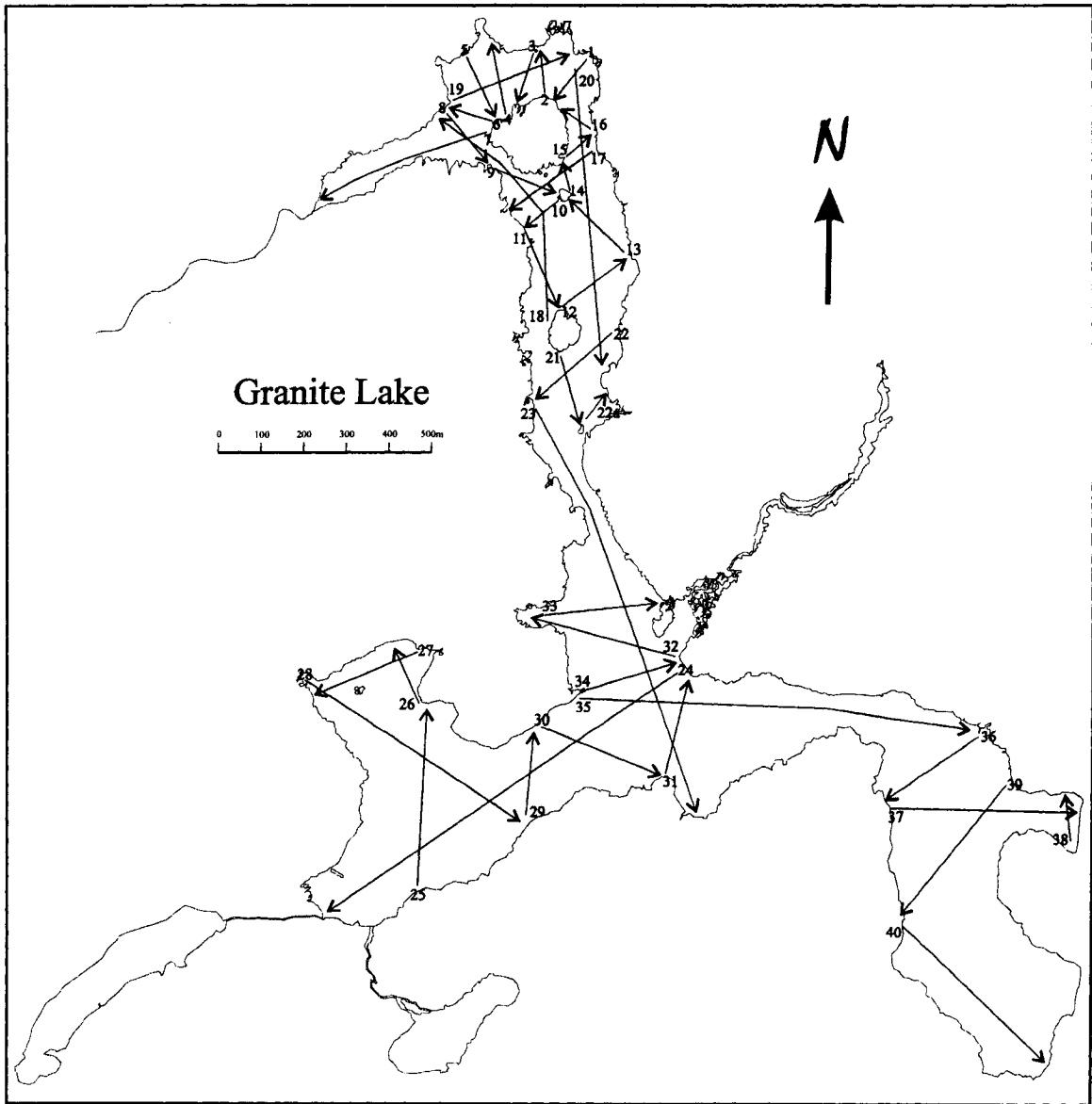


Figure 2.6 - August, 2002 sub-bottom profile runs for Granite Lake.

Figure 2.7 - Figures 2.7a - 2.7e are stratigraphic columns showing locations where cores were sub-sampled for arcellacean and pollen analysis, ^{14}C analysis, sediment compaction analysis, and positions where gastropods, pelecypods and charophytes were observed.

LEGEND

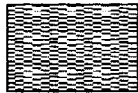
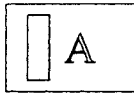
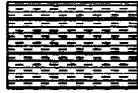

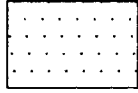
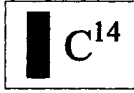



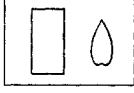
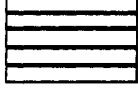

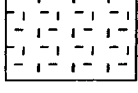
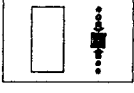
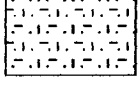
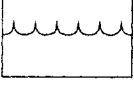
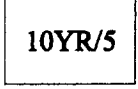
	Gyttja		Arcellacean Samples
	Layered Gyttja		Pollen Samples
	Silt		C^{14} Sample
	Sand		Gastropods
	Silt and Sand		Pelecypods
	Varves		Charophytes
	Clay		Compaction Sample
	Silt and Clay		Water Level
	Color/Code		

Figure 2.7a

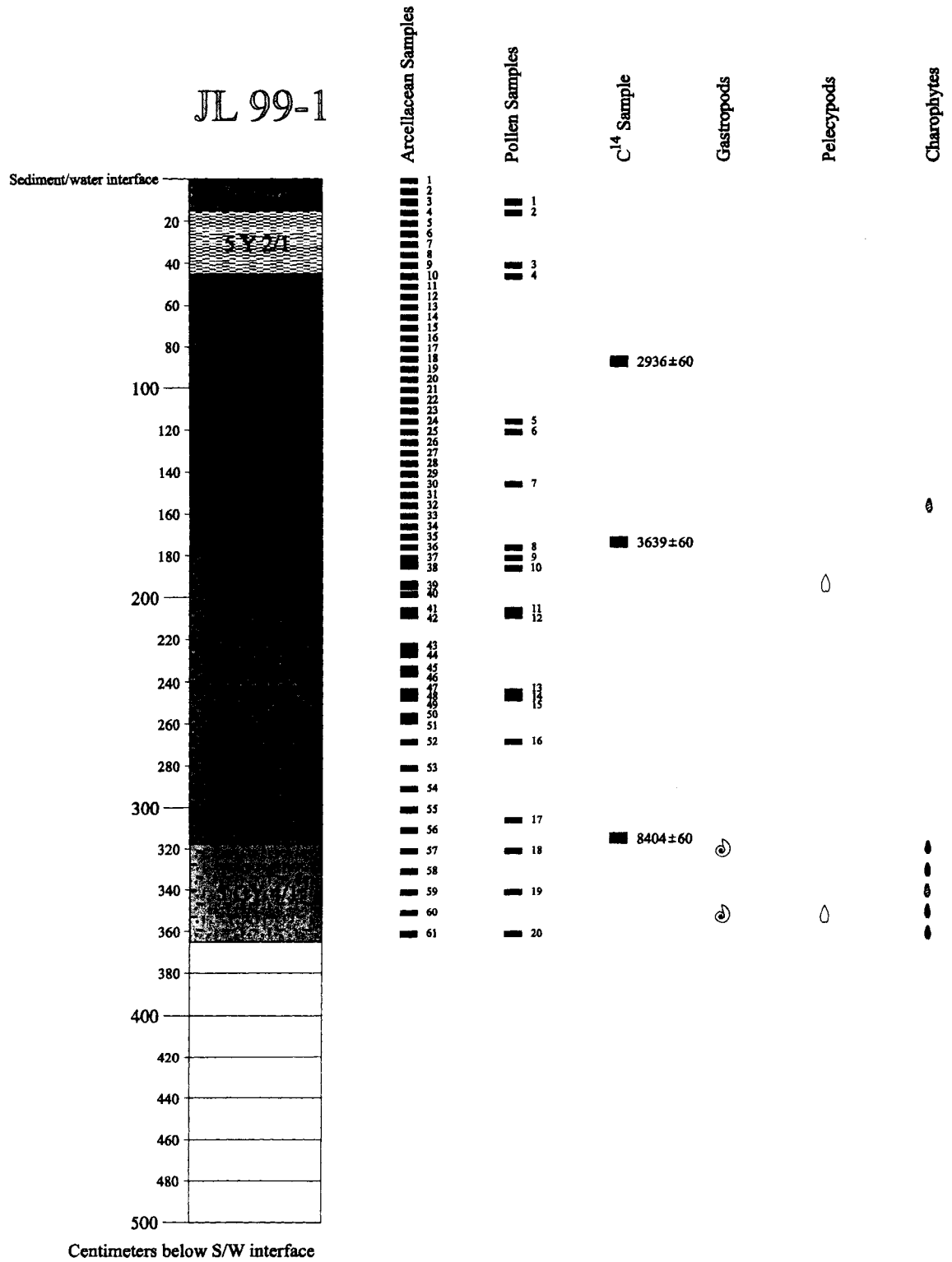


Figure 2.7b

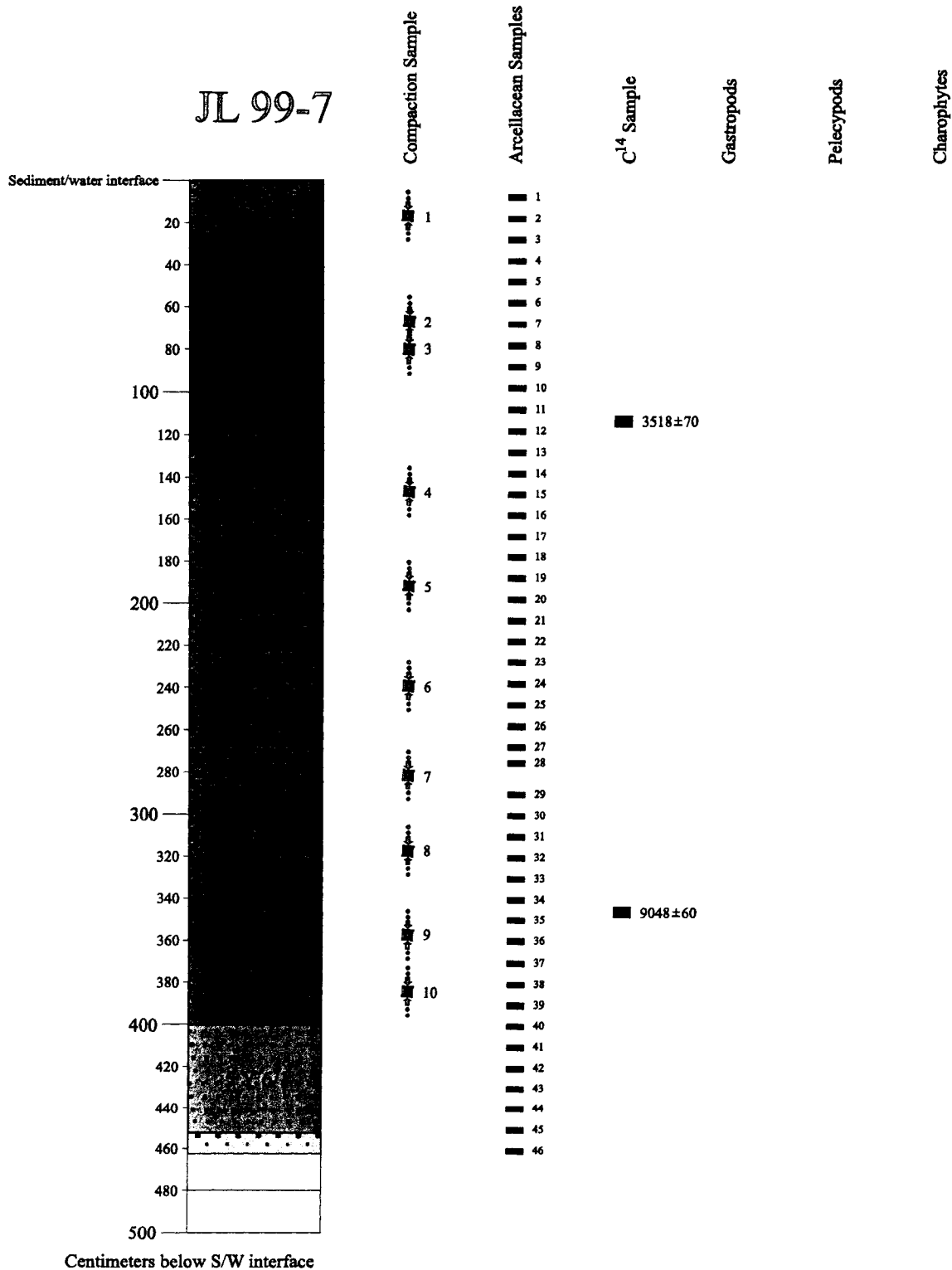


Figure 2.7c

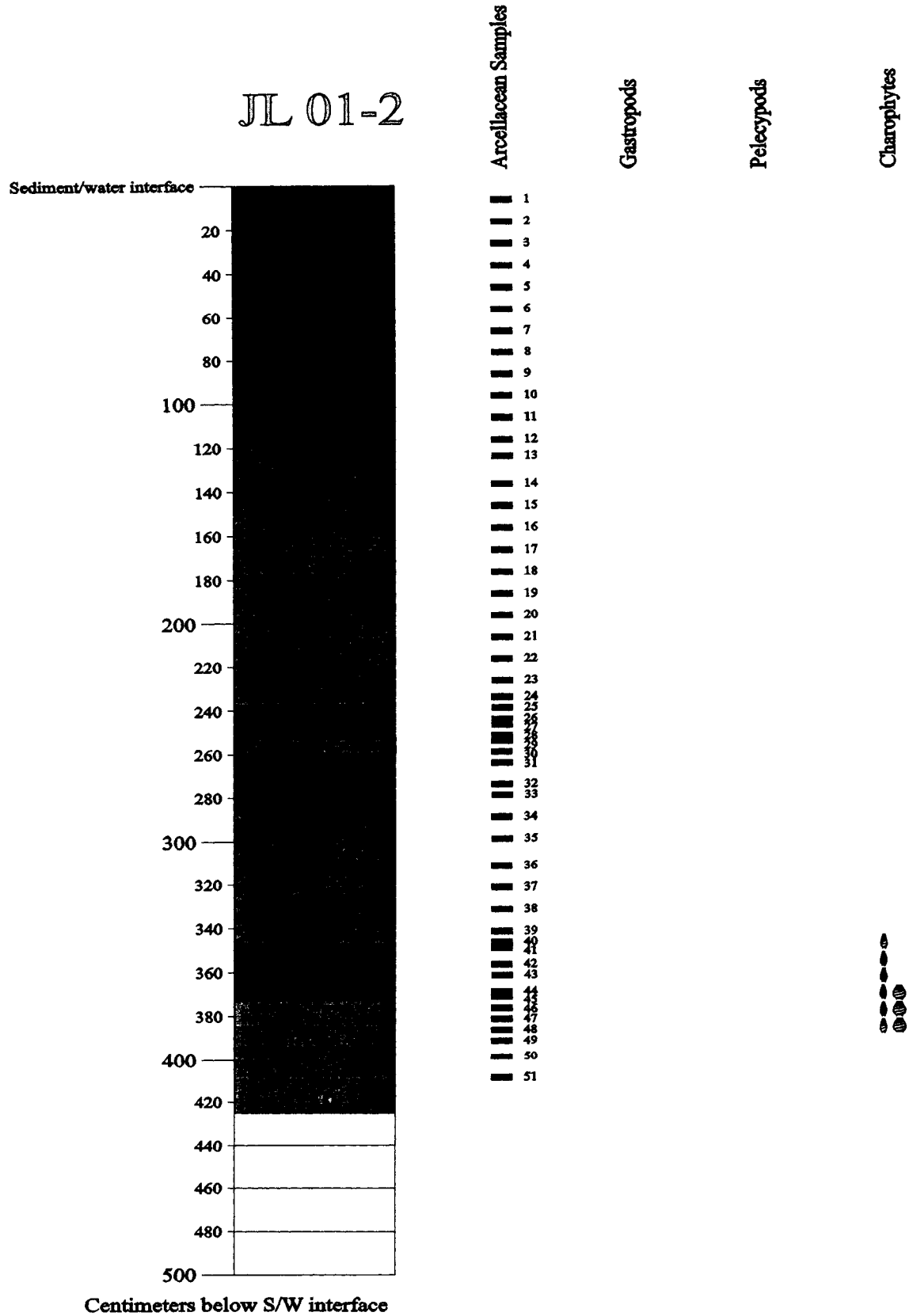


Figure 2.7d

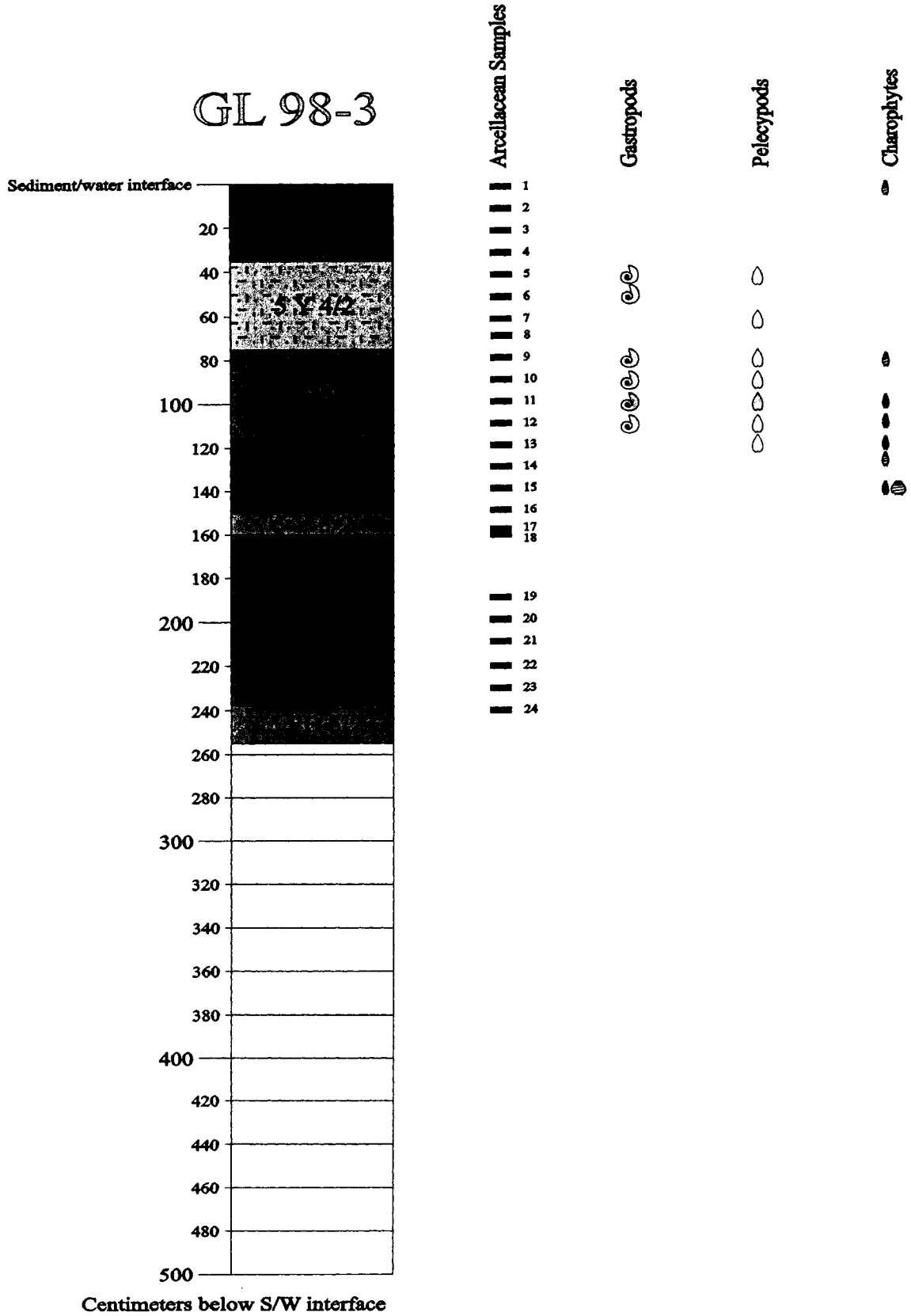
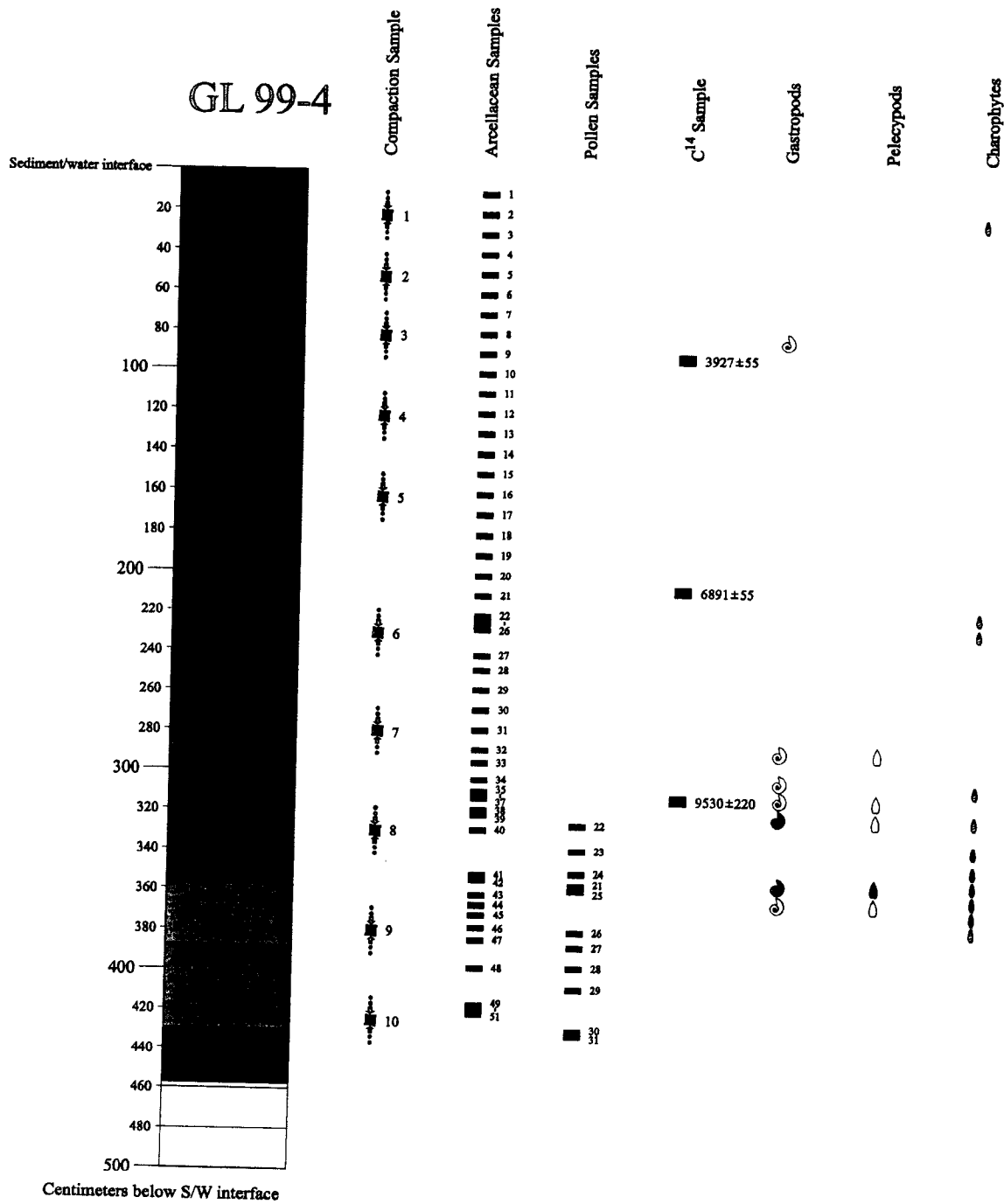


Figure 2.7e



CHAPTER THREE

PALEOSEDIMENTARY MODEL OF THE JAMES AND GRANITE LAKES SYSTEM, USING PALEOLIMNOLOGICAL PROCESSES AS QUATERNARY PALEOINDICATORS

Abstract

The Quaternary sedimentary record in the vicinity of James and Granite lakes ranges from deglaciation prior to $10,800 \pm 220$ yr. BP to the present. This record has been influenced by compaction, a process that results in dewatering, compression and ultimately consolidation of sediment. In order to determine the age and thickness of sedimentary units, the compaction rate and the effect of compression due to coring, were determined with calibrated ^{14}C dating techniques. For James Lake and Granite Lake, the mass accumulation rate was determined to be 0.024 ± 0.001 g/cm²/yr to 0.071 ± 0.003 g/cm²/yr (sedimentation rate: 0.039 ± 0.002 cm/yr) through 5603 ± 227 yrs. The mass compression rate for the system was determined to be 0.002 ± 0.001 g/cm²/yr at 300 cm depth to 0.189 ± 0.0 g/cm²/yr at the surface. This means that the gyttja within the lake system was compressed up to 44%, or a total of 277 cm, to its present thickness of 357 cm.

The results of this research identified seven paleolimnological phases that indicate climate states and relative water depths within the lake system. The glacial fluvial phase

occurred prior to $10,800 \pm 220$ yr. BP, preceding a 100 ± 17 yr. pelagic phase that occurred after 10,800 yr. BP indicating a relatively deep water ice-proximal glacial lake. The end of the Younger Dryas Cool Period occurred during the first of three littoral phases. Littoral phase 1 lasted about 1200 yrs., ending with the beginning of the first of two marsh phases at 9500 ± 220 yr. BP. The first marsh phase was prominent during the Post Younger Dryas warming period, giving way to the warm arid climate of the Holocene Hypsithermal from 7400 ± 77 to 3900 ± 55 yr. BP. At the end of the Holocene Hypsithermal, the first marsh phase gave way to the cool wet climate of the second littoral phase, lasting 1000 yr., until the beginning of the second marsh phase at 2900 ± 86 yr. BP. The second marsh phase would have corresponded to the Medieval Warm Period which ended when the Little Ice Age began at the start of the third littoral phase.

Keywords: compaction, compression, sedimentation rates, radiocarbon dates, paleolimnological phases

Introduction

This chapter investigates sedimentary processes in the James and Granite lakes system (JGLS) in order to develop a model to represent the paleolimnological evolution of the JGLS from the retreat of the Laurentide Ice Sheet to the present.

The continued accumulation of sediment, especially organic-rich lake sediment, led to compaction over time. The volume decrease in unlithified sediment, due to the pressure caused by an overlying column of sediment, is an early stage of diagenesis that

has been extensively investigated by various geologists and engineers during studies of stress-strain relationships, and compression of soils (e.g., Das, 1977; Goldhammer, 1997; Perrier and Quiblier, 1974; Terzaghi, 1943; Whitlow, 1990). Compression in fine-grained organic sediments results in the expulsion of water, and the volume change that results from the readjustment of the wet sediments is called compaction (Al-Shamrani, 1998). When investigating diagenesis with respect to the compaction and decompaction of carbonate sediments, as are found in the Pleistocene clays and varves of the JGLS, Goldhammer (1997) noticed that when the original sediment porosities were in the 70 to 80% range, there was a 50% reduction in thickness, and a 42% reduction in porosity within the first 150 to 200 cm of sediment.

Coring techniques can result in unintentional sediment compression due to uneven sediment capture and extrusion (Livingstone and Imboden, 1996), and the use of methods such as gravity generally fail to capture the top 5 – 15 cm of sediment record at the sediment-water interface (Crusius and Anderson, 1991). Lotter et al. (1997) compared Livingstone coring methods to Kullenberg coring techniques, and investigations with thin section and x-ray revealed no difference in compression of the sediment at the sediment-water interface. Crusius and Anderson (1991) found that compression of cores by up to a factor of three occurred in upper porous sediments, but in deeper less porous sediment, core compression was not noticeable.

To determine the paleolimnological history of the area in the vicinity of JGLS, in the Temagami region of northeastern Ontario (Chapter One), the sediment profiles within the lakes had to be determined. To this end, the porosity of the wet sediment was measured so that the amount of compaction could be assessed (Das, 1977; Freeze and

Cherry, 1979; Terzaghi, 1943; Walton, 1970). In order to measure compaction, one core in Granite Lake (GL 99-4) was sub-sampled and analyzed for porosity (Chapter Two).

Sedimentation rates of lake systems, computed using a linear rate, tend to be 0.01 to 0.1 cm/yr (Scholz, 2001), but in order to account for the density of sediment being deposited into the lake system, mass accumulation rate (MAR) is used to represent sediment accumulation (Boyle, 2001; Meyers and Lallier-Verges, 1999). This chapter investigates these limnological techniques to determine the paleoenvironment recorded in the lake bottom sediments, and to determine whether the difference in rate accumulation outlined by MAR, and the mass compression rate (MCR) is significant.

To understand the significance of the paleosedimentary model on the JGLS, molluscs, crustaceans and charophytes were used as proxies to indicate paleolimnological parameters. Ostracods, small bivalved crustaceans with calcitic shells, have been used to indicate environmental factors in shallow freshwater lakes (Holmes, 2001); and, pelecypods and gastropods reflect non-acidic environments with a wider range of limnological conditions (Clarke, 1981; Miller and Tevesz, 2001). Charophytes or stoneworts are threadlike branching algae that superficially resemble horsetail. They may be found in water depths up to 20 m, but prefer alkaline to weakly acidic waters. In these waters, the oogonium (female reproductive organs) become encrusted in lime and are preserved within the fossil record (Prescott, 1970; Wood and Imahori, 1965).

Analysis and Results

Sedimentary profiles

The stratigraphy, interpreted from core analysis of the JGLS (Chapter Two), and the relationship of the sediment-water interface (SWI) with the lake level of the JGLS system, indicated in meters above sea-level (masl), are displayed in Figure 3.1 (Zone Key is Table 3.1). The lake level in James Lake is currently 312 masl, with the water level dropping to 308 masl in Granite Lake (GL 98-3).

Visual analysis of cores JL 99-1, JL 99-7 and JL 01-2 from James Lake, and cores GL 98-3 and GL 99-4 from Granite Lake indicate that the lake bottom sediment consists of dark brown gyttja to a depth of up to 3.5 m, overlying up to 0.5 m of blue-gray silt and clay. These sediments, in turn, overlie varying thicknesses of gray to dark gray, silt and clay varves, and fat clay (stiff, plastic, blue-gray clay). These sediments are underlain by brown, medium-grained glaciofluvial sands and gravel.

Sheltered areas of the lakes contain 0.25 to 1.0 m of fibrous gyttja (Zone B_{Fi}) at the sediment-water interface, with a water depth of 1.0 to 2.0 m, as found at the sites of cores JL 99-7 and JL 01-2. Zone B_{Fi} is overlain in some locations (cores JL 99-1 and GL 99-4) by 30 - 65 cm of fibrous and rhythmic layered gyttja (Zone B_{Fi-RL}). In southwestern James Lake (JL 99-1), Zone B_{Fi-RL} is overlain by 15 – 20 cm of iron stained silt (Zone A_{Fe}), due to proximity to the mine site. Below the B_{Fi} zone, in all cores except core GL 98-3, is the upper gyttja zone (Zone B-2) which varies between 25 and 100 cm in thickness.

Except for core GL 98-3, the cores from James and Granite lakes contained a series of highly organic rhythmic layered zones (Zones B_{RL-3}, B_{RL-2} & B_{RL-1}), varying from 120 to 230 cm thick, and enclosing either one or two thin peat layers (Zone C). Within the Granite Lake cores, a 35 to 40 cm thick lower gyttja layer (Zone B-1) occurs below Zone B_{RL-1} in core GL 99-4, and at the surface in core GL 98-3. In southeastern Granite Lake (GL 98-3), an erosional or non-depositional surface was noted at the SWI. All Zones above B-1 are absent in core GL 98-3.

Zone B-1 in core GL 99-4 and core GL 98-3, and Zone B_{RL-1} in the James Lake cores unconformably overlie post-glacial lake silts, clays and sands. Below this unconformity, in the James Lake cores, lies 40 to 50 cm of silt to fine sand (Zones E_{f-Si} & E_f), which overlie 20 to 50 cm of silt and clay varves (Zone F_{Si-Cl}). In GL 99-4, 25 cm of fat clay (Zone D_{fat}) and 35 cm of varves (Zone F_{Si-Cl}) overlie at least 30 cm of medium-grained glaciofluvial sand (Zone E_m). In GL 98-3, varying thicknesses of clayey-silt (Zone A_{Cl}; 30 -40 cm) are interbedded with varying thicknesses of fat clay (Zone D_{fat}; 40 – 80 cm), all of which overlies a fine-grained sand (Zone E_f).

Core compaction and compression

Moisture content results from Granite Lake core GL 99-4 indicate that the top 300 to 350 cm of gyttja in the JGLS have bulk densities of 0.2 to 0.3 g/cc, with porosities of 72 to 85%, and dry densities of 0.6 to 1.7 g/cc, as indicated in Table 3.2. Bulk density (ρ) was determined by

$$\rho = \frac{W_s}{V_T} \quad (3-1)$$

where W_s is the weight of the dry sediment, and V_T is the total volume of the sediment sample (App. A to Ch. 3). Dry density (ρ_s) was calculated using the method outlined in Freeze and Cherry (1979)

$$\rho_s = \frac{W_s}{V_s} \quad (3-2)$$

where V_s is the volume of the dry sediment. Porosity (ϕ) was determined by

$$\phi = \frac{V_w}{V_T} \quad (3-3)$$

where V_w is the volume of the water, and V_T is the volume of the wet sediment.

Sediment compression of up to 77%, occurring in the gyttja of the JGLS, was determined using the method outlined in Walton (1970)

$$\Delta h_L = \frac{e_i - e_f}{1 + e_i} b_i \quad (3-4)$$

where Δh_L is the layer subsidence or inelastic compaction, e_i is the initial void ratio, e_f is the void ratio after loading and b_i is the initial thickness of the layer investigated. The void ratio was determined using

$$e = \frac{V_w}{V_s} \quad (3-5)$$

and e_i was taken to indicate the void ratio of the sample at the top of the sediment layer under investigation, while e_f was taken to indicate the void ratio of the sample at the bottom of the layer. The system was divided into five layers based on decreasing void ratio and sediment type as indicated in Figure 3.2, and Table 3.3. The initial and final void ratios were calculated using the rate of change in void ratio between samples as outlined in Appendix A to this chapter. The initial thickness of the layers was determined using

$$b_i = b_f + \Delta h_L \quad (3-6)$$

which when solved with equation (3-4) gives Δh_L in terms of b_f , e_i and e_f ;

$$\Delta h_L = b_i - b_f = b_f \left(\frac{e_i - e_f}{1 + e_f} \right) \quad (3-7)$$

as indicated in Appendix A.

The weight of the water in the samples was determined by subtracting the weight of the dry sediment from the weight of the wet sediment. The volume of the water, V_w was determined by subtracting the volume of the dry sediment from the total volume of the sample, which in turn was verified using the method outlined in Appendix A.

Figure 3.3 displays density, porosity and compaction for the JGLS system.

The propagation of error for the results were added or subtracted in quadrature using the following formula:

$$z = (ax \pm \sigma_x) + (by \pm \sigma_y) - (cu \pm \sigma_u) + \dots \quad (3-8)$$

where σ is the error, and the resulting error for z is

$$\sigma_z = z \sqrt{(a\sigma_x)^2 + (b\sigma_y)^2 + (c\sigma_u)^2 + \dots} \quad (3-9)$$

When multiplication or division was performed, the percentage errors were added in quadrature using the following formula:

$$z = a(x \pm \sigma_x)^n \cdot b(y \pm \sigma_y)^m \cdot c(u \pm \sigma_u)^{-p} \dots \quad (3-10)$$

where the resulting fractional error for z is

$$\sigma_z = z \sqrt{\left(\frac{n\sigma_x}{x}\right)^2 + \left(\frac{m\sigma_y}{y}\right)^2 + \left(\frac{p\sigma_u}{u}\right)^2 + \dots} \quad (3-11)$$

(after Wadden, 1992).

The bulk density of the gyttja is < 1 g/cc, while that of water is equal to 1 g/cc. Therefore, as the porosity increases or decreases, the density also increases or decreases. Figure 3.3 displays density, porosity and compaction for the JGLS system, using data from Granite Lake core GL 99-4. Layer 5, which consists of a 68 cm thick fibrous to rhythmic layered zone (Zone B_{Fi-RL}), indicates a decrease in dry density from 1.7 to 0.8 g/cc and a decrease in porosity from 85 to 75% of the bulk sediment. Calculations indicate that this layer has been compressed 74%, a change in thickness of 195 cm, from 263 cm of deposited sediment to the present 68 cm of gyttja. Below this zone, Layer 4, consists of a fibrous gyttja zone (Zone B_{Fi}) 68 to 95 cm below the SWI (bswi) and an upper gyttja zone (Zone B-2) 95 to 120 cm (bswi). This layer indicates a decrease in dry density from 1.5 to 1.0 g/cc and a decrease in porosity from 80 to 78% of the bulk sediment. Calculations indicate that this layer has been compressed 18%, a change in thickness of 12 cm, from 67 cm of deposited sediment to the present 52 cm of gyttja. Below Zone B-2, Layer 3 consists of a rhythmic layered gyttja (Zone B_{RL-3}), a minor peat zone (Zone C-2) and part of a middle rhythmic layered gyttja zone (Zone B_{RL-2}), from 120 to 224 cm (bswi). This layer indicates a decrease in dry density from 1.1 to 0.6 g/cc and a decrease in porosity from 80 to 73% of the bulk sediment. Calculations indicate that this layer has been compressed 35%, a change in thickness of 52 cm, from 156 cm of deposited sediment to the present 104 cm of gyttja. Layer 2 begins at the bottom of Zone

B_{RL-2}, and consists of the remaining gyttja zones (Zones B_{RL-1}, B_{RL (Si-Gy)} and B-1) at 224 to 360 cm (bswi). This layer indicates an increase in dry density to 1.2 g/cc, and an increase in porosity to 78% of bulk sediment. Calculations indicate that this layer has been compressed 10%, a change in thickness of 12 cm, from 148 cm of deposited sediment to the present 136 cm of gyttja. Overall, the 357 cm thick gyttja layer indicates 44% compression, a change in thickness of 277 cm from 634 cm. Generally, with depth the total amount of compression increases; i.e. the total amount of compression is much less in Layer 5 than it is in Layer 4, and this trend continues through to the bottom of the gyttja.

Layer 1 represents Pleistocene clays and varves underlying the gyttja Zone B-1, from 360 to 430 cm (bswi). The fat clay zone (stiff blue-gray calcitic clay: Zone D_{fat}) from 360 to 386 cm (bswi) shows a porosity of 72%, which drops to 7% by 400 cm (bswi) within the silt and clay varves. This corresponds to an increase in bulk density of 0.3 to 1.7 g/cc within Layer 1.

Compression/decompression also occurs from transportation, storage or core extrusion, and these results are included in Tables 2.2 to 2.14. Compression tended to occur in the upper parts of the cores, decreasing in magnitude with depth. The amount of compression or decompression was derived using the exact core measurements that were marked on the barrels, as they were recovered from the lake bottoms, compared to measurements of core immediately after extrusion. Measurements indicated that overall compressions of 9.47% in core JL 99-7, 1.14% in core GL 99-3 and 1.36% in core JL 01-2 occurred, while decompression of 1.59% occurred in core GL 99-3.

Sub-bottom profiles

To more accurately match core with the sedimentary profile in James and Granite lakes, seventy-five sub-bottom echograms were obtained using sonar equipment (Chapter Two), analyzed using Knudsen Engineering Ltd. proprietary software, "Post Survey", on an IBM laptop computer in order to help construct the stratigraphy of the JGLS.

Profiles that crossed the locations of the three James Lake cores are illustrated in Figures 3.4 to 3.6. Within Basin "A" (Fig. 3.4), a transgressive-regressive zone existed (Zone E_f) when fine-grained sand was deposited, as indicated at level 1 in Figure 3.4A. Water-level regression, leading to a lowstand, would have occurred between (1) and (2), forming Zones B_{RL-1}, C and B_{RL-3} (layer (2)), which are high in organic content. Since sonar will not penetrate a void space, darkened areas are returned on the sonargrams when the echo encounters void spaces, such as, gas filled voids that occur when organics decay. Within the basin, in and above level 4 are dark zones on the echogram indicating outgassing (M), caused by decomposing organics within the sediment. This occurs in and above the gyttja layer (Zone B-2), where an increase in bulk and dry density is indicated in Figure 3.3. Between Zone B-2 and Zone B_{Fi} is an unconformity below the transgression indicated by layer (3). Above layer (3), Zones B_{Fi}, B_{Fi-RL} and A_{Fe} are indistinct on the echogram due to outgassing.

The sediment-water interface in Basin "B" (Fig. 3.4B) is indicated by a dense band on the sonargram which upon visual inspection of a test core (JL 01-8) showed redox couplets up to 0.5 cm thick extending to 30 cm in depth (bswi). Outgassing masks most of the area of core JL 99-7 (Fig. 3.5), but an erosional truncation is evident on both sides of the basin, indicating low water levels that correspond to the peat zone (Zone C).

Immediately north of the Northland Pyrite Mine waste rock pile, at the location of core JL 01-2 (Fig. 3.6), outgassing seems to be concentrated within three zones: near the top of Zone B_{RL-3} and pervasive throughout Zone B_{Fi} near the sediment-water interface.

The sonar profiles for Granite Lake cores GL 98-3 and GL 99-4 are not shown because a malfunctioning low frequency sonar transducer caused indistinct echograms below the sediment-water interface.

Radiocarbon dating

Radiocarbon dates, determined from plant fibers and wood fragments in sediment cored from James (JL 99-1 & JL 99-7) and Granite (GL 99-4) lakes, were used to determine sedimentation rates (Fig. 2.1, 2.7a, b, e). The ¹⁴C dates are reported as years before present (BP), and are calculated on the assumption that atmospheric ¹⁴C concentrations from the past are the same as concentrations measured in 1950. This estimate is based on a ¹⁴C carbon half-life of 5568 years (Arnold, 1995). However as the proportion of ¹⁴C has varied over time, and the true half-life of ¹⁴C is actually 5730 years, the dates must be calibrated. Using calibrated ¹⁴C data in conjunction with core depth, sedimentation rates were determined using

$$SR = \frac{D_1 - D_2}{Y_1 - Y_2} \quad (3-12)$$

where *SR* is the sedimentation rate in cm/yr, *D*₁ is the depth where the oldest date, *Y*₁ was determined, and *D*₂ is the depth where the youngest date, *Y*₂ was determined.

To date cores, and determine sedimentation and mass accumulation rates, eight sediment samples were analyzed for radiocarbon content at the University of Waterloo. These data, along with data from previous research, are included in Table 3.4 and Fig. 3.7 (cf. Kumar and Patterson, 1999; Mason, 1998).

The difference in the slopes of the curves between the 1997 data and the 1999 data was the result of the coring techniques used. The material obtained in 1997 was compressed due to pushing a pipe into the sediment to obtain core, as opposed to the material obtained using a Livingstone coring device (1999). Uncompressing core JL 97-2, or taking the ^{14}C date of the deeper sample back to its uncompressed state, suggests that 132 cm must be added onto the core. In other words, JL 97-2 was compressed to 54% of its true length (compressed by 132 cm), and its true length should have been 288 cm. Core JL 97-3 was compressed to 24% of its true length of 322 cm and core JL 97-4 was compressed to 31% of its real length of 290 cm. These results were arrived at by taking the oldest date to the depth at which it would have been if the slope of the line joining the samples were the same as that for the samples obtained using the Livingstone Corer.

The radiocarbon dates for the 1999 data were calibrated using CALIB 4.1 (Stuiver and Reimer, 1993). The calculated ^{14}C results are listed in Table 3.5, and plotted with ^{14}C ages in Figures 3.8 to 3.10. It was decided to use the ^{14}C age to date events, without calibration, because most time lines in the Quaternary are given using ^{14}C yr. BP, such as the Younger Dryas at 10,000 yr. BP and the original data are not available for calibration.

The ^{14}C data resulting from sampling of core JL 99-1 (Fig. 3.8) shows that within Zones B_{RL-1} , C, B_{RL-2} and B-2, a sedimentation rate of 0.029 ± 0.001 cm/yr in 141 cm of sediment occurred over 4765 yrs. Between Zones B-2 and B_{Fi} , a sedimentation rate of

0.121 ± 0.015 cm/yr in 84.5 cm of sediment occurred over 703 yrs. The result for this core, between Zones B_{RL-1} and B_{Fi}, indicate an overall ¹⁴C sedimentation rate was 0.041 ± 0.001 cm/yr in 226 cm of sediment over 5468 yrs.

The ¹⁴C data resulting from sampling of core JL 99-7 (Fig. 3.9) shows that within Zones B_{RL-1}, C-1, C-2 and B_{RL-2}, a sedimentation rate of 0.039 ± 0.001 cm/yr in 228 cm of sediment occurred over 5576 yrs.

The ¹⁴C data resulting from sampling of core GL 99-4 (Fig. 3.10) shows that within Zones B_{RL-1}, C-1 and B_{RL-2}, a sedimentation rate of 0.039 ± 0.003 cm/yr in 104 cm of sediment occurred over 2639 yrs. Between Zones B_{RL-2}, C-2, B_{RL-3} and B-2, a sedimentation rate of 0.039 ± 0.001 cm/yr in 118 cm of sediment occurred over 2964 yrs. The result for this core, between Zones B_{RL-1} and B-2, indicated that the ¹⁴C overall sedimentation rate was 0.039 ± 0.002 cm/yr in 222 cm of sediment over 5603 yrs.

In order to date sediment at depth, a time model was developed for ¹⁴C ages as follows:

$${}^{14}\text{C Age} = \left(\frac{D_1 - D_2}{SR} \right) + A \quad (3-13)$$

where D_1 is the depth in cm of the ¹⁴C Age required, D_2 is the depth of the previous ¹⁴C Age, A , and SR is the sedimentation rate in cm/yr (App. A to Ch. 3). This procedure was followed to 360 cm (bswi), beyond which the ¹⁴C Age was extrapolated using the above information and the rate derived by counting the 52 varves over 44 cm in Zone F_{Si-Cl} from Granite Lake core GL 99-4.

Mass Accumulation Rate

The mass accumulation rates (MAR) for this lake system (Table 3.6) were investigated to take account of the differences in the mass of the sediments deposited over time, and calculated by the equation

$$MAR = SR \times \rho_s \quad (3-14)$$

where ρ_s is the dry density as reported in Table 3.2 and SR is the sedimentation rate as reported in Table 3.5. The MAR for the JGLS ranges from 0.024 ± 0.001 to 0.048 ± 0.002 g/cm²/yr for the gyttja, and 0.048 ± 0.002 to 0.071 ± 0.003 g/cm²/yr for the Pleistocene silts and clays. These data are plotted in Figure 3.11.

Mass Compression Rate

The mass compression rate (MCR) was developed to account for the amount of compression of organic sediment with depth. The MCR was calculated by the equation

$$MCR = \rho_s \left(\frac{\Delta h_L}{\Delta t} \right) \quad (3-15)$$

where ρ_s is the dry density of the sediment in g/cc, Δh_L is the change in thickness, due to compaction, in cm, and Δt is the time during which the change in thickness occurs, in yrs. The MCR for JGLS (Fig. 3.6) ranges from 0.189 ± 0.0001 g/cm²/yr near the sediment-

water interface to 0.002 ± 0.001 g/cm²/yr near the bottom of the gyttja layer, and ranged from 0.019 ± 0.002 g/cm²/yr near the top of the Pleistocene silts and clays to 0.034 ± 0.002 g/cm²/yr within the varved clays. These data are plotted in Figure 3.12.

Paleoindicators

Paleoindicators (micropaleoindicators are dealt with in Chapter Five), such as ostracods, pelecypods, gastropods and charophytes, were observed within the cores, and qualitatively recorded as present, absent or abundant (more than ten). Ostracods were present in the top 10 cm of core JL 99-7 (Zone B_{Fi}) and present discontinuously, in the top 100 cm of core JL 01-2 (Zone B_{Fi}). Ostracods were also present, discontinuously, in the top 40 cm of core JL 99-1 (Zones A_{Fe} & B_{Fi-RL}) and continuous from 180 to 240 cm depth (Zones B_{RL-1}, C & B_{RL-3}). Ostracods were present, continuously, from 240 to 320 cm of Zone B_{RL-1} in core GL 99-4, and from 40 to 120 cm in Zone A_{Cl} of core GL 98-3.

Pelecypods were absent in cores JL 99-7 and JL 01-2. Pelecypods (*Sphaerium transversum* Say, 1829) were present between 190 and 195 cm, in Zone B_{RL-3} of core JL 99-1. Abundant pelecypods (*Pisidium* sp.) were found between 185 and 190 cm in Zone C-1, and between 300 and 365 cm in Zones B_{RL-1} & B-1 of core GL 99-4. Abundant pelecypods (*Pisidium* sp.) were found between 40 and 120 cm in Zone A_{Cl} of core GL 98-3.

Gastropods were absent in cores JL 99-7 and JL 01-2. Gastropods (*Valvata tricarinata*) were present at 320 cm in Zone E_f of core JL 99-1, at 360 cm in the bottom of Zone B-1, and the top of Zone D_{fat} within Granite Lake core GL 99-4. Another gastropod, the Great Pond Snail (*Lymnaea stagnalis* “jugularis” Say, 1817) was found to

be present at 280 cm in Zone B_{RL-1} of core GL 99-4. Gastropods (*Ammicola* sp.) were abundant between 320 and 360 cm in Zone B-1 of core GL 99-4, and, between 40 and 110 cm in Zones A_{Cl} of core GL 98-3.

Two genera of Characeae were found to be present. Charophytes (*Chara vulgaris*) were abundant between 346 and 382 cm in Zones E_{f-Si} & E_f, and a *Nitella* sp. (*Nitella* sp. are cold water tolerant) was abundant between 370 and 382 cm in Zone E_f of core JL 01-2. *Chara vulgaris* was present at 155 cm in Zone B-2, and abundant between 320 and 361 cm in Zone E_f of core JL 99-1. *Chara vulgaris* was present at 20 cm in Zone B-2, between 220 and 225 cm in Zone C-1, at 300 cm in Zone B_{RL-1}, abundant between 315 and 316 cm in Zone B_{RL-1} of core GL 99-4, and between 360 and 380 cm in Zone D_{fat}. Lastly, *Chara vulgaris* was present at the surface in Zone B-2, and abundant from 80 to 140 cm in Zones D_{fat} & A_{Cl} of core GL 98-3. *Nitella* sp. was present in core GL 98-3 at 140 cm in Zone A_{Cl}.

Gastropods and pelecypods were identified using Clarke (1981), photographed using with a Nikon Coolpix digital camera through an Olympus SZH10 zoom stereo microscope, rendered using Adobe® Photoshop 6.0 and displayed in Plate 3.1.

Charophytes were identified using Wood and Imahori (1965), and scanning electron micrographs were obtained using a JEOL 6400 Scanning Electron Microscope at the Carleton University Research Facility for Electron Microscopy (CURFEM). These digital images were also compiled into images using Adobe® Photoshop 6.0 (Plate 3.1).

Paleoindicators for the JGLS and their ranges are indicated in Figure 3.13.

Discussion

A model based on the sedimentology, the invertebrate paleontology, MAR, MCR and ^{14}C dates, describing the Quaternary history of the JGLS, after the retreat of the Laurentide Ice Sheet from the area to the present, is illustrated in Figure 3.13. This model is based on the Granite Lake core GL 99-4, and validated using cores from James and Granite lakes as outlined in Figure 3.1.

Zone E_m occurs below 428 cm (bswi) in Granite Lake core GL 99-4, and contains rounded medium-grained, brown sand interpreted to be deposited as a result of glacial fluvial processes as the Laurentide ice sheet retreated from the area of the JGLS. This zone is present in James Lake (JL 99-7; > 455 cm bswi) below a silt-clay varved zone, and in Granite Lake (GL 99-4) where it undergoes a facies change to fine-grained sand at 240 cm (bswi) in core GL 98-3. This Glacial Fluvial Phase (GFP) occurred before 10,800 yrs. BP, indicating that fluvial reworking of outwashed material was occurring at that time. No MAR data are available for the GFP, and paleo-invertebrates are absent from this zone.

Zone $F_{\text{Si-Cl}}$ occurs from 388 to 428 cm in depth (bswi) in Granite Lake core GL 99-4, and contains grayish-blue silt and greenish-gray clay varves resulting from low energy, deep waters of an ice-proximal glacial lake (Flint, 1971; Lowe and Walker, 1984). Found also in James Lake in core JL 01-2 (14 cm thick; 382 – 396 cm bswi), this Proximal Lake Phase (PLP) lasted for at least 52 yrs, and had a MAR greater than $0.071 \pm 0.003 \text{ g/cm}^2/\text{yr}$. Paleo-invertebrates are absent from this zone.

Zone D_{fat} occurs from 357 to 388 cm in depth (bswi) and contains plastic light olive gray clay. This zone, also part of the PLP, indicates cool deep waters similar to Zone F_{Si-Cl}. The MAR drops from 0.071 g/cm²/yr to 0.048 g/cm²/yr to the top of this zone, where the waters began to shallow as indicated by the following paleo-indicators. *Chara vulgaris* and a *Nitella* sp. were present by 10,800 yrs. BP, and increased in abundance to the bottom of the First Littoral Phase (LP 1), indicating alkaline to slightly acidic waters less than 20 m deep (Wood and Imahori, 1965). *Valvata tricarinata* was present, increasing in abundance to the top of the zone. *V. tricarinata* like to live within the ample vegetation found near the edges of shallow lakes and ponds, in cooler climates south of the tree line (Clarke, 1981). *Pisidium* sp. were also present, increasing in abundance to the top of the zone, and living among the vegetation within shallow lakes and streams (Clarke, 1981). Lowe and Walker (1984) indicated that this type of massive clay could be found above or below varved silt and clay layers as a result of sedimentation in glacial proximal lakes. This clay is found under varves in James Lake (JL 01-2), over varves in Granite Lake (GL 99-4), and mixed within silty-clays and sands found in Granite Lake (GL 98-3). The top of the PLP is indicated in James Lake by gray silty-sand lying unconformably under the silty organic soils or gyttja common to the JGLS today.

Zone B-1 occurs from 313 to 357 cm in depth (bswi) in Granite Lake core GL 99-4 and zero to 37 cm (rswi) in core GL 98-3. It contains 37 to 44 cm of dark yellowish brown gyttja, the bottom of which forms an unconformable boundary with the Pleistocene clays of Zone D_{fat}. LP 1 occurs between 9530 and 10,700 yr. BP, contains the oldest organic sediment in the core record, and marks the beginning of the Post

Younger Dryas warming period. The MAR decreases to $0.048 \text{ g/cm}^2/\text{yr}$ by the top of this zone, indicating lowering water levels. Water levels deepen slightly near the center of the zone, with a reduction in populations of *V. tricarinata*, *pisidium* sp. and *Nitella* sp., but drop again towards the top of the zone with an increase in populations of *Ammicola* sp. (a ramshead gastropod found in shallow waters of lakeshores and streams; Clarke, 1981), *pisidium* sp., *C. vulgaris* and minor ostracods. This zone was not found in the James Lake cores.

Zone B_{RL-1} occurs from 230 to 313 cm in depth (bswi) and contains thick, dark reddish-brown and dusky blue rhythmic layered gyttja (4 – 5 cm thick couplets), with minor silty layers, grading downward to 21 cm of uneven pale yellowish brown and dark yellowish brown layers of gyttja at the bottom of the zone. This zone dates from 7425 to 9530 yr. BP, the Post Younger Dryas warming period, and begins the first marsh phase (MP 1). The MAR remains steady throughout the MP 1 period. Ostracods and charophytes become absent with shallowing lake levels, leaving only gastropods and pelecypods in the silt, but these become absent at the top of the zone. This zone is present in all cores examined except the Granite Lake core GL 98-3, where it is unconformably absent at the top.

Zones C-1, B_{RL-2}, C-2, B_{RL-3} and B-2 occur from 94 to 225 cm in depth (bswi) and contain, from the bottom, one centimeter of dark yellowish-brown peat showing rootlets (C-1), 34.5 cm of 4 to 5 cm thick, dark reddish-brown and dusky blue rhythmic layered gyttja (B_{RL-2}), 0.5 cm dark yellowish brown peat containing bark (C-2) and 66 cm dark reddish-brown and dusky blue rhythmic layered gyttja (B_{RL-3}). This material was found in all cores examined, except the Granite Lake core GL 98-3, and makes up the

remainder of the first marsh phase (MP 1). These zones correspond to the Holocene Hypsithermal, occurring from 3927 ± 55 to 7425 ± 77 yr. BP, and representing about 3500 years of warm arid climate. The MAR varied from a low of 0.024 ± 0.001 to 0.044 ± 0.002 g/cm²/yr from Zone B_{RL-2} to the end of the Hypsithermal. No gastropods, pelecypods or ostracods were found in these zones, but *C. vulgaris* was present at the bottom of zone B_{RL-2}, indicating shallow, slightly acidic to basic waters.

Zone B_{Fi} occurs from 68 to 94 cm in depth (bswi) and contains 3 to 4 cm thick bands of dark reddish-brown gyttja and dark yellowish-brown gyttja that thickens to 5 to 8 cm towards the bottom of the zone, and dates from 2930 ± 86 to 3927 ± 55 yr. BP. This zone, which exists in all cores examined, except Granite Lake core GL 98-3, makes up the second littoral phase (LP 2), with MAR increasing to 0.059 from 0.036 g/cm²/yr. This increase in sediment mass over the sediment mass present during MP 2, corresponds to a cool wet climate previously inferred by McCarthy et al. (1988). They found a period of accelerated water level rise, based on pollen data, indicating a cooler wetter climate existed in the region of Lake Ontario between 4230 and 2000 yr. BP.

The MAR drops to 0.032 ± 0.001 g/cm²/yr in zone B_{Fi-RL}, then rises to 0.067 ± 0.003 g/cm²/yr indicating a possible dropping water level, followed by rising water levels. The uppermost zone, B_{Fi-RL (Si-Gy)}, occurs in James Lake core JL 99-1 and Granite Lake core GL 99-4, and is absent from the other cores examined. This zone, which includes the MP 2 and the present LP 3, contains dark yellowish-brown gyttja, with grass and worms, and dates from 2930 ± 86 yr. BP to the present, notwithstanding any unconformities.

Conclusions

This research indicated that there are four main types of sediment within the five cores investigated within James and Granite lakes system. The first is an organic silt or gyttja, which was found in the top 30 (GL 98-3) to 360 cm (GL 99-4) of sediment below the sediment-water interface. This gyttja varied according to the amount of silt and organics within, and the MAR of this material indicated the relative water level within the system. The MAR varied from a low of 0.024 ± 0.001 g/cm²/yr, indicating the warm arid climate conditions of the Holocene Hypsithermal that occurred in the study area from 3927 ± 55 to 7425 ± 77 yrs BP. The MAR showed a maximum of 0.067 ± 0.003 g/cm²/yr, indicating the wet conditions that exist today. The retreating Laurentide Ice Sheet formed an ice-proximal lake between $10,800 \pm 220$ and $10,700 \pm 240$ yrs. BP, again marked by a high MAR of 0.071 ± 0.003 g/cm²/yr. In effect, the MAR of gyttja acts as an indicator for lake level change, with high MAR indicating higher lake water levels and low MAR indicating low lake water levels.

The second type of sediment found in these lakes are two thin peat layers in the middle of the Holocene Hypsithermal, indicating marsh conditions.

The third type of sediment found in these lakes is composed of silt and clay, deposited within an ice-proximal lake as the Laurentide ice sheet retreated. This material, which varied in proportion of clay and silt content, appeared as fat clay, silty-clay or clay and silt varves, in units from 40 (JL 01-2) to 200 cm (GL 98-3) thick.

The fourth type of sediment, composed of silts and coarse sands (the glacial-fluvial material) was found below the clays in some of the cores (JL 99-7 & GL 99-4) within the JGLS.

References

- Al-Shamrani, M. A., 1998, Application of the C /Cc concept to secondary compression of sabkha soils: *Canadian Geotechnical Journal*, v. 35, p. 15 - 26.
- Arnold, L. D., 1995, Conventional Radiocarbon Dating, in Rutter, N. W. and Catto, N. R. eds., *Dating Methods for Quaternary Deposits*, St. John's Nfld., GSA, 107-115.
- Boyle, J. F., 2001, Inorganic geochemical methods in Paleolimnology, in Last, W. M. and Smol, J. P., eds., *Tracking Environmental Change Using Lake Sediments: Basin Analysis, Coring, and Chronological Techniques*, Kluwer Academic Publishers, v. 1 of 4, 548 p.
- Björck, S., Fromer, B., Johnsen, S., Bennike, O., Hammarlund, D., Lemdahl, G., Possnert, G., Rasmussen, T. L., Wohlfarth, B., Hammer, D. U., and Spurk, M., 1996, Synchronized terrestrial-atmospheric deglacial records around the North Atlantic: *Science*, v. 274, p. 1155 - 1160.
- Coakley, J. P., Crowe, A. S. and Huddart, P. A., 1998, Subsurface sediment profiles below Point Pelee: indicators of postglacial evolution in western Lake Erie: *Canadian Journal of Earth Sciences*, v. 35, p. 88-99.
- Clarke, A. H., 1981, *The Freshwater Molluscs of Canada*: Ottawa, Canada, The National Museum of Natural Sciences; The National Museums of Canada, 446 p.

- Crowder, A. A., Smol, J. P., Dalrymple, R., Gilbert, R., Mathers, A., and Price, J., 1996, Rates of natural and anthropogenic change in shoreline habitats in the Kingston Basin, Lake Ontario: *Canadian Journal of Fisheries and Aquatic Sciences*, v. 53 Suppl. 1), p. 121 - 135.
- Crusius, J., and Anderson, R. F., 1991, Core compression and surficial sediment loss of lake sediments of high porosity caused by gravity coring; *Limnology and Oceanography*, v. 36, p. 1021 - 1031.
- Das, B. M., 1977, *Advanced Soil Mechanics*, Taylor & Francis, Sacramento, 457 p.
- Dean, W. E., Ahlbrandt, T. S., Anderson, R. Y., and Bradbury, J. P., 1996, Regional aridity in North America during the middle Holocene: *The Holocene*, v. 6, p. 145 - 155.
- Flint, R. F., 1971, *Glacial and Quaternary Geology*: New York, John Wiley and Sons, Inc., 892 p.
- Freeze, R. A., and Cherry, J. A., 1979, *Groundwater*: Englewood Cliffs, NJ, Prentice Hall, 604 p.
- Goldhammer, R. K., 1997, Compaction and decompaction algorithms for sedimentary carbonates: *Journal of Sedimentary Research*, v. 67, p. 26-35.
- Gorham, E., Brush, G. S., Graumlich, L. J., Rosenzweig, M. L., and Johnson, A. H., 2001, The value of paleoecology as an aid to monitoring ecosystems and landscapes, chiefly with reference to North America: *Environmental Review*, v. 9, p. 99 - 126.

- Kumar, A., and Patterson, R. T., 1999, Arcellaceans (thecamoebians): new tools for monitoring long and short term changes in lake bottom acidity: *Environmental Geology*, v. 39, p. 689 - 697.
- Liu, K.-B., 1990, Holocene Paleoecology of the Boreal Forest and Great Lakes-St. Lawrence Forest in Northern Ontario: *Ecological Monographs*, v. 60, p. 179-212.
- Livingstone, D. A., and Imboden, D. M., 1996, The prediction of hypolimnetic oxygen profiles: a plea for a deductive approach: *Canadian Journal of Fisheries and Aquatic Sciences*, v. 53, p. 924 - 932.
- Lotter, A. F., Merkt, J., and Sturm, M., 1997, Differential sedimentation versus coring artifacts: a comparison of two widely used piston-coring methods: *Journal of Paleolimnology*, v. 18, p. 75 - 85.
- Lowe, J. J., and Walker, M. J. C., 1984, *Reconstructing Quaternary Environments*: London and New York, Longman, 389 p.
- Mason, G., 1998, A study of the effects of past mining activities on James Lake sediment chemistry: Unpub. B.Sc. thesis, Carleton University, Ottawa, Canada, 28 p.
- Meyers, P. A. and Lallier-Verges, E., 1999, Lacustrine sedimentary organic matter records of Late Quaternary paleoclimates: *Journal of Paleolimnology*, v. 21, p. 345-372.
- Miller, B. B. and Tevesz, M. J. S., 2001, Freshwater Molluscs, in Smol, J. P., Birks, H. J. B. and Last W. M., eds., *Tracking Environmental Change using Lake Sediments*, Kluwer Academic Publishers, Dordrecht, The Netherlands, 4: 217 p.

- Perrier, R., and Quiblier, J., 1974, Thickness changes in sedimentary layers during compaction history: Methods for quantitative evaluation: the American Association of Petroleum Geologists Bulletin, v. 58, p. 507-520.
- Prescott, G. W., 1970, The Freshwater Algae, The Pictured Key Nature Series, William C. Brown Company, Publishers, Dubuque Iowa, 2: 348 p.
- Say, T., 1817, Conchology, in American edition of the British Encyclopedia or Dictionary of Arts and Sciences, W. M. Nicholson, ed., v. II, 15 p.
- _____, 1819, Conchology, United States, 22 p
- _____, 1821, Descriptions of univalve shells of the United States, Philadelphia Journal of the Academy of Natural Sciences, v. 2, p. 149 - 179.
- _____, 1829, Descriptions of some new and fluviatile shells of North America, The Disseminator of Useful knowledge, containing hints to the youth of the United States, School of Industry, v. 2, p. 229 - 356.
- Scholz, C. A., 2001, Applications of Seismic Sequence Stratigraphy in Lacustrine Basins: in Last, W. M. and Smol, J. P., eds., Tracking Environmental Change Using Lake Sediments: Basin Analysis, Coring, and Chronological Techniques, Kluwer Academic Publishers, v. 1 of 4, 548 p.
- Stuiver, M., and Reimer, P. J., 1993, Extended ^{14}C data base and revised CALIB 3.0 ^{14}C age calibration program: Radiocarbon, v. 35, p. 215 - 230.
- Terzaghi, 1943, Theoretical Soil Mechanics: New York, John Wiley & Sons 510 p.
- Björck, S., Fromer, B., Johnsen, S., Bennike, O., Hammarlund, D., Lemdahl, G., Possnert, G., Rasmussen, T. L., Wohlfarth, B., Hammer, D. U., and Spurk, M.,

- 1996, Synchronized terrestrial-atmospheric deglacial records around the North Atlantic: *Science*, v. 274, p. 1155 - 1160.
- Crowder, A. A., Smol, J. P., Dalrymple, R., Gilbert, R., Mathers, A., and Price, J., 1996, Rates of natural and anthropogenic change in shoreline habitats in the Kingston Basin, Lake Ontario: *Canadian Journal of Fisheries and Aquatic Sciences*, v. 53 Suppl. 1), p. 121 - 135.
- Dean, W. E., Ahlbrandt, T. S., Anderson, R. Y., and Bradbury, J. P., 1996, Regional aridity in North America during the middle Holocene: *The Holocene*, v. 6, p. 145 - 155.
- Flint, R. F., 1971, *Glacial and Quaternary Geology*: New York, John Wiley and Sons, Inc., 892 p.
- Gorham, E., Brush, G. S., Graumlich, L. J., Rosenzweig, M. L., and Johnson, A. H., 2001, The value of paleoecology as an aid to monitoring ecosystems and landscapes, chiefly with reference to North America: *Environmental Review*, v. 9, p. 99 - 126.
- Liu, K.-B., 1990, Holocene Paleoecology of the Boreal Forest and Great Lakes-St. Lawrence Forest in Northern Ontario: *Ecological Monographs*, v. 60, p. 179-212.
- Lowe, J. J., and Walker, M. J. C., 1984, *Reconstructing Quaternary Environments*: London and New York, Longman, 389 p.
- McCarthy, F. M. G., and McAndrews, J. H., 1988, Water levels in Lake Ontario 4230 - 2000 years BP; evidence of Grenadier Pond, Toronto, Canada: *Journal of Paleolimnology*, v. 1, p. 99 - 113.

- Vance, R. E., Beaudoin, A. B., and Luckman, B. H., 1995, The paleoecological record of 6 ka bp climate in the Canadian prairie provinces: *Geographie Physique et Quaternaire*, v. 49, p. 81 - 89.
- Wadden, J. S., 1992, *Laboratory Manual; Physics 75.101/102*: Ottawa, Department of Physics, 100 p.
- Walton, W. C., 1970, *Groundwater Resource Evaluation*: New York, McGraw-Hill Book Company, 664 p.
- Whitlow, R., 1990, *Basic Soil Mechanics*: New York, John Wiley & Sons, Inc., 528 p.
- Wood, R. D., and Imahori, K., 1965, *Monograph of the Characeae*: New York, N. Y., Verlag; Cramer, Weldon and Wesley, LTD; Stechert-Hafner Service Agency, Inc., Vol 1, 904 p.

Table 3.1 – Zone Key, and sediment layer indicators for stratigraphic columns in James and Granite lakes. Used in Figures 3.1, 3.3, 3.9, 3.10 and 3.13.

Sediment Layer Key			
Zones Key	Zone	Sediment Modifiers	Modifier Key
A	Silt	Fe	Iron
B	Gyttja	Fi	Fibrous
		RL	Rythmic layered
C	Peat	Si	Silt
D	Clay	Cl	Clay
		Gy	Gyttja
		ma	Massive
		fat	Fat
E	Sand	f	Fine-grained
		m	Medium-grained
F	Varves	Cl	Clay
		Si	Silt

Sample	Final Depth b_f (cm)	Volume V_T (cm)	Wet Sediment W_s (g)	Dry Sediment (g)	Water V_w (g)	Solid V_s (cc)	Void Ratio e	Porosity ϕ (%)	Bulk Density ρ (g/cc)	Dry Density ρ_s (g/cc)
GL 02-4-1	20.4 ± 0.1	20.5 ± 0.1	55.2 ± 0.1	5.3 ± 0.1	17.4 ± 0.1	3.1 ± 0.1	5.6 ± 0.2	0.85	0.3	1.7
GL 02-4-2	47.7 ± 0.1	27.7 ± 0.1	48.9 ± 0.1	5.2 ± 0.1	20.9 ± 0.1	6.8 ± 0.1	3.1 ± 0.0	0.75	0.2	0.8
GL 02-4-3	74.9 ± 0.1	17.1 ± 0.1	41.9 ± 0.1	4.9 ± 0.1	13.7 ± 0.1	3.4 ± 0.1	4.0 ± 0.1	0.80	0.3	1.5
GL 02-4-4	111.1 ± 0.1	27.4 ± 0.1	54.3 ± 0.1	5.9 ± 0.1	21.4 ± 0.1	6.0 ± 0.1	3.6 ± 0.0	0.78	0.2	1.0
GL 02-4-5	149.9 ± 0.1	16.1 ± 0.1	33.4 ± 0.1	3.4 ± 0.1	12.9 ± 0.1	3.2 ± 0.1	4.0 ± 0.1	0.80	0.2	1.1
GL 02-4-6	215.8 ± 0.1	25.6 ± 0.1	41.3 ± 0.1	4.2 ± 0.1	18.8 ± 0.1	6.8 ± 0.1	2.8 ± 0.0	0.73	0.2	0.6
GL 02-4-7	264.3 ± 0.1	23.7 ± 0.1	51.2 ± 0.1	5.8 ± 0.1	18.7 ± 0.1	5.0 ± 0.1	3.7 ± 0.1	0.79	0.2	1.2
GL 02-4-8	312.2 ± 0.1	22.4 ± 0.1	50.2 ± 0.1	6.2 ± 0.1	17.4 ± 0.1	5.0 ± 0.1	3.5 ± 0.1	0.78	0.3	1.2
GL 02-4-9	359.3 ± 0.1	20.4 ± 0.1	45.0 ± 0.1	7.0 ± 0.1	14.6 ± 0.1	5.8 ± 0.1	2.5 ± 0.1	0.72	0.3	1.2
GL 02-4-10	403.5 ± 0.1	23.7 ± 0.1	67.2 ± 0.1	40.6 ± 0.1	1.5 ± 0.1	22.2 ± 0.1	0.1 ± 0.0	0.07	1.7	1.8

Table 3.2 – Porosity and density data for Granite lake.

Sample	Layer	Thickness Range (cm)	Initial Void Ratio e_i	Final Void Ratio e_f	Compression Δh (cm)	Thickness b_i (cm)	% Compression
GL 02-4-1	1	0	7.5		195.2	263.2	74
GL 02-4-2		68		1.2			
GL 02-4-3	2	68	4.1		11.9	66.9	18
GL 02-4-4		123		3.2			
GL 02-4-5	3	123	4.5		54.7	155.7	35
GL 02-4-6		224		2.6			
GL 02-4-7	4	224	3.7		15.4	148.4	10
GL 02-4-8		357		3.2			
GL 02-4-9	5	357	2.6		172.2	243.2	71
GL 02-4-10		428		0.1			
<i>Gytija</i>		357	7.5	3.2	277.2	634.2	44

Table 3.3 – Compression of lake bottom sediment for the JGLS system based on sediment from Granite Lake core GL 99-4. Calculations for volume, void ratio and change of height in a layer are outlined in Appendix A.

Core	Sample	Lab #	Depth (cm)	$\delta^{13}C$	% Modern	^{14}C Age
JL 99-1	JL 99-1-1	NZA 12822	88.5 ± 1.5	-24.5	68.9 ± 0.5	2936 ± 60
	JL 99-1-2	NZA 12823	173.0 ± 2.0	-24.7	63.2 ± 0.5	3639 ± 60
	JL 99-1-4	NZA 11410	314.3 ± 1.3	-30.9	39.9 ± 0.3	8404 ± 60
JL 99-7	JL 99-7-2	NZA 12868	116.5 ± 1.5	-26.3	64.1 ± 0.6	3518 ± 70
	JL 99-7-3	NZA 11411	345.0 ± 1.0	-32.2	32.2 ± 0.2	9049 ± 60
GL 99-4	GL 99-4-1	NZA 12869	91.0 ± 1.0	-25.4	60.9 ± 0.4	3926 ± 55
	GL 99-4-3	NZA 12870	209.0 ± 1.0	-27.4	42.2 ± 0.3	6891 ± 55
	GL 99-4-4	WAT 4178	313.0 ± 1.0	-33.4	30.5 ± 0.8	9530 ± 220
JL 97-2	JL 97-2-1	TO 7343	32.0 ± 1.0	-26.2	N/A	650 ± 50
	JL 97-2-2	WAT 4045	156.0 ± 1.0	-29.4	41.6 ± 0.7	7050 ± 140
JL 97-3	JL 97-3-1	WAT 4028	24.5 ± 0.5	-24.4	84.9 ± 1	1310 ± 90
	JL 97-3-2	WAT 4029	66.5 ± 1.0	-27.5	37.9 ± 0.5	7790 ± 120
	JL 97-3-3	WAT 4030	80.5 ± 0.5	-29.4	33.6 ± 0.5	8760 ± 100
JL 97-4	JL 97-4-1	WAT 4031	47.0 ± 1.0	-24.3	77.1 ± 1.0	2090 ± 100
	JL 97-4-2	TO 7344	91.0 ± 1.0	-31.7	N/A	8170 ± 80

Table 3.4 - ^{14}C data obtained from James and Granite lakes. Data from 1997 were previously reported by Mason (1998) and Kumar (1999). (N/A = not available).

Sample	Lab #	Depth (cm)	¹⁴ C Age BP	¹⁴ C CALIB BP	Sedimentation Rate ¹⁴ C (cm/yr)	Sedimentation Rate ¹⁴ C CALIB (cm/yr)
JL 99-1-1	NZA 12822	88 ± 1	2936 ± 60	3107 ± 67	0.121 ± 0.015	0.101 ± 0.011
JL 99-1-2	NZA 12823	173 ± 2	3639 ± 60	3947 ± 63	0.029 ± 0.001	0.026 ± 0.001
JL 99-1-4	NZA 11410	314 ± 1	8404 ± 60	9452 ± 63	0.041 ± 0.001	0.035 ± 0.001
JL 99-7-2	NZA 12868	116 ± 2	3518 ± 70	3780 ± 84	0.039 ± 0.001	0.036 ± 0.001
JL 99-7-3	NZA 11411	345 ± 1	9049 ± 60	10,200 ± 77	0.039 ± 0.001	0.036 ± 0.001
GL 99-4-1	NZA 12869	91 ± 1	3926 ± 55	4340 ± 125	0.039 ± 0.001	0.035 ± 0.002
GL 99-4-3	NZA 12870	209 ± 1	6891 ± 55	7702 ± 106	0.039 ± 0.003	0.031 ± 0.002
GL 99-4-4	WAT 4178	313 ± 1	9530 ± 220	11,011 ± 222	0.039 ± 0.002	0.033 ± 0.001
JL 97-2-1	TO 7343	32 ± 1	650 ± 50	611 ± 63	0.040 ± 0.001	0.035 ± 0.001
JL 97-2-2	WAT 4045	288 ± 6	7050 ± 140	7895 ± 143	0.040 ± 0.001	0.035 ± 0.001
JL 97-3-1	WAT 4028	24 ± 1	1310 ± 90	2408 ± 181	0.039 ± 0.001	0.041 ± 0.002
JL 97-3-2	WAT 4029	283 ± 6	7790 ± 120	8574 ± 121	0.04 ± 0.01	0.034 ± 0.008
JL 97-3-3	WAT 4030	322 ± 5	8760 ± 100	9719 ± 112	0.039 ± 0.001	0.041 ± 0.001
JL 97-4-1	WAT 4031	47 ± 1	2090 ± 100	2098 ± 263	0.039 ± 0.001	0.035 ± 0.002
JL 97-4-2	TO 7344	290 ± 5	8170 ± 80	9080 ± 92	0.039 ± 0.001	0.035 ± 0.002

Table 3.5 – Bulk sedimentation rates for James and Granite lakes, including uncompressed data for cores obtained in James Lake during 1997.

<i>Sample</i>	<i>Zone</i>	<i>Depth (cm)</i>	<i>Density (ρ) (g/cc)</i>	^{14}C <i>MAR (g/cm²/yr)</i>	^{14}C <i>CR (cm/yr)</i>	^{14}C <i>MCR (g/cm²/yr)</i>
GL 99-4-1	B _{FI-RL}	20.4 ± 0.1	1.70 ± 0.02	0.067 ± 0.003		0.189 ± 0.000
GL 99-4-2	B _{FI-RL}	47.7 ± 0.1	0.80 ± 0.01	0.032 ± 0.001	0.112 ± 0.000	0.145 ± 0.003
GL 99-4-3	B _{FI}	74.9 ± 0.1	1.50 ± 0.02	0.059 ± 0.002		0.005 ± 0.001
GL 99-4-4	B-2	111.1 ± 0.1	1.00 ± 0.04	0.036 ± 0.002	0.004 ± 0.000	0.005 ± 0.000
GL 99-4-5	B _{RL-3}	149.9 ± 0.1	1.10 ± 0.00	0.044 ± 0.002		0.010 ± 0.003
GL 99-4-6	B _{RL-2}	215.8 ± 0.1	0.60 ± 0.01	0.024 ± 0.001	0.009 ± 0.002	0.006 ± 0.002
GL 99-4-7	B _{RL-1}	264.3 ± 0.1	1.20 ± 0.02	0.048 ± 0.002		0.002 ± 0.001
GL 99-4-8	B _{RL(Si-Gy)}	312.2 ± 0.1	1.20 ± 0.02	0.048 ± 0.002	0.002 ± 0.000	0.002 ± 0.001
GL 99-4-9	B-1	359.3 ± 0.1	1.20 ± 0.00	0.048 ± 0.002		0.019 ± 0.002
GL 99-4-10	D _{fat}	403.5 ± 0.1	1.80 ± 0.01	0.071 ± 0.003	0.016 ± 0.002	0.034 ± 0.002

Table 3.6 – Mass accumulation rates (MAR), compression rates (CR) and mass compression rates (MCR) for zones in the JGLS system, based on information from Granite Lake core GL 99-4.

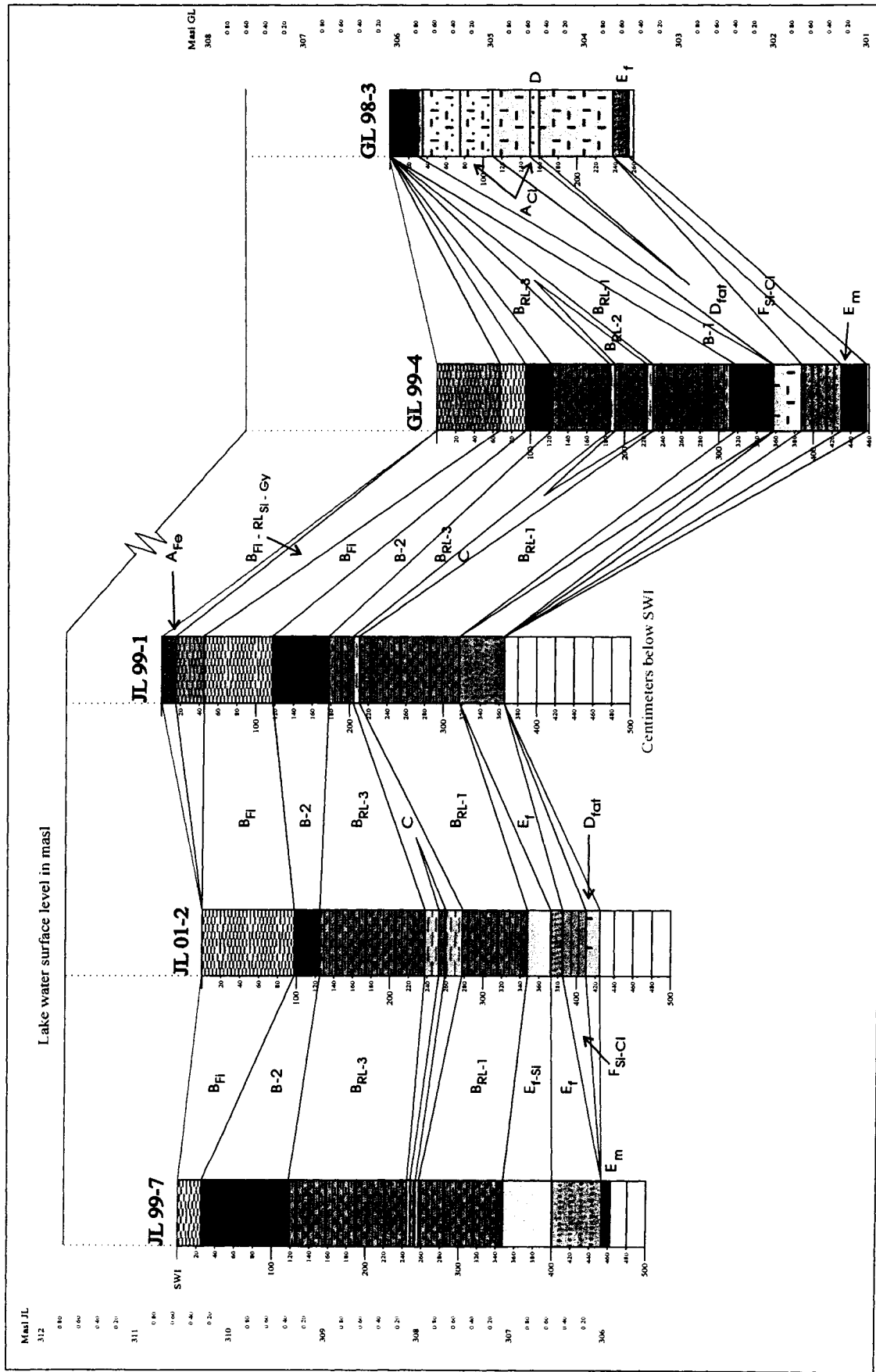


Figure 3.1 - Stratigraphic columns for cores from James and Granite lakes, indicating their relationships to altitude in metres above sea-level (masl) and water depths for James Lake (masl JL) and Granite Lake (masl GL). Zone Key is included in Table 3.1.

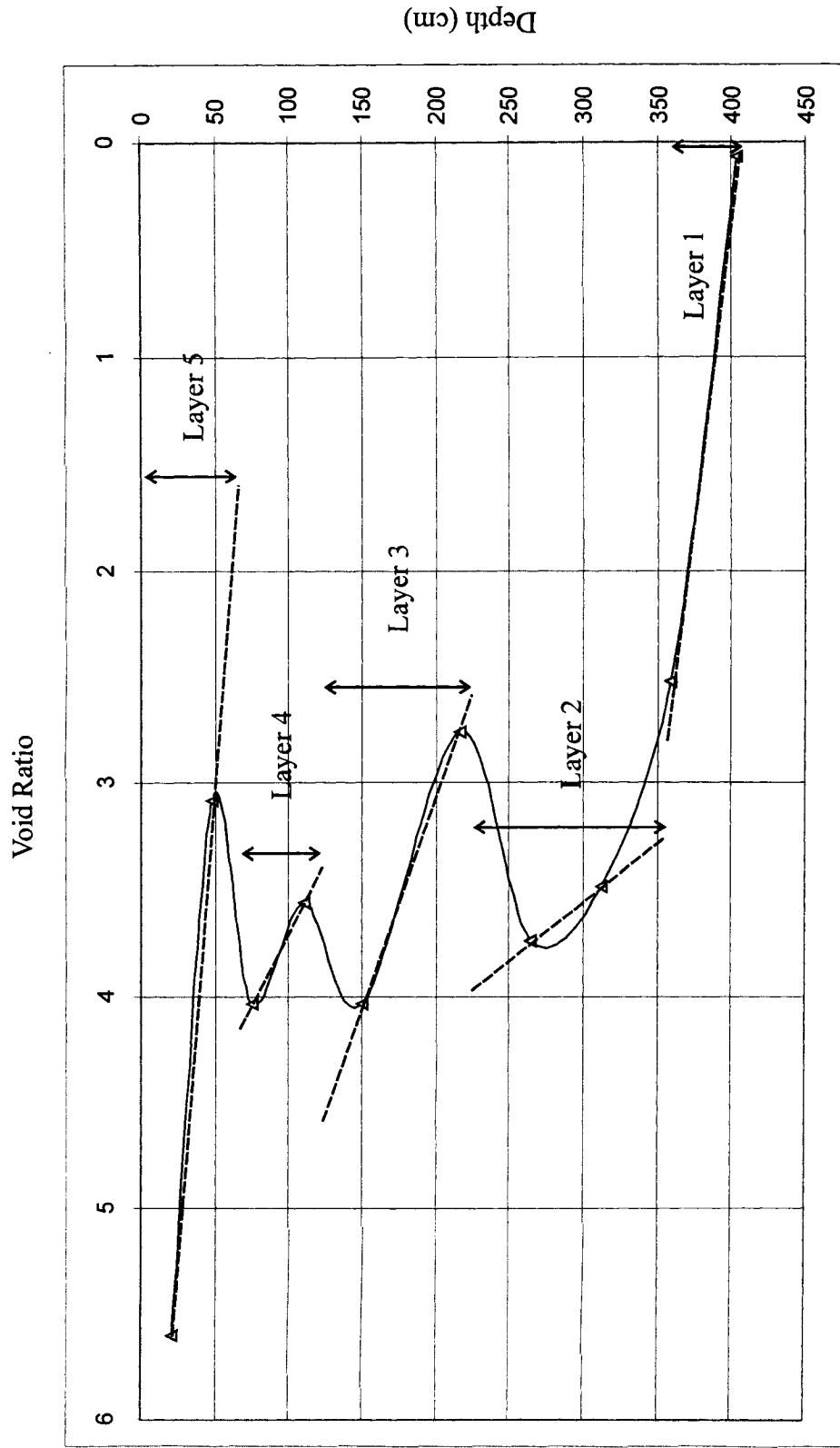


Figure 3.2 - Void ratio plotted against depth for Granite Lake core GL 99-4, indicating layering used to determine compression of the lake bottom sediments in the JGLS.

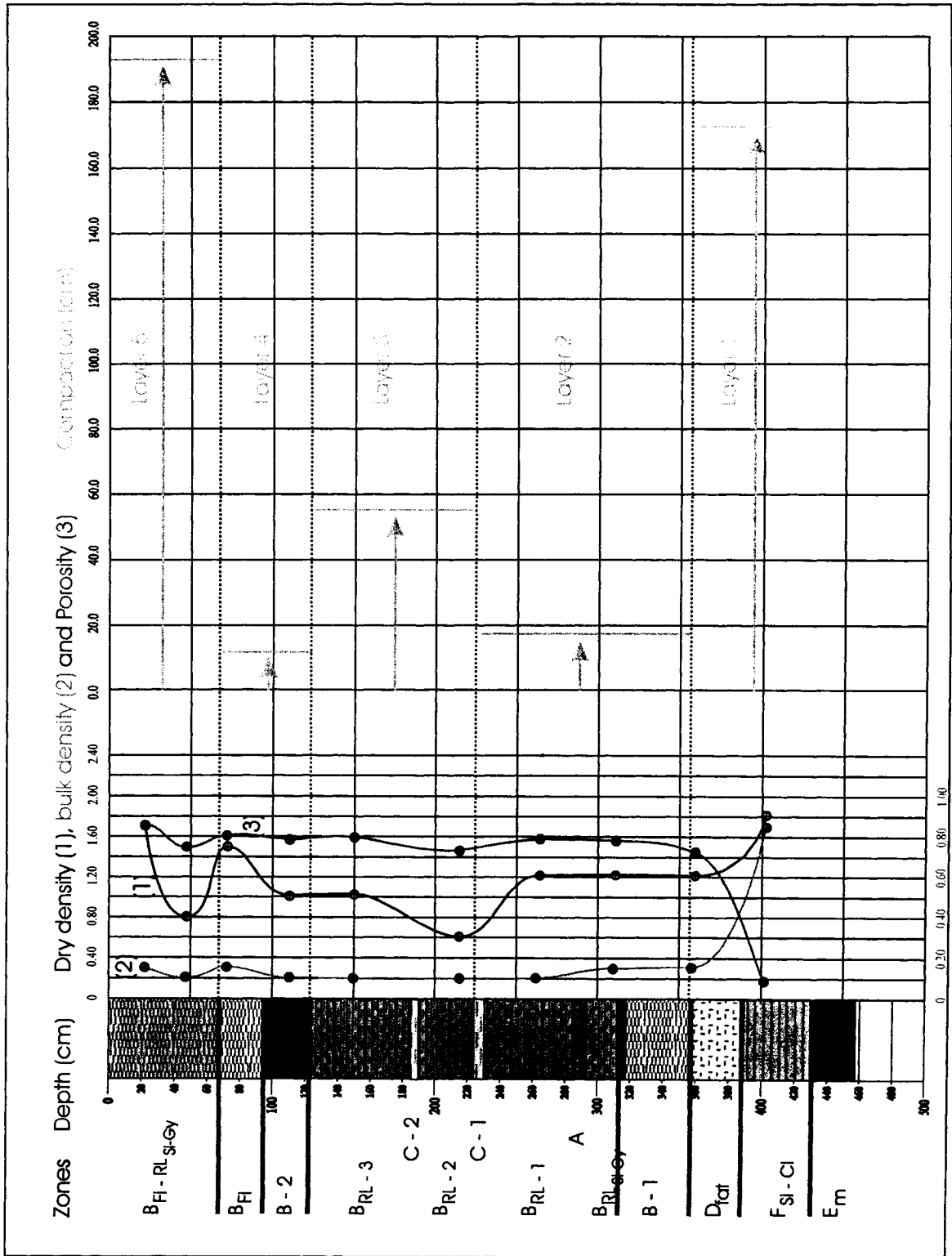


Figure 3.3 - Density, porosity and layer compaction for GL 99-04 core from northern Granite Lake. Top scale = density; bottom scale = porosity.

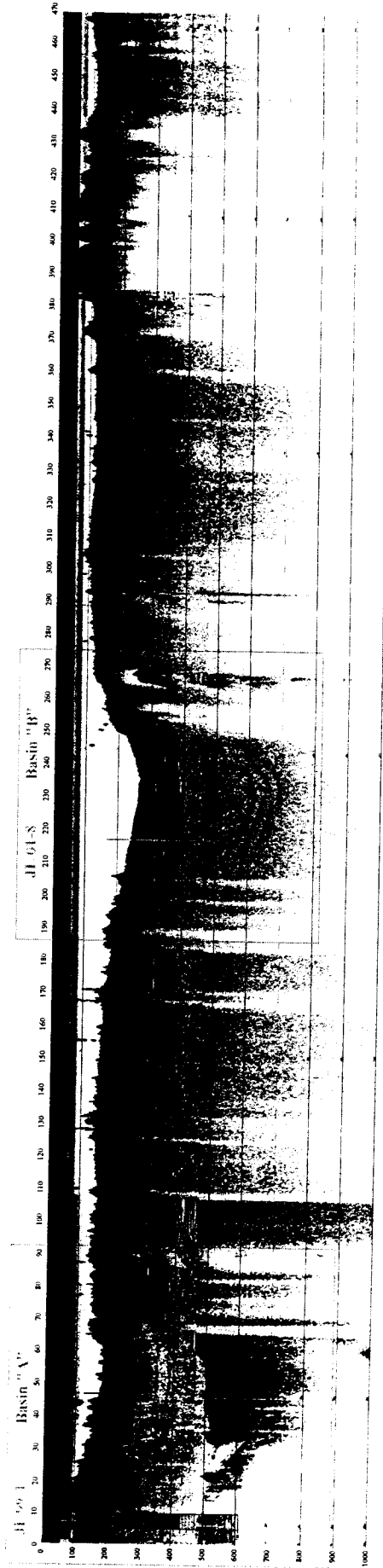


Figure 3.4 - Sonar Profile Run #9 (Fig. 2.5), indicating core sites for JL 99-1 in Basin A, and core site JL 01-8 in Basin B (Fig. 2.1), adjacent to the Northland Pyrite Mine waste rock pile in southwestern James Lake. Depths are in cm below lake surface, and horizontal distances are in metres.

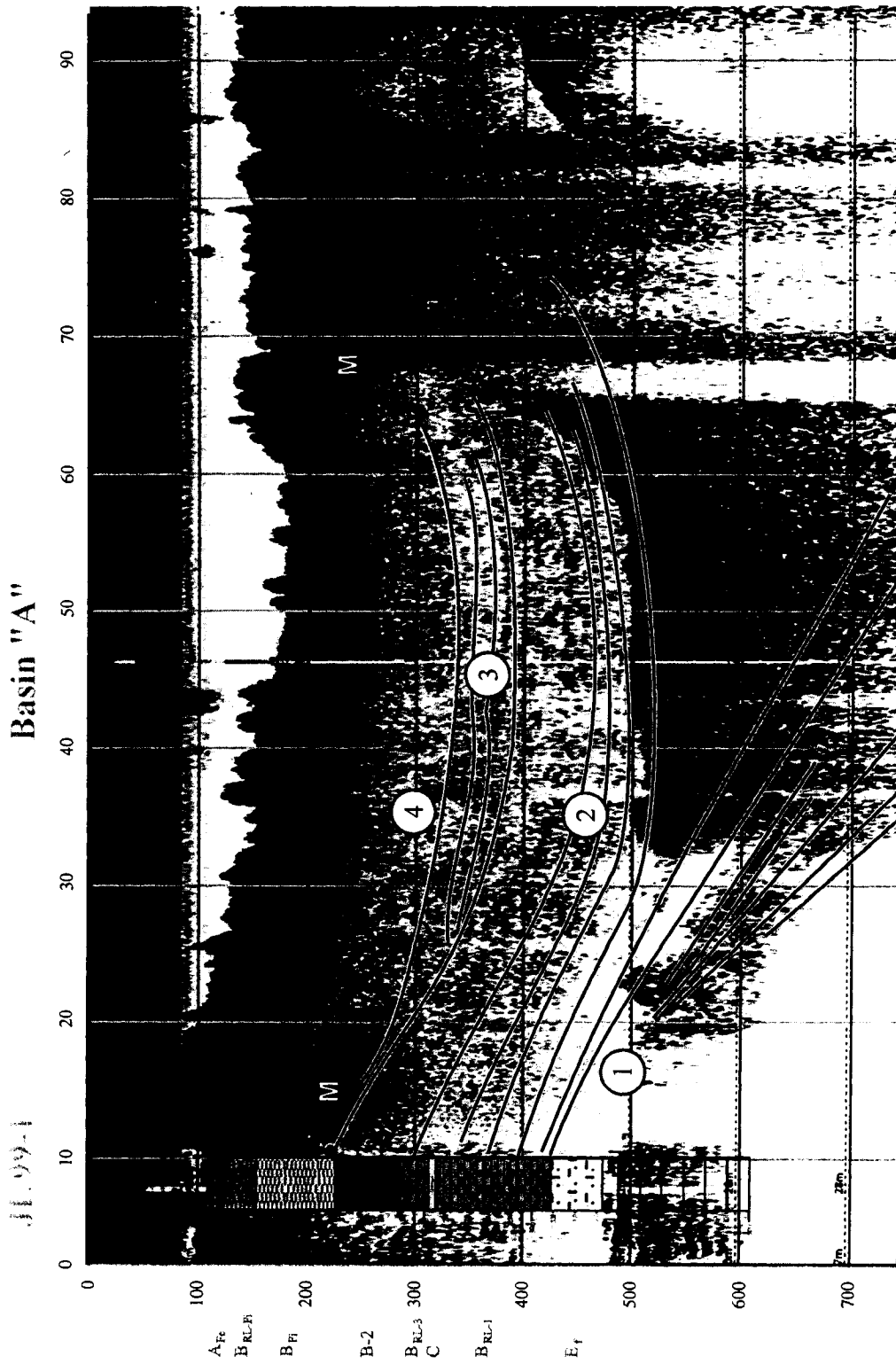


Figure 3.4A - Sonar Profile of Basin A from Run #9 in James Lake, as indicated in Fig. 3.4, showing transgressive-regressive tract (1), lowstand (2), transgression (3), sediment deposition within Basin A (4) and areas of methane outgassing (M). Depths below lake surface are in cm, and horizontal distances are in metres, and the depths indicated on the stratigraphic column are in cm below the SWI. Sediment letter codes are indicated in Table 3-1.

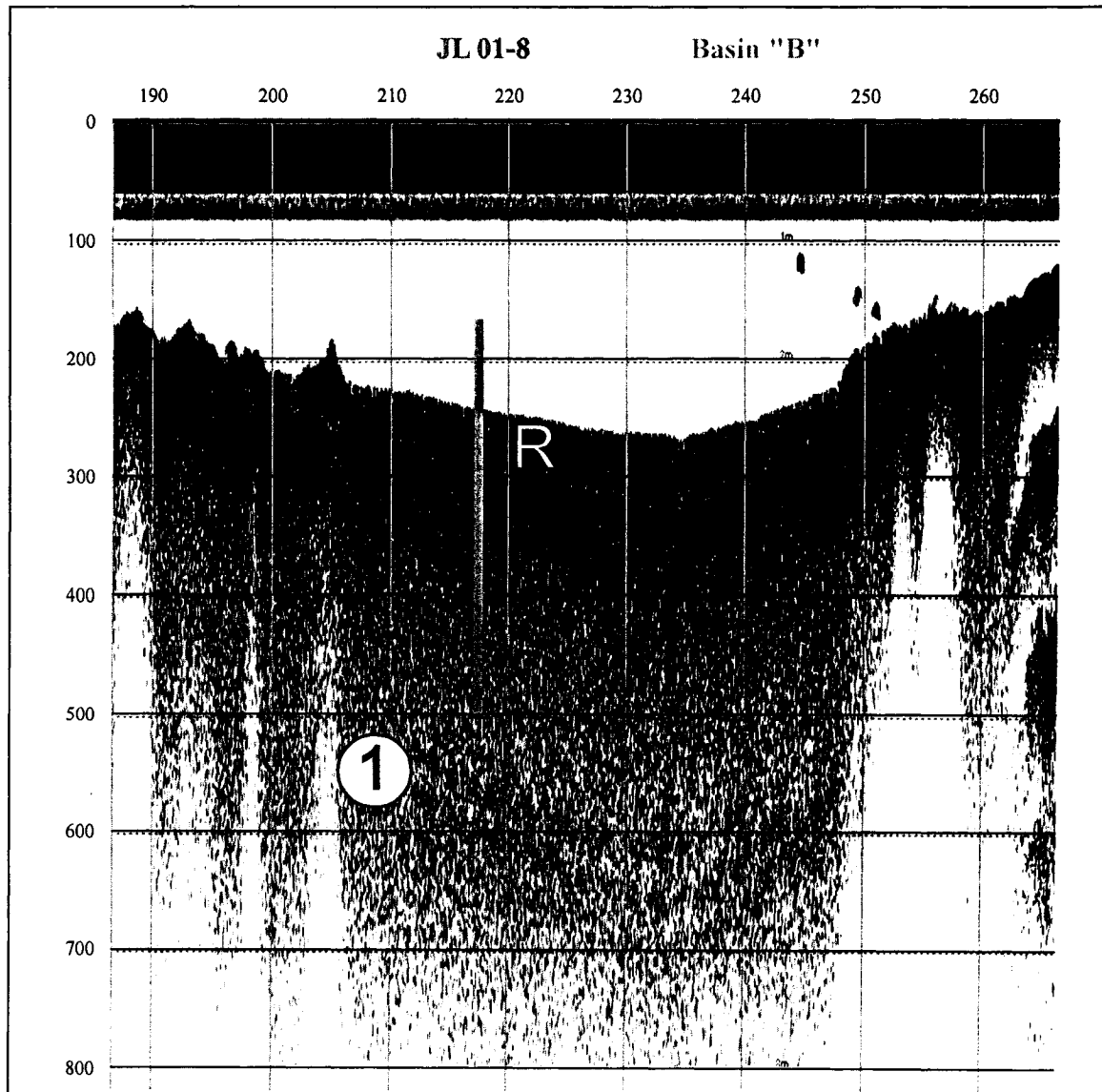


Figure 3.4B - Sonar Profile of Basin B from Run #9 in James Lake, as indicated in Fig. 3.4, showing a depositional sequence (1) and giving the position of core JL 01-8, the top of which indicates a 30 cm section of redox couplets ® near the surface. Depths below lake surface are in cm, and horizontal distances are in metres.

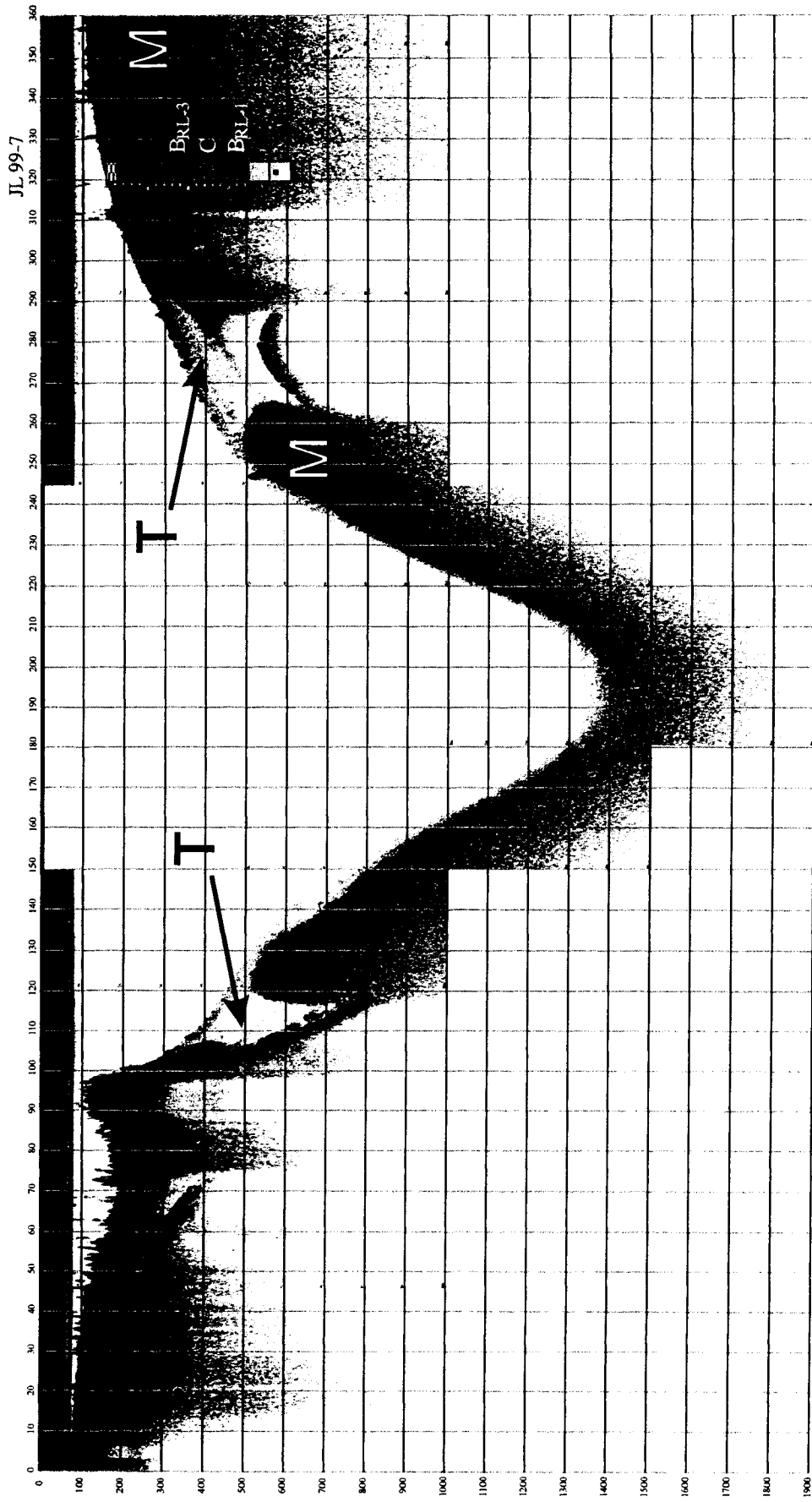


Figure 3.5 - Sonar Profile Run #23 in James Lake as indicated in Fig. 2.1 and Fig. 2.5, showing possible erosional truncation (T) caused by slumping or low water levels, and outgassing (M). Depths below lake surface are in cm, and horizontal distances are in meters.

Waste Rock Pile
3m west of "X"

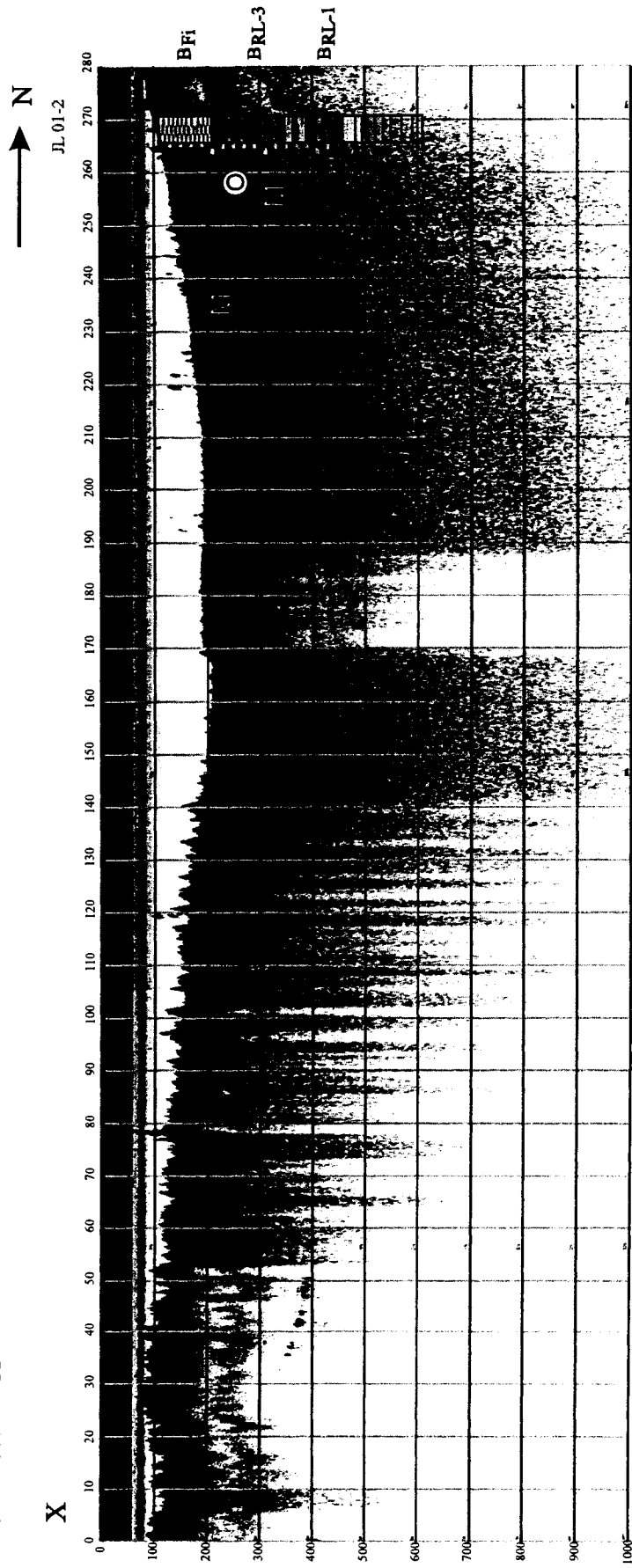


Figure 3.6 - Sonar Profile Run #1 in James Lake as indicated in Fig. 2.1 and Fig. 2.5, showing onlapping (O) immediately north of the Northland Pyrite Mine waste rock pile, and outgassing (M). Depths below lake surface are in cm, and horizontal distances are in meters.

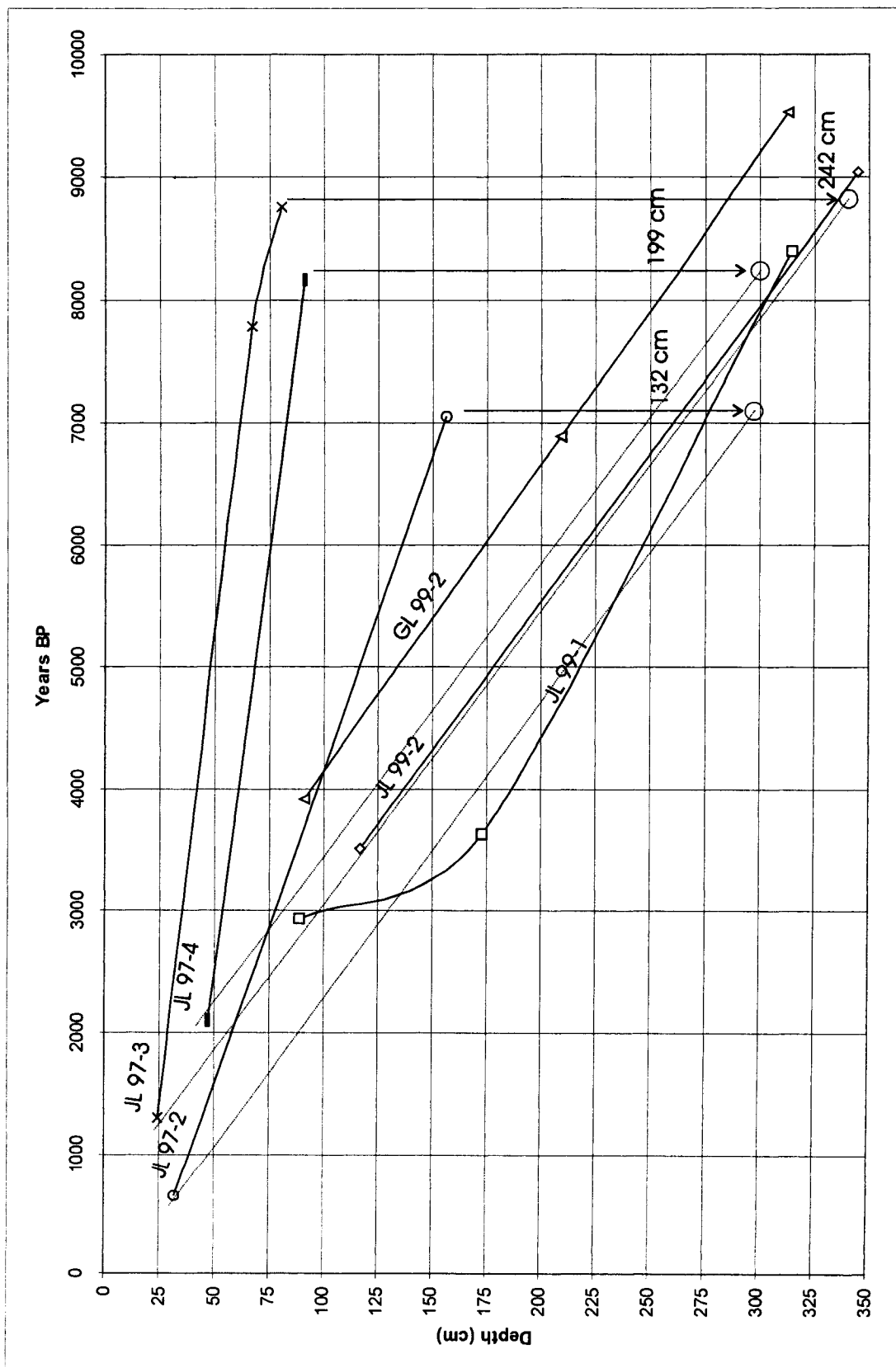


Figure 3.7 - Uncalibrated ¹⁴C dates from 1997 to 1999 in James and Granite lakes. Data from 1997 were previously reported by Mason (1998) and Kumar (1999). Shallow dates from previous data are assumed to be uncompressed.

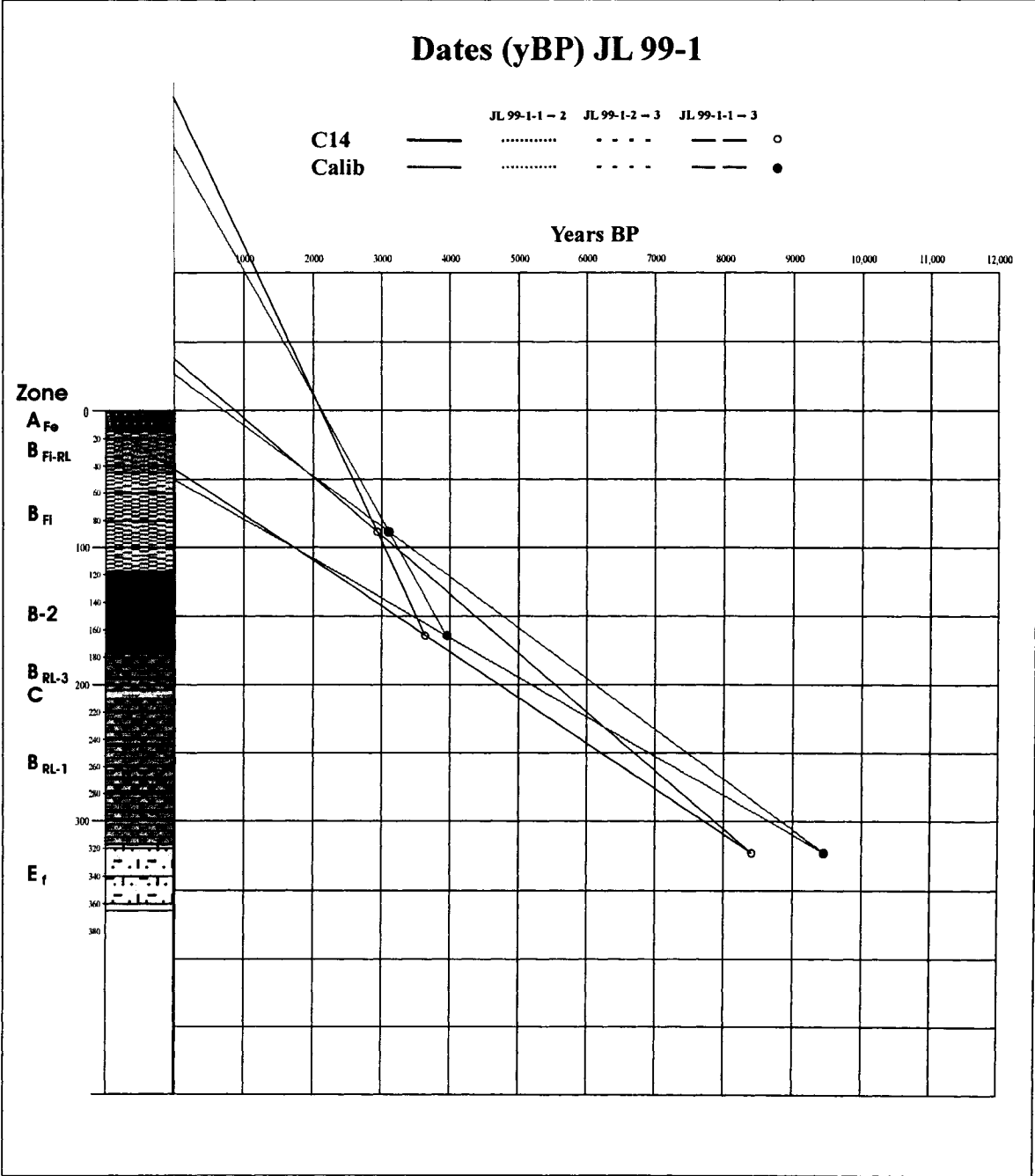


Figure 3.8 - Calibration dates for core JL 99-1 in James Lake.

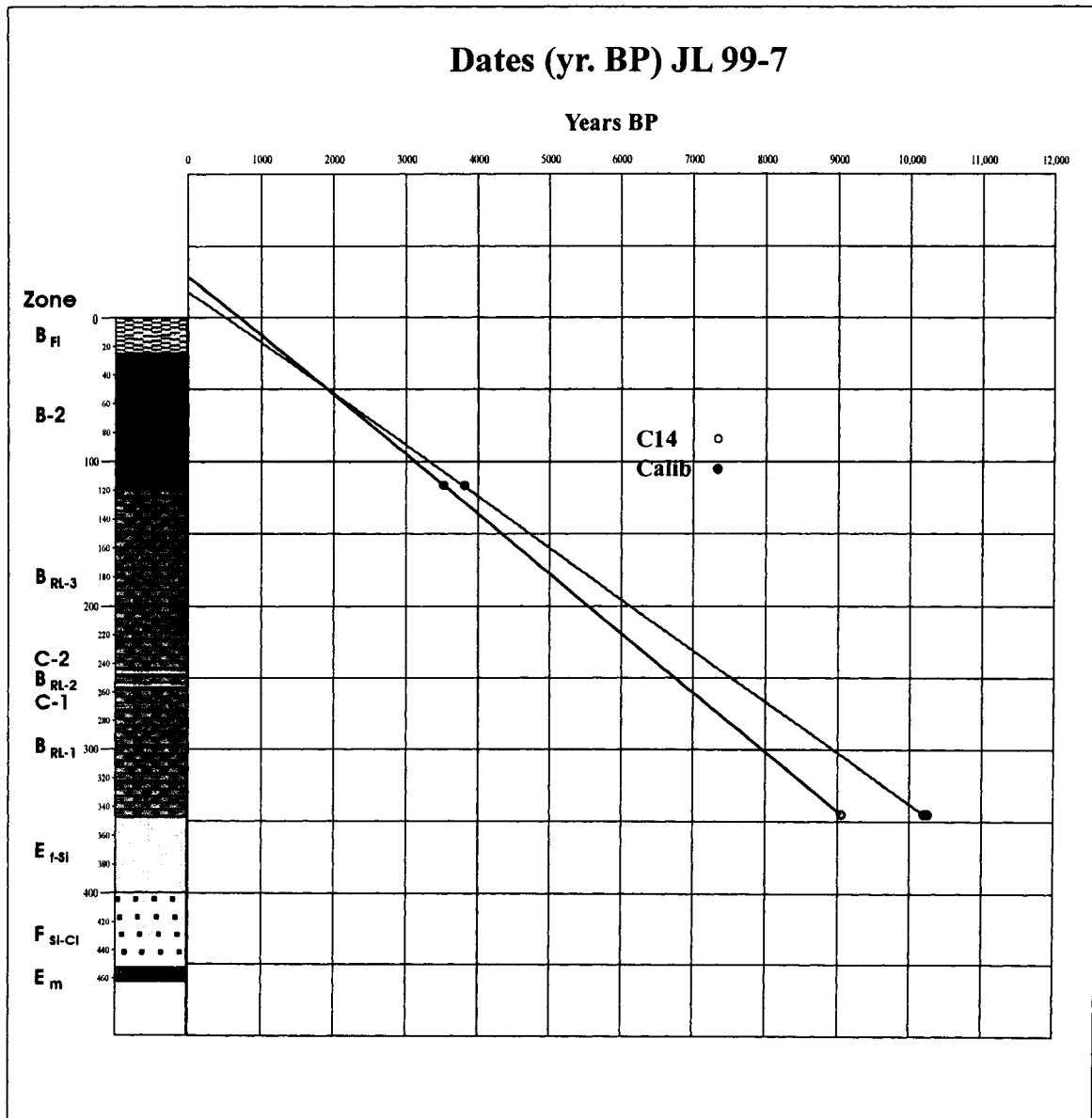


Figure 3.9 - Calibration dates for core JL 99-7 in northern James Lake

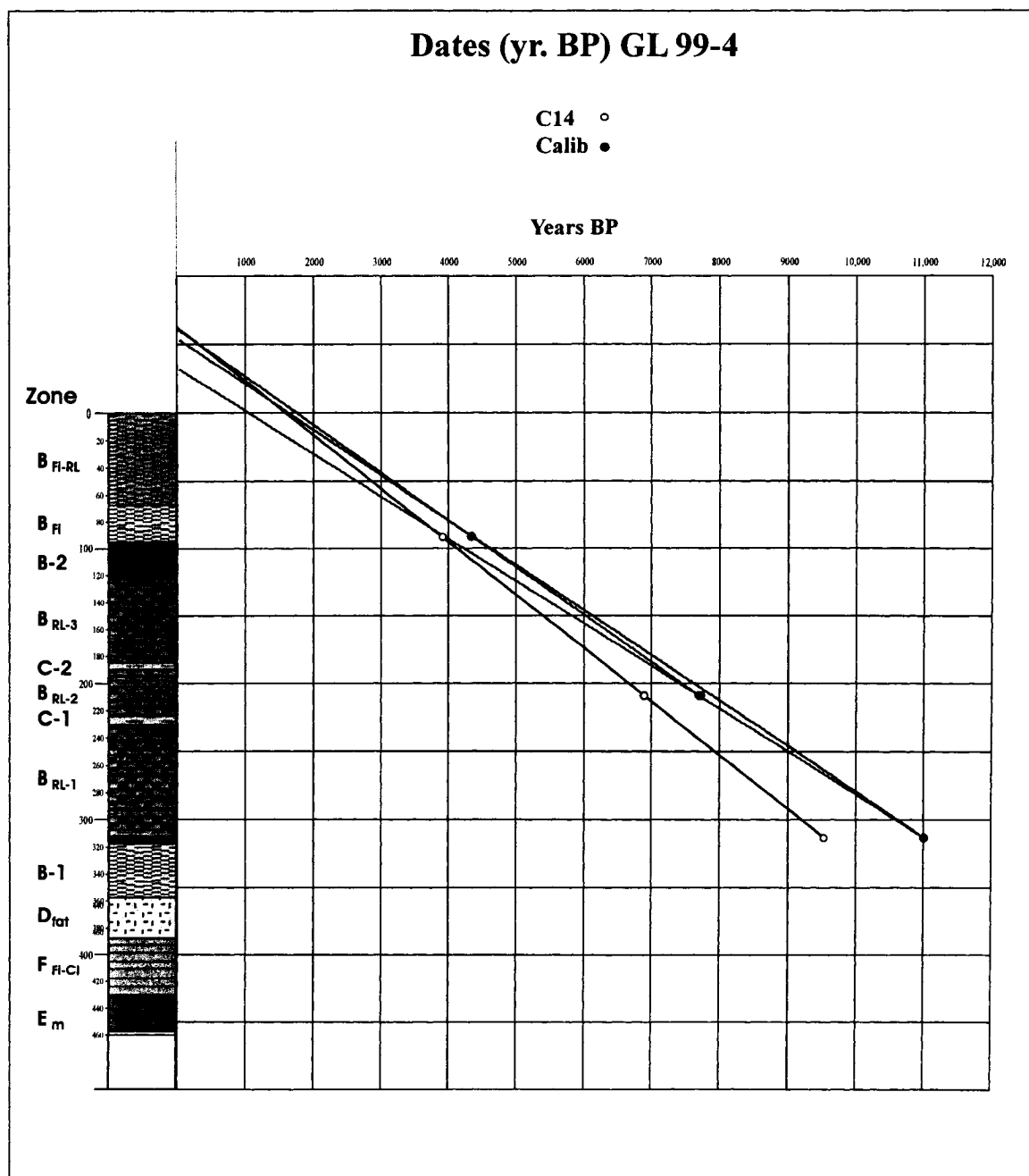


Figure 3.10 - Calibration dates for core GL 99-4 in northern Granite Lake.

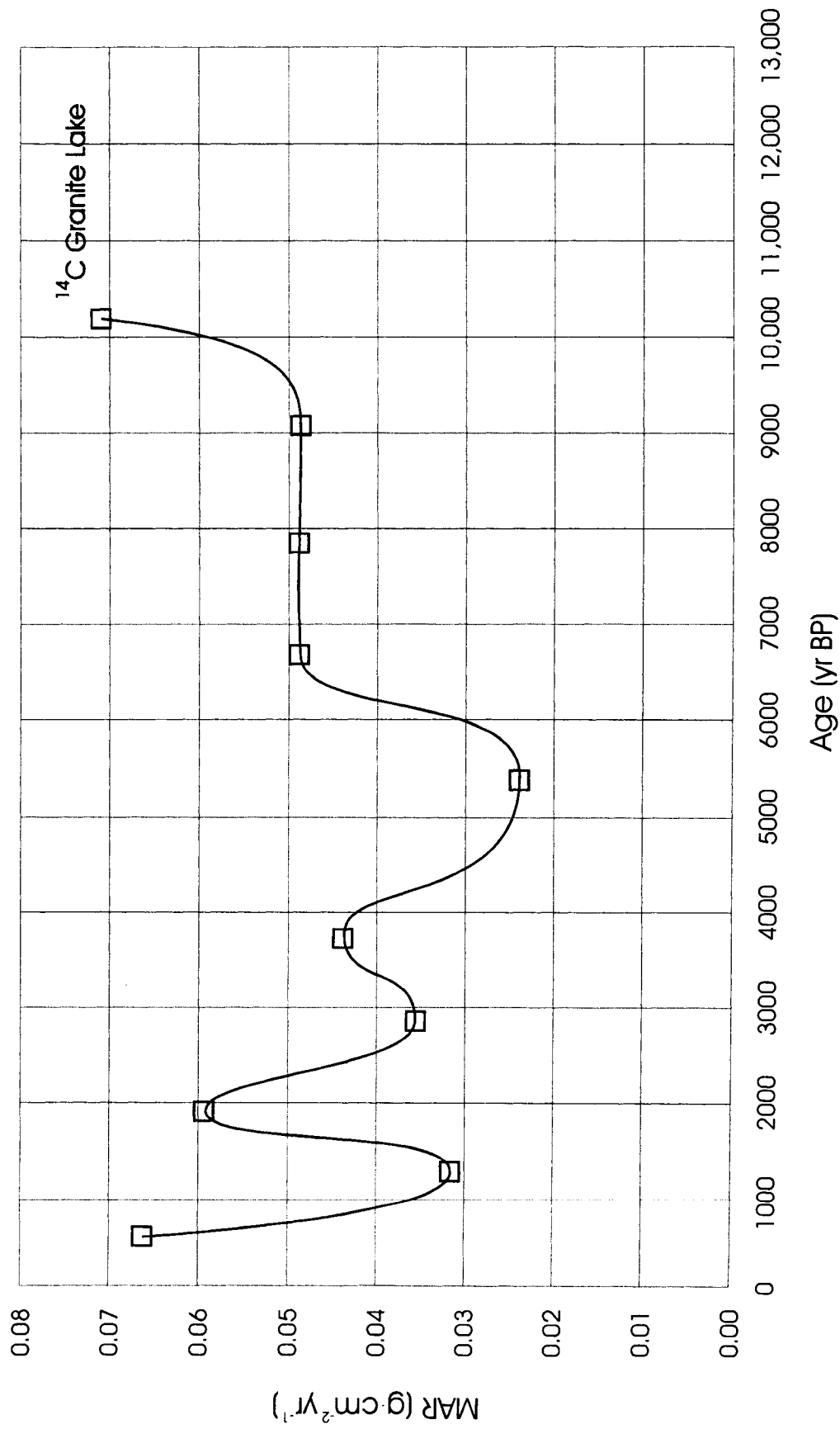


Figure 3.11 - Mass accumulation rates for ^{14}C in the JGLS.

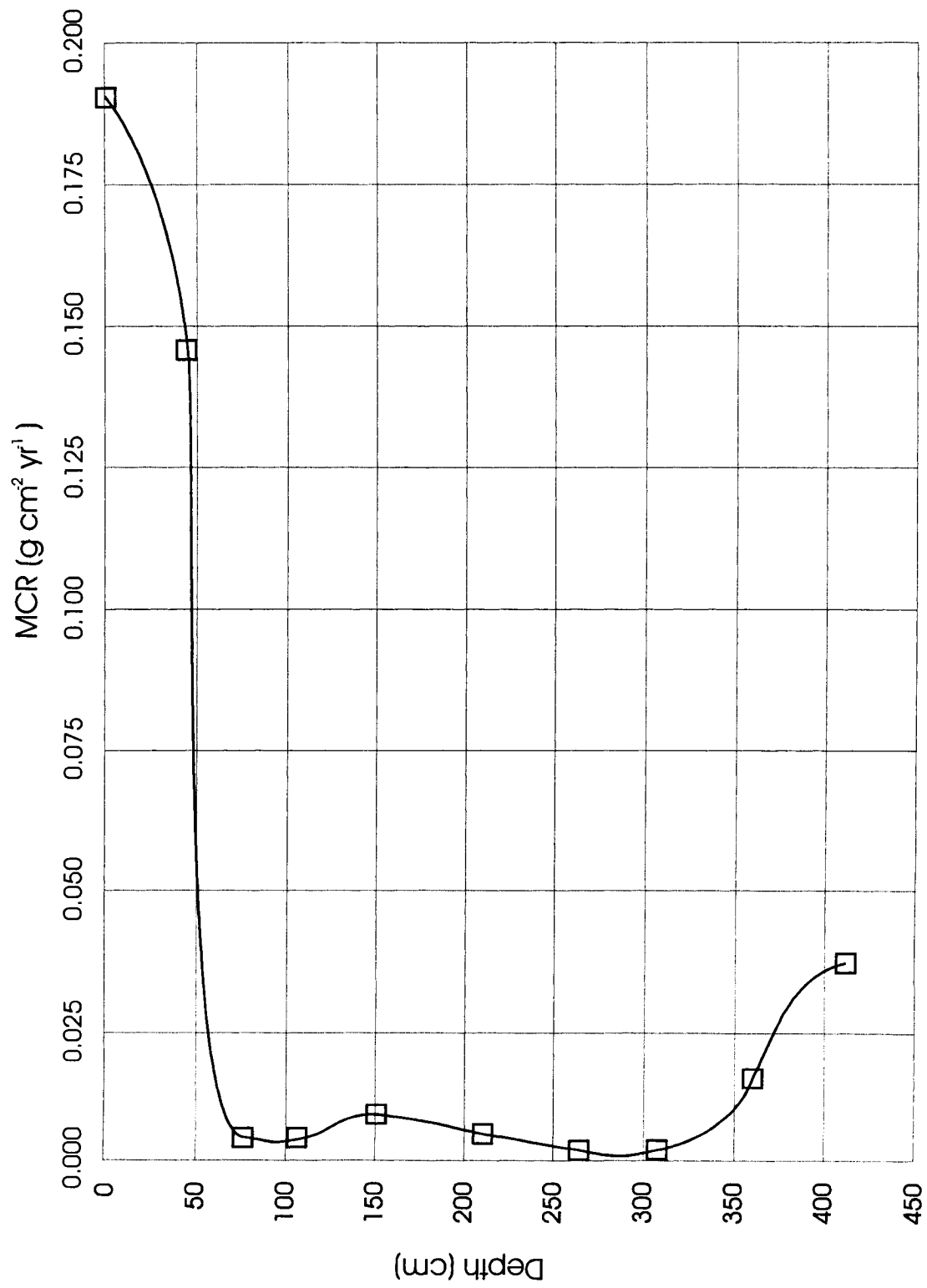


Figure 3.12 - Mass compression rates for ^{14}C in the JGLS.

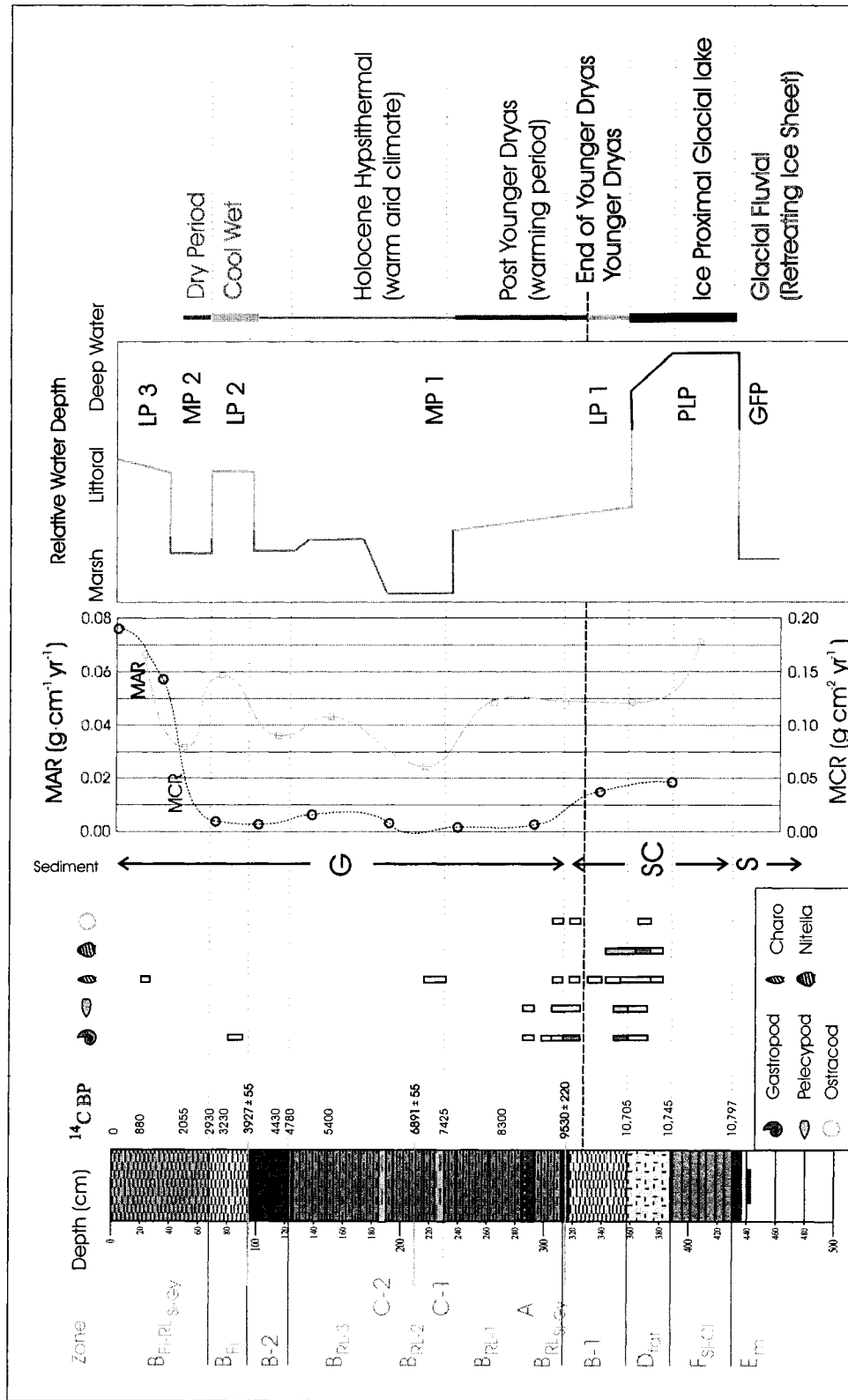
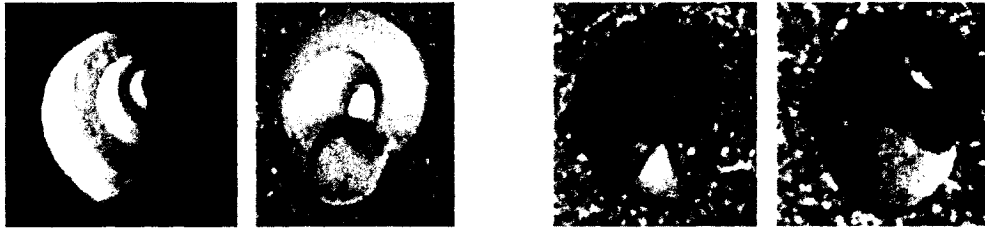


Figure 3.13 - Relative water depths, phases and climate for the James and Granite lakes system, compared to mass accumulation rates and mass compression rates during the Holocene. See text for explanation of relative water depth observations. Zone E_m is of unknown thickness. Sediment types; G - gyttja, SC - silt and clay, S - sand. Darker values of paleoindicators represent greater abundance. LP = Lake Phase; MP = Marsh Phase; PLP = Proximal Lake Phase; and GFP = Glacial Fluvial Phase.

Plate 3.1 – Gastropods: (a), (b) & (j) *Valvata tricarinata* (Say, 1819), found in lakes, rivers, streams and muskeg pools in North America south of the tree line (4 mm wide; 3 mm high); (c), (d) & (k) *Amnicola* sp., found in muddy bottoms of slow moving streams and lakes in the presence of aquatic plants (3 mm wide; 3 mm high); (e) *Lymnaea stagnalis* “stagnalis” (Say, 1817), Great Pond Snail, found with typha in marsh settings (40 mm x 22 mm); (f), (g), (h) & (i) *Helisoma campanulatum* “campanulatum” (Say, 1821), Bell mouth Ramshorn found in lakes and ponds or in slow moving water (1.3 cm wide; 6 mm high); **Pelecypods:** (l) *Sphaerium transversum* (Say, 1829), long fingernail clam, found in lakes and sloughs (12 mm long); (m) *Pisidium* sp. (Schmidt, 1850), Pea clam, found in rivers and lakes (4 mm long; Clarke, 1981); **Charophytes:** (n), (o), (p) and (q) *Chara vulgaris*, oogonium of stoneworts, resembling horsetail, which make up species among macrophyte assemblages in lake and pond edges. Accumulation of lime occurs causing the oogonia to be preserved (700 µm long; 400 µm wide; Wood and Imahori, 1965)



(a)

(b)

(c)

(d)



(e)



(f)



(g)



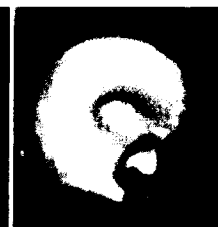
(h)



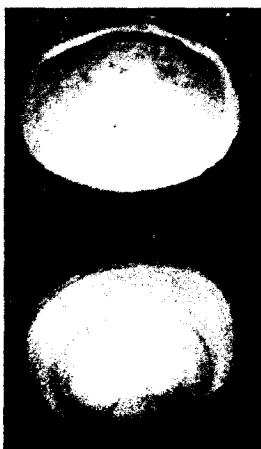
(i)



(j)



(k)



(l)

Plate 3.1



(m)



(n)



(o)



(p)



(q)

1. **Original volume**

The original volumes of the sediment samples were verified using:

$$\rho_T = \rho_w + \rho_s \Rightarrow \frac{W_T}{V_T} = \rho_w + \frac{W_s}{V_s}$$

$$\rho_w = 1.0 \text{ g/cc}$$

$$\Rightarrow \frac{W_T}{V_T} = 1.0 \text{ g/cc} + \frac{W_s}{V_s}$$

$$\frac{W_T}{V_T} = \frac{V_s + W_s}{V_s}$$

$$W_T V_s = V_T (V_s + W_s)$$

$$\therefore V_T = \frac{W_T V_s}{V_s + W_s} \quad (\text{A-3-1})$$

where

ρ_T is the total sample density

ρ_w is the density of the water

ρ_s is the density of the sediment

W_T is the weight of the sample

W_w is the weight of the sediment

V_T is the total volume of the sample

V_s is the volume of the dry sediment

Appendix A to Chapter Three
Mathematical derivations

2. ***Initial and final void ratio***

the initial and final void ratios for a layer were extrapolated using the rate of change in void ratio within that layer;

$$\Delta e_r = \frac{e_1 - e_2}{b_e} \quad (\text{A-3-2})$$

$$e_i = \Delta e_r (b_f - b_{e_i}) \quad (\text{A-3-3})$$

$$e_f = \Delta e_r (b_f - b_{e_2}) \quad (\text{A-3-4})$$

where

Δe_r is the change in void ratio with depth within a layer

e_1 is the void ratio of the upper sample

e_2 is the void ratio of the lower sample

b_e is the thickness of the sediment between samples

b_f is the thickness of the total layer

b_{e1} is the thickness between sample 1 and the bottom of the layer

b_{e2} is the thickness between sample 2 and the top of the layer

3. ***Change in height of layer***

Using Walton's method (1970) to derive the change in height of a layer without the original thickness of the layer;

Appendix A to Chapter Three
Mathematical derivations

$$\Delta h_L = \frac{e_i - e_f}{1 + e_i} b_i \quad (\text{A-3-5})$$

$$b_i = b_f + \Delta h_L \quad (\text{A-3-6})$$

Combining (A-3-1) and (A-3-2):

$$\Delta h_L = \frac{e_i - e_f}{1 + e_i} (b_f + \Delta h_L)$$

$$\Delta h_L (1 + e_i) = (e_i - e_f)(b_f + \Delta h_L)$$

$$\Delta h_L + \Delta h_L e_i = b_f e_i - b_f e_f + \Delta h_L e_i - \Delta h_L e_f$$

$$\Delta h_L + \Delta h_L e_f = b_f e_i - b_f e_f$$

$$\Delta h_L (1 + e_f) = b_f (e_i - e_f)$$

$$\therefore \Delta h_L = \frac{b_f (e_i - e_f)}{(1 + e_f)} \quad (3-6)$$

Where Δh_L is the change in height of the layer with compression
 e_i is the original void ratio
 e_f is the final void ratio
 b_i is the original layer thickness
 b_f is the final layer thickness

4. *Time Model*

Using equation 3-13, all time references with depth in the JGLS gyttja were calculated. Because the sedimentation rate of the Pleistocene varves is greater than that of the gyttja which came later, a ratio was calculated, then, added to the calculated oldest date for the gyttja. It is assumed that the sedimentation rate for all Pleistocene clays and silts was the same. This model further assumes that a constant sedimentation rate exists between actual ^{14}C Age data.

Therefore;

26 cm of massive clay in "x" yrs

44 cm of varves in 52 yrs

so
$$\frac{x}{26} = \frac{52}{44}$$

then
$$x = \frac{26 \times 52}{44} = 30.7 \text{ yr.}$$

the resulting time model is:

Appendix A to Chapter Three
Mathematical derivations

Depth (cm)	^{14}C Age	
20	880 ± 72	
48	2055 ± 78	
68	2930 ± 86	
75	3230 ± 89	
90	3926 ± 55	NZA # 12869
110	4430 ± 67	
120	4655 ± 68	
125	4780 ± 69	
150	5405 ± 76	
210	6891 ± 55	NZA # 12870
216	7065 ± 67	
230	7425 ± 77	
265	8295 ± 125	
312	9510 ± 209	
313	9530 ± 220	WAT # 4178
360	$10,705 \pm 240$	
385	$10,735 \pm 220$	
430	$10,780 \pm 220$	

CHAPTER FOUR

AQUATIC CHEMISTRY

Abstract

Based on aquatic chemistry, the surface waters entering James Lake from the north, are carbonate poor, Na-K waters that mixed with the James Lake Neutral (JLN) waters, bottom waters that display no dominant ions. A waste rock pile associated with the abandoned Northland Pyrite Mine, which operated from 1906 to 1911, forms another water type, the low pH (3.0) Magnesium-Sulfate (Mg-SO_4) waters. These waters mix with the Na-K waters, raising the pH (5.5) and precipitate out excess metals before exiting at the south end of James Lake. The Mg-SO_4 waters are mediated by a man-made dolomitic-limestone causeway, isolating a Ca-SO_4 water variant to the west of James Lake, in the abandoned mine trench. Lastly, a high pH (7.9), Calcium-BiCarbonate (Ca-HCO_3) variant of the JLN waters is found in northern Granite Lake near a beaver lodge.

The above waters correlate with the three bulk chemistry zones at the sediment-water interface in the present lake. These zones are based on the eutrophic indicator phosphorus, and using copper, zinc and manganese as proxies, can be traced back to the end of the Pleistocene glaciation (> 8400 yr. BP). Sediment Zone (SZ) 1 corresponds to the Na-K waters in the present southern James Lake. SZ 2 corresponds to the JLN waters

in northern James Lake, and SZ 3 corresponds to the Mg-SO₄ waters in the southwestern part of James Lake.

Introduction

Natural water systems receive chemical inputs from surrounding ecosystems causing the waters to undergo chemical changes (Stumm and Morgan, 1996). Anion – cation chemistry can be used to classify natural waters and determine changes in the chemical composition of mixtures of these waters (Freeze and Cherry, 1979; Morel and Hering, 1993; Stumm and Morgan, 1996). Trace metal analysis in waters can indicate biological stressors in the present system from world-wide or local sources (Wetzel, 2001; Stumm and Morgan, 1996), while bulk sediment chemistry can reflect metal concentrations of the environment over time (Stumm and Morgan, 1996).

Evaluation of water properties such as electrical conductivity, pH, oxygen content, surface temperatures and temperature depth profiles has been used to display valuable information about the system as a whole. Previous research has indicates that electrical conductivity closely fits a straight line regression with total dissolved solids (TDS), enabling one to approximate TDS (Hem, 1985). The pH gives important information on geochemical equilibrium and solubility conditions in natural and contaminated groundwaters, indicating mixing of different water types and subsequent chemical reactions involving the lacustrine system (Freeze and Cherry, 1979; Hem, 1985; Morel and Hering, 1993; Stumm and Morgan, 1996).

James and Granite lakes are elongated deep mesotrophic lakes (James Lake > 13 m deep; Granite Lake > 27 m deep) that have been investigated in the past by the Ministry of the Environment (MOE) for contamination caused by seepage from the Northland Pyrite Mine waste rock pile and open pit (Gale, 1990). Remediation was attempted during the 1990s by using a crushed limestone causeway to separate James Lake from the waste rock pile and mine trench. Acid mine drainage was investigated to determine the extent of the pollution since the mine site was abandoned in 1911 (Mason, 1998) and the effect of the resulting acidity was investigated using arcellaceans to determine how long the environmental effects of the waste rock pile had been occurring (Kumar and Patterson, 1997).

This research seeks to classify the water types in the lake system, and whether it has changed since remediation was attempted. Anion – cation chemistry, and trace metal chemistry was used to classify the waters, which were then compared to the information contained in the MOE report. In addition, the sediment chemistry was investigated to determine the chemical history through the Holocene. This information was then used to determine whether the only stressors on the water system were as a result of the pyrite vein at the mine site, or if other external influences such as beaver could be involved.

Field and laboratory methods are described in Chapter Two.

Analysis and Results

The results for trace metal analyses of the twelve sediment-water interface pore water trace metal analyses from James Lake are reported in Table 4.1 (Fig. 4.1), while the results for the nine piezometer pore water samples from James Lake and the one sediment-water interface pore water sample from Granite Lake are reported in Table 4.2. The major ion results of the twelve sediment-water interface (SWI) pore water samples from James Lake, one sediment-water interface pore water sample from Granite Lake, and eight MOE surface water samples (Gale, 1990) are reported in Table 4.3. Data for fourteen bulk sediment chemistry samples are reported in Table 4.4.

Anions and Cations

The major ion data are plotted on a Piper trilinear plot, modified with a triangular area (Fig. 4.2), by converting the anion and cation concentrations to millequivalents per litre (meq) and then calculating percentages for the individual major cation (Na^+ , K^+ , Mg^{2+} , Ca^{2+}) and anion (Cl^- , SO_4^{2-} , HCO_3^- , and CO_3^{2-}) species (Table 4.3) (Hill, 1940; Piper, 1944; Freeze and Cherry, 1979; Güller et al., 2002; Hem, 1985; Rao, 1998).

The data from the bottom waters are grouped into two water types as determined from the trilinear plot and mapped in Figure 4.3. The James Lake Neutral waters (JLN) are Mg poor, display no dominant anion or cation, and, are present in the northern and southern parts of James Lake (samples TP 1-4, 7 & 10; Fig. 4.3). The second water type is Na – K poor, with SO_4 almost the sole anion and is present in the vicinity of the Northland Pyrite Mine waste rock pile in the southwestern bay of James Lake (samples

TP 5, 6, 9, 11 & 12; Fig. 4.3). These Magnesium – Sulfate waters (Mg – SO₄) waters have an elevated TDS content compared to JLN waters, and display a range of Ca – Mg values across the man-made dolomitic-limestone causeway separating the Northland Pyrite Mine trench from the southwestern bay of James Lake. The bottom waters in northern Granite Lake are a more Ca and HCO₃ rich version of the JLN waters present in northern James Lake (TP 13). Last, the waters leaving the southern outlet in James Lake (TP 8) are Mg and HCO₃ poor waters similar to those that typify the surface waters of James and Granite lakes during mid June 1989 (TP 14 – 21; Gale, 1990), and enter the James Lake system from Pike Lake to the north.

Water Properties

As indicated in Chapter Two, electrical conductivity, pH, oxygen concentration and temperature measurements were obtained in James and Granite lakes from 2000 to 2003 and the results recorded in Tables 4.5, 4.6 & 4.7.

Electrical conductivity (EC) is the ability of water to conduct an electrical current, and is the reciprocal of electrical resistance. EC reflects total dissolved solids (TDS; mg/L), to which it can be converted using the methods outlined in Hem (1985),

$$TDS = AC \quad (4-1)$$

where C is the electrical conductivity and A , the conversion factor, has a value of 0.54 for Cl⁻ – rich waters and up to 0.96 for SO₄²⁻ – rich waters. The results of this calculation were used to indicate the TDS for TP 13 in Fig. 4.2. EC values varied in the overall lake

system, ranging from 120 to 15,240 $\mu\text{S}/\text{cm}$ (Fig. 4.5, 4.6 & 4.7). The JLN waters, located adjacent to two beaver lodges, indicated an EC of 120 $\mu\text{S}/\text{cm}$ in the surface waters, and 134 to 197 $\mu\text{S}/\text{cm}$ in the pore waters at the SWI. The Mg-SO_4 waters indicated 1297 to 2200 $\mu\text{S}/\text{cm}$ in the surface waters, and up to 7200 $\mu\text{S}/\text{cm}$ in the pore waters at the SWI. The Ca-rich variation of the Mg-SO_4 waters indicated an EC which varied from 1898 to 9490 $\mu\text{S}/\text{cm}$ in the surface waters due to isolation by the limestone causeway. The Na-K-Cl waters contain up to 80 mg/L of TDS in its surface waters, and 82 mg/L in the pore waters at the SWI. The transitional waters between the JLN and Mg-SO_4 waters leaving James Lake indicated an EC in the surface waters of 142 $\mu\text{S}/\text{cm}$. The EC in the surface waters within the marsh range from 142 $\mu\text{S}/\text{cm}$, immediately south of the north beaver dam, to 208 $\mu\text{S}/\text{cm}$ just north of the south beaver dam. From this point, the EC dropped continually until reaching 130 $\mu\text{S}/\text{cm}$ in the surface waters of Granite Lake. The EC was not monitored in northern Granite Lake, but the EC in the surface waters was 127 $\mu\text{S}/\text{cm}$ adjacent to Highway 11.

Surface water pH ranged from 6.0 to 7.0 in northern James Lake, from 4.8 to 6.0 in southern James Lake, from 2.2 to 6.5 in the vicinity of the Northland Pyrite Mine in southwestern James Lake, and from 7.0 to 7.9 in northern Granite Lake (Fig. 4.4). Surface water pH tended to be higher near a beaver lodge, 7.9 in northern Granite Lake and 6.9 in northern James Lake, and lower (pH = 5.0) immediately upstream of the two beaver dams. The pH of the waters traversing the marsh between James and Granite lakes increased to 6.0, then dropped abruptly to 5.0, adjacent to the upstream side of the south beaver dam. Downstream of the south beaver dam, within the mid portion of Granite Lake, the pH was 5.0. Pore-water readings obtained from the piezometers placed

adjacent to the Northland Pyrite Mine waste rock pile indicated a pH range of 2.95 to 3.34, from 1.05 to 1.60 m below the SWI respectively.

Measurements of oxygen concentrations indicate a range of 6.67 to 8.30 mg/L in the surface waters of James Lake, 6.73 to 8.02 mg/L in the marsh and 8.76 to 9.20 mg/L in Granite Lake. Oxygen concentrations as low as 0.12 mg/L in 11.0 m depth of water in northern James Lake, and 0.13 mg/L in 11.0 m depth in the Northland Pyrite Mine trench indicate anoxia at depth. Oxygen profiles were obtained in the mine trench and in northern James Lake (Table 4.8; Figs. 4.7 & 4.8), indicating that the lake was anoxic below 4.5 m during August 2003, and that the mine trench was anoxic below 3 m during August 2003.

Surface water temperature measurements in James Lake ranged from 16.3 to 19.6 °C, while those in Granite Lake ranged from 22.6 °C just south of the marsh to 19.0 °C at the boat launch near Highway 11. Temperatures in the marsh increased from 18.4 °C just south of the northern beaver dam, to a high of 24.7 °C in mid-marsh (mid-day summer temperatures) before dropping to 16.1 °C just to the north of the southern beaver dam.

To determine stratification within the lake waters, three temperature profiles were obtained (Table 4.8). In northern Granite Lake, profile GLTPr 99-1 showed the epilimnion to be 4.3 m deep with a temperature variation from 19.6 to 21.3°C (Fig. 4.6). The metalimnion indicated a temperature drop of 11°C over 3.7 m. The hypolimnion, below 8.0 m, indicated a temperature approaching 7.0°C at 14 m depth.

In northern James Lake, and in the mine trench of the Northland Pyrite Mine site, more sensitive equipment enabled us to obtain profiles that included temperature, oxygen content and electrical conductivity. In the trench of the Northland Pyrite Mine, profile

NPMTPr 02-2 showed a surface temperature of 16.3°C, which dropped to 15.2°C over the 2.0 m thick epilimnion (Fig. 4.7). Within the epilimnion at this site, dissolved oxygen dropped from 6.7 to 0.3 mg/L, and the EC drops from 930 to 667 $\mu\text{S}/\text{cm}$. The metalimnion, which was one meter thick at this site, showed a temperature change of 5.8°C, dropping from 15.2 to 9.4°C at the top of the hypolimnion. The oxygen content dropped 0.14 mg/L, from 0.30 to 0.16 mg/L; and the EC dropped 211 $\mu\text{S}/\text{cm}$, from 667 to 456 $\mu\text{S}/\text{cm}$. Below 3.0 m was the hypolimnion where the temperature dropped slowly from 9.4 to 6.5°C at 11 m depth. The oxygen content showed minor fluctuations between 0.13 and 0.18 mg/L within the hypolimnion, and EC dropped 59 $\mu\text{S}/\text{cm}$, from 456 to 397 $\mu\text{S}/\text{cm}$.

The northern James Lake profile (JLTPr 03-3; Fig. 4.8) showed a surface temperature of 17.8°C, which dropped by 0.1°C over the 3.0 m thick epilimnion. Within the epilimnion at this site, dissolved oxygen dropped from 8.33 to 7.97 mg/L, and the EC was stable at 119 $\mu\text{S}/\text{cm}$. The metalimnion, which is 1.5 m thick at this site, shows a temperature change of 9.9°C, dropping from 17.7 to 7.8°C to the top of the hypolimnion. The oxygen content dropped 7.69 mg/L, from 7.97 to 0.28 mg/L; and the EC increased 52 $\mu\text{S}/\text{cm}$, from 119 to 171 $\mu\text{S}/\text{cm}$. Below 4.5 m was the hypolimnion where temperature dropped from 6.9 to 5.7°C at the bottom. The oxygen content dropped to 0.18 mg/L within the hypolimnion, and the EC increased 10 $\mu\text{S}/\text{cm}$ to 182 $\mu\text{S}/\text{cm}$ at the bottom. These thermal zones show the water stratification in James and Granite lakes (Fig. 4.9).

Trace Metals

Twenty-two water samples were obtained from James and Granite lakes

(Chapter Two) and analyzed for trace metals. The logarithms of the molar concentrations for some of these metals were plotted against pH in order to differentiate zones of supersaturation from zones of undersaturation within the James Lake. Figure 4.10a plots Fe, Al, Ca, Mg, Cu, Zn and P for 11 bottom water samples in James Lake, and one in Granite Lake. Figure 4.10b plots Fe, Al, Ca, Mg, Cu and Zn for seven sub-bottom pore water samples and two surface samples in James Lake. These data plot in two groups depending on proximity to the waste rock pile in southwestern James Lake. Waters near the waste rock pile indicated low pH (2.0 – 3.5) with high metal concentrations, while those further away had higher pH (5.0 – 6.9) with lower metal concentrations.

In order to model precipitation in this lake system, WATEQ4F, Version 2.63 was used to investigate sites of possible mineral precipitation in the lake system. Oversaturated conditions are indicated when the ion activity product (IAP) is greater than the solubility equilibrium constant (K_{SP} ; Stumm and Morgan, 1996). WATEQ4 computes a saturation index (SI), as follows,

$$SI = \log_{10} \left(\frac{IAP}{K_{SP}} \right) \quad (4-2)$$

indicating super saturation (precipitation) by positive results and undersaturation (dissolution) by negative results. Fe, Al, Cu, Pb, Mn and P are supersaturated in the bottom waters in northern James Lake with possible precipitation of Fe and Cu oxides, Fe and Al hydroxides, and Mn and Pb phosphates. Fe, Al and Cu are supersaturated in the

bottom waters in southern James Lake with possible precipitation of Fe and Cu oxides and Fe and Al hydroxides. Ba and Cu are supersaturated near the waste rock pile and within the mine trench, with possible precipitation of Ba sulfate, Cu metal and Cu oxide. Lake surface waters in James and Granite lakes are oversaturated with Fe and Al with possible precipitation of Fe oxides and Fe and Al hydroxides. This oversaturation maximizes in southern James Lake (Table 4.9).

Bulk Sediment Chemistry

Twelve metals (Table 4.4) were analyzed from 14 sediment water interface bulk sediment chemistry samples for distribution characteristics. The relative fractional abundance (X_i) associated with each of the metals was calculated by

$$X_i = \frac{m}{N_i} \quad (4-3)$$

where m is the concentration of the metal in $\mu\text{g/g}$ and N_i is the total concentration of the metals in the sample. The standard error (S_{X_i}) was calculated by

$$S_{X_i} = 1.96 \sqrt{\frac{X_i(1 - X_i)}{N_i}} \quad (4-4)$$

and based on these results, four statistically insignificant species (As, Cd, Co & Ag) were removed and not included in the subsequent multivariate analysis.

Data screening was employed to evaluate the distribution characteristics of each chemical species. Data were log-transformed (except for pH) so that they more closely reflected a normal distribution, then variables were standardized by calculating their z-scores (standard scores), using

$$z_i = \frac{x_i - \bar{x}}{s} \quad (4-5)$$

where z_i is the standard score of the sample i , x_i is the value of the sample i , \bar{x} is the mean, and s is the standard deviation of the concentration of the sample (Boudreau, 1999; Güller et al., 2002). Cluster data from the sediment-water interface bulk sediment samples in James Lake are given in Table 10.

Q-mode cluster analysis was carried out on the standard scores, using Ward's Minimum Variance method to determine the statistically significant populations, resulting in a reduced data set that was recorded with squared Euclidean distances. R-mode was used to determine the chemical species relationships, then combined with the Q-mode results in a hierarchical diagram to illustrate the results (Fig. 4.12a). Three sediment zones (SZ) were determined, all dominated by concentrations of iron greater than five ppm. SZ 1 contains dominant copper (0.48 to 0.66 mg/g) and zinc (0.43 to 0.49 mg/g) and plots to the south in James Lake (Fig. 4.13). SZ 2 contains dominant phosphorus (0.39 to 1.34 mg/g) and manganese (0.23 to 0.64 mg/g) and plots north of the narrows in James Lake. Finally, SZ 3 contains dominant phosphorus (0.14 to 2.07 mg/g) and plots in the vicinity of the waste rock pile in southwestern James Lake. The highest

phosphorus was recorded in the vicinity of a beaver lodge (JLB 96-10) in SZ 3, immediately north of the waste rock pile.

Mason (1998) previously investigated 46 bulk chemistry samples, at various depths from four separate cores taken in 1997 in southern James Lake. The above metals (species of interest), except phosphorus, were analyzed using the same laboratory methods discussed previously. In order to use this information as a proxy for phosphorus (and eutrophism), data screening and cluster analysis were used to investigate six metals from the sediment-water interface bulk chemistry database (Cr, Cu, Pb, Mn, Ni and Zn) that were found with phosphorus, and the results (Fig. 4.12b) indicated the same sediment zones as outlined in Figure 4.12a and plotted in Figure 4.13.

The above fourteen sediment-water interface bulk sediment chemistry samples (Table 4.4) were analyzed with the 46 samples describe by Mason (1998). Following the procedure outlined, the distribution characteristics resulted in a combined Q-mode and R-mode hierarchical diagram (Fig. 4.14) that indicated five SZs existed in this system in the past. SZ 1 indicates a eutrophic zone occurred in southern James Lake, as displayed in three of Mason's cores, since the Medieval Warm Period (> 800 yr. BP). SZ 2 only occurs in the sediment-water interface of the present lake. SZ 3 indicates the chemical environment that is seen adjacent to the Northland Pyrite Mine waste rock pile today, and can be seen to have occurred in the past as far back as 8400 yr. BP. SZ 4 and SZ 5 are not present in the James and Granite lake system today. SZ 4 displays the chemistry of the recent past (last 100 yrs?) at the JL 99-1 core site. Here the iron stained silt is dominated by Fe (412,000 – 428,000 ppm) the greatest amount occurring 100 yr. BP. This sediment also contained dominant As (164 – 420 ppm) and Cu (239 – 325 ppm). SZ

5 displays high concentrations of Fe, Zn, Ni and Co, adjacent to JL 99-1 core site at the unconformable upper boundary of the Holocene Hypsithermal (> 4115 yr. BP).

Discussion

Water Stratification

Both James and Granite lakes are dimictic lakes. Although the lakes are relatively small, lack of water mixing causes anoxia in the deeper basins. At the end of August, 1999, the hypolimnion in Granite Lake was prominent below seven metres, with the temperature dropping to 7°C at the SWI from 20°C at the lake surface in a 16 m deep northern basin. In the Northland Pyrite Mine trench, the epilimnion was less than two metres thick, due to the orientation (N-S) of the open trench, which prevented warming of the waters due to limited sun exposure. The temperature drop was smaller in the trench, dropping 10°C to the measured depth in the hypolimnion (11 m) as opposed to the northern James Lake basin, where the change in temperature to the same depth was 12°C, primarily due to the difference in surface water temperature. The oxygen content within the hypolimnion at both of the James Lake sites was consistently below 0.20 mg/L. Although the oxygen content was not measured at 16 m in Granite Lake, sediment obtained at the SWI was black, reduced gyttja, readily releasing H₂S, and quickly oxidizing upon exposure to the atmosphere.

Major Ion Chemistry

The natural waters of the James Lake system were classified using a Hill-Piper

Trilinear Plot (Fig. 4.2). The diamond shaped plot at the top gives an indication of the types of waters present, and whether mixing occurs. The waters at the north of James Lake are JLN type waters that indicate no dominant cation or anion. These waters, which plot in the neutral zone, in the center of the rectangular area of the trilinear plot, are similar to neutral groundwater (Freeze, 1979; Morel and Hering, 1993; Stumm and Morgan, 1996) with a surface-water pH of 6.6 (SWI pH 6.9). The Na-K waters, which typify the waters leaving James Lake to the south, have a surface pH of 5.5 (SWI pH 5.4) and plot towards the right in the rectangular zone of the Trilinear Plot, indicating that a low amount of carbonate is present in southern James Lake (relative to SO_4 and Cl), past the narrows. This may be due to mixing with the sulfate-rich waters present in the vicinity of the Northland Pyrite Mine waste rock pile. These Mg-SO_4 waters plot at the top of the triangular zone, and result from AMD from the waste rock pile in the southwestern corner of James Lake. They are mediated by a dolomitic-limestone causeway which barricades the mine trench from the lake. The low pH Mg-SO_4 waters (surface water 5.0; SWI 3.0) are neutralized by mixing with the JLN waters before entering the marsh to the south of the lake as Na-K waters. These Na-K (surface) waters are similar to the surface waters investigated by the MOE during June 1989. The waters traversing the marsh between James and Granite lakes have a beaver-mediated pH which increases from 5.0 to 6.0 between two beaver dams, then drops to 5.0 at the southernmost beaver dam before the waters exit into Granite Lake displaying the same surface water signature identified from the 1989 MOE data (Gale, 1990).

The lake-waters in northern Granite Lake are enriched in Ca and bicarbonate. These Ca-HCO_3 waters have a surface-water pH of up to 7.9 (SWI pH as low as 7.0) and

mix with waters from the James and Granite lakes marsh before leaving the southeastern end of Granite Lake with a pH of 5.0.

Dissolution/Precipitation Chemistry

The lake bottom waters adjacent to the Northland Pyrite Mine waste rock pile have low pH due to sulfuric acid generation. This acid is produced through the oxidation of exposed sulfides in the waste rock. Pyrite (FeS_2) and pyrrhotite (Fe_{1-x}S) are the two most dominant sulfides present in the waste rock. Pyrite oxidizes in the presence of water (groundwater or lake water) and oxygen to form sulfate, releasing Fe^{2+} and sulfuric acid to the water. Fe^{2+} can be oxidized to Fe^{3+} which hydrolyzes to form $\text{Fe}(\text{OH})_3(\text{s})$ releasing more acid to the water and coating the lake bottom (Stumm and Morgan, 1996), and ultimately lowering the pH in southwestern James Lake. Although the surface-water pH near the waste rock pile is only slightly lower (5.0) than that which is found in the southern part of the lake (5.6), the waters at the SWI exhibit a pH between 2.0 and 3.0.

This low pH enables the waters to become saturated with high amounts of dissolved metals, resulting in high concentrations of Fe of up to 11,800 mg/L immediately adjacent to the waste rock pile, and concentrations as high as 12,200 mg/L within the pore-waters at one to two meters under the SWI where the pH is as low as 2.9. The saturation of the metals in the waters at this site is controlled by the IAP and the K_{SP} of metal in solution as indicated with eq. 4-2 (Stumm and Morgan, 1996). If the result is negative, the system is undersaturated and dissolution of metals should continue. At this site the TDS within the waters reaches 5600 mg/L at the lake-bottom and reaches 6755 mg/L in the pore-waters below the SWI. As the waters migrate to the south, away from

the waste rock pile, the pH increases to around 5.0 and the system becomes oversaturated ($IAP > K_{SP}$), initiating the precipitation of metals and a reduction in the TDS levels.

The emplacement of a crushed dolomitic-limestone causeway during the 1990s at the southwestern edge of James Lake was an attempt to try to rejuvenate the waters of the mine/trench. This causeway separates the lake from the abandoned mine trench and pond which are exposed to the sulfide vein within the ground. These waters, which contain high amounts of Ca and SO_4^{2-} , have a pH approaching 2.0 and contain TDS levels of up to 5600 mg/L. A side effect of the limestone causeway may be the amount of Ca^{2+} introduced into the system. Although these waters are usually separated from the lake waters, higher spring runoff may let these waters escape into James Lake. In addition, the causeway does not contain the waste rock pile, causing the remediation attempt to fail.

Beaver dams raise the water level in the lake, allowing the waters from behind the causeway to escape, lowering the pH and raising the amount of TDS in the system. The pH in the immediate vicinity of the beaver lodges tends to be higher than the pH at beaver dams, because beaver impoundments generate acid neutralizing capacity by acting as sinks for NO_3 , and sources for NH_4 , Fe and Mn (Cirimo, 1993; Margolis, 2001). In northern James Lake, the pH in the surface waters adjacent to an active lodge is 6.6 (SWI pH is 6.9), while in northern Granite Lake, the pH in the surface waters adjacent to an active lodge is 7.6 (SWI pH is 7.9). The pH drops to 5.0 immediately downstream of both beaver dams, and increases to 6.0 upstream of the beaver dam immediately north of Granite Lake, as corroborated by previous research indicating an increase in pH downstream from a beaver dam (Smith, 1991; Cirimo, 1993; and Margolis, 2001).

Bulk-Sediment Chemistry

When the pH is below 5.5, the amount of P and Mn in the lake-bottom sediment drops because of the solubility of Fe and Al (Lucas and Davis, 1961). SZ 2 has sites with concentrations of P from 1.340 ppm (0.51 ppm Mn) near a beaver lodge in the north (2.44 mg/L Fe), and 2.07 ppm (0.07 ppm Mn) near a beaver lodge in the south (2.26 mg/L Fe). Sites near the waste rock pile (SZ 3) show low concentrations of P (0.084 ppm; 0.019 ppm Mn) with high concentrations of Fe in the bottom water (11,800 mg/L). At low pH, as found in SZ 3, phosphoric acid is the dominant P species, and the aqueous concentration in the vicinity of the waste rock pile corroborates this with concentrations of 7.8 mg/L (as opposed to 0.2 to 0.3 mg/L in the north). Since plants need higher concentrations of soluble reactive phosphorus (SRP), or PO_4^{2-} (SRP tends to dominate at higher pH), as was observed at the SWI near the waste rock pile, plants tended not to grow, leaving the system open to erosion.

Increased P and Mn in the sediment within the lakes and marshes indicates eutrophic conditions. This could have resulted from beaver activity, as is occurring today in most lakes in the Temagami region of Ontario (Klotz, 1998). It is possible that beaver activity had been occurring in the area of James and Granite lakes from the end of the Pleistocene to the present. SZ 1 and SZ 3 indicate that P and Mn was present in the sediment prior to 8400 yr. BP as indicated in the Pleistocene glacial-fluvial silty-sand, and as indicated in the sediment zones B_{Fi} and B_{Fi-RL} in the present.

Conclusions

The aquatic chemistry of the James and Granite lakes system is controlled by surface water entering James Lake from the north. These waters are carbonate poor Na-K waters, which mix with the JLN waters, ultimately displaying no dominant ions. The early summer waters precipitate Fe oxides and Fe and Al hydroxides on their journey to the south of the lake with the exception of the vicinity of the Northland Pyrite Mine waste rock pile in the southwestern part of James Lake. The Na-K lake waters are mixed with the Mg-SO₄ waters resulting from acid mine drainage, before exiting towards Granite Lake to the south.

The effect of metal contamination indicating possible eutrophic conditions has existed at this site since at least 8400 yr. BP. Cluster analyses of sediment can indicate periods in the past where high nutrient content, such as P and Mn, existed in an environment, possibly indicating periods of beaver activity in the lake system.

References

- Boudreau, B. P., 1999, Metals and models: Diagenetic modelling in freshwater lacustrine sediments: *Journal of Paleolimnology*, v. 22, p. 227 - 251.
- Cirno, C. P., and Driscoll, C. T., 1993, Beaver pond biogeochemistry: acid neutralizing capacity generation in a headwater wetland: *Wetlands*, v. 13, p. 277 - 292.
- Freeze, R. A., and Cherry, J. A., 1979, *Groundwater*: Englewood Cliffs, NJ, Prentice Hall, 604 p.

- Gale, P., 1990 James Lake Environmental Assessment, Technical Memorandum.
Ministry of the Environment. Sudbury, ON. 16 pp.
- Güller, C., Thyne, G. D., McCray, J. E., and Turner, A. K., 2002, Evaluation of graphical and multivariate statistical methods for classification of water chemistry data: *Hydrogeology Journal*, v. 10, p. 455 - 474.
- Hem, J. D., 1985, Study and Interpretation of the Chemical Characteristics of Natural Water, Alexandria, Va, U. S. Geological Survey, 264 pp.
- Hill, R. A., 1940, Geochemical patterns in Coachella Valley, California: *American Geophysical Union Transactions*, v. 21, p. 46 - 49.
- Klotz, R. L., 1998, Influence of beaver ponds on the phosphorus concentration of stream water: *Canadian Journal of Fisheries and Aquatic Sciences*, v. 55, p. 1228 - 1236.
- Kumar, A., and Patterson, R. T., 1997, Arcellaceans (Thecamoebians): new tools for monitoring short-term changes in lake bottom acidity: *Environmental Geology* 39 (6), p. 689 - 697.
- Lucas, R. E., and Davis, J. F., 1961, Relationships between pH values of organic soils and availabilities of 12 plant nutrients: *Soil Science*, v. 92, p. 177 - 182.
- Margolis, B. E., Castro, M. S., and Raelsy, R. L., 2001, The impact of beaver impoundments on the water chemistry of two Appalachian streams: *Canadian Journal of Fisheries and Aquatic Sciences*, v. 58, p. 2271 - 2283.
- Mason, G., 1998, A study of the effects of past mining activities on James Lake sediment chemistry: Unpub. B.Sc. Honours thesis, Carleton University 28 p.
- Morel, F. M. M., and Hering, J. G., 1993, Principles and Applications of Aquatic Chemistry: New York, John Wiley & Sons, Inc, 588 p.

- Piper, A. M., 1944, A graphic procedure in the geochemical interpretation of water analysis: American Geophysical Union Transactions, v. 25, p. 914 - 923.
- Rao, N. S., 1998, MHPT.BAS: a computer program for modified Hill-Piper diagram for classification of ground water: Computers & Geosciences, v. 24, p. 991 - 1008.
- Smith, M. E., Driscoll, C. T., Wyskowski, B. J., Brooks, C. M., and Cosentini, C. C., 1991, Modification of stream ecosystem structure and function by beaver (*Castor Canadensis*) in the Adirondack Mountains, New York: canadian Journal of Zoology, v. 69, p. 55 - 61.
- Stumm, W., and Morgan, J. J., 1996, Aquatic chemistry: New York, J. Wiley & Sons, 1022 p.
- Wetzel, R. G., 2001, Limnology: Lake and River Ecosystems: San Diego, Academic Press, 1006 p.

<i>Metals in mg/L</i>	<i>Detection Limit</i>	<i>JLB 97-26</i>	<i>JLB 97-27</i>	<i>JLB 97-28</i>	<i>JLB 97-29</i>	<i>JLB 97-30</i>	<i>JLB 97-31</i>	<i>JLB 97-32</i>	<i>JLB 97-33</i>	<i>JLB 97-34</i>	<i>JLB 97-35</i>	<i>JLB 97-38</i>	<i>JLB 97-39</i>
Aluminum	0.05	0.46	0.38	0.37	0.19	64.0	415	1.11	0.94	146.0	0.43	155.5	1.13
Arsenic	0.002	0.006	0.003	0.002	0.004	0.006	0.95	0.003	0.003	0.013	0.005	Tr	ND
Barium	0.01	0.03	0.03	0.02	0.02	0.03	0.04	0.04	0.03	0.02	0.03	0.04	0.17
Beryllium	0.002	ND	ND	ND	ND	ND	0.002	ND	ND	0.002	ND	0.002	ND
Bismuth	0.05	ND	ND	ND	ND	0.34	3.63	ND	ND	1.39	ND	1.04	ND
Cadmium	0.005	ND	ND	ND	ND	0.035	0.223	0.010	ND	0.113	ND	0.084	ND
Calcium	1.0	12.5	12.4	10.4	12.2	40.2	176	12.0	10.3	75.4	10.8	172	78.2
Chromium	0.01	ND	ND	ND	ND	0.01	3.33	0.01	0.01	0.05	0.01	0.27	ND
Cobalt	0.02	ND	ND	ND	ND	0.19	1.38	ND	ND	0.51	ND	0.65	0.03
Copper	0.01	0.03	0.01	0.06	0.03	0.46	102.5	0.05	0.06	0.49	0.01	8.85	0.16
Iron	0.01	2.44	2.84	2.36	1.52	1240	11,800	59.7	64.9	6200	14.3	4190	32.4
Lead	0.001	0.005	0.004	0.015	0.003	0.018	1.13	0.004	0.024	0.003	0.004	0.032	0.013
Magnesium	1.0	1.8	1.8	1.6	1.9	30.6	214	2.3	1.6	62.9	2.1	65.1	6.5
Manganese	0.005	0.839	0.663	0.356	0.218	3.51	41.7	0.137	0.135	10.2	0.117	10.9	0.827
Molybdenum	0.04	ND	ND	ND	ND	ND	ND	ND	ND	ND	ND	ND	ND
Nickel	0.02	ND	0.02	ND	0.03	0.22	4.03	0.04	0.10	0.65	0.03	0.63	0.20
Phosphorus	0.1	0.2	0.3	0.2	ND	ND	7.8	ND	0.2	ND	0.1	ND	ND
Potassium	1.0	ND	ND	ND	ND	ND	2.9	ND	ND	ND	ND	1.6	4.2
Silver	0.01	ND	ND	ND	ND	ND	ND	ND	ND	ND	ND	ND	ND
Sodium	1.0	13.2	15.8	15.4	18.4	14.5	13.3	14.3	17.2	15.9	16.3	7.0	4.9
Strontium	0.01	0.03	0.03	0.03	0.03	0.12	0.59	0.03	0.03	0.26	0.02	0.38	0.20
Vanadium	0.01	ND	ND	ND	0.01	0.02	0.47	0.02	0.01	0.02	0.01	0.11	ND
Zinc	0.02	0.08	0.08	0.17	0.08	2.34	73.5	0.10	0.32	6.07	0.06	7.0	1.32

Table 4.1 – Trace metal pore water chemistry from sediment-water interface sample locations in James Lake (Fig. 4.1). ND = not detected.

<i>Metals in mg/L</i>	<i>Detection Limit</i>	<i>JLP 99-1</i>	<i>JLP 99-2</i>	<i>JLP 99-3</i>	<i>JLP 99-4</i>	<i>JLP 99-5</i>	<i>JLP 99-6</i>	<i>JLP 99-7</i>	<i>JLP 99-8</i>	<i>JLP 99-9</i>	<i>GLB 02-1</i>
Aluminum	0.01	0.90	240	4.04	0.11	256	918	586	0.22	0.18	0.07
Arsenic	0.1	TR	TR	TR	TR	TR	TR	TR	TR	TR	TR
Barium	0.005	0.015	0.028	0.030	0.067	0.009	TR	TR	0.013	0.013	0.021
Beryllium	0.005	TR	0.014	TR	TR	0.007	0.025	TR	TR	TR	TR
Bismuth	0.05	TR	TR	TR	TR	TR	TR	TR	TR	TR	TR
Cadmium	0.02	TR	0.18	0.08	TR	0.14	0.10	0.11	TR	TR	TR
Calcium	0.03	14.4	465	576	445	496	553	512	13.3	13.3	16.7
Chromium	0.01	TR	TR	TR	TR	TR	TR	0.32	TR	TR	TR
Cobalt	0.01	TR	TR	TR	TR	0.72	0.95	1.68	TR	TR	TR
Copper	0.01	0.02	TR	TR	TR	TR	TR	0.07	TR	TR	0.01
Gallium	0.05	TR	TR	TR	TR	TR	TR	TR	TR	TR	NM
Iron	0.02	12.1	7480	4840	685	11,200	12,200	12,200	5.38	2.26	2.36
Lead	0.1	TR	TR	TR	TR	TR	TR	TR	TR	TR	TR
Lithium	0.005	TR	0.255	0.220	TR	0.300	0.520	0.570	TR	TR	TR
Magnesium	0.01	3.27	220	163	48.3	631	566	588	2.75	2.73	2.44
Manganese	0.01	0.09	33.4	21.9	5.67	47.1	42.0	44.8	0.04	0.04	0.50
Molybdenum	0.02	TR	2.72	0.80	0.18	1.28	2.74	0.11	TR	TR	TR
Nickel	0.02	TR	TR	0.07	TR	1.56	3.72	1.95	TR	TR	TR
Phosphorus	0.1	TR	TR	TR	TR	TR	TR	TR	TR	TR	TR
Potassium	0.4	TR	TR	TR	TR	TR	TR	TR	TR	TR	NM
Silver	0.02	TR	TR	TR	TR	TR	TR	TR	TR	TR	NM
Sodium	0.2	16.9	2.9	13.2	6.7	16.6	58.8	14.6	17.9	17.8	12.5
Strontium	0.005	0.030	0.640	0.878	0.610	1.03	1.32	1.28	0.024	0.024	0.031
Titanium	0.01	TR	TR	TR	TR	TR	0.30	0.12	TR	TR	TR
Vanadium	0.005	TR	TR	TR	TR	TR	TR	0.08	TR	TR	TR
Yttrium	0.005	TR	0.252	TR	TR	0.470	1.67	0.795	TR	TR	TR
Zinc	0.01	0.11	0.14	0.12	0.07	0.14	0.09	3.72	0.03	0.02	0.02

Table 4.2 – 1999 trace metal pore water chemistry results from piezometer locations in James Lake (Fig. 2.4) and one 2002 bottom water trace metal chemistry analysis from northern Granite Lake (Fig. 4.1). Tr = trace.

	JLB97-26	JLB97-27	JLB97-28	JLB97-29	JLB97-30	JLB97-31	JLB97-32	JLB97-33	JLB97-34	JLB97-35	JLB97-38	JLB97-39	GLB02-1	
Data (mg/L)	Species													
	Cation													
	Ca ²⁺	12.5	12.4	10.4	12.2	40.2	1760.0	12.0	10.3	75.4	10.8	172.0	78.2	16.7
	Mg ²⁺	1.8	1.8	1.6	1.9	30.6	2214.0	2.3	1.6	62.9	2.1	65.1	6.5	2.4
	Na ⁺	13.2	15.8	15.4	18.4	14.5	13.3	14.3	17.2	15.9	16.3	7.0	4.9	12.5
	K ⁺	0	0	0	0	0	2.9	0	0	0	0	1.6	1.6	0
Anion	Cl ⁻	18.6	20.1	20.4	23.8	32.0	29.4	20.7	21.9	32.5	20.0	21.3	396.0	17.6
	SO ₄ ²⁻	7.5	7.5	9.2	12.4	2884.0	17,238.0	9.9	25.2	682.0	18.8	668.0	nd	9.0
CCS	HCO ₃ ⁻	nd	nd	nd	nd	nd	nd	nd	nd	nd	nd	nd	nd	nd
	CO ₃ ²⁻	nd	nd	nd	nd	nd	nd	nd	nd	nd	nd	nd	nd	nd
CS	Eq. wt.	0.6238	0.6188	0.5190	0.6088	2.0062	87.8331	0.5989	0.5140	3.7629	0.5389	8.5837	3.9026	0.8334
	Ca	0.1481	0.1481	0.1317	0.1563	2.5180	182.1847	0.1983	0.1317	5.1759	0.1728	5.3569	0.5349	0.2008
CAS	Mg	0.5739	0.6869	0.6696	0.8000	0.6305	0.5783	0.6218	0.7479	0.6913	0.7087	0.3044	0.2130	0.5435
	Na	0	0	0	0	0	0.0742	0	0	0	0	0.0409	0.1074	0
AS	K	1.3458	1.4538	1.3203	1.5651	5.1547	270.6703	1.4190	1.3936	9.6301	1.4204	14.2859	4.7579	1.5777
	Eq. wt.	1.510	1.630	1.460	1.650	71.890	nd	1.410	1.400	nd	2.250	14.860	nd	nd
Calculations (meq/L)	Cl	0.5246	0.5669	0.5754	0.6713	0.9026	0.8293	0.5839	0.6177	0.9167	0.5641	0.6008	0	0.4964
	SO ₄	0.1561	0.1561	0.1915	0.2582	60.0436	358.8872	0.2061	0.5247	14.1989	0.3914	13.9075	8.2445	0.1874
CAS	HCO ₃	nd	nd	nd	nd	nd	nd	nd	nd	nd	nd	nd	nd	nd
	CO ₃	nd	nd	nd	nd	nd	nd	nd	nd	nd	nd	nd	nd	nd
AS	Eq. wt.	0.6807	0.7230	0.7669	0.9295	60.9462	359.7165	0.7899	1.1424	15.1156	0.9555	14.5083	8.2445	0.6838
	Ca	1.440	1.560	1.410	1.610	61.150	nd	1.560	1.310	nd	1.490	14.760	nd	nd
Result (%)	Mg	0.6238	0.6188	0.5190	0.6088	2.0062	87.8331	0.5989	0.5140	3.7628	0.5389	8.5837	3.9026	0.8334
	Na+K	0.1481	0.1481	0.1317	0.1534	2.5180	182.1847	0.1893	0.1317	5.176	0.1728	5.3569	0.5349	0.2008
TDS (mg/L)	Cl	0.5739	0.6869	0.6696	0.8000	0.6305	0.6525	0.6218	0.7479	0.6913	0.7087	0.3453	0.3205	0.5435
	SO ₄	0.5246	0.5669	0.5754	0.6713	0.9026	0.8293	0.5839	0.6177	0.9167	0.5641	0.6008	0	0.4964
Result (%)	HCO ₃ + CO ₃	0.6651	0.7308	0.5533	0.6358	10.740	358.8872	0.2061	0.5246	14.1989	0.3914	13.9075	8.2445	0.1874
	Ca	46.35	42.56	39.31	38.98	38.92	32.45	42.48	36.89	39.07	37.94	60.06	82.02	52.83
Result (%)	Mg	11.01	10.19	9.97	9.99	48.84	67.31	13.42	9.45	53.75	12.17	37.49	11.24	12.73
	Na+K	42.64	47.25	50.72	51.11	12.23	0.24	44.10	53.67	7.18	49.89	2.42	6.74	34.45
Result (%)	Cl	38.98	38.99	43.58	42.89	1.26	0.23	41.41	44.33	6.07	39.71	4.14	0	31.47
	SO ₄	11.60	10.74	14.51	16.49	83.76	99.77	14.62	37.65	93.95	27.55	95.86	100	11.88
Result (%)	HCO ₃ + CO ₃	49.42	50.27	41.91	40.62	14.98	0	43.97	18.02	0	32.73	0	0	56.66
	TDS (mg/L)	58	63	47	71	4320	30180	127	150	7257	84	5328	527	65

Table 4.3 – Sediment-water interface pore water cation and anion data from James and Granite lakes (Fig. 4.1). CAS = Cal Anion Sum; CCS = Cal Cation Sum; CS = Cation sum; AS = Anion sum; nd = no data; Eq. wt. is the equivalent weight taking valence into account. TDS results for JLB samples were summed from the data supplied by ARECO Canada as presented in Chapter Two; and the TDS for GLB02-1 was calculated from the electrical conductivity using the method outlined in the text.

		MOE 1	MOE 2	MOE 3	MOE 4	MOE 5	MOE 6	MOE 7	MOE 8
Data (mg/L)	Cation	Ca ²⁺	8.4	8.5	8.9	8.8	9.0	9.6	11.0
		Mg ²⁺	2.1	1.8	1.9	1.8	1.9	2.0	2.1
		Na ⁺	14.0	9.6	10.0	12.0	12.0	12.0	11.0
		K ⁺	0.4	0.3	0.3	0.3	0.4	0.4	0.4
Anion	Cl ⁻	28.0	17.0	17.0	19.0	20.0	19.0	20.0	19.0
	SO ₄ ²⁻	10.7	9.8	10.0	15.1	13.8	18.7	19.5	17.2
	HCO ₃ ⁻	nd	nd	nd	nd	nd	nd	nd	nd
	CO ₃ ²⁻	nd	nd	nd	nd	nd	nd	nd	nd
CCS	Eq. wt.	Ca	0.4941	0.4242	0.4442	0.4392	0.4491	0.4791	0.5489
		Mg	0.1728	0.1481	0.1564	0.1481	0.1564	0.1646	0.1728
		Na	0.6087	0.4174	0.4348	0.5218	0.5218	0.5218	0.4783
		K	0.0092	0.0074	0.0074	0.0084	0.0092	0.0097	0.0099
CS	Eq. wt.	1.2848	0.9921	0.9807	1.0437	1.1365	1.1752	1.1752	1.2100
		nd	nd	nd	nd	nd	nd	nd	nd
Calculations (meq/L)	Eq. wt.	Cl	0.7898	0.4795	0.5359	0.5641	0.5359	0.5641	0.5359
		SO ₄	0.2228	0.2042	0.2082	0.3144	0.3893	0.4059	0.3581
		HCO ₃	nd	nd	nd	nd	nd	nd	nd
		CO ₃	nd	nd	nd	nd	nd	nd	nd
CAS	Eq. wt.	1.0126	0.6838	0.6877	0.8503	0.8514	0.9252	0.9701	0.8940
		nd	nd	nd	nd	nd	nd	nd	nd
Result (%)	TDS (mg/L)	Ca	0.4941	0.4242	0.4442	0.4392	0.4491	0.4791	0.5489
		Mg	0.1728	0.1481	0.1563	0.1481	0.1563	0.1646	0.1728
		Na+K	0.6179	0.4248	0.4432	0.5302	0.5309	0.5314	0.4883
		Cl	0.7878	0.4795	0.5359	0.5641	0.5359	0.5641	0.5359
		SO ₄	0.2228	0.2042	0.2082	0.3144	0.3893	0.4059	0.3581
		HCO ₃ + CO ₃	0.2722	0.3084	0.2929	0.1934	0.2112	0.2050	0.3159
		Ca	38.45	42.25	43.26	42.55	39.29	40.77	45.37
		Mg	13.45	14.93	13.43	14.98	13.25	13.76	14.28
		Na+K	48.09	42.82	43.32	42.47	47.44	46.72	40.35
		Cl	61.47	48.33	48.89	51.35	50.48	47.16	44.29
		SO ₄	17.34	20.59	21.23	30.12	25.71	34.26	29.59
		HCO ₃ + CO ₃	21.19	31.08	29.87	18.53	23.81	18.58	17.45
	89	64	65	71	74	72	78		

Table 4.3 (continued) – Sediment-water interface pore water cation and anion data from James and Granite lakes (Fig. 4.1). CAS = Cal Anion Sum; CCS = Cal Cation Sum; CS = Cation sum; AS = Anion sum; nd = no data; Eq. wt. is the equivalent weight taking valence into account. TDS for MOE data was calculated from the electrical conductivity using the method outlined in the text.

Metals in mg/g	Detection Limit	JLB96-1	JLB96-2	JLB96-3	JLB96-4	JLB96-6	JLB96-7	JLB96-8	JLB96-10	JLB96-13	JLB96-17	JLB96-19	JLB96-21	JLB96-22	JLB96-23
		Arsenic	0.042	0.0075	0.0033	0.016	0.008	0.015	0.018	0.018	0.023	0.02	0.0039	0.0074	0.0069
Cadmium	0.002	0.008	0.011	0.01	0.0012	0.0004	0.004	0.011	0.012	0.009	0.018	0.018	0.003	0.0002	0.003
Chromium	0.001	0.037	0.056	0.02	0.029	0.03	0.028	0.034	0.045	0.031	0.011	0.09	0.022	0.042	0.03
Cobalt	0.002	0.019	0.011	ND	0.023	0.012	0.023	0.02	0.006	0.023	ND	ND	0.011	0.016	0.024
Copper	0.001	0.53	0.66	0.22	0.12	0.07	0.16	0.56	0.2	0.48	0.098	0.17	0.12	0.051	0.13
Iron	200	369,000	380,000	422,000	22,700	17,600	31,800	312,000	391,000	238,000	507,000	492,000	11,800	18,100	32,300
Lead	0.01	0.047	0.028	ND	0.078	0.032	0.035	0.039	ND	0.056	0.03	0.028	0.052	0.03	0.14
Manganese	0.001	0.093	0.045	0.026	0.23	0.31	0.3	0.078	0.07	0.12	0.019	0.043	0.29	0.64	0.51
Nickel	0.002	0.044	0.031	0.005	0.049	0.034	0.049	0.049	0.011	0.052	0.004	0.008	0.047	0.043	0.67
Phosphorus	0.04	0.45	0.49	0.14	1.160	0.44	0.39	0.42	2.07	0.33	0.084	0.49	0.89	0.64	1.340
Silver	0.0002	0.0002	0.0004	0.0002	ND	ND	0.0002	0.0002	0.002	0.0002	ND	0.0004	ND	ND	0.0002
Zinc	0.002	0.46	0.43	0.09	0.25	0.15	0.24	0.43	89	0.49	0.051	0.095	0.22	0.13	0.27

Table 4.4 – Bulk chemistry data from 1996 sediment-water interface sediment samples in James Lake (Fig. 4.1).

Piezometer	Depth (m)	8 September 1999		9 September 1999	
		pH	Conductivity ($\mu\text{S}/\text{cm}$)	pH	Conductivity ($\mu\text{S}/\text{cm}$)
JLP 99-2	1.70	3.03	8100	4.01	8860
JLP 99-3	1.80	3.02	4520	3.33	7580
JLP 99-4	1.60	3.34	2280	5.35	2440
JLP 99-5	1.05	2.95	10190	3.63	13760
JLP 99-6	1.70	3.00	5650	3.08	14610
JLP 99-7	1.60	2.97	11450	3.56	15240
JLP 99-8	surface	6.19	144		
JLP 99-9	surface	6.54	144		

Table 4.5 – Electrical conductivity and pH readings obtained for pore waters from piezometers placed near the Northland Pyrite Mine waste rock pile in the southwestern corner of James Lake. The depths indicated in the table are the depths below the sediment-water interface. TDS, the total dissolved solids in the waters was calculated using conductivity as discussed in the text.

Table 4.6 – Water depth, pH, electrical conductivity and temperature of lake waters. The numbers in brackets indicate readings from a second sample taken for that site at sediment-water interface. Water depth indicates the depth of water to the sediment-water interface at the locations indicated in Fig. 2.4. SW = surface waters. The total dissolved solids (TDS) are calculated as discussed in the text.

<i>Site</i>	<i>Sample</i>	<i>Water Depth (m)</i>	<i>pH</i>	<i>Conductivity ($\mu\text{S/cm}$)</i>	<i>TDS (mg/L)</i>	<i>Temperature ($^{\circ}\text{C}$)</i>
<i>James Lake (2001)</i>	JLpH 01-1	1.2	4.8			16.5 (15.5)
	JLpH 01-2	1.0	5.0			16.0
	JLpH 01-3	2.0	5.3 (7.0)			15.0 (16.0)
	JLpH 01-4	1.0	5.5 (5.4)			17.0 (15.0)
	JLpH 01-5	0.6	6.6 (6.9)			15.0
	JLpH 01-6	1.0	6.5			
	JLpH 01-7	2.0	(6.8)			17.5 (17.5)
	JLpH 01-8	0.6	6.6 (7.1)			16.0 (15.5)
<i>James Lake Creek (2001)</i>	JLpH 01-9		5.0			
	JLpH 01-10					
	JLpH 01-11		5.8			
	JLpH 01-12		6.0			
<i>Granite Lake (2001)</i>	GLpH 01-1	3.9	7.6 (7.7)			22.0 (22.0)
	GLpH 01-2	2.5	7.6 (7.7)			21.0 (21.0)
	GLpH 01-3	14.0	7.7 (7.0)			21.0 (7.0)
	GLpH 01-4	1.8	7.5			21.0
	GLpH 01-5	3.6	7.7			
	GLpH 01-6	2.0	7.9 (7.8)			21.0 (20.0)
	GLW 01-7	14.0	7.3			20.0 (7.0)
<i>Vicinity of Northland Pyrite Mine (2002)</i>	JLW 02-1	2.0	2.6	2800	1652	21.0
	JLW 02-2	0.5	2.2	4800 (7500)	2832 (4425)	(20.0)
	JLW 02-3	0.3	2.2	7800	4602	21.0
	JLW 02-4	0.3	5.3	2200	1298	22.0
	JLW 02-5	SW		9500	5605	
	JLW 02-6	SW	5.4	1900	1121	22.0
	JLW 02-7	SW	5.7	1800	1062	21.0
	JLW 02-8	SW	5.3	1800	1062	20.0
	JLW 02-9	SW		1700	1003	22.0
	JLW 02-10	SW	5.6			
	JLW 02-11	SW	7.0			
	JLW 02-12	SW	7.0 (7.0)			

Table 4.7 – pH, electrical conductivity, TDS, oxygen concentration and temperature readings at the James and Granite lakes site (Fig. 2.4) during 2003. Depths indicated in brackets are depths at which samples were obtained. TDS was calculated using the method discussed in the text. Red in sample JL 03-19 indicates Fe-oxidized bottom sediment; and green in sample JL 03-20 indicates reduced bottom sediment. Abbreviations in sample names are indicated in Table 2.1.

	<i>Sample</i>	<i>pH</i>	<i>Conductivity (μS/cm)</i>	<i>TDS (mg/L)</i>	<i>Oxygen (mg/L)</i>	<i>Temperature ($^{\circ}$C)</i>
3 September 2003	JL 03-1	2.5	930.0	548.7	6.67	16.3
	JL 03-1 (10 m)	2.0	401.2	236.7	0.18	6.8
	JL 03-2	4.5	812.0	479.1	7.34	17.8
	JL 03-3	5.0	190.1	112.2	7.97	19.6
	JL 03-4	5.0	154.3	91.0	8.01	19.0
	JL 03-5	5.0	142.7	84.2	8.33	19.2
	JL 03-6	5.0	141.6	83.5	8.23	18.6
	JLM 03-7	5.0	138.5	81.7	8.03	18.4
	JLM 03-8	5.0	149.5	88.2	7.92	20.4
	JLM 03-9	5.0	156.3	92.2	8.02	24.7
	JLM 03-10	5.5	224.4	132.4	8.22	23.4
	JLM 03-11	5.5	208.7	123.1	7.55	20.9
	JLM 03-12	6.0	200.5	118.3	6.73	20.1
	JLM 03-13	5.0	186.6	110.1	7.80	16.1
	JL 03-14	5.0	160.5	94.7	7.32	17.2
	GL 03-15	5.0	140.4	82.8	9.20	22.6
GL 03-16	5.0	130.4	76.9	9.08	19.9	
5 September 2003	JL 03-17	6.0	119.4	70.5	8.33	17.8
	JL 03-18	6.0	138.0	81.4	8.24	17.3
	JL 03-19 (red 0.5 m)	4.0	139.5	82.3	9.00	17.0
	JL 03-20 (green 0.5 m)	3.0	1296.0	764.6	8.09	17.2
	JL 03-21	5.0	137.9	81.4	8.24	17.6
	JL 03-22	5.0	136.1	80.3	8.25	17.4
	GL 03-23	5.5	127.0	74.9	8.76	19.0

<i>Mineral</i>	<i>Formula</i>	<i>JLB 97-26</i>	<i>JLB 97-27</i>	<i>JLB 97-28</i>	<i>JLB 97-29</i>	<i>JLB 97-30</i>	<i>JLB 97-31</i>	<i>JLB 97-32</i>	<i>JLB 97-33</i>	<i>JLB 97-34</i>
Gibbsite	Al(OH) ₃	3.25	2.65	2.94	2.93					
Boehmite	AlOOH	2.68	2.08	2.38	2.36					
Magnetite	Fe ₃ O ₄	9.51	7.94	8.03	5.68			9.64	4.28	
Hematite	Fe ₂ O ₃	8.58	7.39	7.47	5.76			8.34	4.31	
Goethite	FeOOH	3.30	2.71	2.75	1.89			3.18	1.17	
	Al(OH) ₃	0.49		0.19	0.17					
Barite	BaSO ₄					0.72	0.96			
Diaspore	AlOOH	4.45	3.85	4.14	4.13			1.01		
	Fe(OH) ₂₋₇ Cl _{0.3}	2.59	2.07	2.10	1.33			2.63	0.82	
	MnHPO ₄	1.69	1.59	1.19						
Cu metal	Cu	2.68	2.19	2.98	2.66	3.76	6.12	2.89	2.96	3.77
Cuprite	Cu ₂ O	2.36	0.95	2.59	1.52		0.02	1.79	0.58	
Cuprous Ferrite	CuFeO ₂	11.76	10.46	11.32	9.93			11.36	8.74	
Cupric Ferrite	CuFe ₂ O ₄	2.94	0.83	1.77				1.93		
Cl pyromorphite	Pb ₅ (PO ₄) ₃ Cl	6.25	5.23	7.79						
Plattnerite	PbO ₂			8.99						
Basaluminite	Al ₄ (OH) ₁₀ SO ₄	6.69	4.73	5.91	6.41					

Table 4.9 – Log₁₀ (IAP/K_{SP}) for dissolved metals from bottom waters in James and Granite lakes indicating modeled precipitated minerals.

<i>Mineral</i>	<i>Formula</i>	<i>JLB 97-35</i>	<i>JLB 97-38</i>	<i>JLB 97-39</i>	<i>GLB 02-01</i>	<i>JLP 99-2</i>	<i>JLP 99-4</i>	<i>JLP 99-7</i>	<i>JLP 99-8</i>	<i>JLP 99-9</i>
Gibbsite	Al(OH) ₃	2.95			2.87		0.77		2.91	2.88
Boehmite	AlOOH	2.38			2.14		0.85		2.36	2.33
Magnetite	Fe ₃ O ₄	8.40			6.59		3.57		6.42	8.10
Hematite	Fe ₂ O ₃	7.56			6.46		3.62		6.17	7.52
Goethite	FeOOH	2.79			2.27		0.84		2.09	2.77
	Al(OH) ₃	0.19			0.01				0.17	0.14
Barite	BaSO ₄		1.24							
Diaspore	AlOOH	4.15			40.1	0.95	1.93	0.04	4.12	40.9
	Fe(OH) _{2.7} Cl _{0.3}	2.22			2.01					
	MnHPO ₄	0.13								
Cu metal	Cu	2.19	5.06	3.41	2.71			3.34		
Cuprite	Cu ₂ O	0.55		0.34	1.39					
Cuprous Ferrite	CuFeO ₂	10.35			10.47			2.37		
Cupric Ferrite	CuFe ₂ O ₄	0.60								
Cl pyromorphite	Pb ₅ (PO ₄) ₃ Cl	2.45								
Plattnerite	PbO ₂									
Basaluminite	Al ₄ (OH) ₁₀ SO ₄	6.69			8.12					

Table 4.9 (continued) – Log₁₀ (IAP/K_{SP}) for dissolved metals from bottom waters in James and Granite lakes indicating modeled precipitated minerals.

<i>Mineral</i>	<i>Formula</i>	<i>MOE 1</i>	<i>MOE 2</i>	<i>MOE 3</i>	<i>MOE 4</i>	<i>MOE 5</i>	<i>MOE 6</i>	<i>MOE 7</i>	<i>MOE 8</i>
Gibbsite	Al(OH) ₃	3.21	3.00	2.89	3.13	3.95	4.38	4.14	3.79
Boehmite	AlOOH	2.66	2.47	2.39	2.62	3.24	3.66	3.42	3.09
Magnetite	Fe ₃ O ₄	17.97	17.92	18.21	20.72	21.37	21.67	21.51	20.55
Hematite	Fe ₂ O ₃	18.80	18.70	18.84	20.54	21.40	21.69	21.56	20.94
Goethite	FeOOH	8.41	8.36	8.43	9.27	9.74	9.88	9.82	9.50
	Al(OH) ₃	0.47	0.27	0.19	0.42	1.10	1.52	1.28	0.96
Barite	BaSO ₄								
Diaspore	AlOOH	4.41	4.31	4.12	4.35	5.10	5.53	5.28	4.95
	Fe(OH) _{2.7} Cl _{0.3}	7.71	7.47	7.46	8.35	9.38	9.62	9.554	9.19
	MnHPO ₄	0.31							
Cu metal	Cu								
Cuprite	Cu ₂ O								
Cuprous Ferrite	CuFeO ₂								
Cupric Ferrite	CuFe ₂ O ₄								
Cl pyromorphite	Pb ₅ (PO ₄) ₃ Cl								
Plattnerite	PbO ₂								
Basaluminite	Al ₄ (OH) ₁₀ SO ₄	6.45	4.77	3.85	5.18	11.92	14.40	13.34	11.74

Table 4.9 (continued) – Log₁₀ (IAP/K_{SP}) for dissolved metals from bottom waters in James and Granite lakes indicating modeled precipitated minerals.

Table 4.10 – Bulk sediment chemistry data from sediment-water interface sediment in James Lake, including transfer logarithm and standard scores used to produce Q-mode and R-mode cluster diagrams. LEL = Lowest Effect Level; SEL = Severe Effect Level; X_i = fractional abundance; S_{Xi} = standard error; TX log = transfer logarithm; z = standard score

Element	Provincial Sediment Quality Standards		Units	JLB 96-1	JLB 96-2	JLB 96-3	JLB 96-4	JLB 96-6	JLB 96-7
	LEL	SEL							
Arsenic	6.00	33.00	X_i	0.0243	0.0042	0.0064	0.0082	0.0121	0.0074
			S_{Xi}	0.0223	0.0094	0.0116	0.0131	0.0158	0.0124
			$\mu\text{g/g}$	42.00	7.50	3.30	16.00	15.00	8.00
			TX log	1.6232	0.8751	0.5185	1.2041	1.1761	0.9031
			z	-0.00776	-0.74171	-0.53461	-0.30275	-0.27418	-0.40141
Cadmium	0.60	10.00	X_i	0.0046	0.0062	0.0194	0.0006	0.0032	0.0004
			S_{Xi}	0.0126	0.0146	0.0257	0.0046	0.011	0.0036
			$\mu\text{g/g}$	8.00	11.00	10.00	1.20	4.00	0.40
			TX log	0.9031	1.0414	1.0000	0.0792	0.6021	-0.3979
			z	-0.78224	-0.56698	-0.02661	-1.47057	-0.87105	-1.74551
Chromium	26.00	110.00	X_i	0.0214	0.0316	0.0389	0.0148	0.0225	0.0276
			S_{Xi}	0.0126	0.0153	0.0169	0.0105	0.0129	0.0143
			$\mu\text{g/g}$	37.00	56.00	20.00	29.00	28.00	30.00
			TX log	1.5682	1.7482	1.3010	1.4624	1.4472	1.4771
			z	-0.06696	0.218	0.291004	-0.03463	0.007679	0.191629
Cobalt	50.00		X_i	0.0110	0.0062	0.0000	0.0188	0.0185	0.0110
			S_{Xi}	0.0149	0.0112	0.0000	0.0154	0.0193	0.0149
			$\mu\text{g/g}$	19.00	11.00	0.00	23.00	23.00	12.00
			TX log	1.2788	1.0413	0.0000	1.3617	1.3617	1.0792
			z	-0.37824	-0.56698	-1.08169	-0.13914	-0.08115	-0.21949
Copper	16.00	110.00	X_i	0.3063	0.3729	0.4276	0.0613	0.1286	0.0644
			S_{Xi}	0.0151	0.0159	0.0162	0.0079	0.0109	0.0081
			$\mu\text{g/g}$	530.00	660.00	220.00	120.00	160.00	70.00
			TX log	2.7243	2.8195	2.3424	2.0792	2.2041	1.8451
			z	1.176302	1.407871	1.389758	0.605666	0.794766	0.571787
Lead	31.00	250.00	X_i	0.0272	0.0158	0.0000	0.0399	0.0281	0.0295
			S_{Xi}	0.0131	0.0100	0.0000	0.0157	0.0133	0.0136
			$\mu\text{g/g}$	47.00	28.00	0.00	78.00	35.00	32.00
			TX log	1.6721	1.4471	0.0000	1.8921	1.5441	1.5051
			z	0.044768	-0.11633	-1.08169	0.411448	0.108446	0.220585
Manganese	460.00	1100.00	X_i	0.0538	0.0254	0.0505	0.1176	0.2411	0.2853
			S_{Xi}	0.0084	0.0059	0.0082	0.0119	0.0159	0.0168
			$\mu\text{g/g}$	93.00	45.00	26.00	230.00	300.00	310.00
			TX log	1.9685	1.6532	1.4149	2.3617	2.4771	2.4914
			z	0.363507	0.112518	0.411223	0.898983	1.078632	1.239446
Nickel	16.00	75.00	X_i	0.0254	0.0175	0.0097	0.0250	0.0394	0.0313
			S_{Xi}	0.0140	0.0117	0.0087	0.0155	0.0151	0.0173
			$\mu\text{g/g}$	44.00	31.00	5.00	49.00	49.00	34.00
			TX log	1.6435	1.4914	0.6989	1.6902	1.6902	1.5315
			z	0.013963	-0.06724	-0.34422	0.201854	0.260389	0.247786
Phosphorus	600.00	2000.00	X_i	0.2601	0.2769	0.2721	0.5930	0.3135	0.4050
			S_{Xi}	0.0089	0.0091	0.0090	0.0099	0.0094	0.0099
			$\mu\text{g/g}$	450.00	490.00	140.00	1160.00	390.00	440.00
			TX log	2.6532	2.6902	2.1461	3.0645	2.5911	2.6434
			z	1.099879	1.264214	1.182651	1.628499	1.19711	1.396572
Silver	0.50		X_i	0.0001	0.0002	0.0004	0.0000	0.0002	0.0000
			S_{Xi}	0.0105	0.0147	0.0193	0.0000	0.0124	0.0000
			$\mu\text{g/g}$	0.20	0.40	0.20	0.00	0.20	0.00
			TX log	-0.6989	-0.3979	-0.6989	0.0000	-0.6989	0.0000
			z	-2.50513	-2.16554	-1.81916	-1.55277	-2.22386	-1.33439
Zinc	120.00	820.00	X_i	0.2659	0.2430	0.1749	0.1278	0.1929	0.1381
			S_{Xi}	0.0149	0.0144	0.0128	0.0112	0.0133	0.0116
			$\mu\text{g/g}$	460.00	430.00	90.00	250.00	150.00	240.00
			TX log	2.6628	2.6335	1.9542	2.3979	2.3802	2.1761
			z	1.110144	1.201211	0.980196	0.936575	0.977865	0.913728

Table 4.10 (Continued) – Bulk sediment chemistry data (continued) from sediment-water interface sediment in James Lake, including transfer logarithm and standard scores used to produce Q-mode and R-mode cluster diagrams. X_i = fractional abundance; S_{Xi} = standard error; TX log = transfer logarithm; z = standard score

Element	Units	JLB 96-8	JLB 96-10	JLB 96-13	JLB 96-17	JLB 96-19	JLB 96-21	JLB 96-22	JLB 96-23
Arsenic	X_i	0.0108	0.0091	0.0124	0.0122	0.0078	0.0042	0.0049	0.0014
	S_{Xi}	0.0150	0.0138	0.0161	0.0159	0.0128	0.0093	0.0101	0.0055
	$\mu\text{g/g}$	18.00	23.00	20.00	3.90	7.40	6.90	7.90	3.60
	TX log	1.2553	1.3617	1.3010	0.5911	0.8692	0.8388	0.8976	0.5563
	z	-0.36515	-0.081515	-0.32556	-0.77617	-0.54095	-0.60326	-0.54504	-0.84825
Cadmium	X_i	0.0066	0.0047	0.0056	0.0564	0.0190	0.0018	0.0012	0.0012
	S_{Xi}	0.0151	0.0128	0.0139	0.0430	0.0254	0.0079	0.0066	0.0064
	$\mu\text{g/g}$	11.00	12.00	9.00	18.00	18.00	3.00	2.00	3.00
	TX log	1.0414	1.0792	0.9542	1.2553	1.2553	0.4771	0.3010	0.4771
	z	-0.59717	-0.39639	-0.70118	-0.17839	-0.11068	-0.98128	-1.1893	-0.91944
Chromium	X_i	0.0205	0.0178	0.0192	0.0345	0.0948	0.0132	0.0262	0.0120
	S_{Xi}	0.0124	0.0115	0.0119	0.0159	0.0255	0.0099	0.0139	0.0095
	$\mu\text{g/g}$	34.00	45.00	31.00	11.00	90.00	22.00	42.00	30.00
	TX log	1.5315	1.6532	1.4914	1.0414	1.9542	1.3424	1.6232	1.4771
	z	-0.06553	0.24334	-0.11941	-0.12899	0.66838	-0.07699	0.23855	-0.02042
Cobalt	X_i	0.0121	0.0024	0.0143	0.0000	0.0000	0.0066	0.1000	0.0096
	S_{Xi}	0.0156	0.0069	0.0169	0.0000	0.0000	0.0116	0.0142	0.0139
	$\mu\text{g/g}$	20.00	6.00	23.00	0.0000	0.0000	11.00	16.00	24.00
	TX log	1.3010	0.7782	1.3617	0.0000	0.0000	1.0414	1.2041	1.3802
	z	-0.31552	-0.76188	-0.25982	-1.62561	-1.50978	-0.39159	-0.21406	-0.10754
Copper	X_i	0.3375	0.0791	0.2979	0.3073	0.1790	0.0722	0.0318	0.0518
	S_{Xi}	0.0155	0.0089	0.0150	0.0151	0.0126	0.0085	0.0058	0.0073
	$\mu\text{g/g}$	560	200	480	98	170	120	51	130
	TX log	2.7482	2.3010	2.6812	1.9912	2.2304	2.0792	1.7076	2.1139
	z	1.25435	0.95303	1.16938	1.23605	0.97308	0.69296	0.32961	0.55210
Lead	X_i	0.0235	0.0000	0.0348	0.0941	0.0295	0.0313	0.0187	0.0558
	S_{Xi}	0.0122	0.0000	0.0147	0.0235	0.0136	0.0139	0.0109	0.0184
	$\mu\text{g/g}$	39.00	0.0000	56.00	30.00	28.00	52.00	30.00	140.00
	TX log	1.5911	0.0000	1.7482	1.4991	1.4472	1.7160	1.4771	2.1461
	z	-0.00089	-1.59909	0.15876	0.49722	0.10319	0.31342	0.08075	0.59104
Manganese	X_i	0.0470	0.0277	0.0745	0.0596	0.0453	0.1745	0.3995	0.2032
	S_{Xi}	0.0079	0.0061	0.0098	0.0088	0.0077	0.0141	0.0182	0.0149
	$\mu\text{g/g}$	78.00	70.00	120.00	19.00	43.00	290.00	640.00	510.00
	TX log	1.8921	1.8451	2.0792	1.2787	1.6335	2.4623	2.8062	2.7076
	z	0.32567	0.45719	0.51727	0.21213	0.31085	1.06344	1.51599	1.0858
Nickel	X_i	0.0295	0.0044	0.0323	0.0125	0.0084	0.0283	0.0268	0.0235
	S_{Xi}	0.0151	0.0059	0.0157	0.0099	0.0081	0.0148	0.0144	0.0135
	$\mu\text{g/g}$	49.00	11.00	52.00	4.00	8.00	47.00	43.00	59.00
	TX log	1.6902	1.0414	1.7160	0.6021	0.9031	1.6721	1.6335	1.7709
	z	0.10665	-0.43851	0.12391	-0.76037	-0.50321	0.26754	0.24959	0.24366
Phosphorus	X_i	0.2531	0.8188	0.2048	0.2634	0.5159	0.5355	0.3995	0.5339
	S_{Xi}	0.0088	0.0078	0.0082	0.0089	0.0101	0.0101	0.0099	0.0101
	$\mu\text{g/g}$	420.00	2070.00	330.00	84.00	490.00	890.00	540.00	1340.00
	TX log	2.6232	3.3159	2.5186	1.9243	2.6902	2.9194	2.8062	3.1271
	z	1.11882	2.09641	0.99312	1.13984	1.48866	1.60238	1.51599	1.46296
Silver	X_i	0.0001	0.0008	0.0001	0.0000	0.0004	0.0000	0.0000	0.0001
	S_{Xi}	0.0108	0.0276	0.0109	0.0000	0.0201	0.0000	0.0000	0.0088
	$\mu\text{g/g}$	0.20	2.00	0.20	0.00	0.40	0.00	0.00	0.20
	TX log	-0.69897	0.30103	-0.69897	0.0000	-0.39794	0.0000	0.0000	-0.69897
	z	-2.4851	-1.2636	-2.4818	-1.6256	-1.9533	-0.4799	-1.5144	-1.9768
Zinc	X_i	0.2592	0.0352	0.3041	0.1599	0.1000	0.1324	0.0812	0.1076
	S_{Xi}	0.0147	0.0062	0.0155	0.0123	0.0101	0.0114	0.0092	0.0104
	$\mu\text{g/g}$	430.00	89.00	490.00	51.00	95.00	220.00	130.00	270.00
	TX log	2.6335	1.9494	2.6902	1.7076	1.9777	2.3424	2.1139	2.4314
	z	1.1299	0.5734	1.1791	0.8284	0.6946	0.9681	0.7684	0.8375

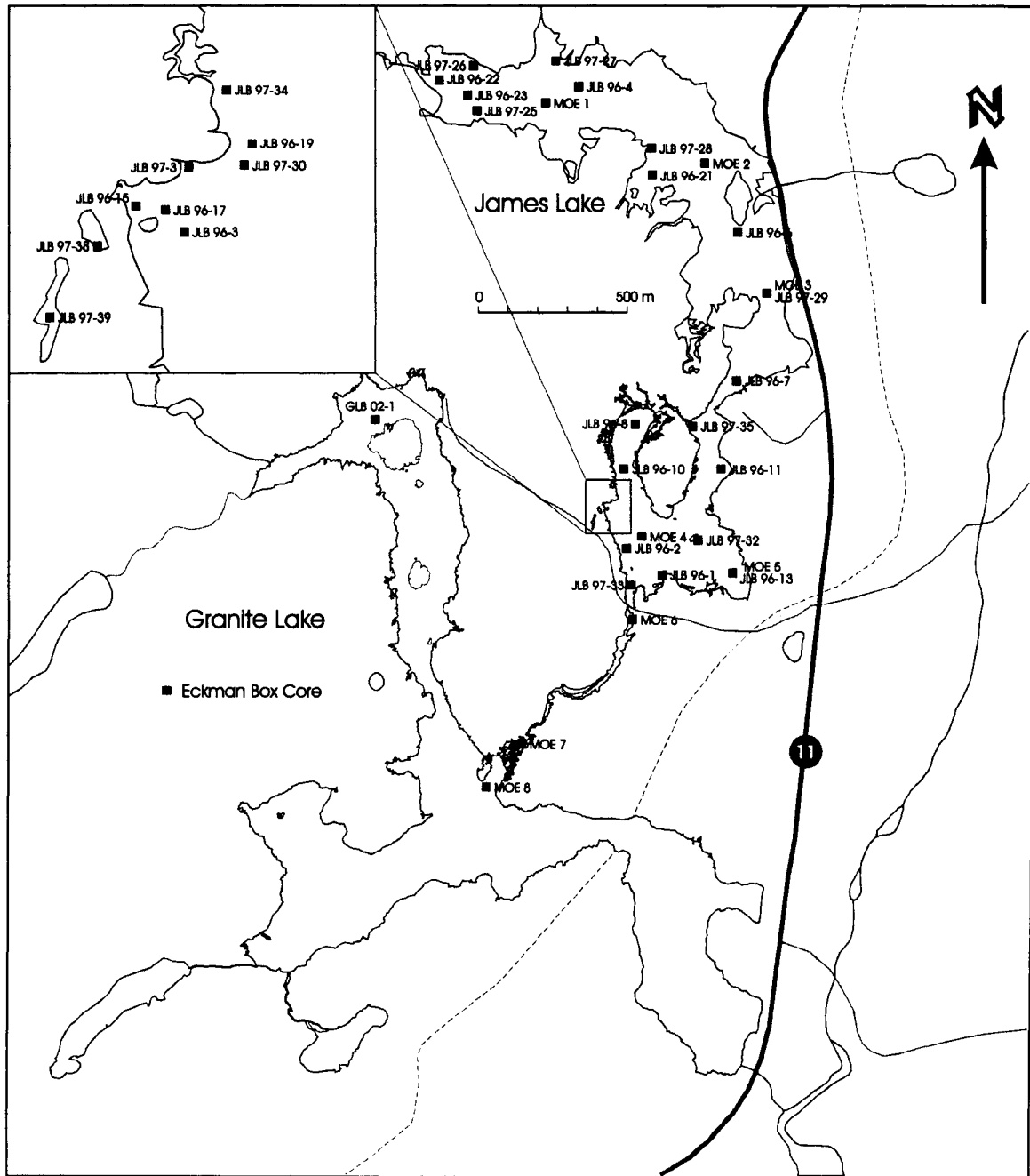


Figure 4.1 - Locations of sediment-water interface pore-water samples from 1997 (Table 4.1 & 4.3); sediment-water interface bulk sediment samples from 1996 (Table 4.4); and sampling sites used by the Ministry of the Environment (MOE) during 1989 in James and Granite lakes.

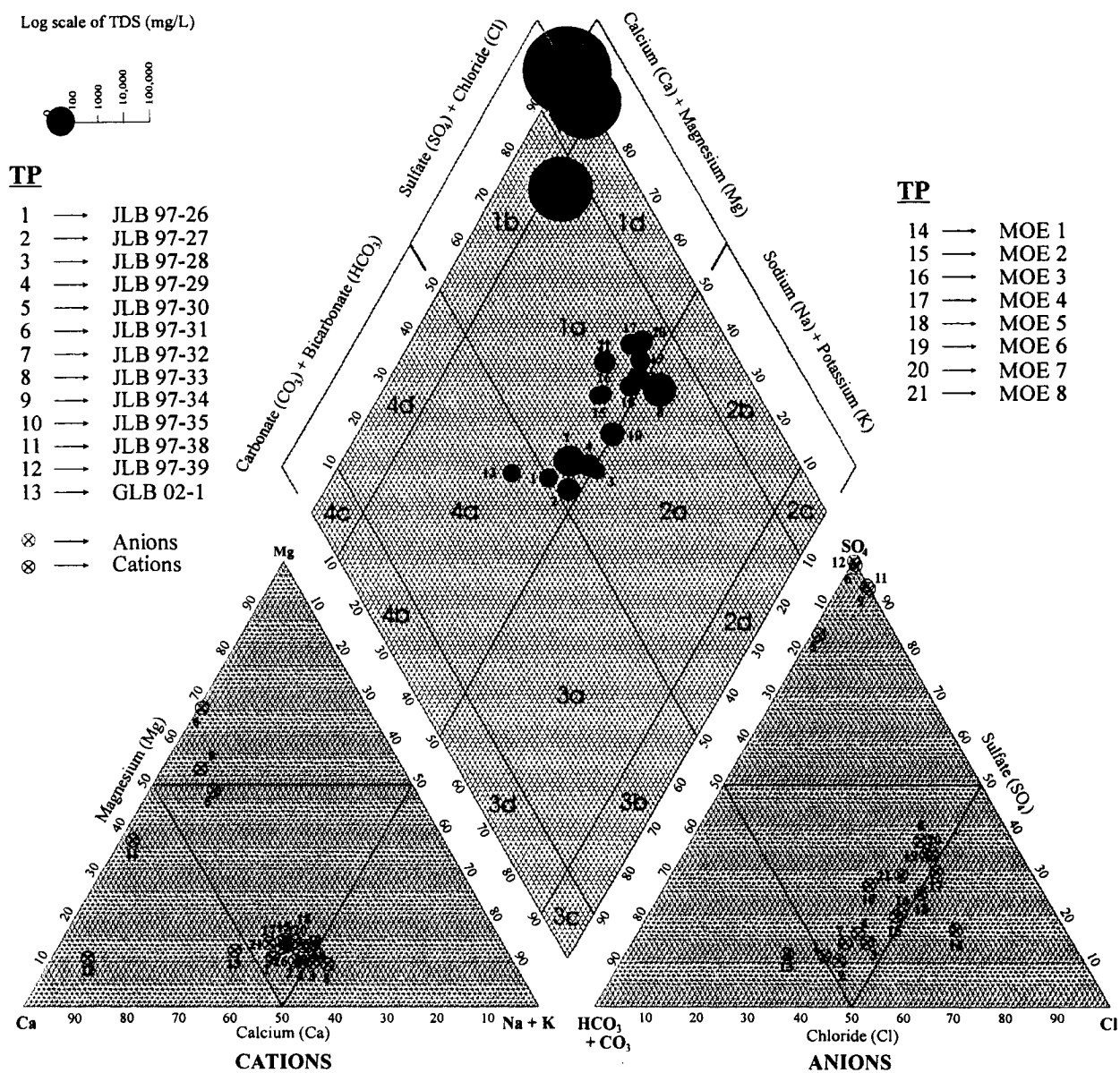


Figure 4.2 - Trilinear Plots (TP) for sediment-water interface pore waters for James and Granite lakes (Table 4.3a & b). The concentrations of the TDS in mg/L are indicated by the size of the circles.

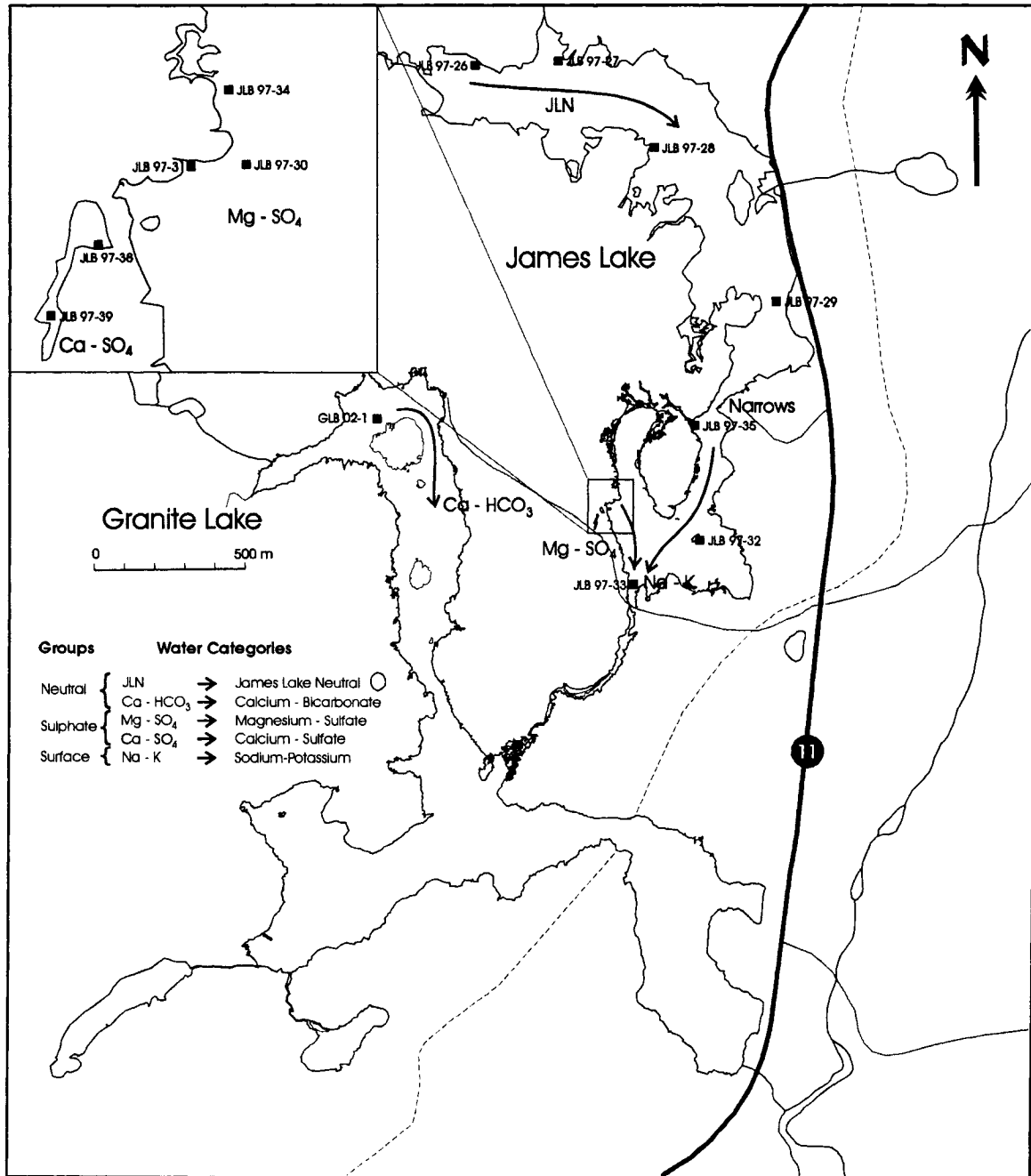


Figure 4.3 - Water groups and categories derived from sediment-water interface pore-water samples and analyzed in trilinear plot from James and Granite lakes.

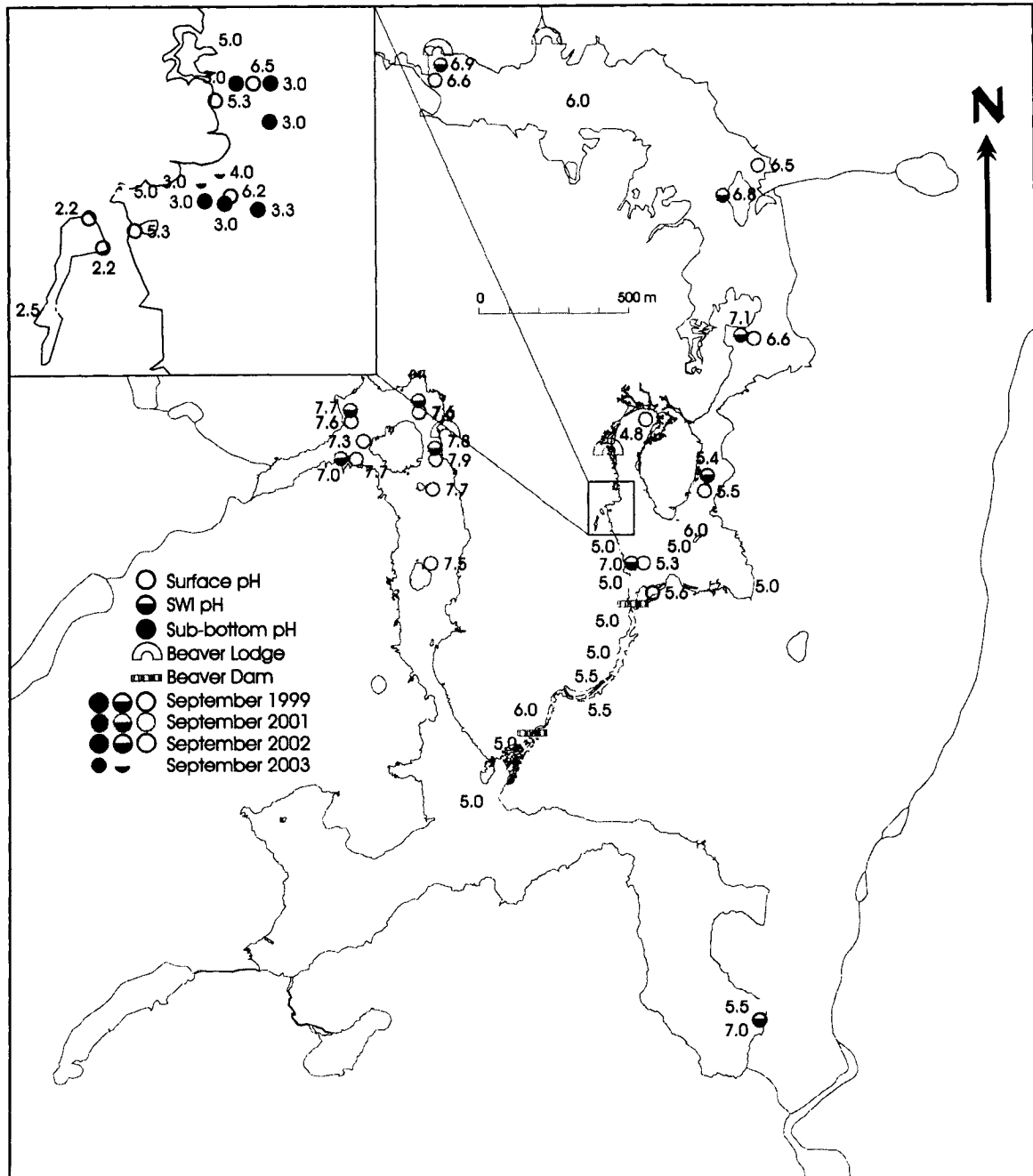


Figure 4.4 - pH map for the James and Granite lake system showing surface water, bottom water and sub-surface pore water readings. Locations of beaver dams and beaver lodges are indicated.

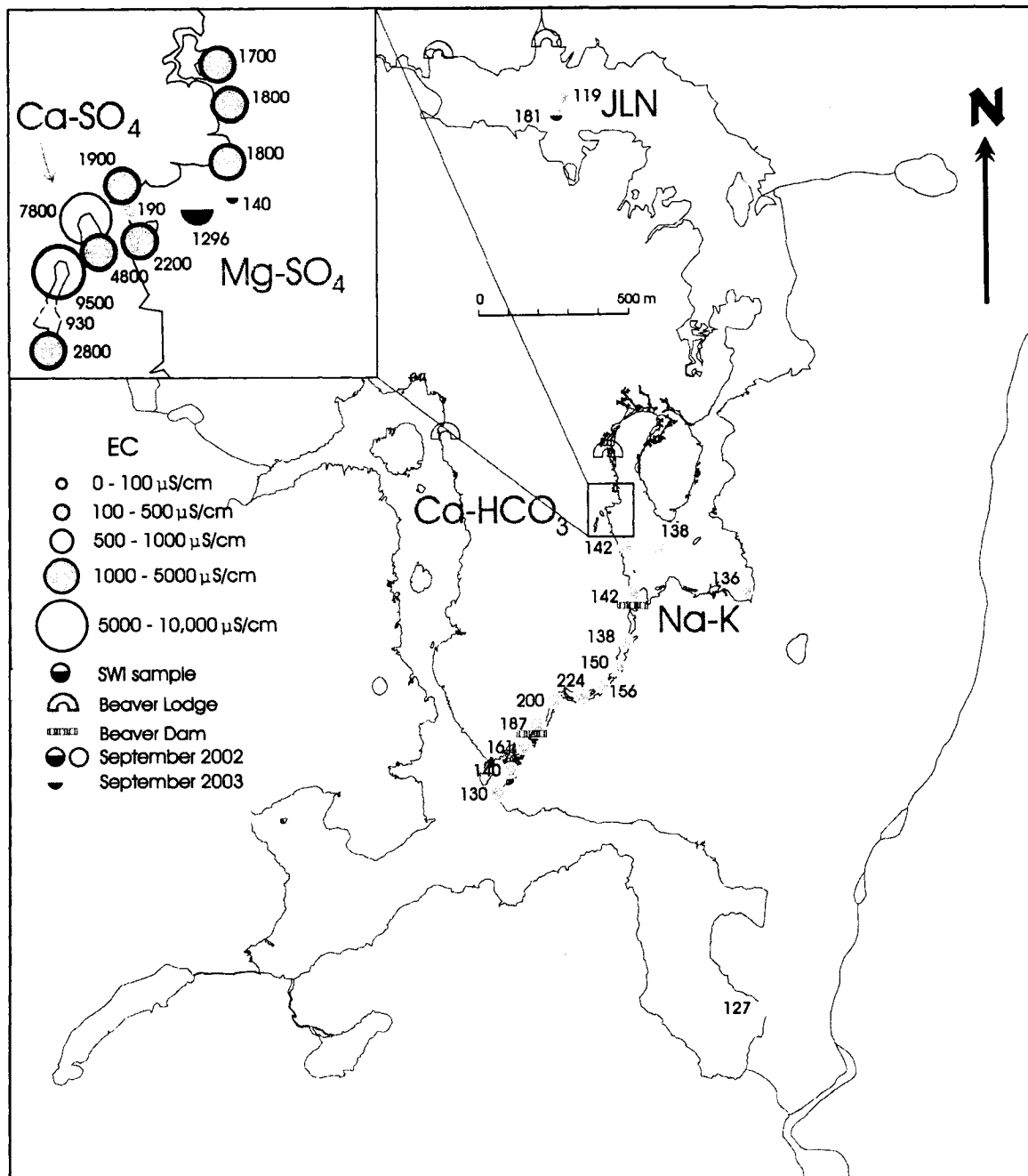


Figure 4.5 - Electrical Conductivity (EC) in the James and Granite lakes system. Lake surface and sediment-water interface (SWI) readings are marked, with increasing size of the circles indicating increasing dissolved solids. Locations of beaver dams and beaver lodges are indicated.

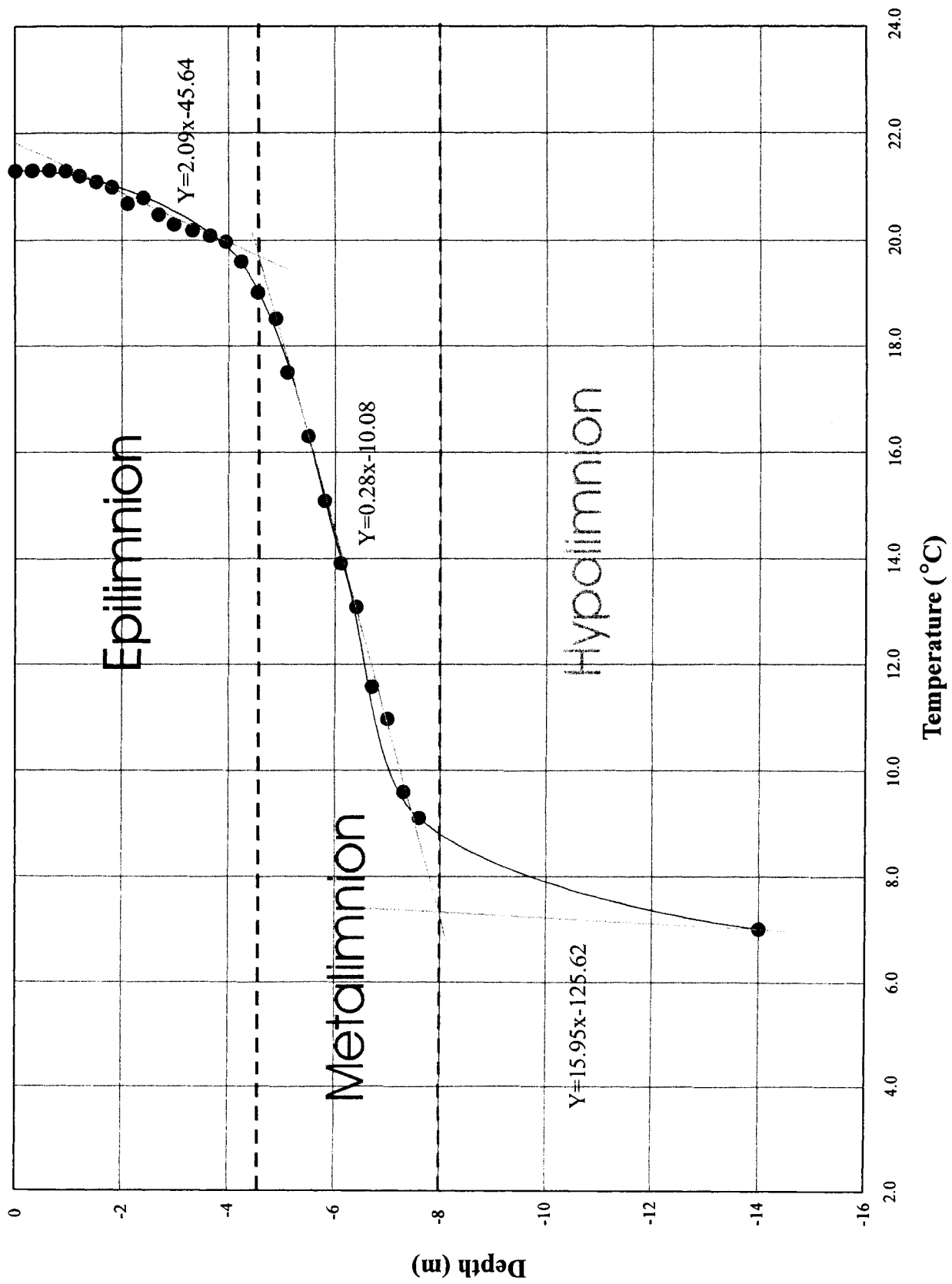


Figure 4.6 - Bathymetric temperature profile (GLTPr 99-1) indicating change in temperature with respect to depth in northern Granite Lake. Boundaries of thermal layers are indicated by intersection of slopes of regression lines.

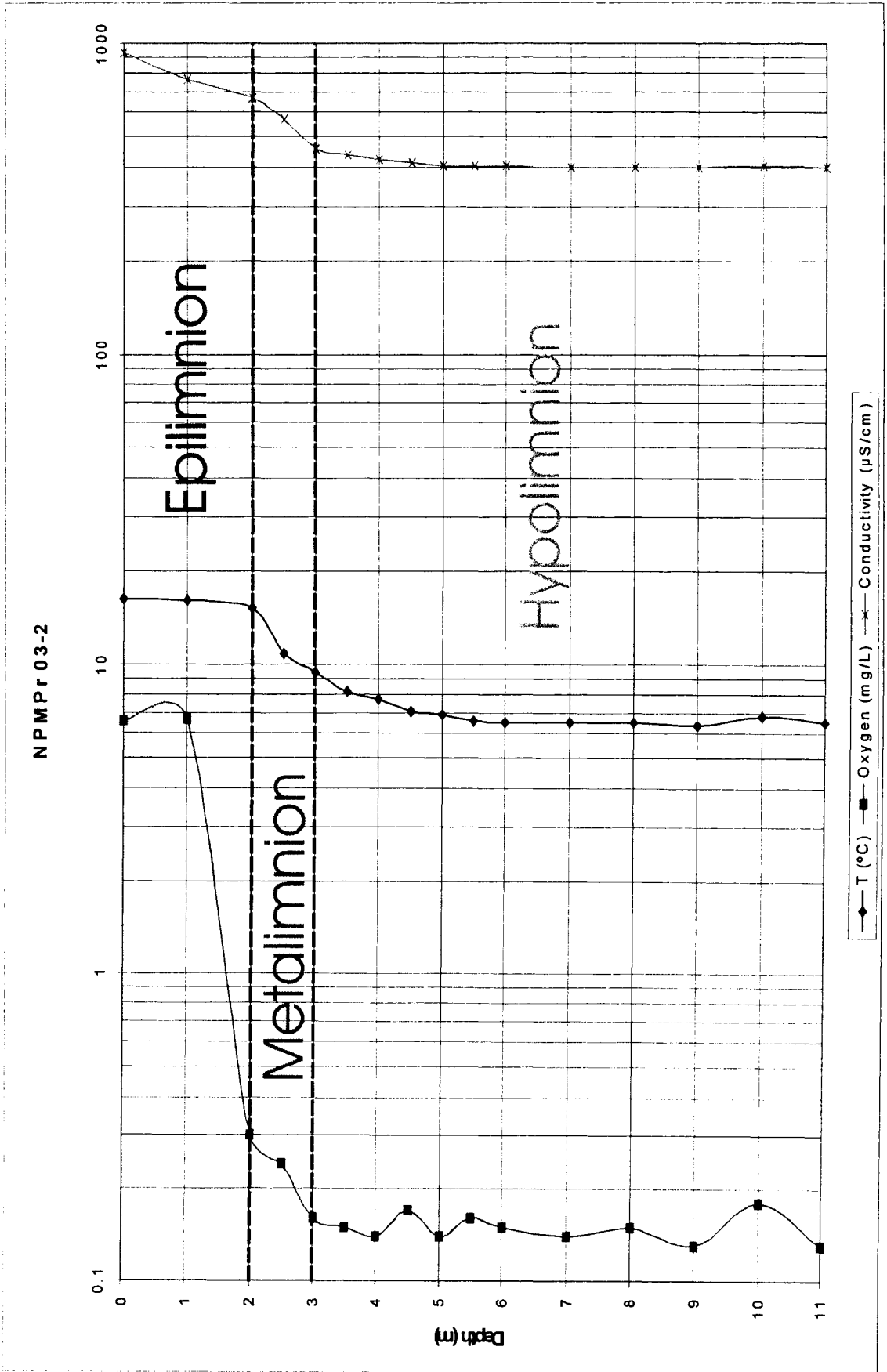


Figure 4.7 - Temperature, oxygen and EC profiles with respect to depth at NPMTPr 03-2 in the Northland Pyrite Mine trench. Data is presented in a semi-log graph in order to more clearly discern the temperature and oxygen profiles. The boundaries for the epilimnion and metalimnion were derived using the method shown in figure 4.6.

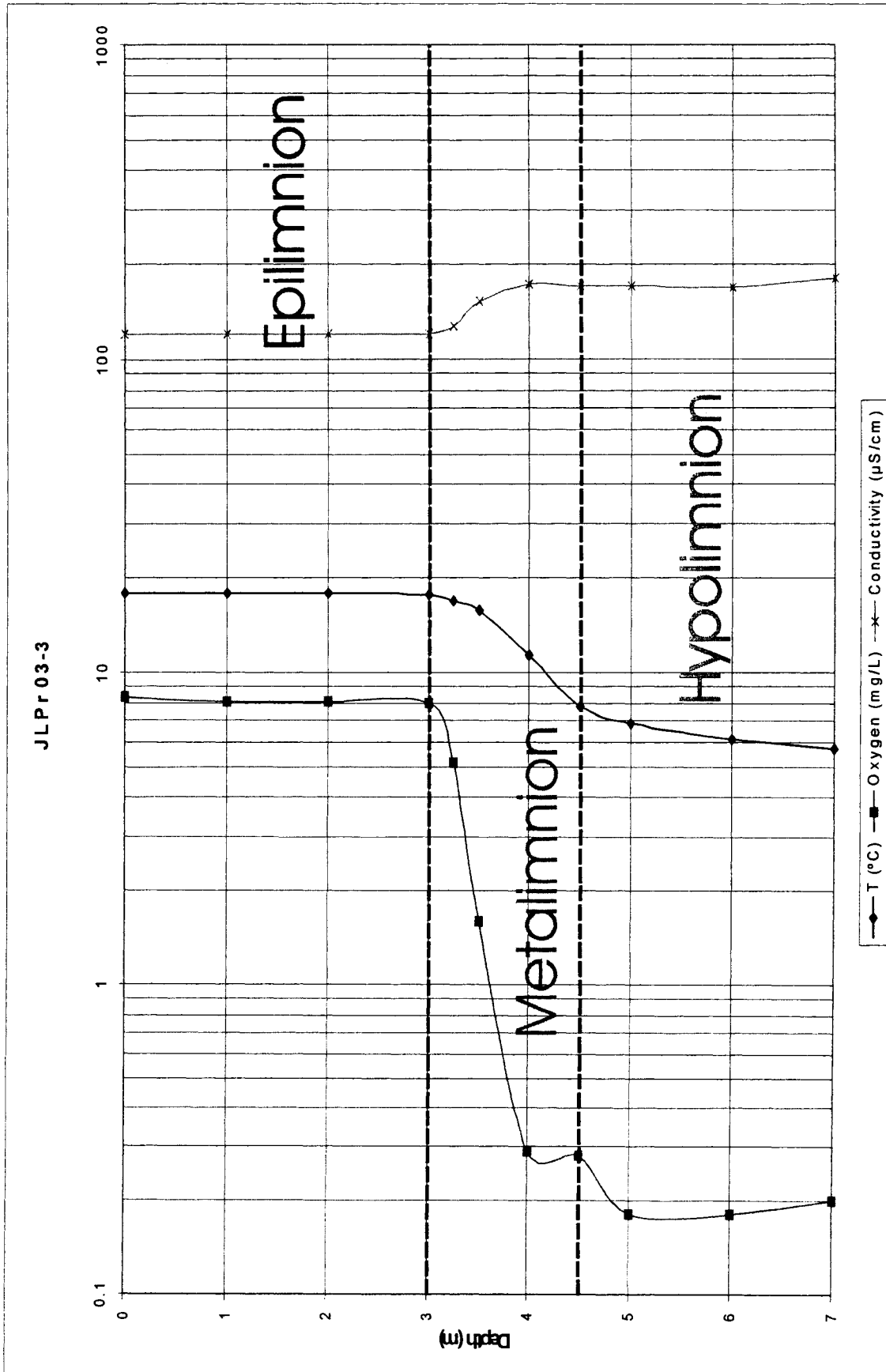


Figure 4.8 - Temperature, oxygen and EC profiles with respect to depth in northern James Lake. Data is presented in a semi-log graph in order to more clearly discern the temperature and oxygen profiles. The boundaries for the epilimnion and metalimnion were derived using the method shown in figure 4.6.

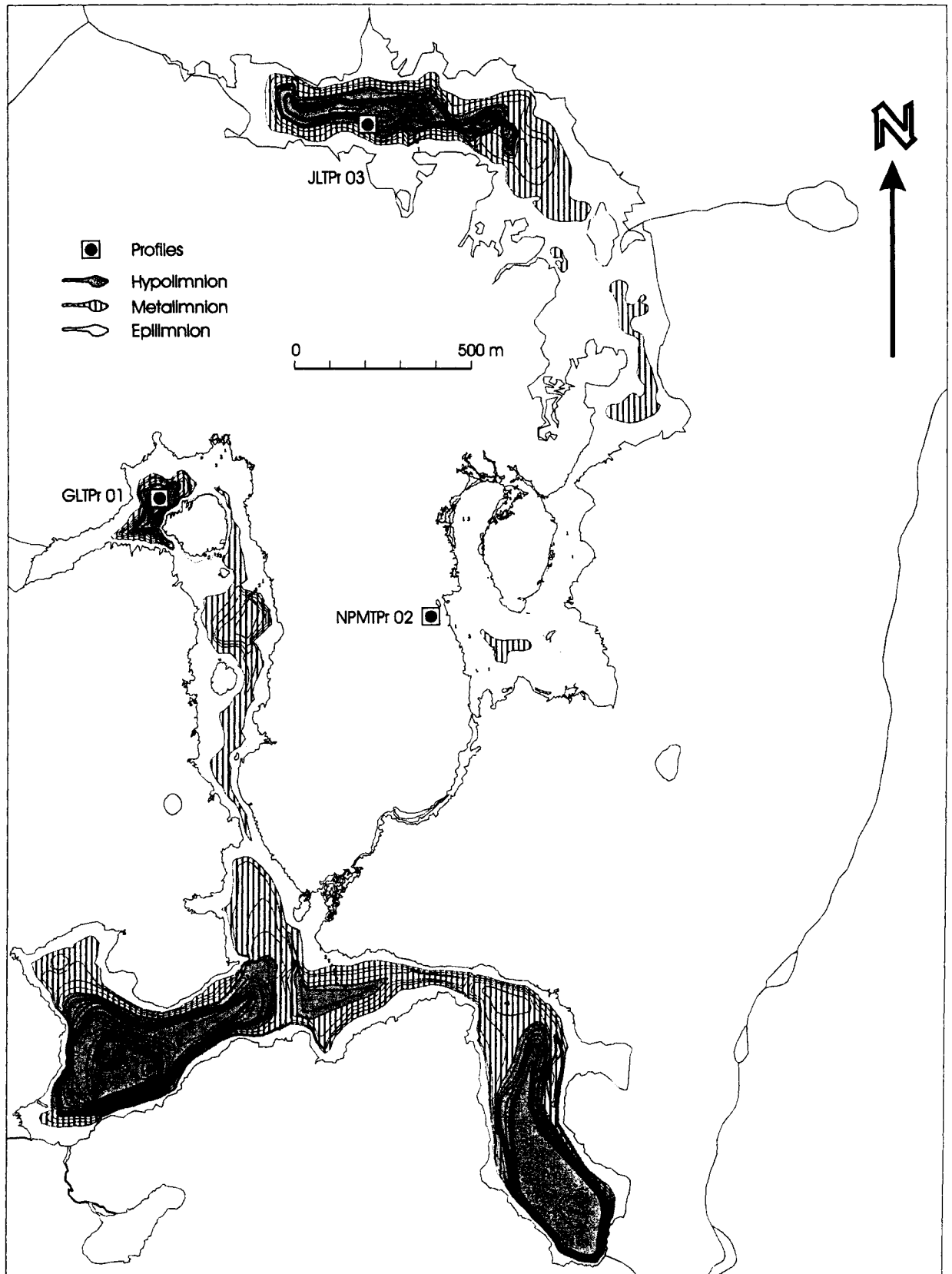


Figure 4.9 - Bathymetric map of James and Granite lakes, showing hypolimnion, metalimnion and epilimnion zones based on temperature profiles taken at indicated stations. Depths in metres (numbers and contours).

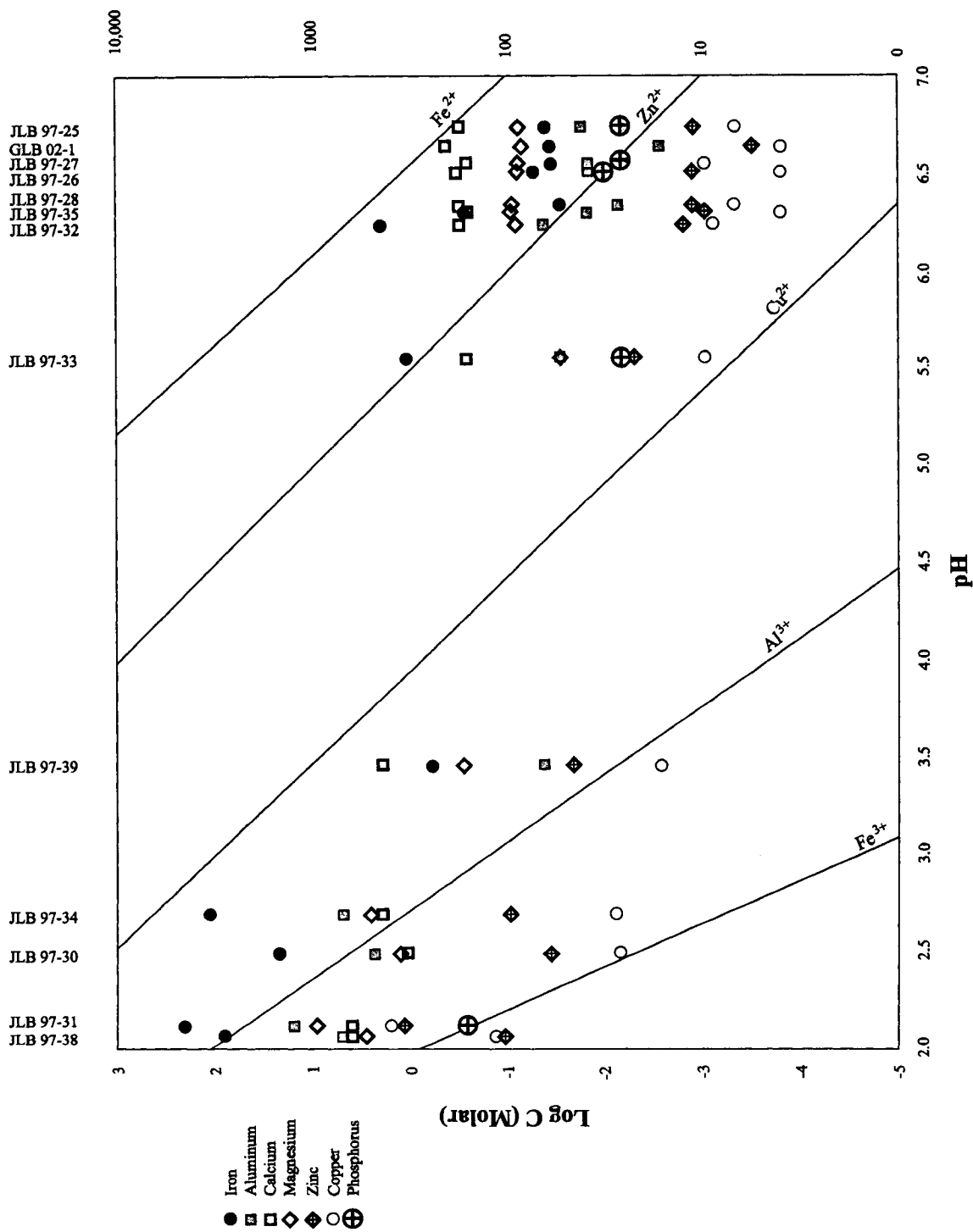


Figure 4.10 - Logarithms of the molar concentrations of metals in bottom waters plotted against pH and compared to their supersaturation/undersaturation zones in James and Granite lakes (after Stumm and Morgan, 1996).
Supersaturation/undersaturation lines for Ca, Mg and P plot to the right of the diagram.

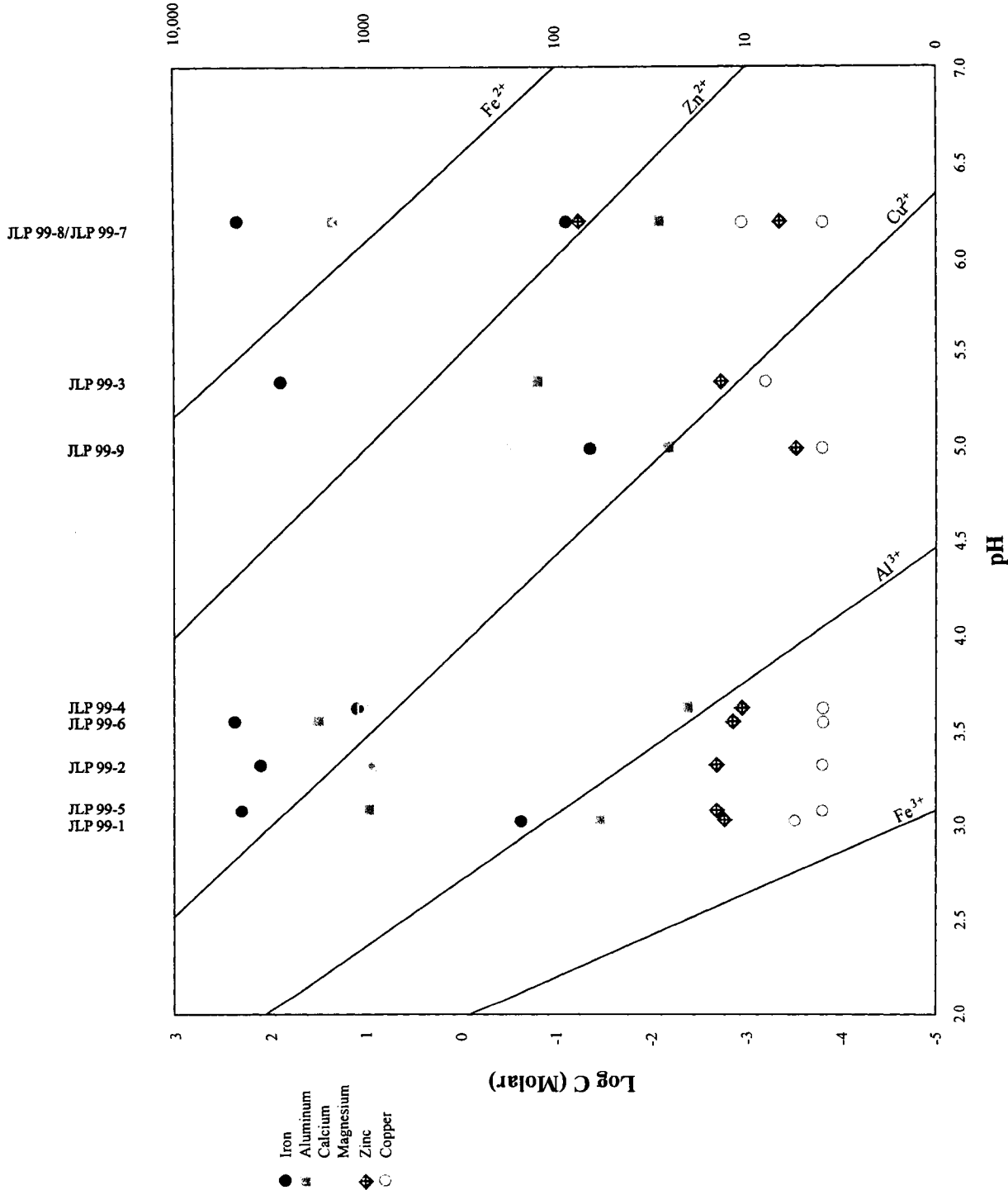


Figure 4.11 - Logarithms of the molar concentrations of metals from pore-waters plotted against pH and compared to their supersaturation/undersaturation zones for piezometer sites in James Lake (after Stumm and Morgan, 1996).

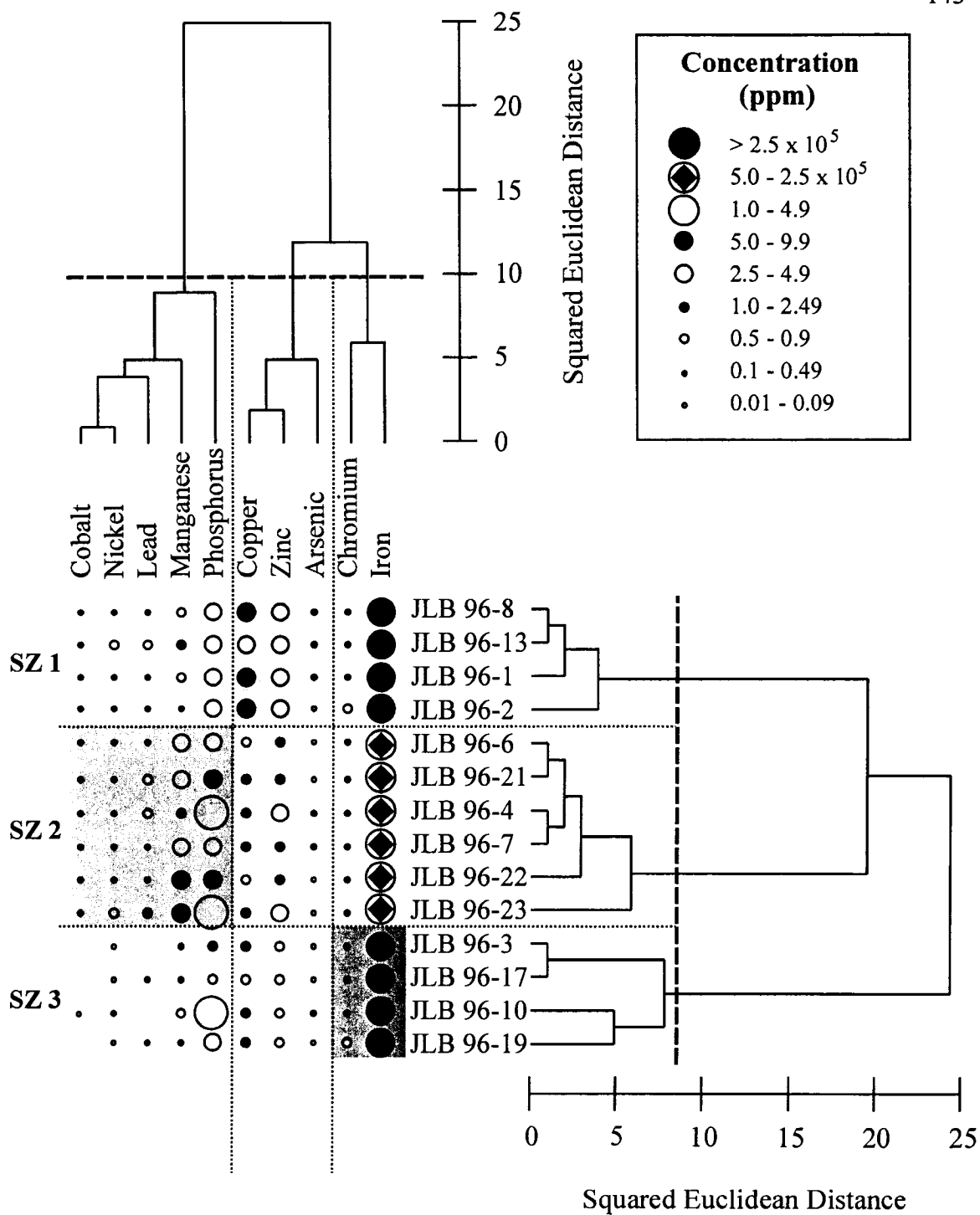


Figure 4.12a - R-mode vs Q-mode cluster analysis for sediment-water interface bulk sediment chemical analysis for James Lake

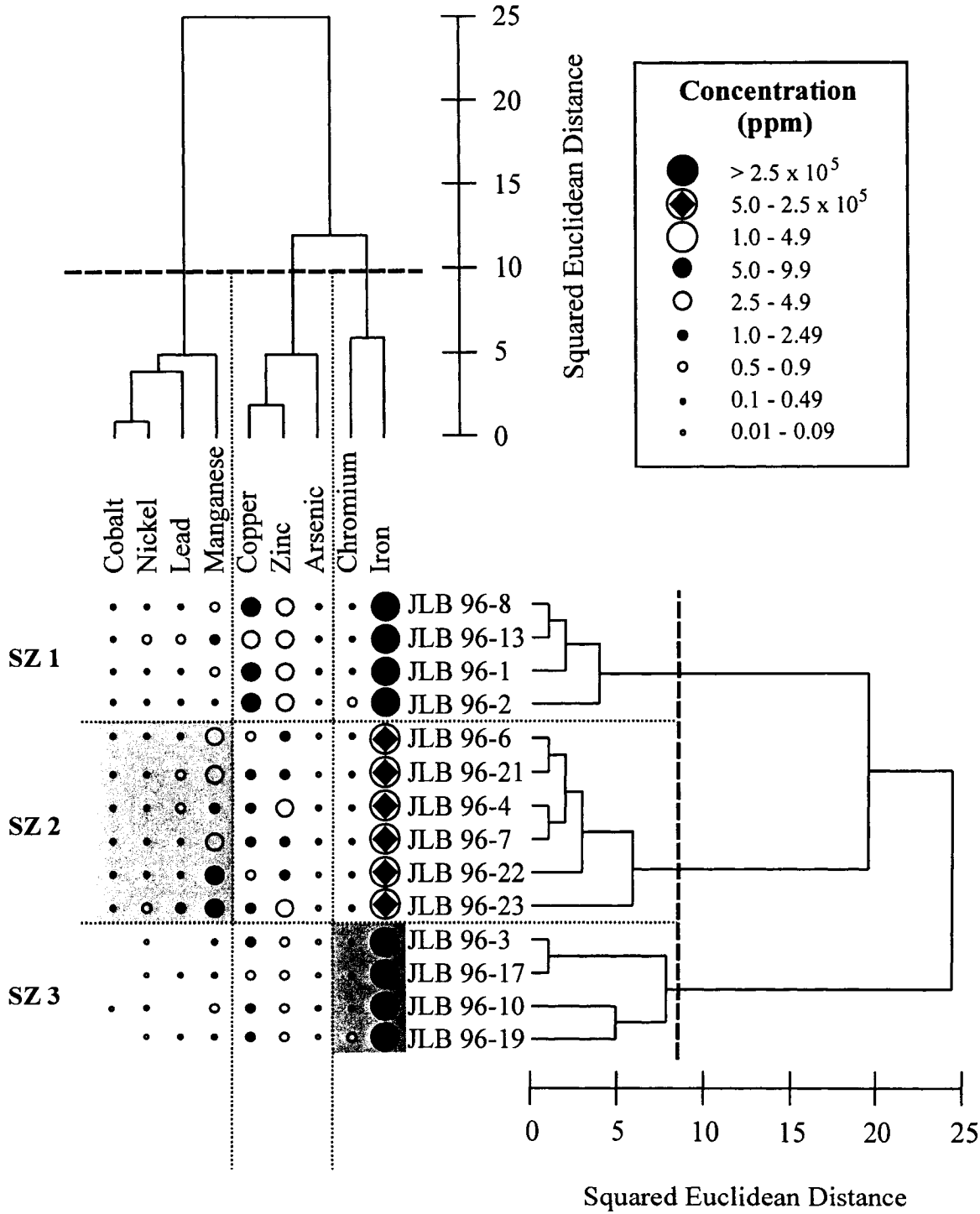


Figure 4.12b - R-mode vs Q-mode cluster analysis for sediment-water interface bulk sediment chemical analysis minus phosphorus in James Lake

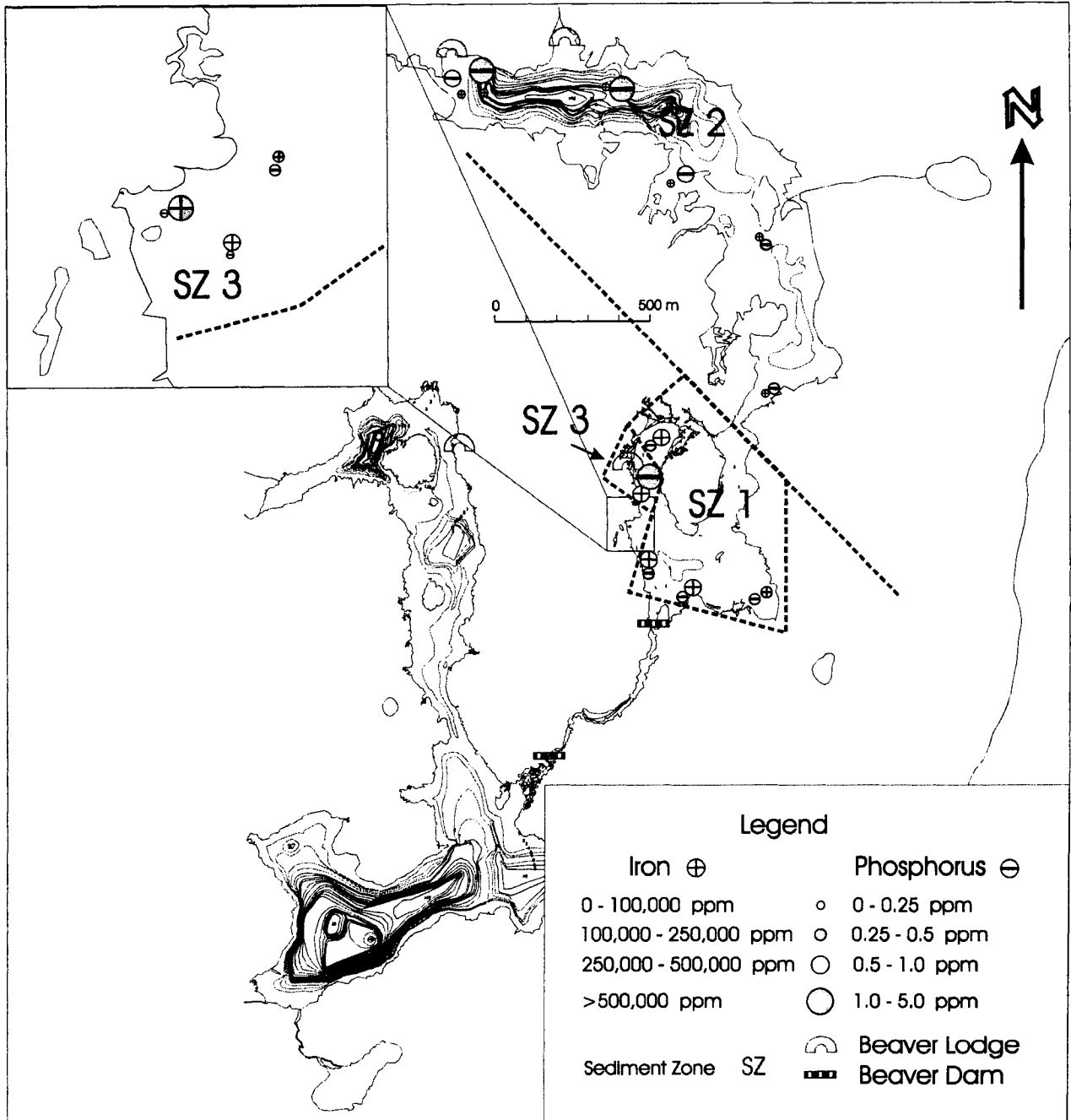


Figure 4.13 - Lake bottom Sediment Zones (SZ) showing phosphorus and iron concentrations from sediment-water interface bulk sediment chemistry in James Lake.

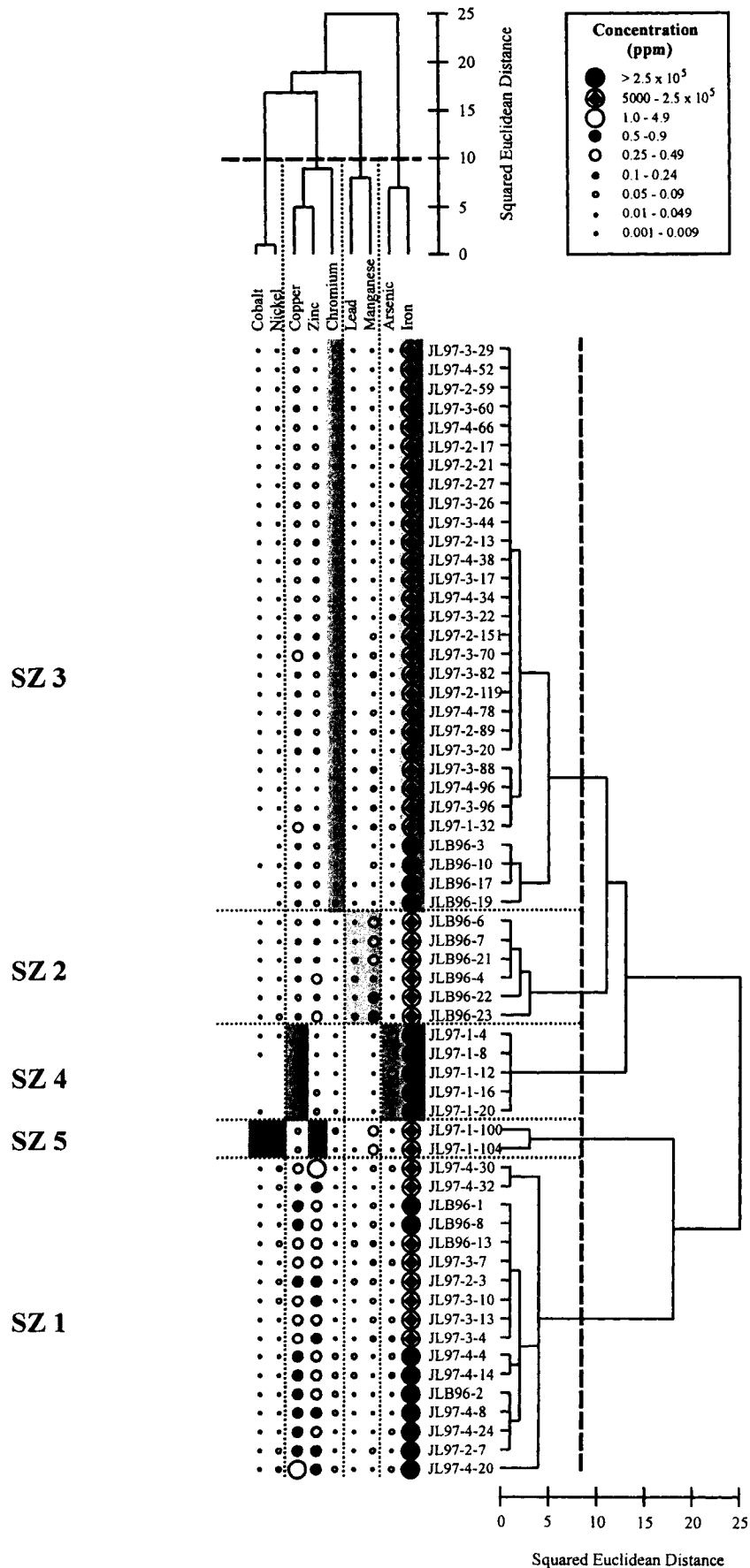
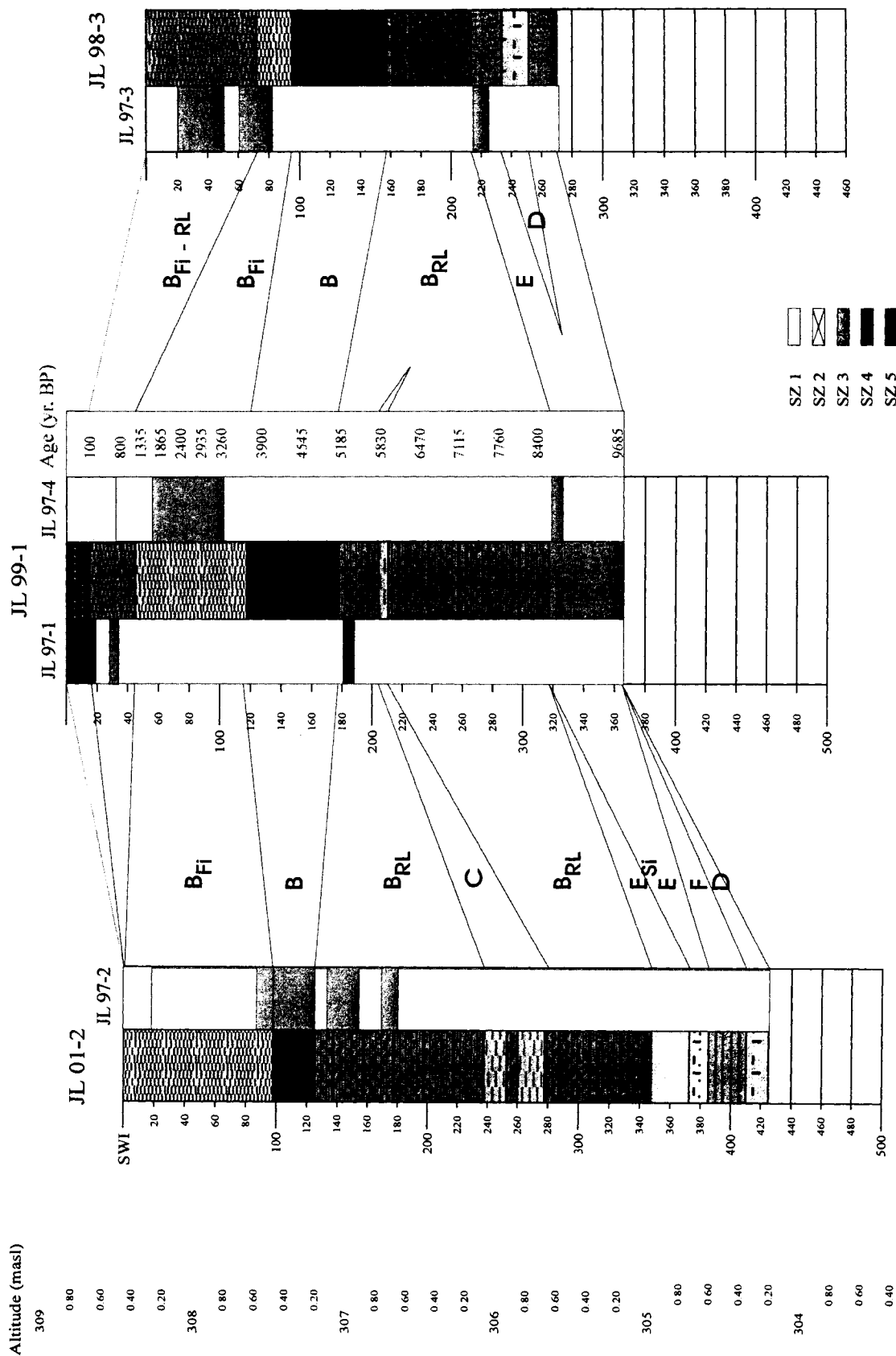


Figure 4.14 - R-mode vs Q-mode cluster analysis for sediment-water interface sediment chemical analysis and bulk sediment core chemical analysis in James Lake



CHAPTER FIVE

APPLICATION OF MICROPALAEONTOLOGICAL PROXIES TO ASSESS HOLOCENE PALEOENVIRONMENTAL AND PALEOCLIMATIC CHANGES IN JAMES AND GRANITE LAKES

ABSTRACT

Arcellacean (Thecamoebian) fauna were assessed from five Holocene sediment cores obtained from James and Granite lakes, and a palynological analysis was carried out on one core from each of James and Granite lakes. The first indication of colonization by plants is the occurrence of rare *Cupressaceae* pollen, dated to 10,800 yr. BP. Plant diversity began to increase by 10,770 yr. BP when *Pinus* sps. and *Larix* migrated into the area. The first appearance of arcellaceans occurred after 9650 yr. BP in low to medium diverse assemblages dominated by *Centropyxis aculeata* and *Centropyxis constricta*. Until 8800 yr. BP, high abundances of charophytes indicated macrophyte blooms were taking place. This is interpreted as having occurred during the draining of an ice-marginal lake after the retreat of the Laurentide Ice Sheet.

Based on pollen analysis, warmer conditions associated with the Holocene Hypsithermal prevailed in this area from 6250 to 4115 yr. BP. A stable, open Great Lakes – St. Lawrence type forest that developed here at the beginning of the Hypsithermal has prevailed here to the present. The presence of beavers (*Castor*

canadensis) in the lake acted as a control on water-level and eutrophism through the Holocene. Eutrophism was indicated by the abundance of high levels of the algae *Pediastrum* and the arcellacean *Cucurbitella tricuspis*, and occurs when beavers dam a site, causing the rate of flow in drainage streams to slow and the development of stagnant conditions. When the site became depleted of nearby beaver preferred trees (*Betula*, *Alnus* and *Populus*), it would be abandoned and the water-level would drop. Stagnant conditions would become reduced as flow levels increased, reducing eutrophism and resulting in recovering forest stands. In addition, the lowering water levels would result in some parts of the lake becoming forested. This cycle occurred many times in the history of this lake as indicated by diversity in the arcellacean populations.

INTRODUCTION

Arcellaceans (Thecamoebians) are freshwater amoeboid protozoans, characterized by an agglutinated test held together by organic cement, that occur in a variety of wetland habitats including moss, soil, peat and standing water from tropical to polar environments (Dalby et al., 2000; Dallimore et al., 2000; Medioli et al., 1990; Scott, 2001).

Arcellaceans have been used as proxies to indicate paleolimnological conditions such as pH, eutrophication, oxygen level (Asioli et al., 1996; Patterson et al., 1996; Patterson et al., 2002; Patterson and Kumar, 2000a; Patterson and Kumar, 2000b; Reinhardt et al., 1998a; Reinhardt et al., 1998b), and to infer climate change, as arcellacean faunas have been found to respond rapidly to changes in their environment (McCarthy et al., 1995).

Environmental changes can be indicated by measuring changes in faunal or floral diversity, a measure of species richness (Sageman and Bina, 1997).

A major cause of paleolimnological and environmental change in lakes results from the activities of beavers (*Castor canadensis* Kuhl). Beavers fell trees to construct dams and lodges, which ultimately raises the water level in the local lowlands (Broschart et al., 1989; Johnston and Naiman, 1990a; Johnston and Naiman, 1990b; Ray et al., 2001; Snodgrass, 1997). Beavers also use trees found near the water ways where they live for food, preferring birch (*Betula*), aspen (*Populus*) and alder (*Alnus*). These tree species, and others found in the vicinity of beaver induced wetlands, such as willow (*Salix*), tamarack (*Larix*) and spruce (*Picea*), decompose rapidly on land, resulting in elevated nutrient levels downstream (Francis et al., 1985). The release of products of decomposition is slower underwater and within beaver dams as both aspen and birch preserve well. Beaver dams are effective overall nutrient traps, causing $[Ca^{2+}]$ cations to increase in ponds and adjacent bogs, raising the overall pH, and causing eutrophication by injecting large amounts of nutrients into the system (Adamowicz, 1980; Watt and Heinselman, 1965).

Eutrophication causes an increase in the biomass of algae and macrophytes (De Nie, 1987). Freshwater macrophytes are aquatic plants that include charophytes, a typical part of the biomass in most lakes. Charophytes or stoneworts are thread-like branching algae that prefer alkaline to weakly acidic waters, where the oogonium, or female reproductive organ can become encrusted with lime and remain in the fossil record (Prescott, 1970; Wood and Imahori, 1965). Abundances of these organisms peaks in July and August, slowing water flow, trapping sediment, altering temperature and

water chemistry profiles (Chambers et al., 1999). *Pediastrum*, another freshwater algae has been linked to sediment erosion and nutrient depletion of exposed upland soils due to deforestation, which is related to the introduction of high-yield chemical fertilizers after World War II (Burden et al., 1986; Patterson et al., 2002). *Cucurbitella tricuspis*, an arcellacean that has a symbiotic relationship with *Pediastrum*, tends to increase proportionally to increases in *Pediastrum*, and is therefore a good indicator of eutrophic conditions (Honig and Scott, 1987; Medioli and Scott, 1983; Patterson et al., 2002; Patterson et al., 1985; Scott and Medioli, 1983).

This research traces the paleoenvironmental and paleoclimatic changes in the area of James and Granite lakes, which are located 10 km north of Temagami, Ontario, adjacent to Highway 11 (Fig. 1.1), and characterized by a mixture of Great Lakes – St. Lawrence Forest and a Boreal Forest (Liu, 1981). Because arcellaceans are better suited than pollen to recognize short-lived phenomena such as the mid-Holocene Hypsithermal (Patterson et al., 2002), palynology was used to describe the long-term effects of climate change during the Holocene, and arcellaceans were used to infer short-term environmental changes caused by native wildlife such as beaver, pollution caused by mineralization within the country rock and pollutants introduced as a result of anthropogenic activity.

Field and laboratory methods are described in Chapter Two.

ANALYSIS AND RESULTS

One cc samples were collected from 73 sediment-water interface (SWI) sediment samples (Fig. 2.3), and 235 one cc samples were obtained from five sediment cores (Fig. 2.1) from James and Granite lakes for quantitative arcellacean analysis. Thirty-one additional sediment samples were analyzed for pollen from James Lake core JL 99-1 (JLP 99-1) and Granite Lake core GL 99-4 (GLP 99-4) to assess past vegetation trends in the area.

Forty-one SWI sediment samples from James Lake and 32 SWI sediment samples from Granite Lake yielded 40 stations in James Lake (Table 5.1) and 26 stations in Granite Lake with statistically significant populations (SSP) of arcellaceans. A sample was judged to contain a SSP if the total counts obtained for each taxon was greater than the probable error (pe), calculated by

$$pe = 1.96 \left(\frac{s}{\sqrt{X_i}} \right) \quad (5-1)$$

where s is the standard deviation of the population counts, and X_i is the number of counts at the station being investigated (Patterson and Fishbein, 1989).

Quantification of arcellaceans from the 235 sediment core samples from James and Granite lakes yielded 75 samples with populations large enough for statistical analysis, as follows: Sixty-one core samples from James Lake core JL 99-1 yielded 24 samples with SSP; 45 core sediment samples from James Lake core JL 99-7 yielded only

one sample with SSP; 51 core sediment samples from James Lake core JL 01-2 yielded 19 samples with SSP; 24 core sediment samples from Granite Lake core GL 98-3 yielded 10 samples with SSP; and 54 core sediment samples from Granite Lake core GL 99-4 yielded 21 samples with SSP. Thirty-one pollen sediment core samples analyzed for pollen from James Lake core JLP 99-1 (Table 5.2) and Granite Lake core GLP 99-4, yielding 26 sediment samples with statistically significant pollen populations.

Twenty-nine species of arcellaceans and two species of charophyte from SWI sediment samples and core sediment samples in James and Granite lakes, and 21 palynomorphs from pollen sediment core samples in James Lake were identified in this investigation. The relative fractional abundance (X_i) of each taxonomic unit for each sample or station was calculated as follows:

$$X_i = \frac{C_i}{N_i} \quad (5-2)$$

where C_i is the species count and N_i is the total of all species counts at that station or sample. Using this information, the standard error (S_{X_i}) associated with each taxonomic unit was calculated using the following equation:

$$S_{X_i} = 1.96 \sqrt{\frac{X_i(1 - X_i)}{N_i}} \quad (5-3)$$

Based on these results, if the standard error was greater than the fractional abundance of the species or palynomorph at a station or sample, then the species or palynomorph was not included in the subsequent multivariate analysis for that station or sample (Patterson and Fishbein, 1989).

Twenty-five arcellacean species and one charophyte species remained after five statistically insignificant arcellaceans and one charophyte were removed from the database and not included in subsequent multivariate analysis. The statistically insignificant species removed from the James and Granite lake database were *Diffflugia bacillariarum* (Perty, 1849); *Diffflugia Bidens* (Pénard, 1902); *Diffflugia globulus* (Ehrenberg, 1849); *Diffflugia oblonga* (Leidy, 1879) strain “triangularis” and *Heliopera sphagni* (Leidy, 1874). Twelve palynomorphs remained after the following 9 statistically insignificant palynomorphs were removed from the pollen database containing James Lake core JLP 99-1 and Granite Lake core GLP 99-4: Aceraceae, Alnus, Ambrosia, Chenopodiaceae, Nuphar, Pteridium, Pteropsida monolete, Saliceace, and Tsuga.

Shannon - Weaver Diversity Index

A measure of species richness is the diversity measure known as the Shannon – Weaver diversity index (SDI) (Shannon and Weaver, 1949), where high values (2.5 – 3.5) indicate a stable environment, while lower values (0.1 – 1.5) may indicate a stressed environment. The arcellacean population diversity of each station or sample was calculated using the SDI,

$$SDI = -\sum_1^S \left(\frac{X_i}{N_i} \right) \times \ln \left(\frac{X_i}{N_i} \right) \quad (5-4)$$

where X_i is the fractional abundance of each taxon in the sample, N_i is the total abundance of the sample and S is the species richness of the sample. The SDI values obtained using the James and Granite lakes database indicate increasing diversity with increasing population size (Fig. 5.1). When the number of arcellacean species per sample is low (2 – 12), the SDI is low (0.5 – 1.1). As the number of species per sample increases (6 – 20), the SDI increases to middle ranges for this system (1.2 – 1.9), and when the number of species becomes stable at higher values (16 – 25) the SDI becomes a maximum in this system (2.0 – 2.6). The SDI was calculated for the pollen data using the same criteria as above.

Cluster Analysis

R-mode and Q-mode cluster analysis was carried out on 26 species present in SSP in the 139 samples from the James and Granite lakes database. R-mode cluster analysis was used to determine which species best characterized an assemblage (Scott and Medioli, 1980), and Q-mode cluster analysis was carried out to group statistically similar populations using Ward's Minimum Variance method. This resulted in a reduced data set recorded as Euclidean distances and arranged in a combined R-mode and Q-mode hierarchical diagram (Fishbein and Patterson, 1993; Figs. 5.2, 5.2a & b). These samples yielded six assemblages (AS) based on the dominance of certain arcellaceans, and the diversity of their populations.

AS I exhibits low diversity ($0.5 \leq \text{SDI} \leq 0.7$), is dominated by *Arcella vulgaris* (Ehrenberg, 1830) ($0.59 \leq X_i \leq 0.83$) and *C. tricuspis* ($0.17 \leq X_i \leq 0.40$), and plots in the immediate vicinity of the Northland Pyrite Mine waste rock site in southwestern James Lake (Fig. 5.3). AS IIa exhibits low to medium diversity ($0.7 \leq \text{SDI} \leq 1.6$), is dominated by *C. tricuspis* ($0.47 \leq X_i \leq 0.77$) and *A. vulgaris* ($0.03 \leq X_i \leq 0.48$), and plots in southwestern James Lake near beaver lodges and the waste rock pile, and in northern James Lake near beaver lodges, and also proximal to the metalimnion of an anoxic basin. AS IIb exhibits low to high diversity ($1.0 \leq X_i \leq 2.6$), is dominated by *C. tricuspis* ($0.09 \leq X_i \leq 0.44$) and plots throughout James Lake, and in the vicinity of an anoxic basin in northern Granite Lake. AS IIIa exhibits low - medium diversity ($1.0 \leq \text{SDI} \leq 1.7$), is dominated by *Lagenodifflugia vas* (Leidy, 1874) ($0.29 \leq X_i \leq 0.59$) and *Centropyxis aculeata* (Ehrenberg, 1832) strain “aculeata” ($X_i \leq 0.42$), and plots in James Lake cores JL 99-1 (Fig. 5.4) and JL 01-2 (Fig. 5.6), and in Granite Lake core GL 99-4 (Fig. 5.8), and the stratigraphic relationships are explored in Figure 5.9. AS IIIb exhibits a medium – high diversity ($1.9 \leq \text{SDI} \leq 2.6$), is dominated by *L. vas* ($X_i \leq 0.31$) and *C. aculeata* “aculeata” ($X_i \leq 0.27$), and plots in the marsh between the lakes, throughout Granite Lake, in marshy areas scattered around James Lake and near the surface in James Lake cores JL 01-2 and JL 99-1. AS IVa exhibits a medium diversity ($1.2 \leq \text{SDI} \leq 1.6$), is dominated by *C. aculeata* “aculeata” ($0.33 \leq X_i \leq 0.71$) and *Centropyxis constricta* (Ehrenberg, 1843) strain “aerophila” ($X_i \leq 0.30$), and plots in James Lake cores JL 99-1, JL 01-2 and in Granite Lake core GL 99-4, and also in the marsh between the two lakes. AS IVb exhibits a medium diversity ($1.1 \leq \text{SDI} \leq 1.8$), is dominated by *A. vulgaris* ($0.15 \leq X_i \leq 0.51$), *C. aculeata* “aculeata” ($0.07 \leq X_i \leq 0.39$) and *C. constricta* “aerophila” (X_i

≤ 0.27), and plots in James Lake cores JL 99-1 and JL 01-2. AS V exhibits a low – medium diversity ($0.8 \leq \text{SDI} \leq 1.5$), is dominated by charophytes ($0.34 \leq X_i \leq 0.67$) with the centropxyxids *C. aculeata* “aculeata” ($0.05 \leq X_i \leq 0.26$), *Centropxyxis aculeata* (Ehrenberg, 1832) strain “discoides” ($0.05 \leq X_i \leq 0.20$) and *C. constricta* “aerophila” ($0.09 \leq X_i \leq 0.15$), and plots in James Lake cores JL 99-1 and JL 99-7 (Fig. 5.5) and in Granite Lake core GL 99-4. AS VI exhibits a low – medium diversity ($0.7 \leq \text{SDI} \leq 1.8$), is dominated the centropxyxids *C. aculeata* “aculeata” ($X_i \leq 0.53$), *C. aculeata* (Ehrenberg, 1832) strain “discoides” ($0.09 \leq X_i \leq 0.52$) and *C. constricta* “aerophila” ($0.08 \leq X_i \leq 0.53$), and plots in the James and Granite lakes cores JL 99-1, JL 01-2, GL 99-4 and GL 99-3 (Fig. 5.7). Certain stations throughout the James and Granite lakes system were sterile with respect to arcellaceans. These are listed in AS 0, and are located within the mine trench (JLB 97-39) and pond (JLB 97-36 – 38) barricaded by a limestone causeway (Ch. 4), in sediment with visible metal precipitation in the marsh immediately south of a beaver dam, at the south of James Lake (JLM 01-1), proximal to the downstream side of a second beaver dam south of the marsh (GLB 01-7 – 8) and in anoxic basins in northern and central Granite Lake (GLB 99-1 – 2, & GLB 02-1).

Pollen cluster analysis

Statistical analysis for palynomorphs in SWI sediment samples was not carried out in the James and Granite lakes system, but the surrounding forest and marshlands was visually ascertained to be a mixed conifer forest containing white and black spruce, white, red and jack pine, tamarack and balsam fir. Birch trees were dominant near the lakes and poplar tends to populate the higher ground. Cattails, sedges and grasses, and

other marsh plants such as St. John's wort populated the marsh areas, which were ringed by a mixed forest containing birch, alder, willow and cedar, inside of the above mixed conifer forest.

Multivariate statistical analysis was carried out on 26 pollen samples from James Lake core JLP 99-1 and Granite Lake core GLP 99-4, yielding five pollen zones (PZ) based on the dominance of palynomorphs (Fig. 10). PZ I exhibits a medium - high diversity ($1.8 \leq \text{SDI} \leq 2.1$), is dominated by *Pinus strobus* ($0.12 \leq X_i \leq 0.29$), *Pinus* sp. ($0.12 \leq X_i \leq 0.26$) and *Picea* ($0.11 \leq X_i \leq 0.26$) with prominent Cupressaceae ($0.05 \leq X_i \leq 0.17$), *Populus* ($0.02 \leq X_i \leq 0.11$), *P. banksiana/resinosa* ($0.06 \leq X_i \leq 0.16$) and *Pediastrum* ($0.02 \leq X_i \leq 0.09$). PZ I plots in one band from the SWI to ~250 cm (rswi), and representing the current forest type that existed in the area since ~7000 yr. BP (Fig. 11). PZ II exhibits a medium diversity ($1.2 \leq \text{SDI} \leq 1.8$), is dominated by *Pinus* sp. ($0.21 \leq X_i \leq 0.39$), *Pinus strobus* ($0.17 \leq X_i \leq 0.32$) and Cupressaceae ($0.08 \leq X_i \leq 0.20$) with prominent *Pediastrum* ($0.04 \leq X_i \leq 0.24$). PZ II plots in three bands, the first from 320 cm to 250 cm in depth (rswi), with minor bands at 350 cm and 390 cm (rswi). PZ III exhibits a medium diversity ($1.1 \leq \text{SDI} \leq 1.1$), is dominated by *Pinus strobus* ($0.56 \leq X_i \leq 0.62$) with *P. banksiana/resinosa* ($0.06 \leq X_i \leq 0.10$) *Pediastrum* ($0.08 \leq X_i \leq 0.12$). PZ III plots in a two bands, from 315 to 335 cm (rswi) and 360 to 370 cm (rswi). PZ IV exhibits a medium diversity ($1.0 \leq \text{SDI} \leq 1.7$), is dominated by *P. strobus* ($0.21 \leq X_i \leq 0.39$) with prominent Cupressaceae ($0.15 \leq X_i \leq 0.37$) and *Pinus* sp. ($0.10 \leq X_i \leq 0.25$), and plots in four narrow bands between 340 and 430 cm (rswi).

DISCUSSION

The end of the Pleistocene

The Laurentide Ice Sheet retreated from the Temagami region between 11,000 and 10,100 yr. BP (Saarnisto, 1974), and the initial vegetation of the region was open Boreal forest dominated by white spruce and tamarack (Hall et al., 1994a). The first vegetation recorded in the James and Granite lakes system was Cupressaceae pollen (juniper vs cedar), found in sediment dated at $10,800 \pm 220$ yr. BP, indicating that the Laurentide Ice Sheet had already retreated from the region of James and Granite Lake by this time. Plant diversity had increased by 10,770 yr. BP, with white pine and *Cupressaceae* dominating the forest with some Larch and red/jack pine present. White pine is an early successional species after deglaciation, indicating cool conditions (Kearney and Luckman, 1983), as does Juniper which also indicates high effective moisture (Minckley and Whitlock, 2000).

Post Younger Dryas warming period

By 9850 yr. BP (after the end of the Younger Dryas cool period), the abundance of Cupressaceae and *Larix* became lower, as the water levels dropped, and *Pediastrum* increased in abundance. This eutrophic indicator was found in association with abundant charophytes, indicating that the falling water levels had reached levels below 20 m, and the lime-rich waters were encrusting the charophyte oogonium. The first evidence of arcellaceans in the lake system following the retreat of the Laurentide Ice Sheet, was the appearance of a low to medium diversity assemblage of centropxyids, dominated by *C.*

aculeata strain “discoides” at 9650 yr. BP. *C. aculeata* strain “discoides” is a dominant species in many modern Arctic lakes (Dallimore et al, 2000). This centropixid assemblage characterized the lakes until 8600 yr. BP.

Post Younger Dryas cool period

By 8600 yr. BP, pollen diversity had decreased significantly, indicating a cooling period, during which time, the charophytes became statistically insignificant. This cooling trend ended at 8400 yr. BP with the appearance of *Betula* in the record suggesting that the climate was beginning to warm. During the cooling event populations of the arcellacean *C. aculeata* strain “aculeata” increased in abundance, replacing *C. aculeata* strain “discoides” as the dominant strain (Vb).

Early Holocene warming

In addition to *Betula*, *Cupressaceae* and *Pediastrum* increased in abundance after 8400 yr. BP, while pine and spruce decreased in abundance, indicating a warmer drier climate. Immediately prior to 8250 yr. BP the thecamoebian *A. vulgaris* first appears in the system, indicating a possible drop in pH of the lake waters (Patterson and Kumar, 2000a). This warm dry phase is marked by statistically insignificant arcellacean populations between 7950 and 6800 yr. BP (PZ II), and a significant drop in the MAR (Chapter Three) suggesting that the lake may have all but dried up during this interval.

Holocene Hypsithermal

By 6250 yr. BP, a drop in the abundance of White pine, coupled with increases in

Red/Jack pine, Aspen, Birch and *Pediastrum* indicate a change in the forest type to that of a Great Lakes – St. Lawrence type. Terasme (1970) and Liu (1990) suggested that the beginning of the Holocene Hypsithermal warm period was indicated by an increase in the flux of red and jack pine, which occurred here at 6250 yr. BP. At 4115 yr. BP, the abundance of White spruce pollen crashed, as did the pollen of Aspen, Birch and *Pediastrum*. A slight but distinct increase in *Abies* through the interval indicates the onset of a climatic change towards cooler and moister conditions, marking the end of the Holocene Hypsithermal (Liu, 1990).

Two types of arcellacean assemblages developed simultaneously in the two lakes involved in this research during the Holocene Hypsithermal. The first, which dominated in Granite Lake, was a medium to high diverse population of arcellaceans dominated by *L. vas*, a higher pH indicator (Boudreau, 1999) and *C. aculeata* “aculeata” (Assemblage III) indicating stressed environmental conditions (Patterson and Kumar, 2000a). The second type of assemblage dominated in James Lake. A medium diversity assemblage dominated by the low pH indicators centropxyxids and *A. vulgaris*, found off and on throughout the whole of the Holocene in the vicinity of the abandoned Northland Pyrite Mine site.

Medieval Warm Period and Little Ice Age

By 650 AD, an increase in white, red and jack pine, and tamarack, coupled with declining populations of cedar suggests the beginning of the Medieval Warm Period which lasted until 1650 AD. The beginning of the Little Ice Age is indicated by a decrease in white pine and increases in cedar, tamarack and red/jack pine (Gribbin, 1978)

which occurred from 1650 to 1800 AD. The current forest community in the Temagami region, today, is similar to that which existed from 6250 yr. BP to the inception of the Little Ice Age (Hall et al., 1994b). The forest community is dominated by white & red pine (*Pinus strobus* & *P. resinosa*), spruce and yellow birch (*Betula alleghaniensis*), with lesser amounts of alder, oak (*Quercus*), elm (*Ulmus*), beech (*Fagus grandifolia*) and sugar maple (*Acer saccharum*) of the Great Lakes – St. Lawrence Forest type. The abundance of white pine attained a maximum at the peak of the Hypsithermal (~4000 yr. BP), but declined with the period of Neoglacial cooling (450 to 150 yr. BP), to be replaced by white and black spruce (*Picea glauca* & *P. mariana*), jack pine (*Pinus banksiana*), tamarack and balsam fir (*Abies balsamea*) (Hall et al., 1994a). Birch and *Ambrosia lativa* have increased over the last 180 years due to farming, mining and logging (Hodgins and Benedickson, 1989).

Present Conditions

Micropaleontological analysis indicates that the arcellacean populations in the James and Granite lakes system today are not completely analogous to those which existed in the past. The development of eutrophic conditions due to human influence has been cited as a possible explanation (Patterson and Kumar, 2002). However, several studies elsewhere have shown that anthropogenic influences are not the exclusive cause of eutrophism (Paterson et al., 2004). Generally the arcellacean assemblages present in James and Granite lakes show medium to high diversity, with exceptions in some parts of the lakes caused by various stress factors. Stress factors influencing the James and Granite lakes system include; 1) the Northland Pyrite Mine waste rock pile, which lowers

the pH in the immediate vicinity of southwestern James Lake, and 2) the influence of beavers, which build lodges and dams, altering the lake chemistry (Chapter Four), resulting in an increase nutrient levels, resulting in eutrophication and the raising of water levels in the system (Chapter Three and Four).

The waste rock site in the vicinity of the southwest corner of James Lake has been previously investigated by Patterson and Kumar (2000), and the waters of the SDI in the immediate vicinity are dominated by low diversity populations dominated by *A. vulgaris*. The two remaining arcellacean assemblages of this study are found mainly at the sediment water interface of James Lake (minor exceptions in northern Granite Lake). The first (Assemblage I) is a low diversity assemblage found in the vicinity of the Northland Pyrite Mine waste rock pile, dominated by *A. vulgaris* and minor *C. tricuspis*, indicating low pH conditions with high nutrient (chemical) content. The second (Assemblage II) is dominated by *C. tricuspis*, found throughout James Lake, but shows the highest fractional abundances of *C. tricuspis* proximal to beaver lodges or dams.

Possible impact of beavers on lake ecology

Within a decade of beaver invading an area, submerged macrophytes, such as pondweed (*Potamogeton*) colonize the ponds (Ray et al., 2001), followed by the common cattail (*Typha latifolia*) in the second decade resulting in the formation of extensive *Typha* marshes, such as exists today between James and Granite lakes. As discussed in Chapter four, high levels of P exist in the sediments of James Lake, especially in the vicinity of the numerous beaver lodges present in the area. This high nutrient levels can cause eutrophication, by beaver induced increases in the biomass of macrophytes, and

rotting vegetation both in and around the area of beaver influence. *Pediastrum*, a strong indicator of eutrophication has been found in James Lake since the invasion of vegetation at the end of the Pleistocene glaciation greater than 10,800 yr. BP. *C. tricuspis*, an arcellacean indicator of eutrophication (Patterson and Kumar, 2002) has been found to spike in Assemblage zones III and IV, suggesting the presence of beaver in the past. Alternating low diversity populations and statistically insignificant populations (low or no water conditions) can be explained by cycling of beaver populations. Beaver will remain at a site until it is too difficult for them to get birch, aspen and alder near their ponds. When this happens, the beaver move to a new site and start over, causing water-level cycling in the area, from a stream or brook through a marshy area to a lake or pond as exists today.

CONCLUSIONS

Holocene arcellacean proxies in the area of James and Granite lakes were influenced by local factors, such as changes in pH, nutrient content, while pollen was influenced by regional factors such as the retreat of the Laurentide Ice Sheet, which occurred prior to 10,800 yr. BP, causing a change in climate from glacial to periglacial.

The stressed climate of the early Holocene was reflected in the initial boreal forest fauna and low diversity assemblages of arcellaceans present at that time. These in turn were affected by local environmental conditions like low pH, first indicated 8400 yr. BP by the arcellacean *A. vulgaris*. From this one can suppose that the Northland Pyrite Mine sulfide vein was exposed to the lake waters at this time.

Eutrophic conditions were indicated to exist as far back as 9700 yr. BP when the first indications of *Pediastrum* (and *Charophyta*) were found to be present in the system. Slow moving waters can be caused by the beaver influenced ponding which increases both the water and nutrient levels behind the dams. These conditions exist today around beaver dams and lodges in James Lake, and throughout most of Granite Lake. The cyclic high and low water levels caused by beavers, over time, is a method of exposing the sulfide vein to the oxygenated waters sulfides require to oxidize. This can be tracked by the presence of algae (as mentioned above) and by the presence of proxies such as *C. tricuspis*.

SYNONYMY

Numerous arcellacean species have been separated and defined through the years (Medioli and Scott, 1983; Medioli and Scott, 1988). The systematic approaches utilized range from the opinion of Wallich (1864) who believed that all arcellaceans belonged to the same species, to that of some modern specialists who have described new species for almost every variety recognized (Deflandre, 1928). Both approaches may be partially right as several distinct morphological populations can be observed within many arcellacean species. These strains develop in response to different environmental stresses, and can be considered ecomorphs. An abbreviated taxonomy as well as photomicrographs of the species discriminated (based on Medioli and Scott 1983) is provided along with diagnosis for infrasubspecific designation (Reinhardt and others, 1998a).

Subphylum SARCODINA Schmarda 1871

Class RHIZOPODEA von Siebold 1845

Subclass LOBOSA Carpenter 1861

Order ARCELLINIDA Kent 1880

Superfamily ARCELLACEA Ehrenberg 1830

Family **ARCELLIDAE** Ehrenberg 1830

Genus *Arcella* Ehrenberg 1830

Arcella vulgaris Ehrenberg 1830

(Plate 5.2, figures i, j)

Arcella vulgaris EHRENBERG 1830, p. 40, pl. 1, fig. 6

Arcella vulgaris Ehrenberg 1830 REINHARDT and others 1998, pl. 1, fig. 3

Diagnosis: Test without spines, hyaline and transparent, aperture sub-terminal or occasionally central, circular or oval, invaginated.

Family **CENTROPYXIDIDAE** Deflandre 1953

Genus *Centropyxis* Stein 1859

Centropyxis aculeata (Ehrenberg 1832)

strain “aculeata”

(Plate 5.1, figures a - k)

Arcella aculeata EHRENBERG 1832, p. 91

Centropyxis aculeata “*aculeata*” REINHARDT and others 1998, pl. 1, fig. 1

Diagnosis: Test depressed, circular with 1 – 8 spines in postero-lateral margin.

Centropyxis aculeata (Ehrenberg 1832)

strain “*discoides*”

(Plate 5.1, figures 1 - n)

Arcella discoides EHRENBERG 1843, p. 139

Arcella discoides Ehrenberg, EHRENBERG 1872, p. 259, pl. 3, fig. 1

Arcella discoides Ehrenberg, LEIDY 1879, p. 173, pl. 28, figs. 14 – 38

Centropyxis aculeata var. *discoides* PENARD 1890, p. 151, pl. 5, figs. 38 – 41

Centropyxis discoides Penard [sic], OGDEN and HEDLEY 1890, p. 54, pl. 16, figs. a – e

Centropyxis aculeata “*discoides*” REINHARDT and OTHERS 1998, pl. 1, fig. 2

Diagnosis: Test depressed, circular almost “doughnut shaped” without spines.

Centropyxis constricta (Ehrenberg 1843)

strain “*aerophila*”

(Plate 5.1, figures o – ad; Plate 5.2, figure a)

Centropyxis aerophila DEFLANDRE 1929

Centropyxis aerophila Deflandre OGDEN and HEDLEY 1980, p. 48 – 49

Cucurbitella [sic.] *constricta* REINHARDT and others 1998, pl. 1, fig. 6

Centropyxis constricta “*aerophila*” KUMAR and DALBY 1998, Issue 1, fig. 5-1

Diagnosis: Test varies from spherical, subspherical to elongated with thick apertural lip at an angle of 45° to 60° with respect to the test. Spines absent.

Centropyxis constricta (Ehrenberg 1843)

strain “spinosa”

Centropyxis spinosa CASH and HEDLEY 1980, p. 62. pl. 20, figs. a – d

Centropyxis spinosa Cash, OGDEN and HEDLEY 1980, p. 62, pl. 20, figs. a – d

Centropyxis constricta “spinosa” REINHARDT and others 1998, pl. 1, fig. 5

Diagnosis: Test more flattened than strain “constricta” with three or more spines on the fundus.

Family **DIFFLUGIDAE** Stein 1859

Genus *Diffugia* Leclerc in Lamarck 1816

Diffugia bacilliarum Perty 1849

Diffugia bacilliarum Perty 1849b, p. 27, Perty, 1852, p. 187, pl. 9, fig. 7

Diffugia acuminata Ehrenberg, Leidy, 1879, p. 109, pl. 13, figs. 10 – 17

Diffugia elegans Leidy 1874, p. 140, pl. 4, figs. 4 – 11

Diffugia mammillaris Pénard 1893, p. 176, pl. 3, figs. 18 – 19

Diffugia elegans var. *teres* Pénard 1899, p. 27, pl. 2, figs. 16 – 20

Diffugia acuminata var. *inflata* Pénard 1899, p. 29, pl. 3, fig. 1

Diffflugia acuminata var. *elegans* Pénard. West, 1901, p. 319, pl. 28, figs. 11 – 12

Diffflugia bacilliarum var. *elegans* Pénard. Cash and Hopkinson, 1909, p. 28, text-fig.

48, pl. 20, figs. 2 – 5

Diffflugia elegans var. *angustata* DEFLANDRE, 1926, p. 523, text-fig. 10

Diffflugia elegans forma *tricornis* Jung, 1936, p. 45

Diffflugia curvicaulis var. *inflata* DECLOITRE, 1951, p. 105, text-fig. 16

Diagnosis: Test broad in relation to its length, at times the maximum width is reached at its aperture. Fundus is always somewhat conical.

Diffflugia bidens Pénard 1902

Diffflugia bidens PENARD 1902, p. 264, figs. 1 – 8

Diffflugia bidens Pénard MEDIOLI and SCOTT 1983, p. 21 – 22, pl. 1, figs. 1 – 5

Diagnosis: Test laterally compressed with two or three short spines. Aperture round and simple.

Diffflugia corona Wallich 1864

Diffflugia protaeiformis (sic) Ehrenberg subsp. *D. globularis* (Dujardin) var. *D. corona*

WALLICH 1864, p. 244, pl. 15, fig. 4a – c; pl. 16, figs. 19 – 20

Diffflugia corona (Wallich 1864) ARCHER 1866, p. 186

Diffflugia corona Wallich REINHARDT and OTHERS 1998, pl. 2, fig. 1

Diagnosis: Fundus with one to ten short spines, aperture circular, crenulated by six to 20 indentations forming a thin collar.

Diffugia fragosa HEMPEL 1898

Diffugia fragosa HEMPEL 1898, p. 320, text-figs. 1 – 2

Diffugia fragosa Pénard 1902, p. 573, fig. 2

Diffugia fragosa Averintsev 1906, p. 216

Diffugia fragosa Schoutenden 1906, p. 344

Diffugia fragosa Harnisch 1958, p. 40, pl. 8, fig. 21 (after Pénard, 1902)

Diffugia fragosa Scott and Medioli, 1983, p. 818, fig. 9o

Diffugia globulus (Ehrenberg, 1848)

Diffugia proteiformis (sic) Lamarck. Ehrenberg, 1838, p. 131 (part), pl. 9, figs. 1a – b

Arcella globulus Ehrenberg, 1848, p. 379

D. proteiformis (sic) (Ehrenberg) subspecies of *D. globularis* (Dujardin). Wallich, 1864, p. 241, pl. 15, fig. 4h

Diffugia globulosa Dujardin. Leidy, 1879, p. 96, pl. 15, figs. 25 – 31

Diffugia globulosa var. *globularis* Wallich, Pénard, 1902, p. 257, text-figs. 1 – 6

Diffugia globulosa forma *genuine* Pénard, 1902, p. 257

Diffugia globulus (Ehrenberg) CASH and HOPKINSON, 1909. p. 33, text-figs. 52 – 54, pl. 21, figs. 5 – 9

Diagnosis: Shell spheroidal to ellipsoidal with the oral pole truncated by a circular aperture.

Diffugia oblonga Ehrenberg 1832

strain “bryophila”

Diffugia pyriformis var. *bryophila* PENARD 1902, p. 221, text-fig. 7

Diffugia bryophila Pénard [sic.], OGDEN and ELLISON 1988, p. 234, pl. 1, figs. 1 – 3

Diffugia oblonga “bryophila” REINHARDT and OTHERS, 1998, pl. 2, fig. 9

Diagnosis: Test flask shaped, elongated, pyriform, neck long but sometimes obscure due to coarse agglutination, aperture narrow, circular and without lips.

Test is made of conspicuously large sand grains.

Diffugia oblonga Pénard 1902

strain “glans”

(Plate 5.2, figure k)

Diffugia oblonga “glans” PENARD 1902

Diffugia oblonga “glans” REINHARDT and OTHERS 1998, pl. 2, fig. 7

Diagnosis: Test oval to ovoid, slightly elongated, fundus rounded, neck absent, aperture circular with smooth lip, test made of fine sand particles.

Diffugia oblonga Pénard 1890

strain “lanceolata”

Diffugia lanceolata PENARD 1890, p. 145, pl. 4, figs. 59 – 60*Diffugia lanceolata* Pénard – OGDEN and HEDLEY 1980, p. 140, pl. 59, figs. a – d*Diffugia oblonga* “lanceolata” REINHARDT and OTHERS 1998, pl. 2, fig. 6

Diagnosis: Test elongate, pyriform and smooth, fundus rounded, neck long,
aperture circular with lip

Diffugia oblonga Ehrenberg 1832

strain “oblonga”

Diffugia oblonga EHRENBERG 1832, p. 90*Diffugia oblonga* Ehrenberg 1832, OGDEN and HEDLEY 1980, p. 148, pl. 63, figs. a - c*Diffugia oblonga* Ehrenberg 1832, HAMAN 1982, p. 367, pl. 3, figs. 19 – 25*Diffugia oblonga* Ehrenberg 1832, SCOTT and MEDIOLI 1983, p. 818, figs. 9a – b*Diffugia oblonga* “oblonga” REINHARDT and OTHERS 1998, pl. 2, fig. 10

Diagnosis: Test pyriform, elongated to oblong, fundus rounded, neck long,
aperture circular without lip, test made generally of fine sand grains

Diffugia oblonga Ehrenberg 1832

strain “spinosa”

Diffflugia oblonga var. *spinosa* REINHARDT and OTHERS 1998, p. 140, pl. 2, figs. 11a-

b

Diagnosis: Test pyriform, elongated, fundus large and with a distinct spine, neck short and constricted, aperture narrow, circular without lip, test made of fine sand grains

Diffflugia oblonga Ehrenberg 1832 “tenuis”

Diffflugia pyriformis var. *tenuis* PENARD 1980, p. 138, pl. 3, figs. 47 – 49

Diffflugia oblonga “tenuis” REINHARDT and OTHERS 1998, pl. 2, fig. 12

Diagnosis: Test elongated, ovoid almost bean shaped, fundus subrounded to subacute, neck indistinct or absent, aperture narrow and circular with crenulated lip, test made of generally medium to fine sand.

Diffflugia oblonga Ehrenberg 1832

strain “triangularis”

Diffflugia oblonga Ehrenberg 1832 MEDIOLI and SCOTT 1983, p. 25 – 28, pl. 2 fig. 26

Diffflugia oblonga Ehrenberg 1832 PATTERSON et al. 1985, p. 134, pl. 1, figs. 5, 9

Diffflugia oblonga Ehrenberg 1832 “triangularis” PATTERSON et al. 2002, figs. 8, 4a – b

Diagnosis: Test pyriform, elongated to oblong, fundus rounded with two or three protrusions resembling fins, neck indistinct or absent, aperture narrow and circular, test made of medium to fine sand grains.

Diffugia protaeiformis Lamarck 1816

strain "acuminata"

Diffugia protaeiformis LAMARCK 1816, p. 95 (with reference to material in a manuscript by Leclerc)

Diffugia acuminata EHRENBERG 1830, p. 95

Diffugia acuminata Ehrenberg 1830, OGDEN and HEDLEY 1980, p. 118, pl. 4, figs, a - c

Diffugia acuminata Ehrenberg 1830, SCOTT and MEDIOLI 1983, p. 818, fig. 9d

Diffugia protaeiformis "acuminata" REINHARDT and others 1998, pl. 2, fig. 5

Diagnosis: Distinguished from *Diffugia protaeiformis "claviformis"* by having a thinner wall which appears transparent under a light microscope.

Diffugia protaeiformis REINHARDT and others 1998

strain "amphoralis"

Diffugia amphoralis HOPKINSON in CASH and HOPKINSON 1909, p. 43, pl. 21, fig.

13

Diagnosis: Test almost biconical, elongated, fundus subangular tapering to form a spine, neck absent, aperture circular, narrow without lip, test smooth, almost hyaline and small.

Diffflugia protaeiformis Lamark 1816

strain "claviformis"

Diffflugia protaeiformis LAMARK 1816, p. 95 (with reference to material in a manuscript by Leclerc)

Diffflugia pyriformis var. *claviformis* PENARD 1899, p. 25, pl. 2, figs. 12 - 14

Diffflugia claviformis OGDEN and HEDLEY 1980, p. 126, pl. 52, figs. a - d

Diffflugia protaeiformis strain "protaeiformis" ASIOLI and others, 1996, p. 250, pl. 2, fig. 1, a - b

Diffflugia protaeiformis "claviformis" REINHARDT and others 1998, pl. 2, fig. 3

Diagnosis: This strain is similar to "acuminata" except that it has a coarser test made up of medium to coarse grained sand.

Diffflugia urceolata Carter 1864

strain "elongata"

Diffflugia urceolata CARTER 1864, p. 27, pl. 1, fig. 7

Diffflugia urceolata Carter 1864 REINHARDT and others 1998, pl. 2, fig. 2a

Diagnosis: Test elongate; aperture a distinct hanging collar.

Diffflugia urceolata Carter 1864

strain "urceolata"

Diffugia urceolata CARTER 1864, p. 27, pl. 1, fig. 7

Diffugia urceolata Carter 1864 REINHARDT and others 1998, pl. 2, fig. 2b

Diagnosis: Test spheroidal to ovoidal; aperture a distinct hanging collar.

Genus *Lagenodiffugia* MEDIOLI and SCOTT 1983

Lagenodiffugia vas (Leidy 1874)

Diffugia vas LEIDY 1874, p. 155

Pontigulasia elisa (Pénard 1893) OGDEN and HEDLEY 1980, p. 164 – 165, p. 71 a - d

Lagenodiffugia vas (Leidy 1874) MEDIOLI and SCOTT 1983, p. 33, pl. 2, figs. 18 - 23,

27, 28

Lagenodiffugia vas (Leidy 1874) PATTERSON et al. 1985, p. 135, pl. 1, figs. 13 - 16

Lagenodiffugia vas (Leidy 1874) REINHARDT et al. 1998, p. 142, pl. 1, figs. 8a - b

Lagenodiffugia vas (Leidy 1874) PATTERSON and KUMAR 2000, p. 230, pl. 2, fig. 11

Lagenodiffugia vas (Leidy 1874) PATTERSON et al. 2000, figs. 7. 6a - d

Diagnosis: Test elongate, pyriform, fundus bulbous and wide, neck arising from its narrow end with a prominent constriction at its base.

Genus *Pontigulasia* Rhumbler 1895

Pontigulasi compressa (Carter 1864)

Diffugia compressa CARTER 1864, p. 22, pl. 2, figs. 5 – 6

Pontigulasi compressa (Carter 1864) OGDEN and HEDLEY 1980, p. 162 – 163, pl. 70a

– d

Pontigulasi compressa (Carter 1864) MEDIOLI and SCOTT 1983, p. 35 – 36, pl. 6, figs.

5 – 7

Pontigulasi compressa (Carter 1864) ASIOLI et al. 1996, p. 252, pl. 1, figs. 3a – b

Pontigulasi compressa (Carter 1864) PATTERSON et al. 1985, p. 135, pl. 2, figs. 7 – 8

Pontigulasi compressa (Carter 1864) PATTERSON et al. 2002, figs. 7 – 9

Diagnosis: Test ovoid to pyriform, laterally compressed, with a distinct V-shaped constriction at the base of the neck. Aperture simple and ovoid.

Family **HYALOSPHEIIDAE** Schultze 1877

Genus *Cucurbitella* Penard 1902

Cucurbitella tricuspis (Carter 1856)

Diffugia tricuspis CARTER 1856, p. 221, fig. 80

Cucurbitella tricuspis (Carter 1856) MEDIOLI, SCOTT, and ABBOTT, 1987, p. 42, pls.

1 - 4, text figs. 1 - 4

Cucurbitella tricuspis (Carter 1856) REINHARDT and others 1998, pl. 1, fig. 7

Diagnosis: Test varies from spherical, subspherical to elongated. It is characterized by a thick apertural lip.

Genus *Heleopera* Leidy, 1879

Heleopera sphagni (Leidy, 1874)

Diffflugia (Nebela) sphagni Leidy, 1874, p. 174.

Nebela sphagni (Leidy), Leidy, 1876, p. 118, text-figs. 16, 17.

Heleopera picta Leidy, 1879, p. 162, pl. 26, figs. 1-11.

Heleopera petricola Leidy, 1879, p. 165, pl. 26, figs. 12 – 20.

Heleopera petricola var. *amethystea* Penard, 1899, p. 53, pl. 5, figs. 1-5.

Heleopera sphagni (Leidy) CASH and HOPKINSON, 1909, p. 143, pl. 30, figs. 4-9

Heleopera petricola var. *major* CASH in CASH and HOPKINSON, 1909, p. 139, pl. 29, figs. 20, 21.

Diagnosis: Shell strongly compressed , ovoid (Medioli and Scott, 1983).

Genus *Lesquereusia* Schlumberger 1845

Lesquereusia spiralis (Ehrenberg 1840)

Diffflugia spiralis (Ehrenberg 1840), p. 199

Diffflugia spiralis Ehrenberg, (Ehrenberg 1872), p. 274, pl. 3, figs. 25 – 27

Lesquereusia spiralis (Ehrenberg) Patterson et al. 1985, pl. 2, figs. 9, 12

Lesquereusia spiralis (Ehrenberg) Reinhardt et al. 1998, pl. 1, fig. 9

Diagnosis: Test made of curved siliceous rods, with neck. Apertural neck curved, spiralling away from the centre of the test.

Genus *Nebela* Leidy 1879

Nebela collaris Ehrenberg 1848

Diffflugia collaris Ehrenberg 1848, p. 218

Nebela collaris (Ehrenberg) Leidy 1879, p. 150

Nebela collaris (Ehrenberg) Ogden and Hedley 1980, p. 94 - 95

REFERENCES

- Adamowicz, S. J., 1980, A Study on the effects of beaver activity on bog vegetation in an area of the Mer Bleue Bog near Ottawa, Canada and an analysis of some of the factors that control bog plant distribution and abundance: Unpub. M.Sc. thesis, Carleton University 443 p.
- Archer, W., 1866, Quarterly Journal of Microscopical Science, new series, v. 6, p. 185 - 188.
- Asioli, A., Medioli F. S., and Patterson, R. T., 1996, Thecamoebians as a tool for reconstruction of paleoenvironments in some Italian lakes in the foothills of the southern Alps (Orta, Varese and Candia): Journal of Foraminiferal Research, v. 26, p. 248 - 263.
- Averintsev, S., 1906, Rhizopoda prêsnykh vod. Imperatorskoe Sankt-Peterburgskoe Obshchestvo Estestvoispytatelei Trudy:, v. 36, p. 1 - 346.
- Boudreau, R. E. A., 1999, Foraminifer and Arcellaceans from non-marine environments in northern Lake Winnipegosis, Manitoba, Unpub. M. Sc. Thesis, Department of Earth Sciences, Carleton University, 113 p.

- Broschart, M. R., Johnston, C. a., and Naiman, R. J., 1989, Predicting beaver colony density in boreal landscapes: *Journal of Wildlife Management*, p. 929 - 934.
- Burden, E. T., McAndrews, J. H., and Norris, G., 1986, Palynology of Indian and European forest clearance and farming in lake sediment cores from Awenda Provincial Park, Ontario: *Canadian Journal of Earth Sciences*, v. 23, p. 43-54.
- Carpenter, W. B., 1861, On the systematic arrangement of the Rhizopoda: *Natural History Review*, v. 1, p. 456 - 472.
- Carter, H. J., 1856, Notes on the freshwater Infusoria of the island of Bombay: No. 1. Organization. *Annals and Magazine of Natural History*, series. 2, v. 18, p. 221 - 249.
- , 1864, On freshwater Rhizopoda of England and India: *Annals and Magazine of Natural History*, v. 13, p. 18 - 39.
- Cash, J., and Hopkinson, J., 1905, The British freshwater Rhizopoda and Heliozoa; Volume I, Rhizopoda, Ray Society, London:, v. I, p. 151.
- , 1909, The British freshwater Rhizopoda and Heliozoa; Volume II, part 2; Ray Society, London:, p. 1 - 166.
- Chambers, P. A., DeWreede, R. E., Irlandi, E. A., and Vandermeulen, H., 1999, Management issues in aquatic macrophyte ecology: a Canadian perspective: *Canadian Journal of Botany*, v. 77, p. 471 - 487.
- Dalby, A., Kumar, A., Moore, J. M., and Patterson, R. T., 2000, Preliminary survey of arcellaceans (thecamoebians) as limnological indicators in tropical Lake Sentani, Irian Jaya, Indonesia: *Journal of Foraminiferal Research*, v. 30, p. 135 - 142.

- Dallimore, A., Schröder-Adams, C. J., and Dallimore, S. R., 2000, Holocene environmental history of thermokarst lakes on Richards Island, Northwest Territories, Canada: thecamoebians as paleolimnological indicators: *Journal of Paleolimnology*, v. 23, p. 261 - 283.
- Deflandre, G., 1928, Le genre *Arcella* Ehrenberg. Morphologie - Biologie. Essai phylogénétique et systématique; Protozoen-Algen-Pilze: *Archiv für Protistenkunde*, v. 64, p. 152 - 287.
- Deflandre, G., 1928, Le genre *Arcella* Ehrenberg. Morphologie - Biologie. Essai phylogénétique et systématique; Protozoen-Algen-Pilze: *Archiv für Protistenkunde*, v. 64, p. 152 - 287.
- , G., 1929, Le genre *Centropyxis* Stein: *Archiv für Protistenkunde*, v. 67, p. 322 - 375.
- , 1953, Ordres des Testaceolobosa (De Saedeleer, 1834), Testaceofilosa (De Saedeleer, 1834), *Thalamia* (Haeckel, 1862) ou thécamoebiens (Auct.) (Rhizopoda Testacea): in P.-P. Grass, (ed.), *Trait, de Zoologie*, Masson, Paris, v. 1, p. 97 - 148.
- De Nie, H., 1987, The decrease in aquatic vegetation in Europe and its consequences for fish population. Occasional Paper No. 19: European Inland Fisheries Advisory Commission, Food and Agricultural Organization of the United Nations, Rome.
- Ehrenberg, C. G., 1830, Organisation, systematik und geographisches Verhältnis der Infusionsthierchen; Berlin: Druckerei der Königl. Akademie der Wissenschaften:., p. 108.
- , 1832, Über die Entwicklung und Lebensdauer der Infusionsthierchen, nebst ferneren Beiträgen zu einer Vergleichung ihrer organischen Systeme: Königl.

- Akademie der Wissenschaften zu Berlin Physikalische Abhandlungen, 1831, p. 1 - 154.
- , 1843, Verbreitung und Einfluss des mikroskopischen Lebens in Süd-und Nord Amerika: Königliche Akademie der Wissenschaften zu Berlin Physikalische Abhandlungen, 1841, p. 291 - 446.
- , 1848, Fortgesetzte Beobachtungen über jetzt herrschende atmosph.,rische mikroskopische Verh.,ltnisse: Bericht über die zur Bekanntmachung geeigneten Verhandlungen der K"niglichen Preussischen Akademie der Wissenschaften zu Berlin, v. 13, p. 370 - 381.
- , 1872, Nachthrag zur Übersicht der organischen Atmosphärlilien: Königliche Akademie der Wissenschaften zu Berlin Physikalische Abhandlungen, 1871, p. 233 - 275.
- Eichwald, C. E. v., 1830, Zoologia specialis, Vilnae: D.E. Eichwaldus, v. 2, p. 1 - 323.
- Fishbein, E. and Patterson, R. T., 1993, Error-wieghted maximum likelihood (EWML): a new statistically based method to cluster quantitative micropaleontological data. *Journal of Paleontology*, v. 67 (3) p. 475 - 485.
- Francis, M. M., Naiman, R. J., and Melillo, J. M., 1985, Nitrogen fixation in sub-arctic streams influenced by beaver (*Castor canadensis*): *Hydrobiologia*, v. 121, p. 193 - 202.
- Hall, R. I., Duff, K. E., and Quinby, P. A., 1994a, A 10,000-Year Vegetation History of the Temagami Region of Ontario with Special Emphasis on White Pine: Ancient Forest Exploration and Research@www.ancientforest.org/rr4.html.

- , 1994b, A 10,000-year vegetation history of the Temagami Region of Ontario with special emphasis on white pine, Temagami, Temagami Wilderness Society, p. 1 - 10.
- Haman, D., 1982, Modern Thecamoebinids (Arcellinida) from the Balize Delta, Louisiana: Transactions, Gulf Coast Association of Geological Societies, v. 32, p. 353 - 376.
- Hempel, A., 1898, A list of the Protozoa and rotifera found in the Illinois River and adjacent lakes at Havana, Illinois: Illinois State Laboratory of Natural History Bulletin, v. 5, p. 301 - 388.
- Hodgins, B. W., and Benedickson, J., 1989, The Temagami experience: recreation, resource, and aboriginal rights in the northern Ontario wilderness: Toronto, Canada, University of Toronto Press, 370 p.
- Honig, C. A., and Scott, D. B., 1987, Post-glacial stratigraphy and sea level change in southwestern New Brunswick: Canadian Journal of Earth Sciences, v. 24, p. 354 - 364.
- Johnston, C. A., and Naiman, R. J., 1990a, Aquatic patch creation in relation to beaver population trends: Ecology, p. 1617 - 1621.
- , 1990b, Browse selection by beaver: effects on riparian forest composition: Canadian Journal of Forest Resources, p. 1036 - 1043.
- Kearney, M. S., and Luckman, B. H., 1983, Postglacial vegetational history of Tonquin Pass, British Columbia: Canadian Journal Of Earth Science, v. 20, p. 776-786.
- Kent, W. S., 1880, A Manual of the Infusoria: London: Bogue:, v. 1, p. 1 - 472.

- Lamarck, J. B., 1816, *Histoire naturelle des animaux sans vertèbres*: Verdière, Paris, v. 2, p. 1 - 568.
- Leidy, J., 1874, Notice of some Rhizopods: Academy of Natural Sciences of Philadelphia Proceedings, v. 3, p. 155 - 157.
- , 1879, Fresh water rhizopods of North America: United States Geological Survey of the Territories, Report 12, p. 1 - 324.
- Liu, K.-B., 1981, Pollen evidence of Late Quaternary Climatic changes in Canada: A review. Part II - Eastern Arctic and subArctic Canada: *Ontario Geography*, v. 17, p. 61 - 82.
- McCarthy, F. M. G., Collins E. S., McAndrews J. H., Kerr H. A., Scott D. B., and Medioli, F. S., 1995, A comparison of postglacial arcellacean ("thecamoebian") and pollen succession in Atlantic Canada, illustrating the paleoclimatic reconstruction: *Journal of Paleontology*, v. 69, p. 980 - 993.
- Medioli, F. S., and Scott, D. B., 1983, Holocene Arcellacea (Thecamoebians) from Eastern Canada: Cushman Foundation for Foraminiferal Research, Special Publication, v. 21, p. 1 - 63.
- , 1988, Lacustrine thecamoebians (mainly arcellaceans) as potential tools for palaeolimnological interpretations: *Palaeogeography, Palaeoclimatology, Palaeoecology*, v. 62, p. 361 - 386.
- Medioli, F. S., Scott, D. B., Collins, E. S., and McCarthy, F. M. G., 1990, Fossil thecamoebians: present status and prospects for the future, in Hemleben, C., Kaminski, M.A., Kuhnt, W. and Scott, D.B., eds: *Paleoecology, Biostratigraphy*,

- Paleoceanography and Taxonomy of Agglutinated Foraminifera, NATO ASI series; Volume C, Mathematical and Physical Sciences, v. 327, p. 813 - 839.
- Minckley, T., and Whitlock, C., 2000, Spatial variation of modern pollen in Oregon and southern Washington, USA: *Review of Paleobotany and Palynology*, v. 112, p. 97-123.
- Ogden, C. G., and Ellison, R. L., 1988, The value of the organic cement matrix in the identification of the shells of fossil testate amoeba: *Journal of Micropalaeontology*, v. 7, p. 233 - 240.
- Ogden, C. G., and Hedley, R. L., 1980, *An Atlas of Freshwater Testate Amoeba*; British Museum (Natural History), Oxford University Press:., p. 222.
- Paterson, A. M., Cumming, B. F., Smol, J. P., and Hall, R. I., 2004, Marked recent increases of colonial scaled chrysophytes in boreal lakes: implications for the management of taste and odour events: *Freshwater Biology*, v. 49, p. 199-207.
- Patterson, R. T., Barker, T., and Burbidge, S. M., 1996, Arcellaceans (Thecamoebians) as proxies of Arsenic and Mercury contamination in Northeastern Ontario lakes: *Journal of Foraminiferal Research*, v. 26, p. 172 - 183.
- Patterson, R. T., Dalby, A., Kumar, A., Henderson, L. A., and Boudreau, R. E. A., 2002, Arcellaceans (thecamoebians) as indicators of land-use change: settlement history of the Swan Lake area, Ontario as a case study: *Journal of Paleolimnology*, v. 28, p. 297 - 316.
- Patterson, R. T., and Fishbein, E., 1989, Re-Examination of the Statistical Methods used to Determine the Number of Point Counts Needed for Micropaleontological Quantitative Research: *Journal of Paleontology*, v. 63, p. 245 - 248.

- Patterson, R. T., and Kumar, A., 2000a, Assessment of Arcellacean (Thecamoebian) Assemblages, Species, and Strains as Contaminant Indicators in James Lake, Northeastern Ontario, Canada: *Journal of Foraminiferal Research*, v. 30, p. 310 - 320.
- , 2000b, Use of Arcellacea (Thecamoebians) to Gauge Levels of Contamination and Remediation in Industrially Polluted Lakes, *in* Martin, R. E., ed., *Environmental Micropaleontology: Topics in Geobiology*, New York, Kluwer Academic/Plenum Publishers, p. 257 - 278.
- , 2002, A review of current testate rhizopod (thecamoebian) research in Canada: *Palaeogeography, Palaeoclimatology, Palaeoecology*, Elsevier, v. 180, p. 225 - 251.
- Patterson, R. T., MacKinnon, K. D., Scott, D. B., and S., M. F., 1985, Arcellaceans (Thecamoebians) in small lakes of New Brunswick and Nova Scotia: modern distribution and Holocene stratigraphic changes: *Journal of Foraminiferal Research*, v. 15, p. 114-137.
- Penard, E., 1890, Études sur les Rhizopodes d'eau douce: *Mémoires de la Société de Physique et d'Histoire Naturelle de Genève*, v. 31, p. 1 - 230.
- , 1899, Les Rhizopodes de faune profonde dans le lac du Léman, *Revue Suisse de Zoologie*, v. 7, p. 1 - 142.
- , 1902, Faune rhizopodique du Bassin du Léman; Henry Kundig, Genève., p. 714 p.
- Prescott, G. W., 1970, *The Freshwater Algae: The Pictured Key Nature Series*: Dubuque, Iowa, Wm. C. Brown Company Publishers, 348 p.

- Ray, A. M., Rebertus, A. J., and Ray, H. L., 2001, Macrophyte succession in Minnesota beaver ponds: *Canadian Journal of Botany*, v. 79, p. 487 - 499.
- Reinhardt, E. G., Dalby, A., Kumar, A., and Patterson, R. T., 1998a, Utility of Arcellacean Morphotypic Variants as Pollution Indicators in Mine Tailing Contaminated Lakes Near Cobalt, Ontario, Canada: *Micropaleontology*, v. 44, p. 131 - 148.
- Reinhardt, E. G., Dalby, A. P., Kumar, A., and Patterson, R. T., 1998b, Arcellaceans as Pollution Indicators in Mine Tailing Contaminated Lakes Near Cobalt, Ontario, Canada: *Micropaleontology*, v. 44, p. 131 - 148.
- Rhumbler, L., 1895, Entwurf eines natürlichen Systems der Thalomophoren: Nachrichten der Gesellschaft für Wissenschaft Göttingen: mathematischephysikalisch Klasse, v. 1, p. 51 - 98.
- Saarnisto, M., 1974, The deglaciation history of the Lake Superior region and its climatic implications: *Quaternary Research*, v. 4, p. 316 - 339.
- Sageman, B. B., and Bina, C. R., 1997, Diversity and Species Abundance Patterns in Late Cenomanian Black Shale Biofacies, Western Interior, U.S: *Palaios*, v. 12, p. 449 - 466.
- Schlumberger, P., 1845, Observations sur quelques nouvelles especes d'Infusoires de la famille des Rhizopodes: *Annales des Sciences Naturelles. B. Zoologie*, v. 3, p. 254 - 256.
- Schmarda, L. K., 1871, *Zoologie*, v. I: Braumuller, Wien, 372 p.
- Schouteden, H., 1906, Les Rhizopodes testacés d'eau douce d'après la Monographie du Prof. A. Awerintzew: *Annales de Biologie lacustre*, v. 1, p. 327 - 382.

- Schultze, F. E., 1877, Rhizopodenstudien VI: Archiv fuer Mikroskopische Anatomie, v. 13, p. 9 - 30.
- Scott, D. B., 2001, Monitoring of Coastal Environments Using Foraminifera and Thecamoebian Indicators: Cambridge, USA, Cambridge University Press, 192 p.
- Scott, D. B., and Medioli, F. S., 1980, Quantitative studies of marsh foraminiferal distributions in Nova Scotia: their implications for the study of sea level changes: Cushman Foundation for Foraminiferal Research, Special Publication, v. 17, p. 58 p.
- , 1983, Testate rhizopods in Lake Erie: modern distribution and stratigraphic implications: Journal of Paleontology, v. 57, p. 809 - 820.
- Shannon, E. L., and Weaver, W., 1949, The Mathematical Theory of Communication: Urbana, University of Illinois Press, 117 p.
- Snodgrass, J. W., 1997, Temporal and spatial dynamics of beaver-created patches as influenced by management practices in a south-eastern North American landscape: Journal of Applied Ecology, p. 1043 - 1056.
- Stein, S. F. N., 1859, Über die ihm aus eigener Untersuchung bekannt gewordenen Süsswässer-Rhizopoden: Abhandlungen der Koeniglichen Boehmischen Gesellschaften der Wissenschaften, v. 5, p. 41 - 43.
- von Siebold, C. T. E., 1845, Wirbellose Thiere, *in* von Siebold, C. T. E., and von Stannius, H., eds., Lehrbuch der Vergleichenden Anatomie, p. 1 - 679.
- Wallich, G. C., 1864, On the extent, and some of the principal causes, of structural variation among the difflugian rhizopods: Annals and Magazine of Natural History, series 3, v. 13, p. 215 - 245.

Watt, R. F., and Heinselman, M. L., 1965, Foliar nitrogen and phosphorus level related to site quality in a northern Minnesota spruce bog: *Ecology*, v. 46, p. 357 - 361.

Wood, R. D., and Imahori, K., 1965, *Monograph of the Characeae*: New York, N. Y., Verlag; Cramer, Weldon and Wesley, LTD; Stechert-Hafner Service Agency, Inc.

Station	JL1-01	JLM-01-1	JLM-01-2	JLM-01-3	JLM-01-4	JLB-01-1	JLB-01-2	JLB-01-3	JLB-01-4	JLB-01-5	JLB-01-6	JLB-01-7	JLB-01-8	JLB-01-9	JLB-01-10	JLB-01-11	JLB-01-12	JLB-01-13	JLB-01-14	JLB-01-15	JLB-01-16	
<i>Arctia vulgaris</i>	0.029	0.000	0.029	0.042	0.112	0.005	0.059	0.342	0.387	0.026	0.008	0.010	0.006	0.039	0.028	0.013	0.003	0.006	0.003	0.003	0.006	0.144
Standard error 1	0.015	0.000	0.025	0.019	0.039	0.010	0.031	0.068	0.059	0.014	0.008	0.006	0.007	0.021	0.018	0.012	0.006	0.012	0.007	0.007	0.006	0.037
<i>Ceratopogon acidus - aculeatus</i>	0.159	0.188	0.234	0.134	0.326	0.097	0.032	0.005	0.000	0.021	0.012	0.022	0.050	0.071	0.090	0.067	0.065	0.036	0.057	0.000	0.057	0.051
Standard error 1	0.033	0.191	0.085	0.057	0.142	0.042	0.023	0.010	0.000	0.012	0.009	0.013	0.019	0.029	0.031	0.028	0.028	0.020	0.026	0.000	0.026	0.011
<i>Ceratopogon acidus - bicoloratus</i>	0.102	0.000	0.069	0.116	0.217	0.113	0.068	0.010	0.000	0.021	0.041	0.070	0.087	0.039	0.025	0.067	0.046	0.101	0.067	0.000	0.067	0.002
Standard error 1	0.027	0.000	0.038	0.050	0.060	0.044	0.033	0.014	0.000	0.017	0.022	0.022	0.017	0.025	0.017	0.028	0.023	0.024	0.028	0.000	0.028	0.005
<i>Ceratopogon constrictus - arripallus</i>	0.058	0.563	0.225	0.223	0.136	0.149	0.063	0.000	0.000	0.000	0.008	0.000	0.004	0.003	0.015	0.000	0.022	0.029	0.024	0.015	0.000	0.000
Standard error 1	0.021	0.243	0.082	0.058	0.042	0.050	0.032	0.000	0.000	0.008	0.008	0.005	0.005	0.006	0.013	0.000	0.016	0.019	0.016	0.015	0.000	0.000
<i>Ceratopogon constrictus - constrictus</i>	0.054	0.000	0.133	0.122	0.050	0.108	0.131	0.000	0.000	0.000	0.037	0.074	0.048	0.052	0.046	0.000	0.087	0.049	0.119	0.060	0.000	0.000
Standard error 1	0.026	0.000	0.051	0.030	0.027	0.044	0.045	0.000	0.000	0.020	0.023	0.019	0.019	0.025	0.023	0.000	0.031	0.024	0.035	0.027	0.000	0.000
<i>Ceratopogon constrictus - spinipes</i>	0.000	0.162	0.000	0.000	0.000	0.021	0.000	0.015	0.000	0.000	0.000	0.000	0.000	0.006	0.013	0.013	0.013	0.014	0.011	0.000	0.000	0.000
Standard error 1	0.000	0.125	0.000	0.000	0.000	0.000	0.015	0.000	0.000	0.000	0.000	0.000	0.000	0.006	0.013	0.013	0.013	0.014	0.011	0.000	0.000	0.000
<i>Ctenophora thompsoni</i>	0.092	0.000	0.069	0.065	0.019	0.036	0.090	0.633	0.398	0.647	0.160	0.164	0.161	0.310	0.393	0.502	0.225	0.154	0.238	0.351	0.007	0.771
Standard error 1	0.026	0.000	0.038	0.023	0.017	0.026	0.038	0.067	0.058	0.041	0.032	0.032	0.032	0.051	0.053	0.065	0.045	0.047	0.039	0.050	0.051	0.041
<i>Diptera Acuticrura</i>	0.000	0.000	0.000	0.002	0.000	0.000	0.000	0.000	0.000	0.000	0.000	0.000	0.000	0.000	0.000	0.000	0.000	0.000	0.000	0.000	0.000	0.000
Standard error 1	0.000	0.000	0.000	0.004	0.000	0.000	0.000	0.000	0.000	0.000	0.000	0.000	0.000	0.000	0.000	0.000	0.000	0.000	0.000	0.000	0.000	0.000
<i>Diptera blattis</i>	0.000	0.000	0.000	0.000	0.000	0.000	0.000	0.000	0.000	0.000	0.000	0.000	0.000	0.000	0.000	0.000	0.000	0.000	0.000	0.000	0.000	0.000
Standard error 1	0.000	0.000	0.000	0.000	0.000	0.000	0.000	0.000	0.000	0.000	0.000	0.000	0.000	0.000	0.000	0.000	0.000	0.000	0.000	0.000	0.000	0.000
<i>Diptera crenata</i>	0.004	0.000	0.000	0.000	0.000	0.000	0.000	0.000	0.000	0.004	0.022	0.016	0.028	0.039	0.009	0.012	0.045	0.024	0.040	0.007	0.000	0.000
Standard error 1	0.020	0.000	0.033	0.023	0.028	0.049	0.023	0.010	0.010	0.005	0.013	0.011	0.014	0.021	0.010	0.012	0.023	0.021	0.016	0.022	0.000	0.008
<i>Diptera foveata</i>	0.000	0.000	0.000	0.000	0.000	0.000	0.000	0.000	0.000	0.000	0.000	0.000	0.000	0.000	0.000	0.000	0.000	0.000	0.000	0.000	0.000	0.000
Standard error 1	0.000	0.000	0.000	0.000	0.000	0.000	0.000	0.000	0.000	0.000	0.000	0.000	0.000	0.000	0.000	0.000	0.000	0.000	0.000	0.000	0.000	0.000
<i>Diptera oblonga - hydropila</i>	0.010	0.000	0.000	0.004	0.000	0.000	0.131	0.000	0.000	0.017	0.067	0.252	0.161	0.097	0.043	0.112	0.118	0.148	0.107	0.000	0.000	0.000
Standard error 1	0.008	0.000	0.000	0.008	0.000	0.000	0.045	0.000	0.000	0.002	0.038	0.032	0.032	0.033	0.022	0.035	0.036	0.033	0.035	0.000	0.000	0.000
<i>Diptera oblonga - flemis</i>	0.050	0.000	0.040	0.060	0.000	0.005	0.136	0.000	0.000	0.077	0.098	0.096	0.117	0.087	0.084	0.112	0.114	0.107	0.110	0.000	0.012	0.011
Standard error 1	0.020	0.000	0.029	0.022	0.000	0.010	0.045	0.000	0.000	0.023	0.026	0.028	0.028	0.028	0.030	0.035	0.036	0.033	0.036	0.000	0.000	0.011
<i>Diptera oblonga - fuscicollis</i>	0.004	0.000	0.000	0.000	0.000	0.000	0.000	0.000	0.000	0.000	0.000	0.000	0.000	0.000	0.000	0.000	0.000	0.000	0.000	0.000	0.000	0.000
Standard error 1	0.006	0.000	0.000	0.000	0.000	0.000	0.000	0.000	0.000	0.000	0.000	0.000	0.000	0.000	0.000	0.000	0.000	0.000	0.000	0.000	0.000	0.000
<i>Diptera globus</i>	0.000	0.000	0.000	0.000	0.000	0.000	0.000	0.000	0.000	0.000	0.000	0.000	0.000	0.000	0.000	0.000	0.000	0.000	0.000	0.000	0.000	0.000
Standard error 1	0.000	0.000	0.000	0.000	0.000	0.000	0.000	0.000	0.000	0.000	0.000	0.000	0.000	0.000	0.000	0.000	0.000	0.000	0.000	0.000	0.000	0.000
<i>Diptera oblonga - fuscipes</i>	0.000	0.000	0.000	0.000	0.000	0.000	0.020	0.000	0.000	0.000	0.000	0.016	0.009	0.000	0.006	0.019	0.019	0.020	0.019	0.000	0.000	0.000
Standard error 1	0.000	0.000	0.000	0.000	0.000	0.000	0.020	0.000	0.000	0.000	0.000	0.016	0.009	0.000	0.006	0.019	0.019	0.020	0.019	0.000	0.000	0.000
<i>Diptera oblonga - fuscipes</i>	0.033	0.063	0.006	0.004	0.000	0.005	0.027	0.000	0.000	0.033	0.033	0.025	0.036	0.016	0.006	0.019	0.010	0.021	0.015	0.015	0.000	0.000
Standard error 1	0.016	0.119	0.011	0.008	0.000	0.010	0.021	0.000	0.000	0.013	0.033	0.025	0.036	0.016	0.006	0.019	0.010	0.021	0.015	0.015	0.000	0.000
<i>Diptera oblonga - spinipes</i>	0.010	0.000	0.000	0.004	0.000	0.005	0.000	0.000	0.000	0.006	0.018	0.018	0.016	0.016	0.013	0.000	0.003	0.000	0.003	0.010	0.000	0.000
Standard error 1	0.009	0.000	0.000	0.008	0.000	0.010	0.000	0.000	0.000	0.006	0.011	0.011	0.011	0.013	0.000	0.006	0.000	0.006	0.011	0.000	0.000	0.000
<i>Diptera oblonga - tenuis</i>	0.008	0.000	0.000	0.000	0.000	0.000	0.000	0.000	0.000	0.000	0.000	0.000	0.000	0.000	0.000	0.000	0.000	0.000	0.000	0.000	0.000	0.000
Standard error 1	0.008	0.000	0.000	0.000	0.000	0.000	0.000	0.000	0.000	0.000	0.000	0.000	0.000	0.000	0.000	0.000	0.000	0.000	0.000	0.000	0.000	0.000
<i>Diptera oblonga - tringularis</i>	0.004	0.000	0.000	0.000	0.000	0.005	0.000	0.000	0.000	0.000	0.000	0.000	0.000	0.000	0.000	0.000	0.000	0.000	0.000	0.000	0.000	0.000
Standard error 1	0.008	0.000	0.000	0.000	0.000	0.010	0.000	0.000	0.000	0.000	0.000	0.000	0.000	0.000	0.000	0.000	0.000	0.000	0.000	0.000	0.000	0.000
<i>Diptera presuliformis - acuminatus</i>	0.008	0.000	0.000	0.000	0.000	0.010	0.000	0.000	0.000	0.000	0.000	0.000	0.000	0.000	0.000	0.000	0.000	0.000	0.000	0.000	0.000	0.000
Standard error 1	0.008	0.000	0.000	0.000	0.000	0.010	0.000	0.000	0.000	0.000	0.000	0.000	0.000	0.000	0.000	0.000	0.000	0.000	0.000	0.000	0.000	0.000
<i>Diptera presuliformis - ampullatus</i>	0.019	0.000	0.016	0.008	0.011	0.024	0.015	0.000	0.000	0.040	0.057	0.051	0.073	0.065	0.030	0.038	0.032	0.021	0.047	0.003	0.002	0.000
Standard error 1	0.017	0.000	0.016	0.008	0.011	0.024	0.015	0.000	0.000	0.017	0.020	0.019	0.023	0.027	0.030	0.021	0.025	0.021	0.024	0.009	0.005	0.000
<i>Diptera presuliformis - ampullatus</i>	0.019	0.000	0.006	0.002	0.000	0.000	0.000	0.000	0.000	0.032	0.239	0.055	0.071	0.016	0.031	0.000	0.035	0.062	0.027	0.027	0.000	0.000
Standard error 1	0.012	0.000	0.011	0.004	0.000	0.000	0.000	0.000	0.000	0.015	0.037	0.020	0.022	0.014	0.019							

Station	GL-99-43	GL-99-44	GL-99-45	GL-99-46	GL-99-47	GL-99-48	GL-99-49	GL-99-50	GL-99-51	GL-99-53	GL-99-54
Depth (cm)	284	302	309	311	317	322	328	332	333	342	344
Taxa per core	7	9	10	10	10	10	10	10	10	10	10
Number of Species	38	589	308	1545	681	540	38	156	195	655	7
Diversity	0.73	1.32	1.50	1.30	1.43	1.46	1.58	1.46	1.77	0.86	0.00
<i>Arcella sulcata</i>	0.000	0.000	0.002	0.006	0.004	0.001	0.000	0.000	0.000	0.000	0.000
Standard error 1	0.000	0.000	0.004	0.007	0.006	0.003	0.000	0.000	0.000	0.000	0.000
<i>Campylopus aculeatus</i>	0.421	0.462	0.370	0.344	0.193	0.256	0.289	0.118	0.075	0.051	0.000
Standard error 1	0.157	0.044	0.054	0.042	0.036	0.032	0.144	0.041	0.028	0.012	0.000
<i>Campylopus aculeatus "bicoloris"</i>	0.053	0.166	0.162	0.295	0.327	0.137	0.026	0.130	0.092	0.125	0.000
Standard error 1	0.071	0.033	0.041	0.039	0.043	0.043	0.043	0.043	0.030	0.018	0.000
<i>Campylopus compressus "arabopolis"</i>	0.342	0.347	0.240	0.241	0.229	0.099	0.211	0.126	0.150	0.105	0.000
Standard error 1	0.151	0.038	0.048	0.037	0.036	0.022	0.130	0.042	0.038	0.017	0.000
<i>Campylopus compressus "constrictus"</i>	0.053	0.073	0.019	0.031	0.029	0.048	0.000	0.008	0.006	0.016	0.000
Standard error 1	0.071	0.023	0.015	0.012	0.015	0.016	0.000	0.012	0.008	0.007	0.000
<i>Campylopus compressus "spinosa"</i>	0.000	0.002	0.016	0.002	0.002	0.001	0.000	0.000	0.006	0.002	0.000
Standard error 1	0.000	0.004	0.014	0.004	0.004	0.006	0.000	0.008	0.003	0.000	0.000
<i>Cocconeis trioculata</i>	0.000	0.000	0.000	0.000	0.000	0.000	0.000	0.000	0.000	0.000	0.000
Standard error 1	0.000	0.000	0.000	0.000	0.000	0.000	0.000	0.012	0.000	0.000	0.000
<i>Difflugia bacilliformis</i>	0.000	0.000	0.000	0.000	0.000	0.000	0.000	0.000	0.000	0.000	0.000
Standard error 1	0.000	0.000	0.000	0.000	0.000	0.000	0.000	0.000	0.000	0.000	0.000
<i>Difflugia kansas</i>	0.000	0.000	0.000	0.000	0.000	0.000	0.000	0.000	0.000	0.000	0.000
Standard error 1	0.000	0.000	0.000	0.000	0.000	0.000	0.000	0.000	0.000	0.000	0.000
<i>Difflugia coreana</i>	0.000	0.000	0.000	0.000	0.000	0.000	0.000	0.000	0.000	0.000	0.000
Standard error 1	0.000	0.000	0.000	0.000	0.000	0.000	0.000	0.000	0.000	0.000	0.000
<i>Difflugia fragilis</i>	0.000	0.000	0.000	0.000	0.000	0.000	0.000	0.000	0.000	0.000	0.000
Standard error 1	0.000	0.000	0.000	0.000	0.000	0.000	0.000	0.000	0.000	0.000	0.000
<i>Difflugia oblonga "hydropolis"</i>	0.000	0.000	0.000	0.000	0.000	0.000	0.000	0.000	0.000	0.000	0.000
Standard error 1	0.000	0.000	0.000	0.000	0.000	0.000	0.000	0.000	0.000	0.000	0.000
<i>Difflugia oblonga "plum"</i>	0.000	0.000	0.003	0.006	0.000	0.000	0.132	0.021	0.068	0.000	0.000
Standard error 1	0.000	0.000	0.006	0.007	0.000	0.000	0.107	0.018	0.008	0.000	0.000
<i>Difflugia oblonga "retus"</i>	0.000	0.000	0.000	0.000	0.000	0.000	0.000	0.000	0.000	0.000	0.000
Standard error 1	0.000	0.000	0.000	0.000	0.000	0.000	0.000	0.000	0.000	0.000	0.000
<i>Difflugia rotunda</i>	0.000	0.000	0.000	0.000	0.000	0.000	0.000	0.000	0.000	0.000	0.000
Standard error 1	0.000	0.000	0.000	0.000	0.000	0.000	0.000	0.000	0.000	0.000	0.000
<i>Difflugia oblonga "venezis"</i>	0.000	0.000	0.000	0.000	0.000	0.000	0.000	0.000	0.000	0.000	0.000
Standard error 1	0.000	0.000	0.000	0.000	0.000	0.000	0.000	0.000	0.000	0.000	0.000
<i>Difflugia oblonga "ablonga"</i>	0.026	0.051	0.000	0.006	0.006	0.017	0.026	0.050	0.040	0.005	0.000
Standard error 1	0.026	0.026	0.000	0.009	0.007	0.004	0.021	0.028	0.021	0.004	0.000
<i>Difflugia oblonga "spinosa"</i>	0.051	0.000	0.013	0.004	0.002	0.009	0.025	0.025	0.026	0.000	0.000
Standard error 1	0.051	0.000	0.005	0.004	0.004	0.009	0.071	0.020	0.017	0.000	0.000
<i>Difflugia oblonga "frenis"</i>	0.000	0.000	0.000	0.000	0.000	0.000	0.051	0.012	0.000	0.000	0.000
Standard error 1	0.000	0.000	0.000	0.000	0.000	0.000	0.000	0.000	0.000	0.000	0.000
<i>Difflugia oblonga "virgatilis"</i>	0.000	0.000	0.000	0.000	0.000	0.000	0.000	0.000	0.000	0.000	0.000
Standard error 1	0.000	0.000	0.000	0.000	0.000	0.000	0.000	0.000	0.000	0.000	0.000
<i>Difflugia praesiformis "acuminata"</i>	0.000	0.000	0.003	0.000	0.000	0.000	0.105	0.003	0.003	0.000	0.000
Standard error 1	0.000	0.000	0.006	0.000	0.000	0.001	0.098	0.014	0.006	0.000	0.000
<i>Difflugia praesiformis "amplicornis"</i>	0.000	0.000	0.000	0.000	0.000	0.000	0.026	0.008	0.014	0.000	0.000
Standard error 1	0.000	0.000	0.000	0.000	0.000	0.003	0.051	0.012	0.000	0.000	0.000
<i>Difflugia praesiformis "dentiformis"</i>	0.000	0.000	0.000	0.000	0.000	0.000	0.105	0.000	0.000	0.000	0.000
Standard error 1	0.000	0.000	0.000	0.000	0.000	0.000	0.098	0.000	0.000	0.000	0.000
<i>Difflugia arcuolana "arcedana"</i>	0.000	0.000	0.000	0.000	0.000	0.000	0.000	0.004	0.009	0.000	0.000
Standard error 1	0.000	0.000	0.000	0.000	0.000	0.000	0.000	0.008	0.010	0.000	0.000
<i>Difflugia arcuolana "fingera"</i>	0.000	0.000	0.000	0.000	0.000	0.000	0.000	0.000	0.009	0.000	0.000
Standard error 1	0.000	0.000	0.000	0.000	0.000	0.000	0.000	0.010	0.000	0.000	0.000
<i>Heteropora Spangeli</i>	0.000	0.000	0.000	0.000	0.000	0.000	0.000	0.000	0.000	0.000	0.000
Standard error 1	0.000	0.000	0.000	0.000	0.000	0.000	0.000	0.000	0.000	0.000	0.000
<i>Leptoneis fusca</i>	0.079	0.039	0.159	0.060	0.182	0.059	0.000	0.084	0.098	0.022	0.000
Standard error 1	0.066	0.017	0.041	0.021	0.035	0.017	0.000	0.031	0.008	0.000	0.000
<i>Leptoneis spallans</i>	0.000	0.000	0.000	0.000	0.000	0.000	0.000	0.000	0.000	0.000	0.000
Standard error 1	0.000	0.000	0.000	0.000	0.000	0.000	0.000	0.000	0.000	0.000	0.000
<i>Nitidulites collaris</i>	0.000	0.000	0.000	0.000	0.000	0.000	0.000	0.000	0.000	0.000	0.000
Standard error 1	0.000	0.000	0.000	0.000	0.000	0.000	0.000	0.000	0.000	0.000	0.000
<i>Pezomachus compressus</i>	0.000	0.000	0.000	0.000	0.000	0.000	0.000	0.000	0.000	0.000	0.000
Standard error 1	0.000	0.000	0.000	0.000	0.000	0.000	0.000	0.000	0.000	0.000	0.000
<i>Chamaepoma</i>	0.000	0.004	0.000	0.000	0.002	0.364	0.000	0.345	0.667	0.837	0.000
Standard error 1	0.000	0.006	0.000	0.000	0.004	0.035	0.000	0.060	0.038	0.110	0.000

Table 5.1 (continued) - Taxonomic unit counts, Shannon-Weaver Diversity, fractional abundances and standard error for sediment-water interface and core samples from James and Granite lakes.

Station	JLP 99-1-1	JLP 99-1-2	JLP 99-1-3	JLP 99-1-4	JLP 99-1-5	JLP 99-1-6	JLP 99-1-7	JLP 99-1-8	JLP 99-1-9	JLP 99-1-10	JLP 99-1-11	JLP 99-1-12	JLP 99-1-13	JLP 99-1-14
Depth (cm)	10	15	40	45	115	120	145	175	180	181	207	209	243	245
Taxonomic Counts	420	345	286	269	285	268	283	305	273	293	283	286	310	347
Counts per cc	472	405	352	325	324	314	330	343	317	335	331	323	364	411
Number of Species	12	13	11	11	10	13	13	14	12	12	10	14	14	13
Diversity	1.96	1.94	2.14	2.08	1.99	1.92	1.95	1.99	1.88	1.90	1.80	1.91	1.91	1.62
<i>Abies</i>	0.026	0.035	0.028	0.030	0.018	0.015	0.007	0.016	0.007	0.003	0.007	0.010	0.010	0.006
Standard error ±	0.015	0.019	0.019	0.020	0.015	0.015	0.010	0.014	0.010	0.007	0.010	0.012	0.011	0.008
<i>Aceraceae</i>	0.002	0.000	0.000	0.000	0.000	0.000	0.000	0.000	0.000	0.000	0.000	0.000	0.000	0.000
Standard error ±	0.005	0.000	0.000	0.000	0.000	0.000	0.000	0.000	0.000	0.000	0.000	0.000	0.000	0.000
<i>Alnus</i>	0.000	0.000	0.000	0.000	0.000	0.000	0.000	0.000	0.004	0.000	0.000	0.000	0.000	0.000
Standard error ±	0.000	0.000	0.000	0.000	0.000	0.000	0.000	0.000	0.007	0.000	0.000	0.000	0.000	0.000
<i>Ambrosia</i>	0.000	0.003	0.000	0.000	0.000	0.000	0.000	0.000	0.000	0.000	0.000	0.000	0.000	0.000
Standard error ±	0.000	0.006	0.000	0.000	0.000	0.000	0.000	0.000	0.000	0.000	0.000	0.000	0.000	0.000
<i>Betula</i>	0.019	0.003	0.007	0.015	0.014	0.026	0.028	0.033	0.084	0.044	0.025	0.028	0.006	0.006
Standard error ±	0.013	0.006	0.010	0.014	0.014	0.019	0.019	0.020	0.033	0.024	0.018	0.019	0.009	0.008
<i>Chenopodiaceae</i>	0.000	0.000	0.000	0.000	0.000	0.000	0.000	0.003	0.000	0.000	0.000	0.000	0.000	0.000
Standard error ±	0.000	0.000	0.000	0.000	0.000	0.000	0.000	0.006	0.000	0.000	0.000	0.000	0.000	0.000
<i>Cypressaceae</i>	0.112	0.087	0.108	0.152	0.126	0.149	0.113	0.128	0.150	0.167	0.046	0.066	0.116	0.110
Standard error ±	0.030	0.030	0.036	0.043	0.039	0.043	0.037	0.037	0.042	0.043	0.024	0.029	0.036	0.033
<i>Equisetaceae</i>	0.000	0.003	0.024	0.011	0.000	0.000	0.000	0.000	0.000	0.000	0.000	0.017	0.019	0.006
Standard error ±	0.000	0.006	0.018	0.013	0.000	0.000	0.000	0.000	0.000	0.000	0.000	0.015	0.015	0.008
<i>Larix</i>	0.007	0.003	0.049	0.067	0.028	0.007	0.021	0.016	0.004	0.007	0.004	0.010	0.010	0.003
Standard error ±	0.008	0.006	0.025	0.030	0.019	0.010	0.017	0.014	0.007	0.009	0.007	0.012	0.011	0.006
<i>Populus</i>	0.110	0.090	0.115	0.067	0.098	0.108	0.085	0.052	0.022	0.051	0.028	0.042	0.045	0.026
Standard error ±	0.030	0.030	0.037	0.030	0.035	0.037	0.032	0.025	0.017	0.025	0.019	0.023	0.023	0.017
<i>Nuphar</i>	0.000	0.000	0.000	0.000	0.000	0.000	0.000	0.003	0.000	0.000	0.000	0.000	0.000	0.000
Standard error ±	0.000	0.000	0.000	0.000	0.000	0.000	0.000	0.006	0.000	0.000	0.000	0.000	0.000	0.000
<i>Pediastrium</i>	0.024	0.087	0.084	0.089	0.053	0.026	0.039	0.049	0.055	0.072	0.071	0.049	0.084	0.043
Standard error ±	0.015	0.030	0.032	0.034	0.026	0.019	0.023	0.024	0.027	0.030	0.030	0.025	0.031	0.021
<i>Picea</i>	0.179	0.203	0.168	0.234	0.253	0.123	0.173	0.230	0.260	0.160	0.226	0.112	0.132	0.133
Standard error ±	0.038	0.042	0.043	0.051	0.050	0.039	0.044	0.047	0.052	0.042	0.049	0.037	0.038	0.036
<i>Pinus banksiana/resinosa</i>	0.190	0.096	0.084	0.059	0.063	0.101	0.106	0.089	0.088	0.078	0.148	0.161	0.097	0.089
Standard error ±	0.036	0.031	0.032	0.028	0.028	0.036	0.036	0.032	0.034	0.031	0.041	0.043	0.033	0.030
<i>Pinus strobus</i>	0.157	0.212	0.192	0.123	0.232	0.213	0.191	0.213	0.143	0.263	0.191	0.182	0.187	0.170
Standard error ±	0.035	0.043	0.046	0.039	0.049	0.049	0.046	0.046	0.042	0.050	0.046	0.045	0.043	0.040
<i>Unknown Pinus</i>	0.171	0.174	0.140	0.152	0.116	0.209	0.216	0.161	0.172	0.147	0.254	0.290	0.265	0.398
Standard error ±	0.036	0.040	0.040	0.043	0.037	0.049	0.048	0.041	0.045	0.041	0.051	0.053	0.049	0.051
<i>Poaceae</i>	0.000	0.000	0.000	0.000	0.000	0.004	0.007	0.003	0.011	0.000	0.000	0.007	0.000	0.000
Standard error ±	0.000	0.000	0.000	0.000	0.000	0.007	0.010	0.006	0.012	0.000	0.000	0.000	0.000	0.000
<i>Pteridium</i>	0.000	0.000	0.000	0.000	0.000	0.007	0.000	0.000	0.000	0.000	0.000	0.000	0.000	0.009
Standard error ±	0.000	0.000	0.000	0.000	0.000	0.010	0.000	0.000	0.000	0.000	0.000	0.000	0.000	0.010
<i>Pteropsida monoletes</i>	0.000	0.000	0.000	0.000	0.000	0.000	0.004	0.000	0.000	0.003	0.000	0.000	0.003	0.000
Standard error ±	0.000	0.000	0.000	0.000	0.000	0.000	0.007	0.000	0.000	0.007	0.000	0.000	0.006	0.000
<i>Salicaceae</i>	0.000	0.000	0.000	0.000	0.000	0.000	0.000	0.000	0.000	0.000	0.000	0.000	0.000	0.003
Standard error ±	0.000	0.000	0.000	0.000	0.000	0.000	0.000	0.000	0.000	0.000	0.000	0.000	0.000	0.006
<i>Taxus</i>	0.002	0.006	0.000	0.000	0.000	0.011	0.011	0.003	0.000	0.003	0.000	0.007	0.006	0.000
Standard error ±	0.005	0.008	0.000	0.000	0.000	0.013	0.012	0.006	0.000	0.007	0.000	0.010	0.009	0.000

Table 5.2 - Taxonomic unit counts, Shannon-Weaver Diversity, fractional abundances and standard error for core pollen samples from James and Granite lakes.

Station	JLP 99-1-15	JLP 99-1-16	JLP 99-1-17	GLP 99-4-21	GLP 99-4-22	GLP 99-4-23	GLP 99-4-24	GLP 99-4-25	GLP 99-4-26	GLP 99-4-27	GLP 99-4-28	GLP 99-4-29	GLP 99-4-30	GLP 99-4-31
Depth (cm)	246	268	310	325	340	350	355	360	380	390	400	410	430	435
Taxonomic Counts	249	289	253	146	142	90	213	274	57	147	40	69	1	1
Counts per cc	325	398	354	163	162	108	270	325	79	177	57	90	2	2
Number of Species	11	11	10	9	9	9	9	7	7	8	7	8	1	1
Diversity	1.59	1.84	1.74	1.06	1.75	1.25	1.66	1.21	1.23	1.73	1.19	1.34	0.00	0.00
<i>Abies</i>	0.000	0.010	0.004	0.000	0.000	0.000	0.000	0.000	0.000	0.000	0.000	0.000	0.000	0.000
Standard error ±	0.000	0.012	0.008	0.000	0.000	0.000	0.000	0.000	0.000	0.000	0.000	0.000	0.000	0.000
<i>Aceraceae</i>	0.000	0.000	0.000	0.000	0.000	0.000	0.000	0.000	0.000	0.000	0.000	0.000	0.000	0.000
Standard error ±	0.000	0.000	0.000	0.000	0.000	0.000	0.000	0.000	0.000	0.000	0.000	0.000	0.000	0.000
<i>Alnus</i>	0.000	0.000	0.000	0.000	0.000	0.022	0.000	0.000	0.000	0.000	0.000	0.000	0.000	0.000
Standard error ±	0.000	0.000	0.000	0.000	0.000	0.030	0.000	0.000	0.000	0.000	0.000	0.000	0.000	0.000
<i>Ambrosia</i>	0.000	0.000	0.000	0.000	0.000	0.000	0.000	0.000	0.000	0.000	0.000	0.000	0.000	0.000
Standard error ±	0.000	0.000	0.000	0.000	0.000	0.000	0.000	0.000	0.000	0.000	0.000	0.000	0.000	0.000
<i>Betula</i>	0.004	0.059	0.012	0.007	0.014	0.000	0.009	0.000	0.000	0.000	0.000	0.000	0.000	0.000
Standard error ±	0.008	0.027	0.013	0.014	0.000	0.000	0.013	0.000	0.000	0.000	0.000	0.000	0.000	0.000
<i>Chenopodiaceae</i>	0.000	0.000	0.000	0.000	0.000	0.000	0.000	0.000	0.000	0.000	0.000	0.000	0.000	0.000
Standard error ±	0.000	0.000	0.000	0.000	0.000	0.000	0.000	0.000	0.000	0.000	0.000	0.000	0.000	0.000
<i>Cupressaceae</i>	0.096	0.201	0.103	0.096	0.197	0.133	0.150	0.033	0.368	0.075	0.325	0.275	1.000	1.000
Standard error ±	0.037	0.046	0.037	0.048	0.065	0.070	0.048	0.021	0.125	0.043	0.145	0.105	0.000	0.000
<i>Equisetaceae</i>	0.000	0.000	0.000	0.000	0.000	0.000	0.000	0.000	0.000	0.000	0.000	0.000	0.000	0.000
Standard error ±	0.000	0.000	0.000	0.000	0.000	0.000	0.000	0.000	0.000	0.000	0.000	0.000	0.000	0.000
<i>Larix</i>	0.000	0.000	0.000	0.000	0.000	0.000	0.000	0.000	0.000	0.000	0.000	0.000	0.000	0.000
Standard error ±	0.000	0.000	0.000	0.000	0.000	0.000	0.000	0.000	0.000	0.000	0.000	0.000	0.000	0.000
<i>Populus</i>	0.016	0.038	0.036	0.007	0.000	0.000	0.047	0.007	0.053	0.020	0.048	0.061	0.000	0.000
Standard error ±	0.016	0.022	0.023	0.013	0.000	0.000	0.028	0.010	0.058	0.023	0.000	0.000	0.000	0.000
<i>Nuphar</i>	0.000	0.000	0.000	0.000	0.000	0.000	0.000	0.000	0.000	0.000	0.000	0.000	0.000	0.000
Standard error ±	0.000	0.000	0.000	0.000	0.000	0.000	0.000	0.000	0.000	0.000	0.000	0.000	0.000	0.000
<i>Pedicularium</i>	0.084	0.235	0.190	0.123	0.190	0.122	0.155	0.084	0.000	0.061	0.100	0.043	0.000	0.000
Standard error ±	0.035	0.049	0.048	0.053	0.065	0.068	0.049	0.033	0.000	0.039	0.093	0.048	0.000	0.000
<i>Picea</i>	0.096	0.035	0.115	0.000	0.000	0.000	0.000	0.000	0.000	0.000	0.000	0.000	0.000	0.000
Standard error ±	0.037	0.021	0.039	0.000	0.000	0.000	0.000	0.000	0.000	0.000	0.000	0.000	0.000	0.000
<i>Pinus banksiana/fechinosa</i>	0.052	0.055	0.043	0.062	0.042	0.033	0.028	0.102	0.035	0.116	0.050	0.058	0.000	0.000
Standard error ±	0.028	0.026	0.025	0.039	0.033	0.037	0.022	0.036	0.048	0.052	0.068	0.055	0.000	0.000
<i>Pinus strobus</i>	0.237	0.145	0.213	0.623	0.331	0.278	0.399	0.555	0.211	0.320	0.375	0.391	0.000	0.000
Standard error ±	0.053	0.041	0.050	0.079	0.077	0.093	0.066	0.059	0.106	0.075	0.150	0.115	0.000	0.000
<i>Unknown Pinus</i>	0.394	0.208	0.269	0.021	0.120	0.356	0.164	0.208	0.246	0.245	0.100	0.130	0.000	0.000
Standard error ±	0.061	0.047	0.055	0.023	0.053	0.099	0.050	0.048	0.112	0.070	0.093	0.079	0.000	0.000
<i>Poaceae</i>	0.000	0.000	0.000	0.021	0.028	0.011	0.000	0.004	0.018	0.095	0.025	0.014	0.000	0.000
Standard error ±	0.000	0.000	0.000	0.023	0.027	0.022	0.000	0.007	0.034	0.047	0.048	0.028	0.000	0.000
<i>Pteridium</i>	0.004	0.007	0.012	0.000	0.000	0.000	0.000	0.000	0.000	0.000	0.000	0.000	0.000	0.000
Standard error ±	0.008	0.010	0.013	0.000	0.000	0.000	0.000	0.000	0.000	0.000	0.000	0.000	0.000	0.000
<i>Pteropsis monoletae</i>	0.012	0.000	0.000	0.000	0.000	0.000	0.000	0.000	0.000	0.000	0.000	0.000	0.000	0.000
Standard error ±	0.014	0.000	0.000	0.000	0.000	0.000	0.000	0.000	0.000	0.000	0.000	0.000	0.000	0.000
<i>Silicaceae</i>	0.000	0.000	0.000	0.000	0.000	0.000	0.000	0.000	0.000	0.000	0.000	0.000	0.000	0.000
Standard error ±	0.000	0.000	0.000	0.000	0.000	0.000	0.000	0.000	0.000	0.000	0.000	0.000	0.000	0.000
<i>Tsuga</i>	0.004	0.000	0.000	0.000	0.000	0.000	0.000	0.000	0.000	0.000	0.000	0.000	0.000	0.000
Standard error ±	0.008	0.000	0.008	0.000	0.000	0.000	0.000	0.000	0.000	0.000	0.000	0.000	0.000	0.000

Table 5.2 (continued) - Taxonomic unit counts, Shannon-Weaver Diversity, fractional abundances and standard error for core pollen samples from James and Granite lakes.

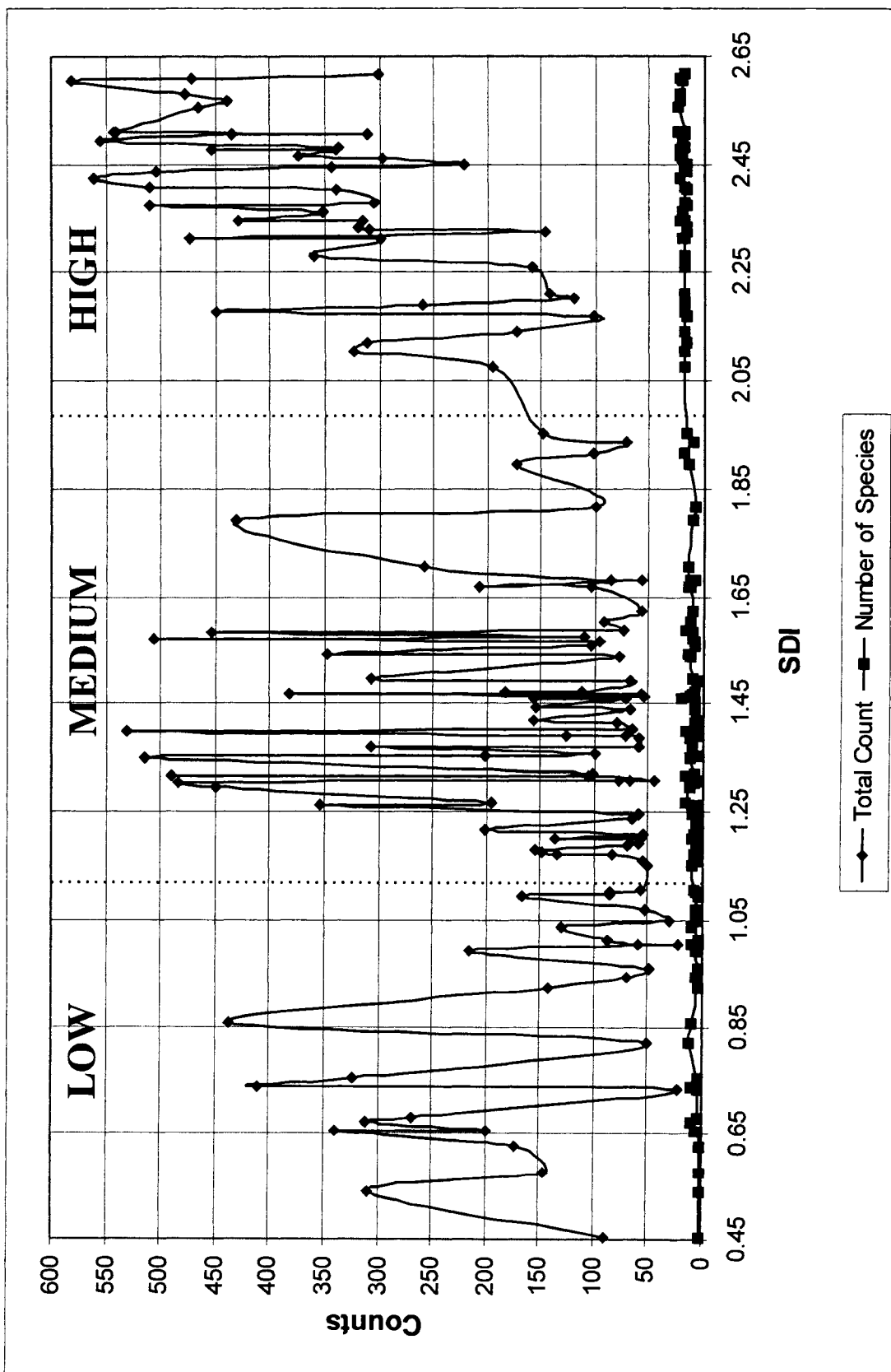


Figure 5.1 - Shannon Diversity Index (SDI) and number of taxa plotted against total counts for SWI stations in the James and Granite lakes system.

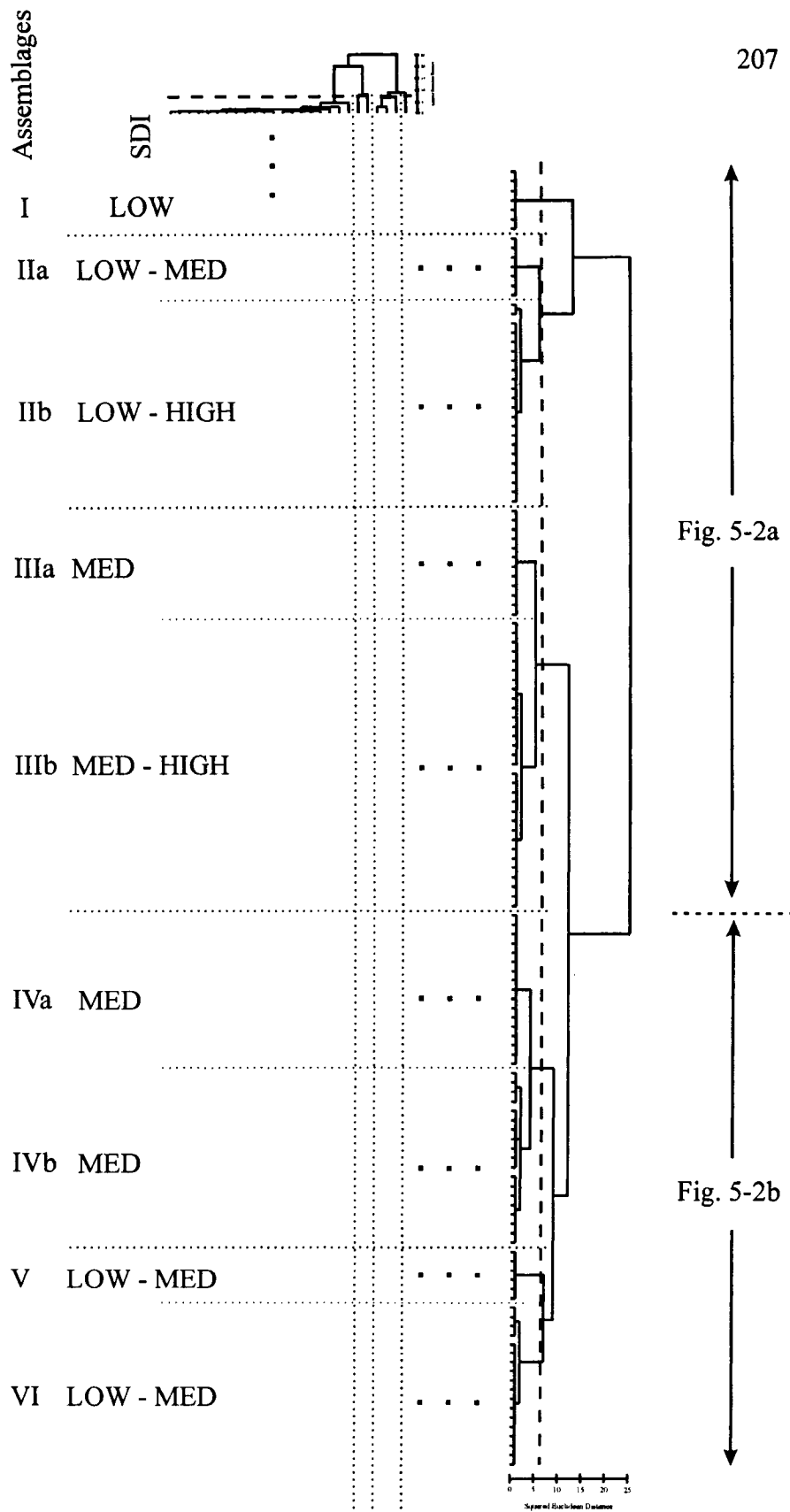


Figure 5.2 - Overall map of R-mode vs Q-mode cluster diagram showing abundances for arcellacean assemblages and their relationships within the James and Granite lakes system. Close-ups of this cluster diagram are as indicated in figures 5.2a & b.

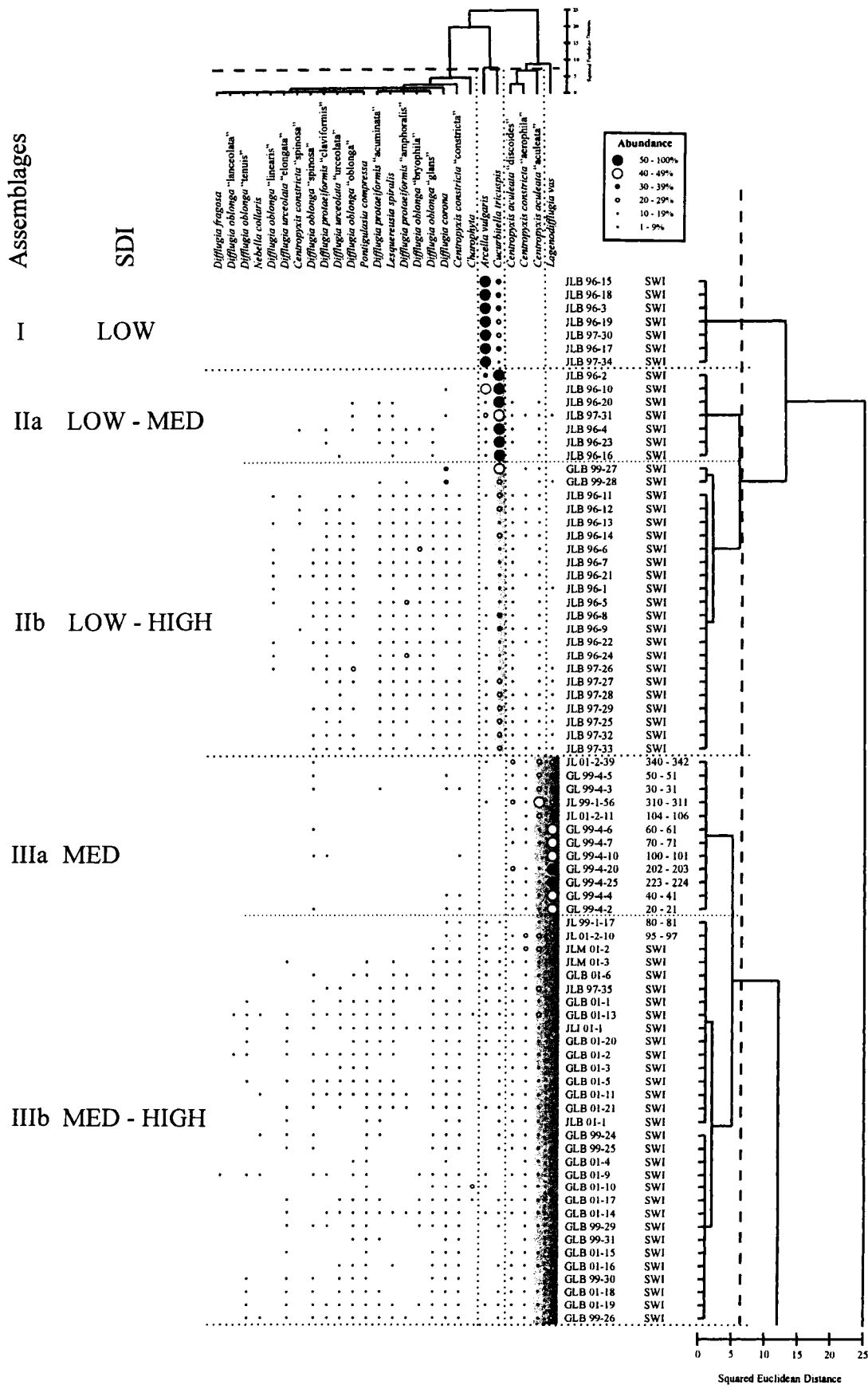


Figure 5.2a - R-mode vs Q-mode cluster diagram for assemblages I, II and III and their relationships with the James and Granite lakes system.

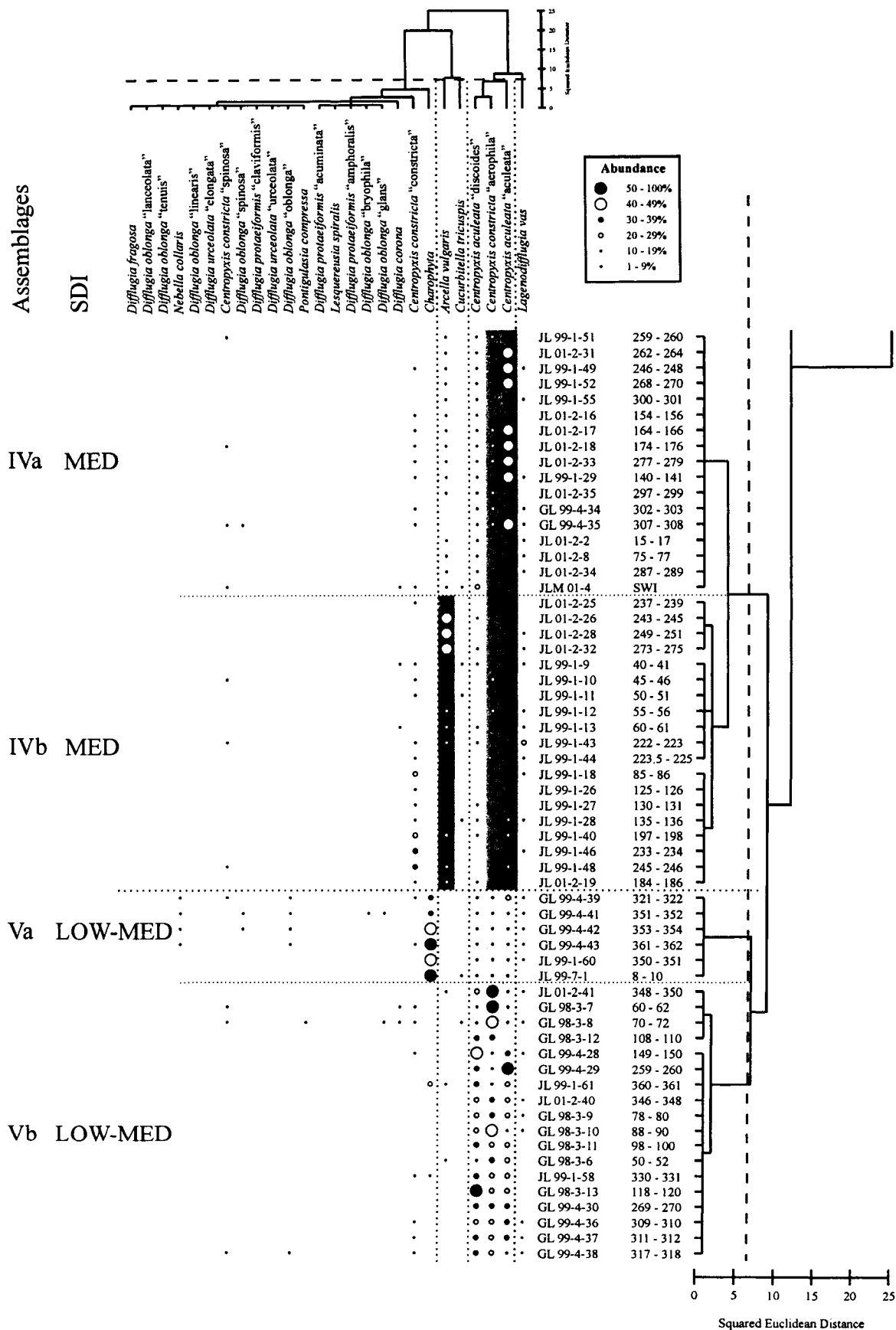


Figure 5.2b - R-mode vs Q-mode cluster diagram for assemblages IV and V and their relationships with the James and Granite lakes system.

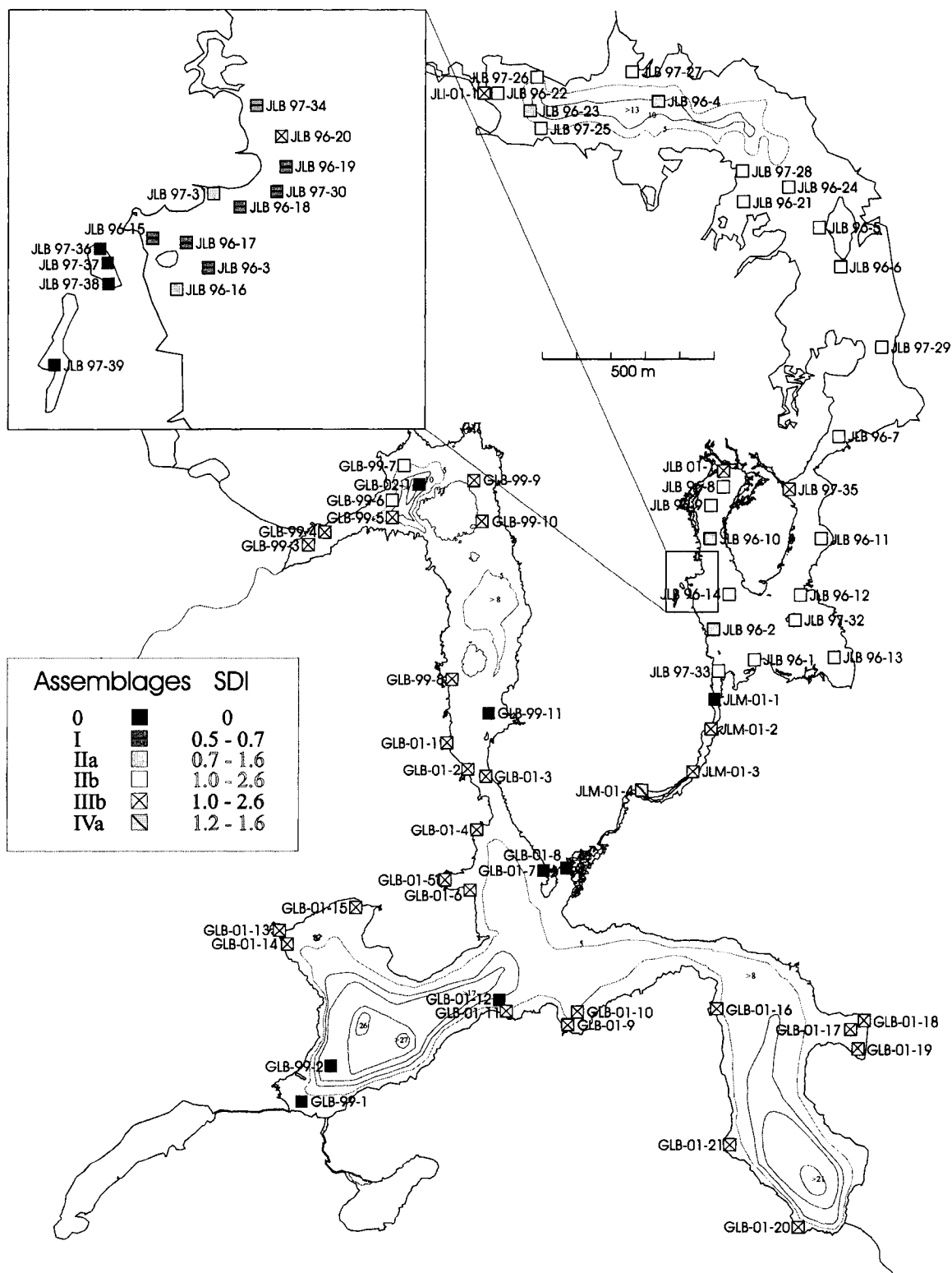


Figure 5.3 - SWI assemblages in the James and Granite lakes system indicating the Shannon diversity. Assemblages IIIa, Va and Vb are represented in sediment core as indicated in figures 5.4 to 5.8. Contour interval 5 m.

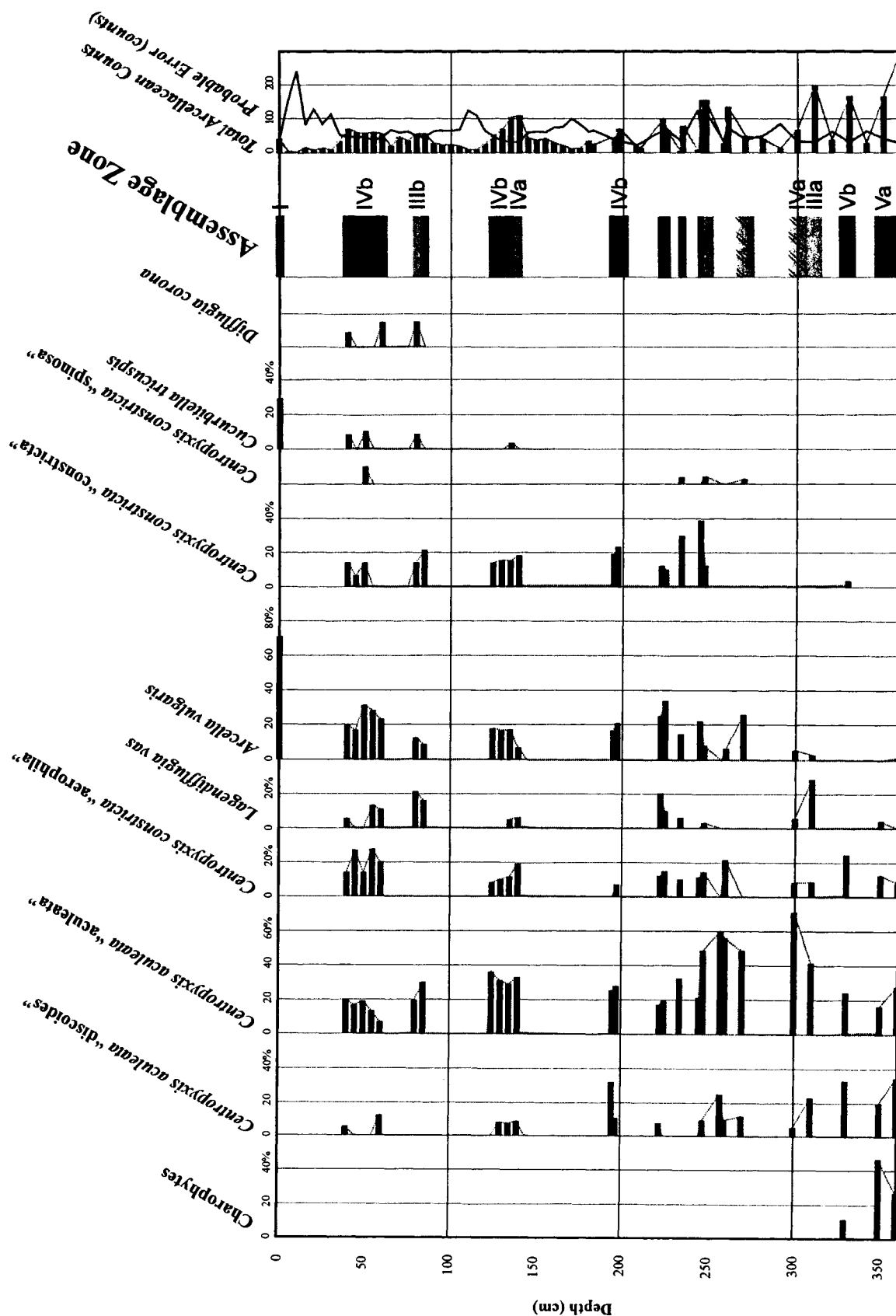


Figure 5.4 - Sawtooth diagram showing relative fractional abundances of arcellaceans and charophytes in reference to assemblage zones obtained through cluster analysis from James Lake core JL 99-1.

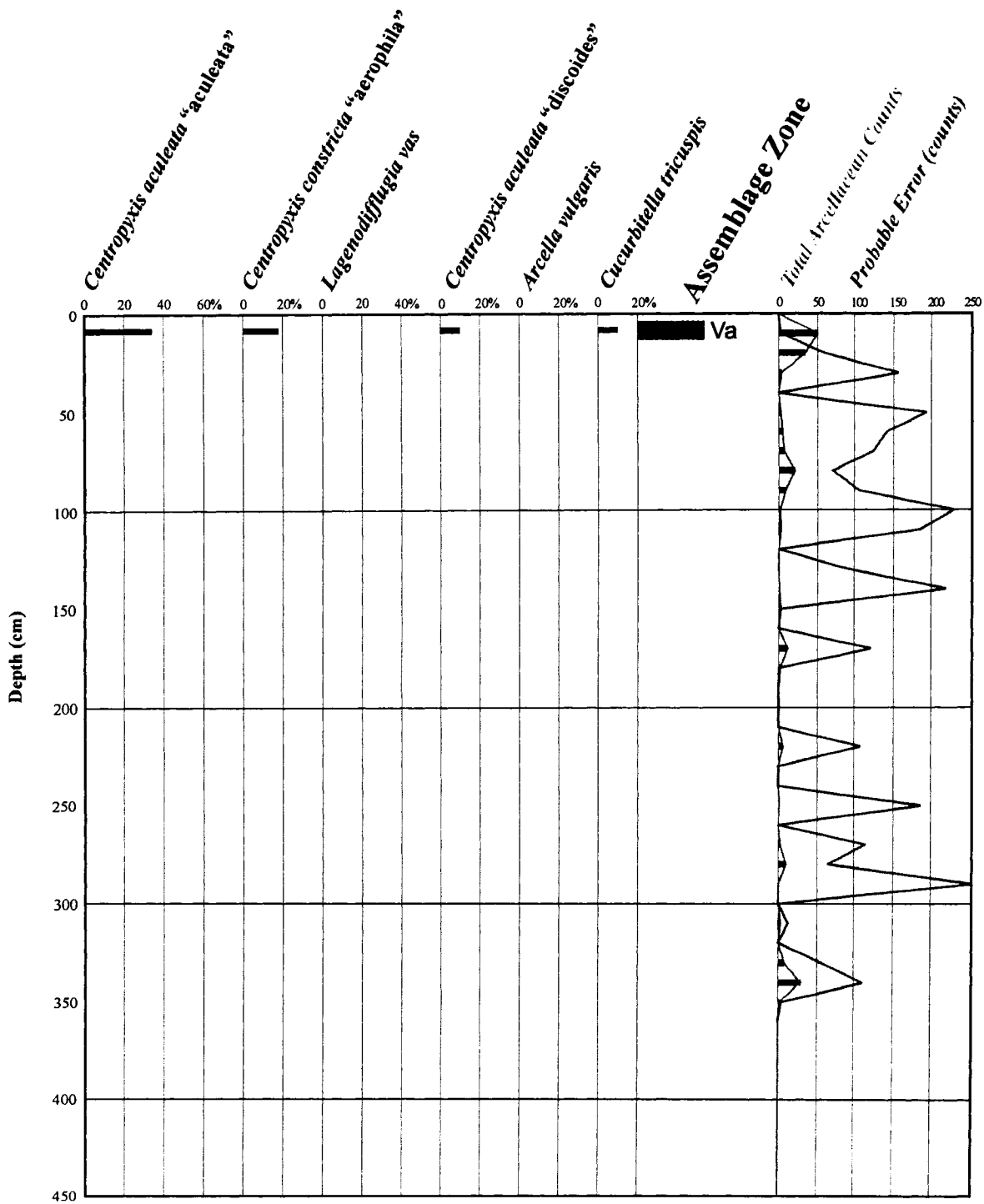


Figure 5.5 - Sawtooth diagram showing relative fractional abundances of arcellaceans in reference to assemblage zones obtained through cluster analysis from James Lake core JL 99-7.

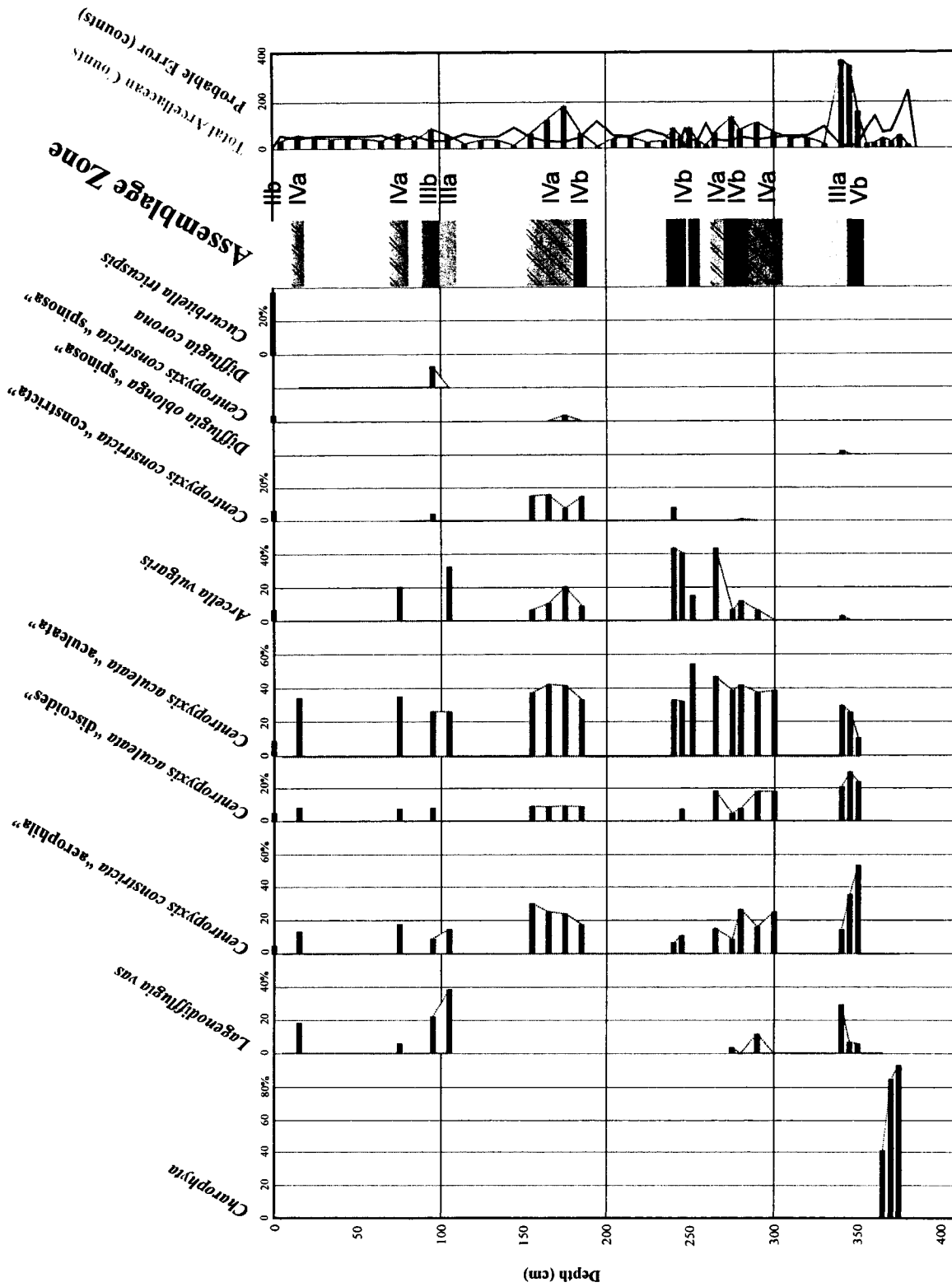


Figure 5.6 - Sawtooth diagram showing relative fractional abundances of acellaceans and charophytes in reference to assemblage zones obtained through cluster analysis from James Lake core JL 01-2.

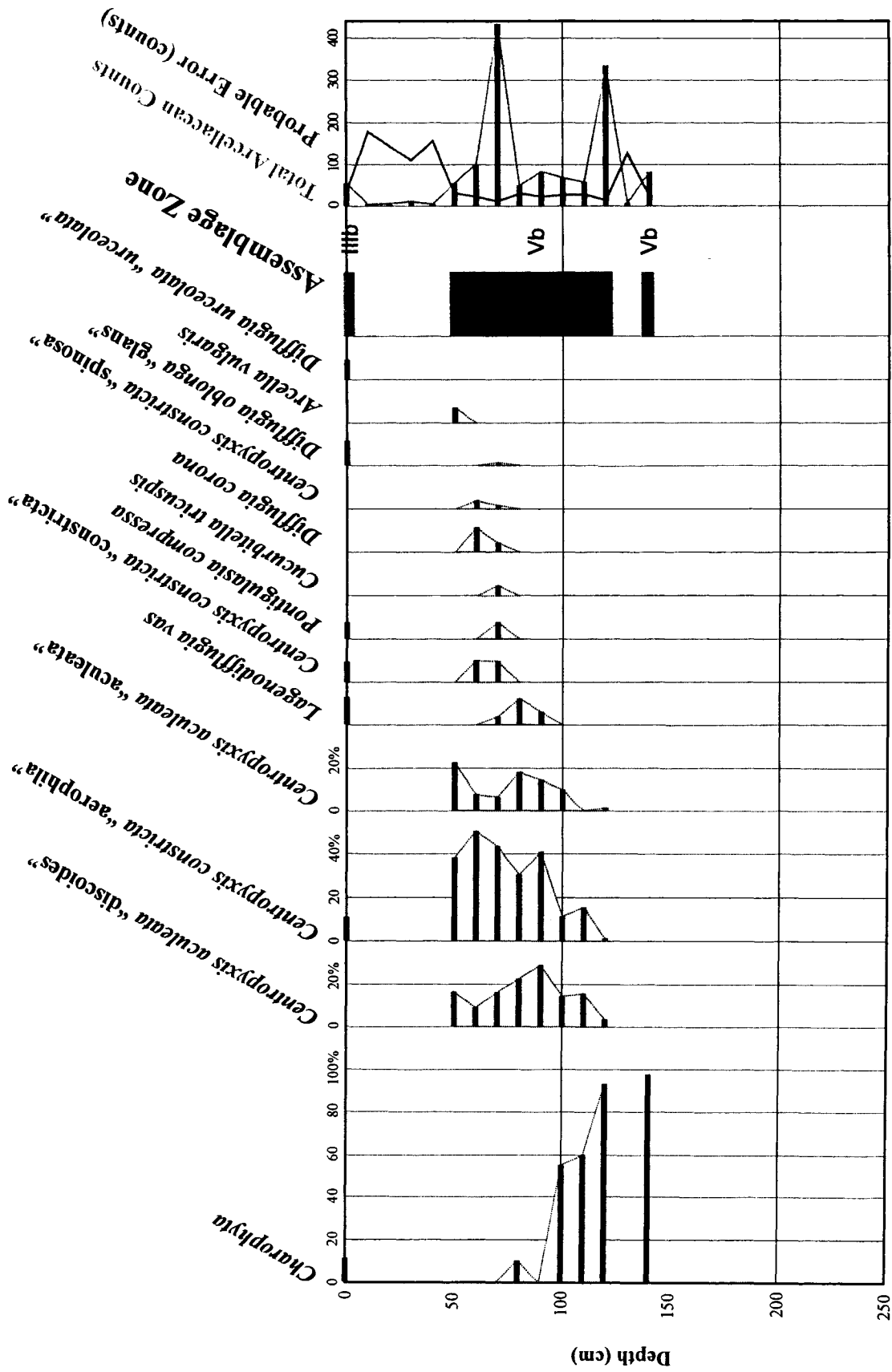


Figure 5.7 - Sawtooth diagram showing relative fractional abundances of arcellaceans and charophytes in reference to assemblage zones obtained through cluster analysis from Granite Lake core GL 98-3.

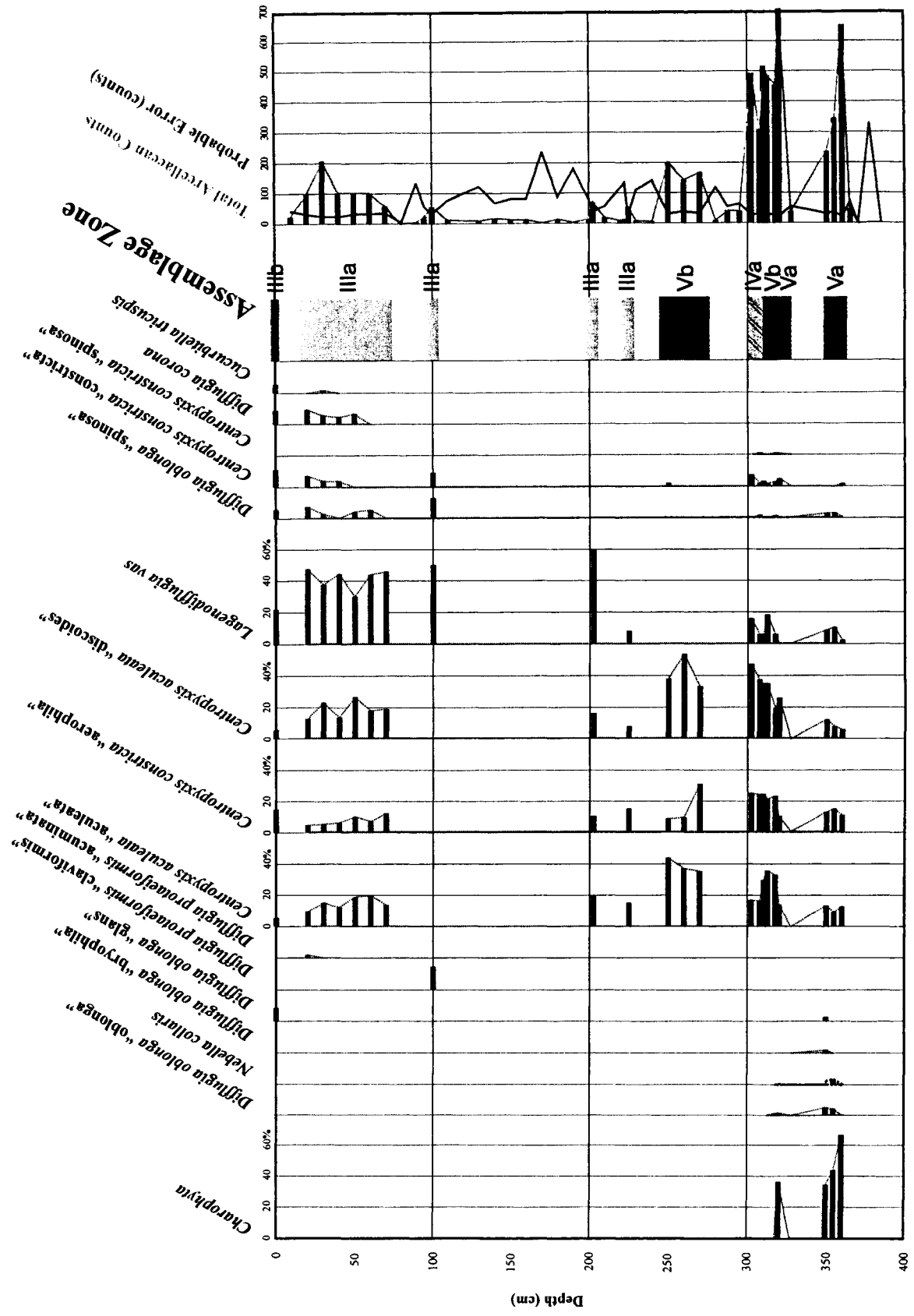


Figure 5.8 - Sawtooth diagram showing relative fractional abundances of arcellaceans and charophytes in reference to assemblage zones obtained through cluster analysis from Granite Lake core GL 99-4.

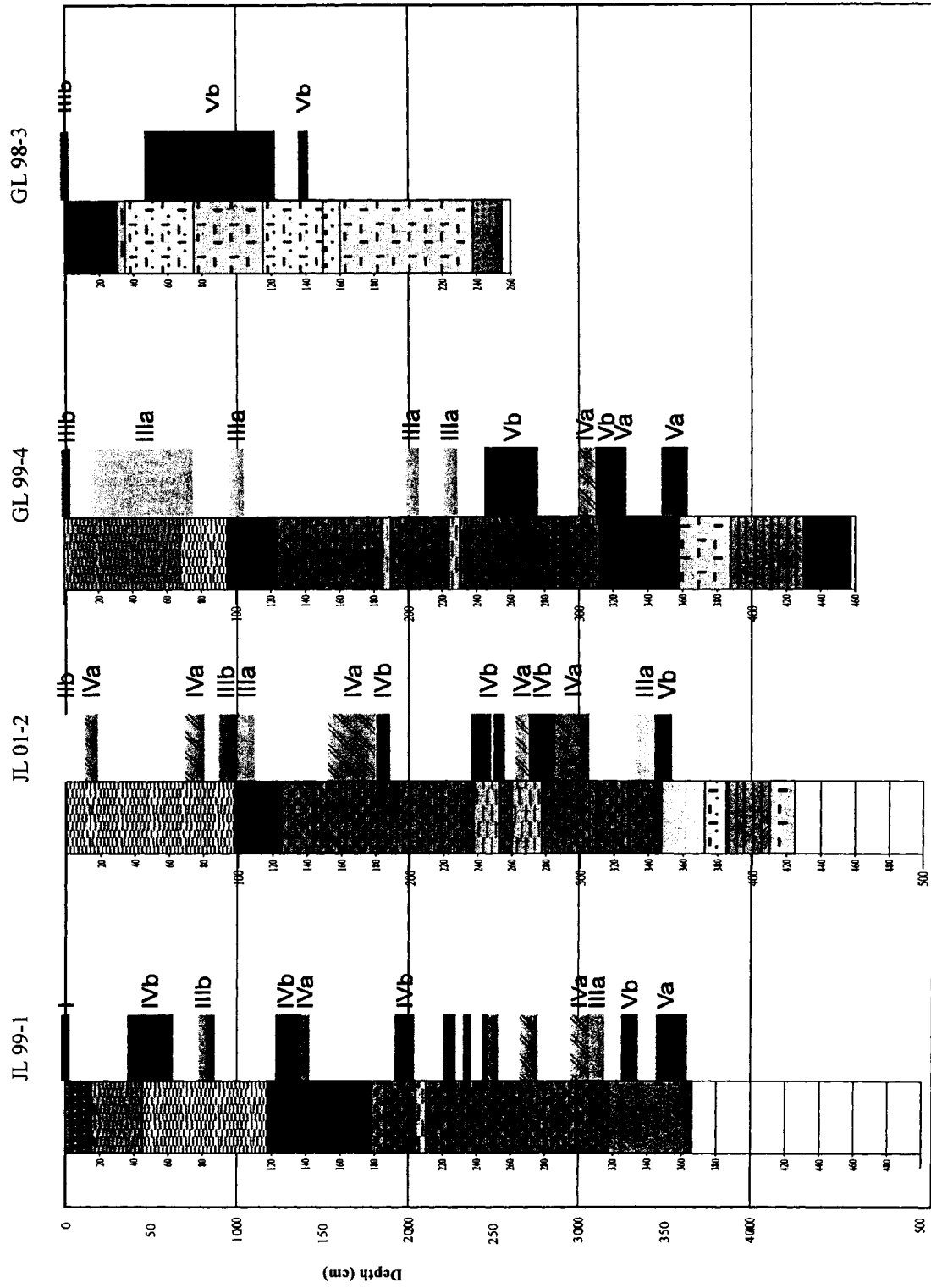


Figure 5.9 - Stratigraphic relationships between assemblages in the James and Granite lakes system during the Holocene.

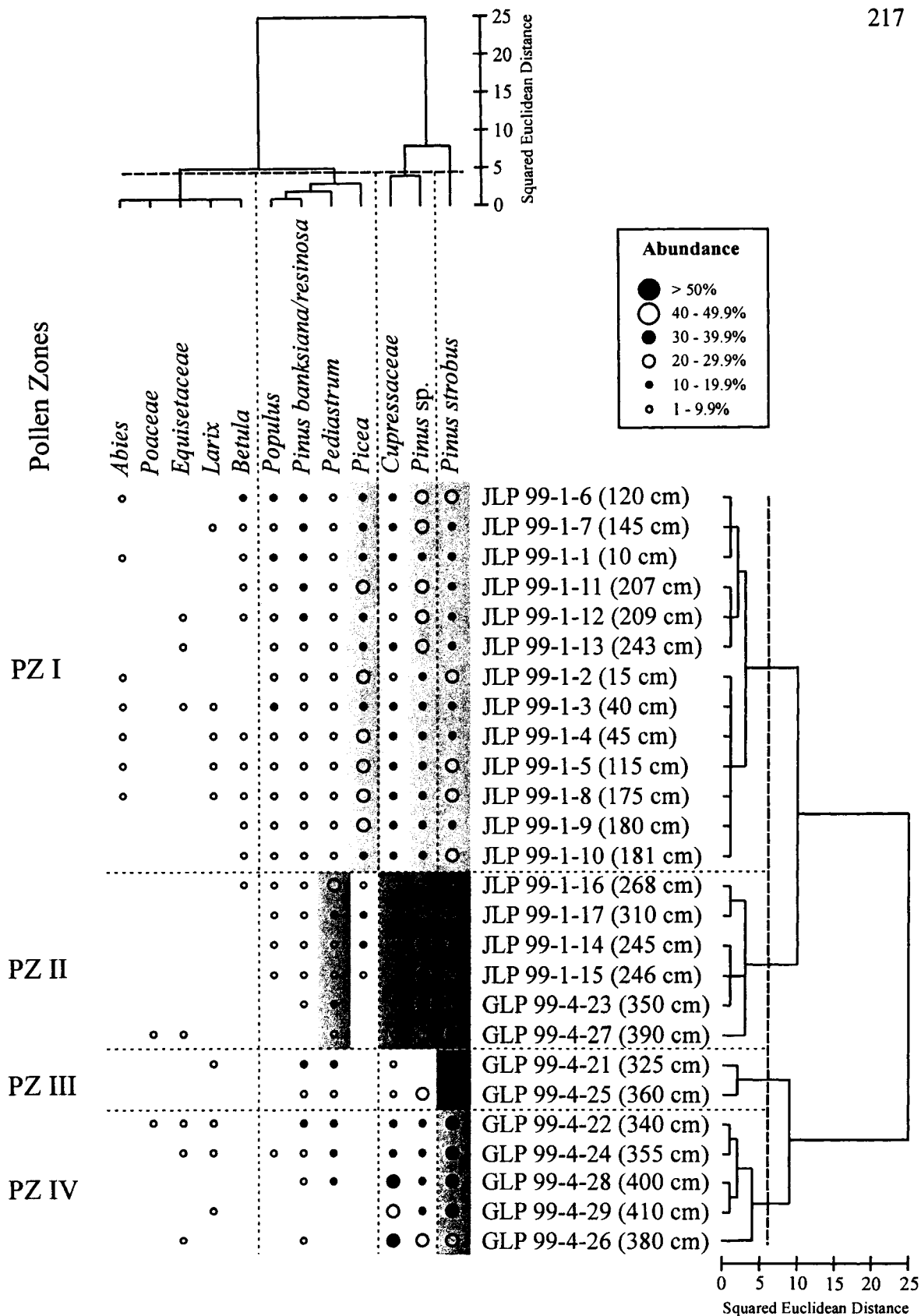


Figure 5.10 - R-mode vs Q-mode cluster diagram showing abundances for pollen assemblages from James Lake core JLP 99-1 and Granite Lake core GLP 99-4..

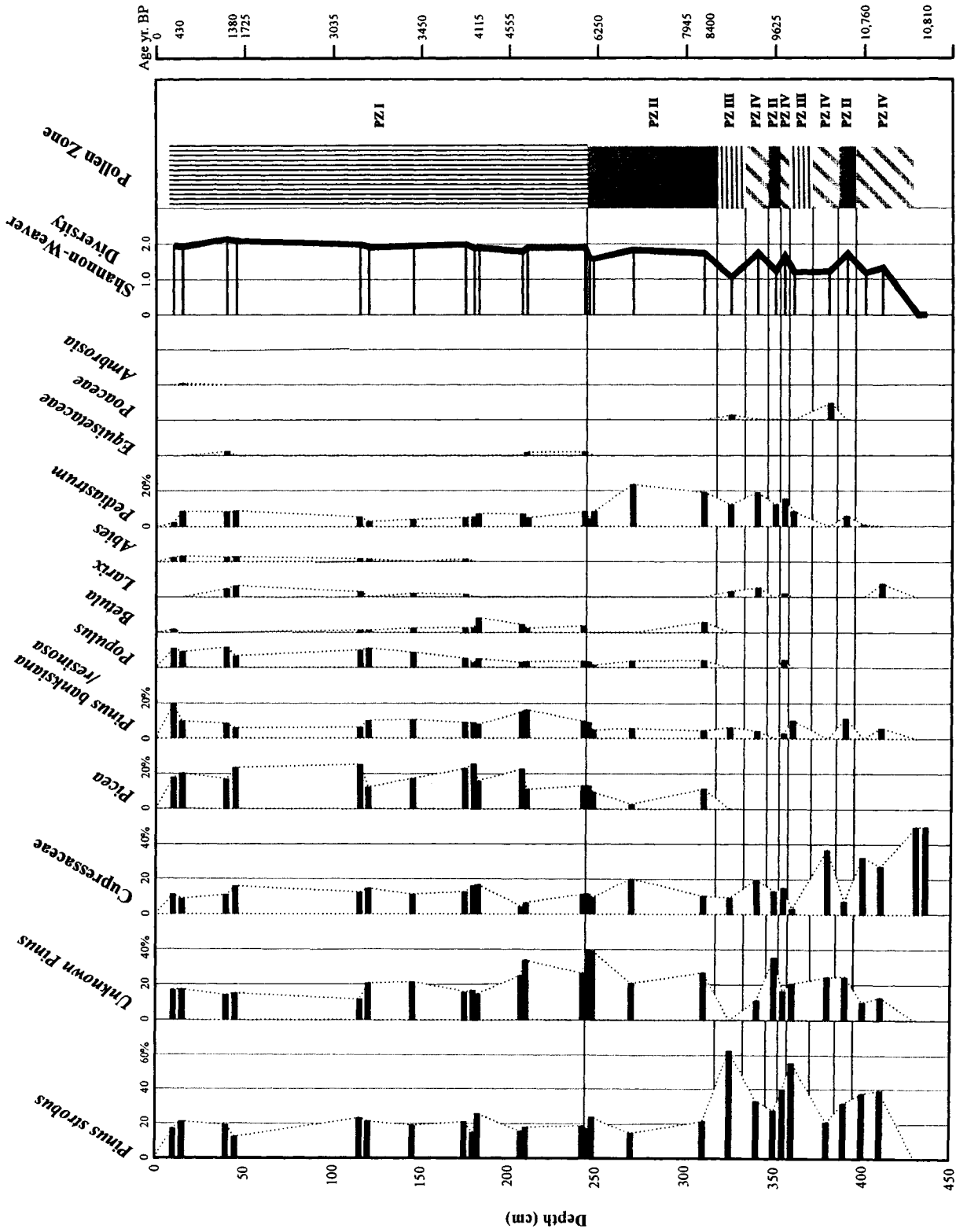


Figure 5.11 - Sawtooth diagram showing relative fractional abundances of pollen in reference to zones obtained through cluster analysis from James Lake core JLP 99-1 and Granite Lake core GLP 99-4. Age scale extrapolated from information in Chapter Three.

Plate 5.1 – a-k. *Centropyxis aculeata* (Ehrenberg, 1832) strain “aculeata”: **a.** side view showing one spine, x105; **b.** dorsal view showing three spines, x140; **c.** dorsal profile of **b**; **d.** apertural view showing three spines, x132; **e.** x118; **f.** x95; **g.** side profile, x90; **h.** x110; **i.** x130; **j.** x90; **k.** x95. **l-n.** *Centropyxis aculeata* (Ehrenberg, 1832) strain “discoides”: **l.** apertural view, x250; **m.** x145; **n.** dorsal view, x200. **o-ad.** *Centropyxis constricta* (Ehrenberg, 1843) strain “aerophila”: **o.** apertural view, x100; **p.** x95; **q.** x75; **r.** x90; **s.** dorsal view, x105; **t.** x130; **u.** x150; **v.** close-up of diatom in aperture of **u**, x390; **w.** x115; **x.** x125; **y.** x84; **z.** side view x115; **aa.** x80; **ab.** x55; **ac.** x70; **ad.** close-up of edge of aperture in **y.**, showing a diatom sp., x480.

Plate 5.2 – a. *Centropyxis constricta* (Ehrenberg, 1843) strain “aerophila”, apertural view, x200. **b-h.** *Lagenodifflugia vas* Leidy, 1874: **b.** side view, x55; **c.** x35; **d.** x65; **e.** x60; **f.** x50; **g.** apertural view x70; **h.** close-up of apertural view from **g.**, x190. **i-j.** *Arcella vulgaris* Ehrenberg, 1830: **i.** apertural view, x70; **j.** angled view of **i.** **k.** *Difflugia oblonga* (Penard, 1902) strain “glans”, apertural view, x170.

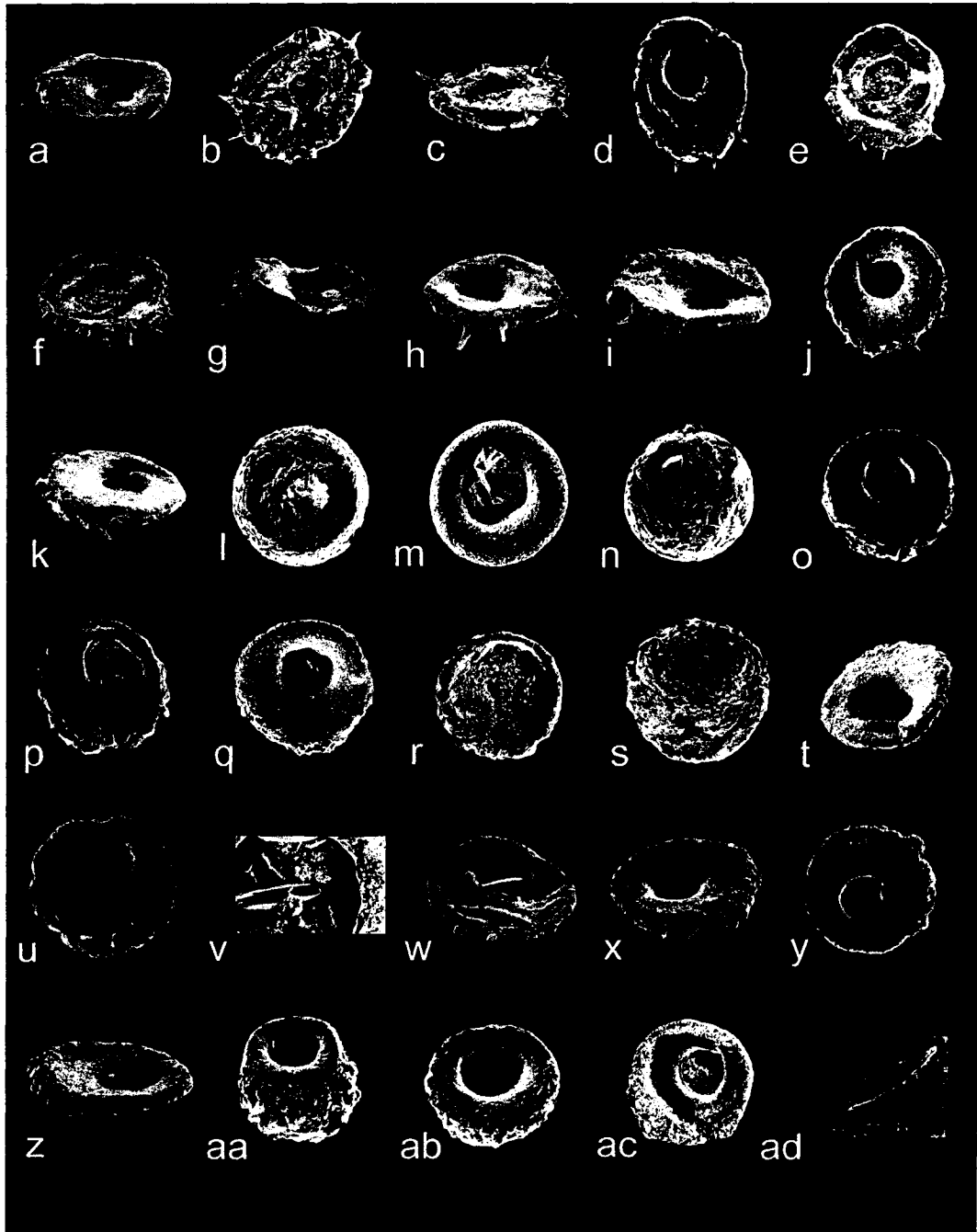


Plate 5.1

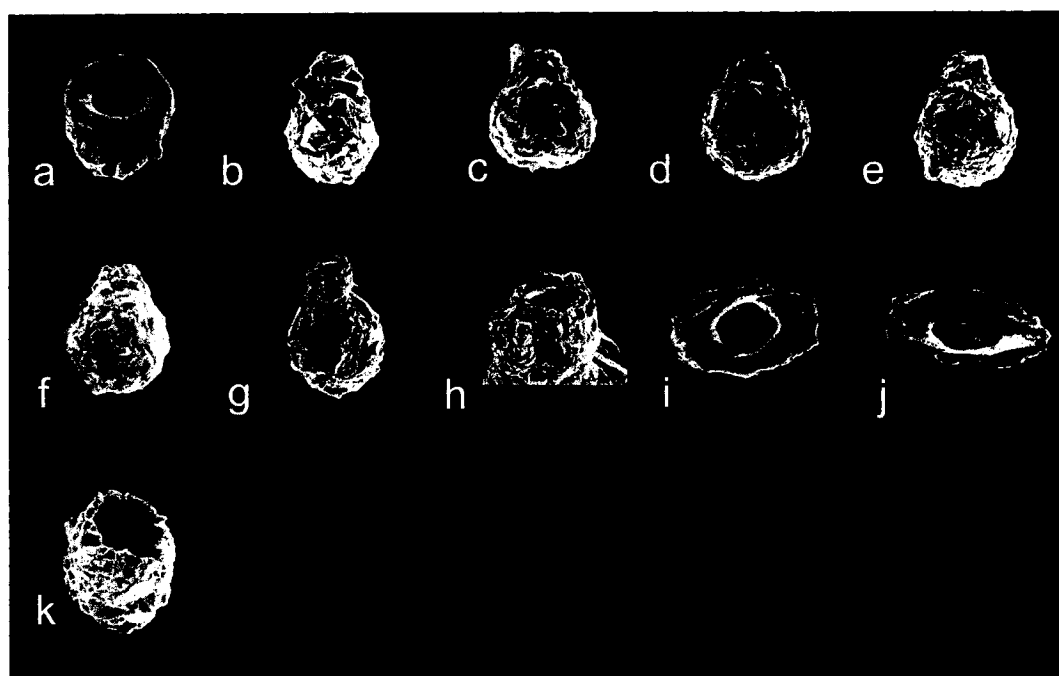


Plate 5.2

CONCLUSIONS

This research described the post glacial paleoenvironmental, hydrogeochemical and sedimentological Holocene history of James and Granite lakes, in Temagami region of northeastern Ontario. Paleontological interpretation was complicated by the presence Northland Pyrite Mine on the southwestern shore of James Lake, which was abandoned in 1911 after being in operation for five years. This mine site contains a waste rock pile which produces sulfuric acid through oxidation of pyrite, lowering the pH to 3.0 in the lake surface waters immediately adjacent to the abandoned mine site.

This research indicated that there are four main types of sediment within the five cores investigated within James and Granite lakes system. The first is an organic silt or gyttja, which was found in the top 30 (GL 98-3) to 360 cm (GL 99-4) of sediment below the sediment-water interface. Gyttja varied according to the amount of silt and organics within, and the mass accumulation rate (MAR) of this material indicated the relative water level within the system. The MAR ranged from a low of 0.024 ± 0.001 g/cm²/yr, indicating a warm or a drier climate conditions that existed during the Holocene Hypsithermal that characterized the study area from 3927 ± 55 to 7425 ± 77 yrs BP; to a maximum of 0.067 ± 0.003 g/cm²/yr, indicating a transition to the wetter conditions that exist today. The retreating Laurentide Ice Sheet formed an ice-proximal lake between $10,800 \pm 220$ and $10,700 \pm 240$ yrs. BP, again marked by a high MAR of 0.071 ± 0.003 g/cm²/yr. In effect, the MAR within gyttja acts as an indicator for lake level change, with high MAR indicating higher lake water levels and low MAR indicating low lake water levels.

The second type of sediment is peat, which was found in thin layers in the middle of the Holocene Hypsithermal, indicating marsh conditions. The third type of sediment is composed of the silts and clays which were deposited within an ice-proximal lake as the Laurentide ice sheet retreated. This material, which varied in proportion of clay and silt content, appeared as fat clay, silty-clay or clay and silt varves, in units from 40 (JL 01-2) to 200 cm (GL 98-3) thick. The fourth sediment type found, at the base of the Holocene sediment cores, is coarse sand which represents glacial fluvial conditions as the Laurentide ice sheet melted.

The accumulation and compression of the unlithified Holocene sedimentary record of the James and Granite lakes system is the result of the climate and the environment that was present from the time of a temporary ice-marginal lake, which drained as the Laurentide ice-sheet retreated through the area more than 10,800 yr. BP. Changes were analyzed using physical techniques such as changes in density and porosity, and by the presence or absence of biological indicators in the sedimentary record.

The aquatic chemistry of the James and Granite lakes system is controlled by carbonate poor Na-K waters surface waters which enter James Lake from the north and mix with the JLN waters. James Lake is dimictic, and in early summer the freshly turned over waters precipitate Fe oxides and Fe and Al hydroxides during their journey to the south of the lake. The Mg-SO₄ anthropogenic waters found in the vicinity of the Northland Pyrite Mine waste rock pile in the southwestern part of James Lake mix with the above waters, then exit James Lake to the south towards Granite Lake.

Analysis indicates that metal contamination has existed at this site since at least 8400 yr. BP. Cluster analyses of sediment analysis data indicates that there were periods in the past when high nutrient content, such as P and Mn, existed at this site. Two possible causes of the high nutrient levels are beaver activity, and low pH conditions with high Fe concentrations in both the sediment and the bottom waters.

Holocene arcellacean proxies in the area of James and Granite lakes were influenced by local factors, such as changes in pH, nutrient content, while pollen was influenced by regional factors such as the retreat of the Laurentide Ice Sheet, which occurred prior to 10,800 yr. BP, causing a change in climate from glacial to periglacial.

The stressed climate of the early Holocene was reflected in the initial boreal forest fauna and low diversity assemblages of arcellaceans present at that time. These in turn were affected by local environmental conditions like low pH, first indicated 8400 yr. BP by the arcellacean *A. vulgaris*. From this one can suppose that the Northland Pyrite Mine sulfide vein was exposed to the lake waters at this time.

Eutrophic conditions were indicated to exist as far back as 9700 yr. BP when the first indications of *Pediastrum* (and *Charophyta*) were found to be present in the system. Slow moving waters can be caused by the beaver influenced ponding which increases both the water and nutrient levels behind the dams. These conditions exist today around beaver dams and lodges in James Lake, and throughout most of Granite Lake. The cyclic high and low water levels caused by beavers, over time, is a method of exposing the sulfide vein to the oxygenated waters sulfides require to oxidize. This can be tracked by the presence of algae (as mentioned above) and by the presence of proxies such as *C. tricuspis*.

The ability to hindcast past environmental conditions in an area is vital to determining what sort of remediation might be required for a contaminated site (eg. the waste rock pile from the abandoned mine site at James Lake). The sediment that accumulates on the lake bottom can archive an important record of sedimentation, chemical change and, changes in the paleofauna and the paleoflora that are critical to determining the natural condition of a lake system.

The Holocene climate of James and Granite lakes was reconstructed using arcellaceans and pollen as environmental proxies. The retreat of the ice sheet from the area prior to 10,800 yr. BP caused a change in climate from glacial to periglacial, which ended at the end of the Younger Dryas with a warming trend. This change in climate was reflected in the pollen present as well as the arcellacean assemblages present.

The metal contamination caused by the waste rock pile has not been contained by the dolomitic-limestone causeway put across the mine site in the 1990s. This could be remedied by extending the causeway to completely encircle the waste rock, and/or place some of the waste rock back into the mine trench. Here it would do minimal damage because the water is anoxic below two m in depth.